Study and development of a 'smart' wound dressing technology which can detect and inhibit/kill the colonisation of pathogenic bacteria

Zhou, Jin

Award date:
2011

Awarding institution:
University of Bath

Study and Development of A 'Smart' Wound Dressing Technology Which Can Detect and Inhibit/Kill the Colonisation of Pathogenic Bacteria

Jin Zhou

A thesis submitted for the degree of Doctor of Philosophy

Department of Chemistry

University of Bath

November 2011

To my parents and my grandfather

Abstract

Bacterial infections are a serious problem for patients with burns and other wounds. Such burn wound infection accounts for the pathogenic bacteria by colonising onto burned areas. Therefore, the need for detection and inhibition of such bacterial colonisation requires a methodology for sensing/killing pathogenic bacteria.

This research project aims to design a 'smart' wound dressing system which can respond to the microbiological environment of the wound via a simple colour change and will release antimicrobials only when required. Two strains of pathogenic bacteria *Staphylococcus aureus* (MSSA 476) and *Pseudomonas aeruginosa* (PAO1) were used in the study. The non-pathogenic bacterium *E.coli* (DH5α) was used as a control organism as it does not secrete virulence factors and therefore does not lyse membranes of vesicles. The key contributions of this thesis are outlined below.

Firstly, an initial responsive nanocapsule system was studied. The fundamental work with giant unilamellar vesicles proved such a responsive system can provide antimicrobial properties when antimicrobial agents were encapsulated within the vesicles.

Secondly, partially polymerised vesicles—polydiacetylene/phospholipid vesicles were then developed to improve vesicle stability. The vesicle system was optimised by varying molar concentration of diacetylene monomers (TCDA) in order to obtain relatively stable vesicles as well as sensitivity to the toxins secreted by the pathogenic strains. Measurements proved that the polydiacetylene/phospholipid vesicles can respond to pathogenic bacteria when fluorescent dye/antimcirobials were encapsulated in the vesicles.

Finally, a simple prototype dressing was constructed. Plasma polymerised maleic anhydride (pp-MA) deposited onto non-woven polypropylene was shown to be a good method to stabilise vesicles via covalent bonding. Vesicle adhered to pp-MA non-woven polypropylene showed the ability to inhibit/kill the pathogenic strains, quantified by the Japanese Industry Standard assay and also gave a fluorimetric colour response in the presence of pathogenic bacteria when a fluorescent dye is encapsulated within vesicles. Other simple prototypes were also attempted by using hydrogels (gelatine and collagen) to maintain vesicle stability as well as promote tissue healing.

Acknowledgements

"*I am digging my way to something,*
To something better"
- James Hetfield -

Studying abroad for PhD degree is certainly never easy at the beginning and especially in a country with different culture and language. Now, looking back from the end of this journey, I am surprised to find that what I have gained is not just professional knowledge but also a wonderful adventure in my life. By this time, I would like to acknowledge the contributions of the following groups and individuals to the development of this thesis.

First of all, I would like to give my sincere thanks to my supervisor Dr. Toby Jenkins for his kind guidance over the course of my research. Especially, he directed me to a wide range of new avenues such as plasma and answered all of my questions as well as asked me questions that helped me to narrow my research. Without him, I will not make such good progress so fast.

Secondly, I am indebted to many people for their contributions into my current project work. I am thankful to Dr. Xavier Muñoz-Berbel and Dr. Geraldine Mulley for their kind guidance about microbiology. Although they have left our group, without them, I will not make such good progress so fast. I also would like to thank my colleagues in Jenkins' group: Dr. Neil Poulter, Dr. June June D. Mercer-Chalmers, Dr. Thet Naing Tun, Andrew Loftus, Charlotte James, Maisem Laabei, David Jamieson, Sung-ha Hong, Jessica Bean, Serena Marshall, and all the other members of EMBEK project.
Thirdly, I would like to thank all of my dear friends for their help and support, who constitute my memorable experience in UK.

The financial aid I received from EMBEK1 project is also appreciated

Last, but most importantly, I would like to give my deepest thanks to my parents, Lizhong Zhou, Xinlian Xia and Xiaojun Wen, it was their boundless love and supports that made me never be devastated by any difficulties. I hope I have not disappointed you.

Table of Contents

Abstract iii
Acknowledgements iv
Table of Contents vi
List of figures xii
List of tables xvi
Acronyms and Abbreviations xvii
List of Symbols xxi

Chapter 1 Introduction 1
1.1 Burn Wound Infection 1
1.1.1 Burn Injuries of Paediatrics 1
1.1.2 Classification of Burn Wound Infection 2
1.1.3 Clinical Management of Burn Wound Infection 3
1.2 Bacteria 5
1.2.1 Classification of Bacteria 6
1.2.2 Bacterial Cell Wall Structure 7
1.2.3 Pathogenic Bacteria 8
1.2.4 Pathogenic Toxins 9
1.2.4.1 Endotoxins 10
1.2.4.2 Exotoxins 11
1.2.4.3 Pore Forming Toxins (PFTs) 12
1.2.4.4 Exoenzymes 13
1.2.4.5 Superantigens 13
1.2.5 Mode of Action of Bacterial Toxins 14
1.2.5.1 Transmembrane Pore Formation 14
1.2.5.2 Lipid Damaging 16
1.2.5.3 Inhibition of Protein Synthesis 18
1.2.5.4 Activation of Secondary Messenger Pathways 19
1.2.5.5 Inhibition of the Release of Neurotransmitters 20
1.2.6 Biofilms 20
1.2.6.1 Biofilm Formation 20
1.2.6.2 Antimicrobial Resistance of Biofilms 22
1.2.6.3 Biofilm Related Infectious Diseases 23
1.3 Pathogenesis of Burn Wound Infection 23
1.4 Antimicrobial Agents Used for the Treatment of Burn Wound Infection 26
1.4.1 Introduction to Antimirobials 26
1.4.2 Topical Antimicrobial Agents 27
1.4.2.1 Silver Products 27
1.4.2.2 Mafenide Acetate 28
1.4.2.3 Nitrofurazone 29
1.4.2.4 Povidone-Iodine 29

1.4.2.5 Gentamicin Sulfate....29
1.4.2.6 Silver Nitrate Solution (0.5%) 30
1.4.2.7 Chlorhexidine....31
1.5 Biomembranes 31
1.5 .1 Basics of Lipid and Cell Membrane Structures 31
1.5.1.1 Glycerophospholipids 32
1.5.1.2 Membrane Fluidity....34
1.5.1.3 Cholesterol 35
1.5.2 Description of the Background for Lipid Vesicles....35
1.5.3 Introduction to Polydiacetylene Vesicles 37
1.5.3.1 Polydiacetylene Vesicles 37
1.5.3.2 Mixed Lipid/PDA Liposomes 39
1.6 Application of Liposomes --- As Drug Carriers 40
1.6.1 Lipid Vesicles/Liposomes 40
1.6.2 Polydiacetylene Vesicles as Drug Carriers 41
1.7 Problem Statement & Aims 42
1.8 References....45
Chapter 2 Instrumentation and Theory 59
2.1 Fundamentals of Plasma Polymerisation and Surface Modification 59
2.1.1 Main Sources of Gas Discharge Plasmas....59
2.1.2 The Plasma Polymerisation Mechanism....60
2.1.3 Plasma Reactor....63
2.2 Fluorescence 64
2.2.1 Principles of Fluorescence 64
2.2.2 Fluorescence Quenching....68
2.3 Instrumentation for Characterisation and Visualisation of Vesicles 69
2.3.1 Fourier-transform Infra-red Spectroscopy 69
2.3.2 Fluorescent tagging....70
2.3.2.1 Fluorescence Spectroscopy....70
2.3.2.2 Fluorescence Microscopy 71
2.3.3 Scanning Electron Microscopy (SEM) 72
2.3.4 UV-Vis Spectroscopy....74
2.4 Microbiology....74
2.4.1 Bacteria Used in the Work 75
2.4.1.1 *Pseudomonas aeruginosa* 75
2.4.1.2 *Staphylococcus aureus* 77
2.4.1.3 *Escherichia coli* 78
2.4.2 Methodology of Detection for Bacteria 79
2.4.2.1 Basics of Bacterial Growth 79
2.4.2.2 Colony Counting....81
2.4.2.3 Solution Turbidity 82
2.4.2.4 Optical Density-CFU Relationship of Bacteria 83
2.4.3 Sterilisation 83
2.4.4 Antimicrobial Evaluation Assays....84

2.4.4.1 Solution Assays 84
2.4.4.2 Surface Assays ---JIS 84
2.4.4.3 Minimum Inhibitory Concentration Assays 85
2.5 Estimation of Minimum Encapsulation Volume 85
2.5.1 Structure and Organisation of Lipid Bilayer 85
2.5.2 GUVs 87
2.5.3 Polydiacetylene Vesicles 88
2.6 References: 90
Chapter 3 Experimental Methods 95
3.1 Material Science 95
3.1.1 Synthesis and Purification of Giant Unilamellar Vesicles 95
3.1.1.1 Formation of GUVs 95
3.1.1.2 Purification of Giant Unilamellar Vesicles (GUVs) 97
3.1.2 Synthesis and Purification of Polydiacetylene/Phospholipid Vesicles 98
3.1.2.1 Preparation of Stock Lipid Solution (SLS) 98
3.1.2.2 Compositions of Phospholipid/PDA Vesicles 99
3.1.2.3 Synthesis of Polydiacetylene/Phospholipid vesicles 99
3.1.2.4 Polymerisation 101
3.1.2.5 Purification of Phospholipid/PDA Vesicles 103
3.2 Physical Science 103
3.2.1 Characterisation of Chromatic Property for Phospholipid/TCDA vesicles 103
3.2.2 Colorimetric Detection of Bacteria-Vesicle Interactions 104
3.2.3 Carboxyfluorescein Fluorescence – Concentration Analysis 104
3.2.4 Carboxyfluorescein Photobleach Analysis 105
3.2.5 Stability Study of Phospholipid/PDA Vesicles–Dehydration & Rehydration Assay 105
3.2.6 Sensitivity Study of Phospholipid/PDA Vesicles to Lytic Agents 106
3.2.7 Plasma Polymerisation 107
3.3 Microbiological Assays 107
3.3.1 Bacterial Culture 108
3.3.2 MIC Assays 108
3.3.3 Antimicrobial Analysis 109
3.3.3.1 Colony Counting 109
3.3.3.2 Solution Turbidity Assay 110
3.3.3.3 JIS Assays –Antimicrobial Test on Modified Surface 110
3.3.4 Fluorescence Response Assay ---Pathogenicity Assay in Suspension. 111
3.4 Attachment of Vesicles to Treated Fabrics 111
3.4.1 Pulse Plasma Polymerisation 112
3.4.1.1 Pathogenicity Assay on pp-MA Treated Fabrics 112
3.4.2 Surface Photografting of Poly (acrylic acid) on Non-woven Polypropylene 112
3.4.2.1 Pathogenicity Assay on UV-Induced PAA Grafed Non-woven Polypropylene 113

3.4.3 Gelatine 113
3.4.4 Collagen Grafted pp-MA Non-woven Polypropylene 114
3.4.4.1 Pathogenicity Assay on Collagen Grafted pp-MA Non-woven Polypropylene 114
3.5 Visualisation of Vesicles 115
3.5.1 Visualisation of GUVs with bacteria by Using Fluorescent Microscopy 115
3.5.2 Visualisation of Phospholipid/PDA Vesicles on pp-MA Treated Fabrics by Scanning Electron Microscopy 115
3.6 References: 115
Chapter 4 Giant Unilamellar Vesicles as Response System for Killing/Inhibiting Growth of Pathogenic Bacteria 116
4.1 Formation and Purification of GUVs 117
4.1.1 Materials 117
4.1.1.1 DMPC 117
4.1.1.2 DMPE 118
4.1.1.3 Cholesterol 118
4.1.1.4 Temperature Effect on Lipid Membranes 119
4.1.2 Mechanism of GUVs Formation 121
4.1.3 Purification of GUVs 122
4.2 Surface Design – Pulsed Plasma Deposited Maleic Anhydride Thin Films as Supports for Vesicles 125
4.2.1 Chemical Structural Characterisation for Plasma Polymerised Maleic Anhydride 126
4.2.2 Chemical Characterisation for Vesicles Attachment to pp-MA Non-woven Polypropylene 127
4.3 Antimicrobial Activity Measurement of GUVs 128
4.3.1 Antimicrobials Studied in this Work for killing Bacteria 128
4.3.1.1 Sodium Azide 128
4.3.1.2 Gentamicin Sulfate 129
4.3.2 Pathogens Studied in This Work 129
4.3.2.1 *In-Vitro* Haemolysis Test 129
4.3.3 Determination of Bacterial Susceptibility 130
4.3.3.1 Minimum Inhibitory Concentration (MIC_{50}) 130
4.3.3.2 Minimum Encapsulation Concentration 133
4.3.4 Solution Assay 134
4.3.4.1 Time Resolved Bacterial Killing by Sodium Azide Vesicles 134
4.3.4.2 Time Resolved Bacterial Killing by Gentamicin Sulfate Vesicles 136
4.3.5 Fabric Assay Japanse Industry Standard (JIS) 138
4.4 Visualisation of Vesicle Lysis by Bacteria under Fluorescence Microscopy. 140
4.5 Conclusion 142
4.6 References 145
Chapter 5 Study of Partially Polymerised Polydiacetylene/Phospholipid Vesicles Based

Upon Construction of a Fluorescence Sensing System 146
5.1 Formation and Purification of TCDA/phospholipid Vesicles 147
5.1.1 Materials 147
5.1.1.1 TCDA 147
5.1.1.2 Structure and Phase Separation 148
5.1.1.3 Temperature Effect of TCDA on Mixed Vesicle System 149
5.1.2 Vesicle Formation and Polymerisability 150
5.1.3 Purification of Phospholipid/TCDA Vesicles 151
5.2 Study of Colorimetric Property of Polydiacetylene/Phospholipid Vesicles 151
5.2.1 UV-Vis Spectra of Vesicles Depending upon the Molar Ratios of Lipid-PDA 151
5.2.2 Thermochromic Property of Phospholipid/PDA Vesicles 153
5.2.3 Colorimetric Detection of Bacteria-Vesicle Interactions 155
5.3 Fluorescence Sensing System 156
5.3.1 Preparatory Work 157
5.3.2 Carboxyfluorescein Fluorescence – Concentration Analysis 158
5.3.3 Calculation of Fluorescence Release from Vesicles After Total Lysis 159
5.3.4 Carboxyfluorescein Fluorescence – Photobleach Analysis by UV Irradiation 159
5.4 Study of Vesicle Stability and Sensitivity 160
5.4.1 Alpha-Haemolysin (α-HL) and Phospholipase A_2 (PLA_2) 160
5.4.2 Stability Study 160
5.4.3 Sensitivity Study 162
5.4.4 Summary 163
5.5 Pathogenicity Assay in Suspension 164
5.6 Conclusion 166
5.7 References: 168
Chapter 6 Construction of a Prototype for Stabilising Vesicles and Assisting Wound Healing 170
6.1 Construction of Wound Dressing 170
6.2 Pulsed Plasma Deposited Maleic Anhydride Thin Films as Supports for Vesicles 172
6.2.1 FT-IR for Surface Characterisation 172
6.2.2 SEM for Analysis of Vesicle Modified Surface 173
6.2.3 Attachment of Vesicles to Fabric and Stability /Response Testing 175
6.3 Graft Polymerisation of Poly(acrylic acid) onto Non-woven Polypropylene 178
6.4 A Simple Prototype Construction 183
6.4.1 Gelatine as Supports for Stabilising Vesicles 183
6.4.2 Plasma Polymerised Maleic Anhydride Deposited onto Non-woven Polypropylene and Following Subsequent Grafting of Collagen onto Polymer Films 185
6.4.2.1 Stability Study of Collagen Grafted pp-MA Non-woven Polypropylene 185
6.4.2.2 Pathogenicity Assay on Collagen Grafted pp-MA Non-woven

Polypropylene 188
6.5 Conclusion 189
6.6 References 191
Chapter 7 Development of Antimicrobial Property for Phospholipid/PDA Vesicles . 192
7.1 Silver Nitrate 192
7.1.1 Determination of Bacterial Susceptibility (MIC_{50}) 193
7.1.2 Minimum Encapsulation Concentration 195
7.1.3 Antimicrobial Activity of Vesicles Containing $AgNO_3$ in Suspension 196
7.1.4 Antimicrobial Activity on Vesicle Modified Fabrics ---JIS 199
7.2 Gentamicin Sulfate 201
7.2.1 Determination of Bacterial Susceptibility (MIC_{50}) 202
7.2.2 Minimum Encapsulation Concentration 202
7.2.3 Antimicrobial Activity of Vesicles Containing Gentamicin Sulphate in Suspension 202
7.2.4 Antimicrobial Activity on Vesicle Modified Fabrics ---JIS 205
7.3 Chlorhexidine 207
7.3.1 Determination of Bacterial Susceptibility (MIC_{50}) 207
7.3.2 Minimum Encapsulation Concentration 210
7.3.3 Antimicrobial Activity of Vesicles Containing Chlorhexidine in Suspension 210
7.4 Conclusion 212
Chapter 8 Conclusions 215
8.1 Summary of Results 215
8.2 Future Research Areas 219
8.2.1 Stability 219
8.2.2 Encapsulating Agents 220
8.2.3 Bacteria Related to Wound Infection 221
8.2.4 Prototype Construction 222
8.3 References 224
Appendix A Detailed Operations of Plasma Reactor 225
Appendix B Original Publications 226

List of Figures

Figure 1.1: A paediatric patient with partial thickness scald injury was cured by Biobrane. 4
Figure 1.2: Construction of the cell walls of Gram-negative and Gram-positive bacterial cell walls. 8
Figure 1.3: Schematic of array of membrane bound bacterial cell and secretion of proteins/toxins that pathogenic bacteria can deploy against healthy tissue. 10
Figure 1.4: Ribbon diagram of the α-haemolysin of *S. aureus.* 16
Figure 1.5: Cleavage sites of different phospholipases (shown with red dashed line) ... 18
Figure 1.6: Stages of biofilm formation with corresponding photomicrographs. 21
Figure 1.7: Basic construction of a typical eukaryotic cell membrane. 32
Figure 1.8: Lipid bilayer containing hydrophilic head and hydrophobic tail. 34
Figure 1.9: Structure of liquid-crystal phase of lipid bilayer 35
Figure 1.10: Basic structure of lipid vesicles with hydrophilic head and hydrophobic tail. 36
Figure 1.11: Schematic of polydiacetylene vesicle formation. 38
Figure 1.12: Diacetylene structures 39
Figure 1.13: Structure of mixed lipid/PDA vesicle. 40
Figure1.14: Schematic of responsive antimicrobial system showing an immobilised vesicle with encapsulated antimicrobial/fluorescent dyes. 44
Figure 2.1: Overall plasma polymerisation mechanism showing a bi-cyclic step-growth. 62
Figure 2.2: Home-made plasma reactor 62
Figure 2.3: Diagram of a plasma reactor. 63
Figure 2.4: Excitation and relaxation of molecules due to absorption and emission of light. 65
Figure 2.5: Spectra of Stokes' shift. 66
Figure 2.6: FLUOstar Omega microplate reader 71
Figure 2.7: Schematic of fluorescence microscope 72
Figure 2.8: Schematic diagram of a SEM; 73
Figure 2.9: *P. aeruginosa* colonies on an agar plate and its micrograph in SEM. 76
Figure 2.10: Micrograph of *S.aureus* in SEM and wound infection caused by MRSA.. 78
Figure 2.11: False colour SEM (×22,000) of hemorrhagic *E. coli* O256:H7 79
Figure 2.12: Foure stages of bacterial growth. 81
Figure 2.13: *S.aureus* (MSSA 476) colonies on an agar plate grown from individual cells 82
Figure 2.14: UV-vis measurement to determine the optical density of bacterial culture 82
Figure 2.15: Optical density of *S. aureus* (MSSA 476) against the number of CFU mL^{-1} 83
Figure 2.16: A typical lipid bilayer with several chemical regions. 86
Figure 2.17: Simplified vesicles with estimation of inner and outer diameter. 87

Figure 3.1: Details of polymerisation of polydiacetylene/phospholipid vesicle induced by UV irradiation and experimental setup in the A.T.A.Jenkins group. ..102
Figure 3.2: Representation of the positions that vesicles were placed.....114
Figure 4.1: Chemical structure of DMPC. 117
Figure 4.2: Chemical structure of DMPE. 118
Figure 4.3: Chemical structure of cholesterol and interaction of cholesterol and lipid bilayers. 119
Figure 4.4: Diagram of the suggested mechanism of GUVs formation. 122
Figure 4.5: Typical traces of NAP-10 column used on 5(6)-carboxyfluorescein containing vesicles. 123
Figure 4.6: Fluorescence intensity change of eluent using NAP-25 column.....124
Figure 4.7: Visual images of eluate from NAP-25 column. 124
Figure 4.8: Chain growth of a polymer growth during the pulsed off period of PPP...125
Figure 4.9: Schematic diagram & simplified reaction showing GUVs attached to pp-MA treated non-woven polypropylene via amide bond. 126
Figure 4.10: FT-IR spectra of pulsed plasma-polymerised maleic anhydride. 127
Figure 4.11: FTIR data for vesicles attachment onto treated non-woven polypropylene. 128
Figure 4.12: Blood agar plate showing the lysis of haemoglobin around colonies of typical pathogenic bacteria 130
Figure 4.13: MIC_{50} of sodium azide and gentamicin sulfate against the three strains of bacteria. 132
Figure 4.14: Reduction in the number of viable bacteria (CFU mL^{-1}) following exposure to vesicles containing sodium azide in aqueous suspension, over a 4 h period. 135
Figure 4.15: Time-course of viable number of pathogenic and non-pathogenic bacteria with GUVs containing gentamicin sulfate. 137
Figure 4.16: JIS results of lipid vesicles (containing sodium azide) against three strains of bacteria.....140
Figure 4.17: Fluorescence imaging of surface attached vesicles exposed to the three strains of bacteria. 142
Figure 5.1: Chemical structure and polymerisation of 10, 12 - tricosadiynoic acid. 148
Figure 5.2: Organisation of phospholipid/TCDA vesicles and their colorimetric sensing. 149
Figure 5.3: SEM image of phoshpolipid/TCDA vesicles composed of 10 mol% TCDA, 20 mol% cholesterol, 2 mol% DMPE and 68 mol% DMPC. 150
Figure 5.4: Colorimetric properties of phospholipid/TCDA vesicles after UV irradiation. 152
Figure 5.5: The transition of backbone structures of polydiacetylene from planar to nonplanar.....153
Figure 5.6: Graph of colorimetric response (CR) calculated from the visible absorption spectra of DMPC/DMPE/ 40 mol % TCDA and DMPC/DMPE/Cholesterol/40 mol % TCDA as a function of the solution temperature. 155

Figure 5.7: UV-Vis absorption spectra showing colour transitions of vesicles (DMPC/DMPE/Cholesterol/ 40 mol % TCDA) induced by three strains of bacteria. 156
Figure 5.8: Chemical structure of 5(6)-carboxyfluorescein and images of the system in its pre-lysis (on left of frame) and post lysis (on right of frame) forms by Triton. 157
Figure 5.9: Graph showing self-quenching behaviour depending upon varying concentrations. 158
Figure 5.10: Graph showing study of vesicle stability 161
Figure 5.11: Graphs of vesicle sensitivity to lytic agents. 163
Figure 5.12: Time course of the kinetics of the interaction of bacteria with phospholipid/TCDA vesicles. 165
Figure 5.13: Similar graphs showing fluorescence release from vesicles (30 mol % TCDA/lipid vesicles) as bacteria grow in different media. 166
Figure 6.1: Schematic representation of the hydrogel-vesicle modified fabric-hydrogel construction. 171
Figure 6.2: FT-IR data showing vesicles attachment onto treated non-woven polypropylene. 173
Figure 6.3: SEM images, recorded with JEM-6480LV scanning electron microscope 174
Figure 6.4: SEM images of vesicles on non-woven polypropylene deposited with plasma polymerised maleic anhydride, recorded with JEM-6480LV scanning electron microscope. 175
Figure 6.5: Polypropylene modified with vesicles containing initially self-quenched carboxyfluorescein (left-hand swatch) and switching on of fluorescence of dye following either vesicle destruction following part drying or direct lysis by Triton, as a function of mol % TCDA 176
Figure 6.6: Fluorescent images of vesicles in 96-well plate. 177
Figure 6.7: A crude 'proof of principle' prototype: response of modified fabric following overnight growth of bacteria on polypropylene fabric with 30 mol% TCDA vesicles. 178
Figure 6.8: Schematic representation of UV-induced graft polymerisation of poly (acrylic acid) on non-woven polypropylene. 180
Figure 6.9: Images of photo-grafting polymerisation of PAA on non-woven polypropylene in the central area with a diameter of 1 cm and fluorescence response induced by toxins secreted by pathogenic bacteria (PAO1 and MSSA 476) after 4h and overnight. 182
Figure 6.10: Schematic of simple prototype in single vial of 96-well plate, phospholipid/PDA vesicles (30 mol% TCDA) containing self-quenched carboxyfluorescein sandwiched between two hydrolysed gelatine sheets. 184
Figure 6.11: Graph showing stability test of phospholipids/PDA vesicles (30 mol% TCDA) in gelatine sheets for 25 days and significant fluorescence increase after lysis by Triton. 185
Figure 6.12: Schematic diagram of prototype construction: pp-MA modified non-woven

polypropylene was dip coated in collagen solution, with vesicles containing self-quenched carboxyfluorescein following attached onto collagen grafted pp-MA surface.....186
Figure 6.13: Graph showing stability test of phospholipids/PDA vesicles (30 mol% TCDA) sandwiched in collagen grafted pp-MA non-woven polypropylene for 25 days and significant fluorescence increase after lysis by Triton. ..187
Figure 6.14: Graph showing stability test of phospholipids/PDA vesicles sandwiched in collagen grafted pp-MA non-woven polypropylene at 37 ^{o}C and fluorescence increase after lysis by Triton.....188
Figure 6.15: Simple prototype dressings: fluorescence response of modified fabric following overnight growth of bacteria on polypropylene fabric with 30 mol % TCDA vesicles.....189
Figure 7.1: MIC_{50} of silver nitrate to the three strains of bacteria. The shapes of bacterial optical density-antimicrobials graphs give a clue that at which concentration of bacteria starts to respond to $AgNO_3$ and at which concentration of bacteria would be completely inhibited by the antimicrobial. Error bars represent standard deviations based on three measurements of each sample.....194
Figure 7.2: Time course of viable numbers of pathogenic and non-pathogenic bacteria incubated with phospholipid/PDA vesicles containing $AgNO_3$. 198
Figure 7.3: JIS result of TCDA vesicle (containing $AgNO_3$) bound to pp-MA nonwoven polypropylene against three strains of bacteria.....201
Figure 7.4: Time course of viable numbers of pathogenic and non-pathogenic bacteria incubated with phospholipid/PDA vesicles containing gentamicin sulphate. 205
Figure 7.5: MIC results of TCDA vesicle (containing gentamicin sulphate) bound to pp-MA nonwoven polypropylene against three strains of bacteria. 206
Figure 7.6: MIC_{50} of chlorhexidine versus the three strains of bacteria. Error bars represent standard deviations based on three measurements of each experiment.....209
Figure 7.7: Overnight growth of pathogenic and non-pathogenic bacteria incubated with phospholipid/PDA vesicles containing chlorhexidine. 211
Figure 8.1: Bilayer arrangements before/after UV irradiation in phospholipid/TCDA vesicles.....220
Figure 8.2: A proposed 'smart' wound dressing. 223

List of Tables

Table 1.1: Lists of microorganisms responsible for causing burn wound infection [a] 24
Table 1.2: Classes of antimicrobials and their mechanisms of action to the host [137] 26
Table 3.1: Encapsulated agents used in this work and the concentration prepared in different buffer systems 96
Table 3.2: Eluent buffer systems for different encapsulating compounds 97
Table 3.3: Description of two types of columns used in the purification of vesicles including the parameters for sample and eluent volumes 98
Table 3.4: Vesicle stock solutions 99
Table 3.5: Constituents of 20,30,40,50,60 mol % TCDA vesicles 99
Table 3.6: Compositions of aqueous bulk solution for encapsulation, solvent is distilled water 99
Table 3.7: Composition of aqueous bulk solution system for 5(6)-carboxyfluorescein (50mM) in 50mL 100
Table 3.8: Eluent buffer (pH 7.4) for 50mM 5(6)-carboxyfluorescein (50 mL) 103
Table 3.9: HEPES buffer system for 95mM carboxyfluorescein 104
Table 3.10: List of lytic agents for their ability to lyse vesicle membrane and hence release the contents 106
Table 4.1: Phase transition temperature with different tail length and number of double bonds[2] 120
Table 4.2: Range finding test of NaN_3 against three strains of bacteria (where '+' is positive growth and '-' indicates no growth.) 131
Table 4.3: Range finding test of gentamicin sulphate against three strains of bacteria (where '+' is positive growth and '-' indicates no growth) 131
Table 4.4: MICs determined for sodium azide and gentamicin sulfate versus three strains of bacteria 133
Table 5.1: Fluorescence intensity of three difference concentrations of 5(6)-carboxyfluorescein before and after irradiation; hard UV was used to irradiate for 5 minutes. 160
Table 7.1: Range finding test of $AgNO_3$ against three strains of bacteria (where '+' is positive growth and '-' indicated no growth) 193
Table 7.2: Summary of MIC_{50} of $AgNO_3$ versus three bacterial strains 194
Table 7.3: Summary of MIC_{50} of gentamicin sulphate versus three bacterial strains 202
Table 7.4: Range finding results for chlorhexidine agains three strains of bacteria (where '+' is positive growth and '-' indicated no growth) 208
Table 7.5: Lists of MIC_{50} of three strains of bacteria 209

Acronyms and Abbreviations

Ag-SD	Silver sulfadiazine
ADP	Adenosine diphosphate
AHL	*N*-acyl homoserine lactone
BSE	Back-scattered electrons
BP	Benzophenone
Ctx	Cholera enterotoxin
CBTs	Cholesterol binding toxins
CPE	*C. perfringens* enterotoxins
C. perfringens	*Clostridium perfringens*
CNFs	Cytotoxic necrotizing factors
c AMP	Cyclic adenosine monophosphate
CNS	Central nervous system (CNS)
CW	Continuous wave
Da	Dalton (atomic mass unit)
Dtx	Diphtheria toxin
DNA	Deoxyribonucleic Acid
DT	Diphtheria toxin
DMPC	1,2-Dimyristoyl-sn-Glycero-3-Phosphocholine
DMPE	Dimyristoyl-sn-Glycero-3-phosphoethanolamine
DPPC	1,2-dipalmitoyl-*sn*-glycero-3-phosphocholine
DSPC	1,2-dioctadecanoyl-*sn*-glycero-3-phosphocholine
DC	Direct current
E. coli	*Escherichia coli*
E. coli DH5α	*Escherichia coli* DH5α
EF2	Elongation factor-2
ExoA	*Pseudomonas* exotoxin A
ER	Endoplasmic reticulum
EPS	Extracellular polymeric substance
ESBLs	Extended-spectrum beta-lactamases
EDTA	Ethylenediaminetetraacetic acid
F	Fluorescence

FT-IR	Fourier-transform infra-red spectroscopy
G-proteins	Guanine nucleotide-binding proteins
GUV	Giant unilamellar vesicle
HlyA	α-Haemolysin
HEPES	4-(2-hydroxyethyl)-1-piperazineethanesulfonic acid
IC	Internal conversion
ISC	Inter system crossing
LPS	Lipopolysaccharides
LPC	Lysophosphatidylcholine
LPI	Lysophosphatidylinositol
LUV	Large unilamellar vesicles
LB	Lysogeny broth
MRSA	Methicillin resistant *Staphylococcus aureus*
MHC	Major histocompatibility molecules
MLV	Multilamellar vesicles
MDROs	Multi-drug resistant organisms
NAD	Nicotinamide adenine dinucleotide
OD	Optical density
P. aeruginosa	*Pseudomonas aeruginosa*
P. aeruginosa PAO1	*Pseudomonas aeruginosa* PAO1
PFTs	Pore forming toxins
PLs	Phospholipases
α-PFTs	α-Pore forming toxins
β- PFTs	β-Pore forming toxins
PNS	Peripheral nervous system
PC	Phosphatidylcholine
PI	Phosphatidylinositol
PE	Phosphatidylethanolamine
PS	Phosphatidylserine
PG	Phosphatidyglycerol
PLA_1	Phospholipase A1
PLA_2	Phospholipase A2
PLB	Phospholipase B
PLC	Phospholipase C

PLD	Phospholipase D
PVP-I	Povidone-iodine (PVP-I)
PDA	Polydiacetylene
PPP	Pulse plasma polymerisation
PAA	Poly acrylic acid
P	Phosphorescence
PBS	Phosphate saline buffer
QCAs	Quaternary ammonium cations (QCAs)
RME	Receptor-mediated endocytosis
Rho G-proteins	Rho guanine nucleotide binding proteins
RF	Radio frequency
S	Ground state
S_0, S_1	Electronic state
S. aureus	*Staphylococcus aureus*
S.aureus MSSA 476	Methicillin susceptible *Staphylococcus aureus*
SLO	Streptolysin O
sn	Stereospecific numbering
sn-1	Stereospecific numbering-1
sn-2	Stereospecific numbering-2
ST	Shiga toxin
SSD	Silver sulphadiazine
SUV	Small unilamellar vesicles
SEM	Scanning electron microscopy
SLS	Stock lipid solution
T	Triplet state
T_1	Lowest triplet state
Tris	Tris(hydroxymethyl)aminomethane
TSS	Toxic shock syndrome
TSST-1	Toxic shock syndrome exotoxin-1
TSB	Tryptic soya broth
RNA	Ribonucleic acid
t- RNA	Transfer ribonucleic acid
TCDA	10, 12- tricosadiynoic acid
T*m*	Phase transition temperature

UV	Ultraviolet
VT	Verotoxin
VR	Vibrational relaxation

List of Symbols

A	absorbance
c	sample concentration
CR	colorimetric response
ε	molar absorptivity or extinction coefficient
I_0	fluorescence intensity of unquenched fluorophore
I	fluorescence intensity of quenched fluorophore
I_0	intensity of incident light
I	transmitted intensity
κ_0	rate constant
κ_F	rate of fluorescence
κ_Q	rate of quenching
κ_{ET}	rate of energy transfer
κ_{ISC}	rate of intersystem crossing
κ_{IC}	rate of internal conversion
κ_D	Stern-Volmer quenching constant
κ_Q	bimolecular quenching constant
κ_S	association constant for the fluorophore-quencher complex
L	length of light path through the sample
P_s	start pressure
P_f	final pressure
PB_0	value of control sample
PB	value of the vesicle solution after colour change
[Q]	concentration of quencher
Q	quantum yield
r	radius
R	gas constant
Δt	time
T	temperature
τ	fluorescence lifetime
τ_0	unquenched lifetime

V	volume
χ	flow rate

Chapter 1 Introduction

Burns are one of the most common and devastating forms of trauma. Patients with thermal injury require immediate care to minimise morbidity and mortality. Once burn injury occurs, bacteria rapidly colonise open skin wounds. Specialized antimicrobials and wound dressings are needed for the treatment of burn wounds. The work described in this thesis aims to create an advanced wound dressing technology which can detect and respond to the presence of pathogenic bacteria and release antimicrobials only when required. Such a responsive system is based on the use of phospholipid and partially polymerised vesicles which provide the cell membrane mimic. This introductory chapter covers the background and literature review of related knowledge and, further, addresses the open research challenges that have constituted the key motivations for the present Ph.D. work.

1.1 Burn Wound Infection

1.1.1 Burn Injuries of Paediatrics

Burns have been recognised as the most painful and devastating injuries. Burn injuries range from the most severe requiring high levels of intensive care and multiple surgeries, to the most trivial, for which self-treatment may be sufficient. Almost all of us will experience a burn injury in our lifetime.

Children under age 4 are at particular risk of infection, with an injury death rate more than two times that of children aged 5 to 14.[1-2] This is because children, especially those who aged 4 and under, may not perceive danger, have less control of their environment, may lack the ability to escape a life-threatening burn situation and may not be able to tolerate the physical stress of a burn injury. One of the most severe infections after burn injury in children with a high mortality is Toxic Shock Syndrome (TSS).[3] TSS is caused by exotoxins commonly produced by *Staphylococcus aureus*. The exotoxin responsible for causing TSS is TSS toxin-1 (TSST-1). Children of age less than 4 normally have low

levels of anti-TSST-1 antibodies, which will render them more susceptible to bacterial infection. Therefore, children of this age range are more susceptible to a scald injury.[3]

1.1.2 Classification of Burn Wound Infection

The majority of burn injuries only affect the epidermis such as sun burn. However, burns can be much more serious and can result in death. Burn wound infections were previously classified by changes in the burn wound and eschar appearance, time of occurrence, and associated mortality into distinct conditions, including impetigo, cellulitis, and invasive infection.[4] The old classification system has now been replaced by a system based on surgical wound infection at the excision sites.[5]

A first-degree burn is considered a superficial wound which does not blister and only affects the outer surface of the skin (epidermis). To manage a first-degree burn or even a minor second-degree burn, the wound is kept moist to reduce topical discomfort and pruritus.

Second-degree burns are partial-thickness burns which can be characterised as superficial or deep. The epidermis is the primarily involved element in superficial partial-thickness burns. Normally, blisters form and the overlying skin sloughs. Healing usually occurs in about 14 days. In comparison, a deep partial-thickness burn may have a dark red or white base, because the wound injures the dermis and associated nerve structures. The healing time will take longer than 14 days. Surgery may be required to secondarily treat hypertrophic scarring and late sequelae.

Burns which result in total destruction of both layers of the skin are termed third-degree burns or full-thickness burns. Because the skin and the surrounding tissues are destroyed, the healing process is slower than in more superficial burn injuries. Third degree burns which cover smaller areas are treated in a similar way as partial thickness burns with regards to the types of dressings used, however larger third degree burns often need a skin-graft to heal.[6]

1.1.3 Clinical Management of Burn Wound Infection

Restoration of a wound after injury is a natural phenomenon, and the resulting wound is the source of complication, and the patient remains at risk unless it is healed. Clinical management aims to close a burn wound infected by pathogens as soon as possible and minimise the chance of complication once burn wound infection occurs. Bacteria are able to infect and colonise open layers of dermis and proliferate with the loss of skin barrier. Toxic factors will then be secreted by pathogenic bacteria which cause tissue damage and deeper penetration of the tissue once bacteria have colonised on the wound. In addition, bacterial attachment and colonisation are able to form complex communities (biofilms) with altered phenotypes resulting in increased resistance to antimicrobial agents and the host's immune systems. This tissue damage will prevent the wound from healing properly and even cause other complications such as toxic shock syndrome (TSS) which would give rise to the biggest challenge to wound-care product researchers. Also there are many factors which affect wound healing, such as infections, quality of healing, speed of healing, fluid loss and other complications. All of these detailed above would increase the healing time and will become a major clinical challenge.[7]

Clinical management for burn wound infection is dependent on the degree of infection. Established treatment for deep partial and full thickness burns involves early excision of necrotized tissue, skin grafting and dressing. This closes the wound immediately and prevents bacterial inoculation and bacteria which are present in the wound area before grafting may form biofilms and prevent the graft adhering. Antimicrobial dressings are also necessary in the treatment of full thickness and deep partial thickness injuries to prevent bacterial infection. The use of temporary skin substitutes such as Biobrane ™ and Transcyte ™ have been widely used in the treatment of superficial and partial burn injury. Currently, various biological, biosynthetic and synthetic wound dressings are used in burn care. Selection and use of these products depends on the condition of the wound bed, the inherent properties of the dressing and the goals of therapy.[8] Various considerations should be taken into account [9] when selecting an ideal wound dressing,

for example, protecting the wound from physical damage and micro-organisms, being comfortable, compliant and durable, non-toxic, non-adherent, and non-irritant, allowing gaseous exchange and high humidity at the wound, being compatible with topical therapeutic agents, being able to allow maximum activity for the wound to heal without retarding or inhibiting any stage of the process.

Biological dressings are designed to promote epitheliation and have improved healing in partial thickness scalds in children which result in the shorter lengths of stay and a reduced need for skin grafting.[3] Biobrane is currently most commonly used for the treatment of superficial burn injuries. Biobrane consists of a silicone layer and nylon fabric which has collagen bonded to it. Collagen, which is a naturally occurring protein in anmimals and is a main component in connective tissues, is often used in food and medical applications such as burns surgery and cosmetic surgery. It often put on a burn wound site and sticks to the wound and stays there until the wound is healed. This provides an ideal environment for promoting tissue healing. Figure 1.1 shows before and after medical photography of a paediatric patient who presented with partial thickness burns and was treated with biobrane.

Figure 1.1: A paediatric patient with partial thickness scald injury was cured by Biobrane.
Left: the patient with scald injury was treated with biobrane; right: the patient made a full recovery with no scarring after treatment (Frenchay hospital).

However, dressings designed to encourage cell growth also assist microbial growth. Dressings such as Acticoat ™ contain silver to inhibit microbial growth. Acticoat ™ has

a more controlled and prolonged release of nanocrystalline silver to the wound area. This mode of silver delivery allows the dressings to be changed with less frequency to reduce risk of nosocomial infection, cost of care, further tissue damage and patient discomfort.[10-11] Although silver products have been recognised as useful antibacterial agents for burn wound treatment, recent findings indicate that the compounds might delay the wound-healing process[12] and that silver may have serious cytotoxic activity on various host cells.[13] Furthermore, silver-containing dressings allow microorganisms on the wound to be continually exposed to a silver-containing environment, which would increase the rate of bacteria evolving resistance.[13] Therefore, there is a need to develop a 'smart' wound dressing which can respond to the microbiological environment of the wound and give a color response in the presence of pathogenic bacteria and which will release an antimicrobial to kill/inhibit the growth of pathogenic bacteria only when required.

1.2 Bacteria

Bacteria comprise a large group of single celled prokaryotes with a variety of sizes in the range of a few microns (10^{-4} – 10^{-7} meters). Bacteria have neither a membrane-enclosed nucleus nor membrane-enclosed organelles like mitochondria and chloroplasts.

Bacteria are ubiquitous on earth and grow in soil, rock, water, and in organic matter and live bodies of plants and animals. There are approximately 40 million bacterial cells in every gram of soil and millilitre of water. It has been estimated that there are approximately 5×10^{23} bacterial cells in the entire planet.[14] The numbers of prokaryotic cells are approximately more than ten times than human eukaryotes on the planet. Eukaryotes with a size range of 10^{-3} – 10^{-5} meters are around two orders of magnitude than prokaryotes (10^{-4} – 10^{-7} meters).[15] Bacteria are extremely adaptable and have adapted over billions of years to survive in extremely unlikely conditions including radioactive waste, volcanic springs and even the surface of the moon. Bacteria can colonise objects and remain dormant. However, they can change very much viable when

that environment changes to be more accommodating. When it comes to surgical and dental equipment, this may be colonised prior to use and once the bacteria are supplied with a constant supply of warmth and nutrients, the dormant bacteria grow and some pathogenic bacteria may cause an infection which is life threatening.

1.2.1 Classification of Bacteria

Most bacteria are collected, identified and grouped based on their sizes and shapes, requirement of oxygen for respiration, role of temperature for their growth, intake of nutrients for their survival and by gram staining of bacterial cell wall. Therefore, correct identification of bacteria is important for precise diagnosis and effective treatment in case of diseases due to bacterial infection.

Based on cellular morphology, bacteria display a range of shapes. Most bacteria are either spherical (coccus), or rod-shaped (bacillus). Some rod-shaped bacteria can be further divided by different variants. Some rod-shaped bacteria are slightly curved or comma-shaped (vibro); others can be spiral-shaped (spirillum) or tightly coiled (spirochaetes) and some other less common forms for example, tetrahedral or cuboidal shapes.[16-17] This wide range of variety is controlled by the bacterial cell wall and cytoskeleton and is important as it can influence the ability of bacteria to acquire nutrients, attach to surfaces, swim through liquids and escape predators.[18-19] Bacterial cells naturally aggregate on surfaces and this gives another classification and identification. When cellular division occurs along a single axis and the bacteria grow in chains or pairs, these bacteria are called Streptococci, the shape of which are like a chain or twisted chain, while Staphylococci forms grapelike clusters. *Staphylococcus aureus* which are gram negative bacteria is clinically important.

Most bacteria are classified as gram-positive and gram-negative in the laboratory. The classification relies on the positive or negative results from Gram's staining method which uses a purple dye and iodine. The staining method was developed by Hans

Christian Gram in 1884 to characterise bacteria based on the structure of their cell wall.[20] Both gram-positive and gram-negative bacteria have a cell wall made up of peptidoglycan and a phospholipid bilayer with membrane-spanning proteins. The thick layers of peptidoglycan in the "gram-positive" cell wall stain purple, while "gram-negative" bacteria have a unique outer membrane with a thinner layer of peptidoglycan, and a periplasmic space between the cell wall and the membrane and the cell wall appears pink. In the outer membrane, gram-negative bacteria have lipopolysaccharides (LPS), porin channels, and murein lipoprotein, all of which gram-positive bacteria lack. Many species of gram-negative bacteria are pathogenic, meaning that they can cause disease in a host organism. This pathogenic capability is usually associated with certain components of "gram-negative" cell walls, in particular the lipopolysaccharide (also known as LPS or endotoxin) layer which blocks antibiotics, dyes, and detergents protecting the sensitive inner membrane and cell wall.[21]

1.2.2 Bacterial Cell Wall Structure

The cell walls of gram-positive bacteria are made up of many layers of peptidoglycan and teichoic acids, whilst gram-negative bacteria have relatively thin cell walls containing a few layers of peptidoglycan. Peptidoglycan in gram-negative bacteria is surrounded by a second lipid membrane containing lipopolysacharides and lipoproteins. The thick outer layer of peptidoglycan, teichoic acid, polysaccharides, and other proteins has many purposes including cell expansion, shape formation and membrane transport regulation.[22] Figure 1.2 shows the structures of cell walls of "gram-negative" and "gram-positive" bacteria. The difference in structures of cell walls results in the differing susceptibilities to antibiotics, e.g. vancomycin was used to fight against gram-positive bacteria, while it is ineffective against gram-negative pathogens such as *Pseudomonas aeruginosa.*[23]

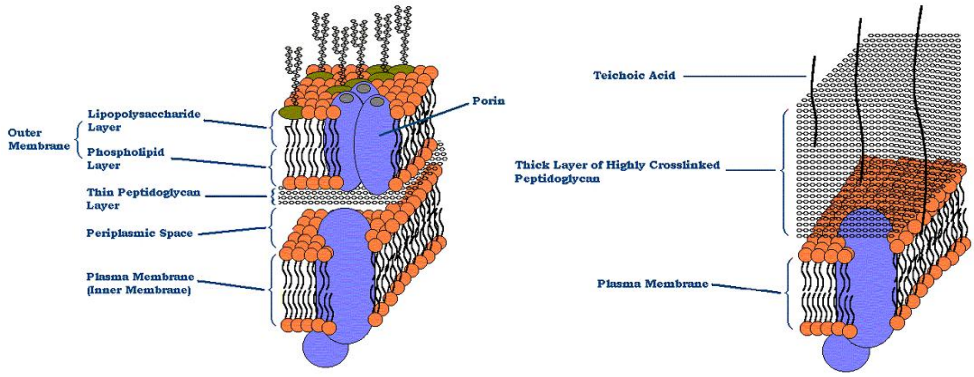

Gram-negative Gram-positive

Figure 1.2: Construction of the cell walls of Gram-negative and Gram-positive bacterial cell walls.[24]

1.2.3 Pathogenic Bacteria

There are ten times more bacteria inhabiting the human flora than the total number of human cells.[25] Most of bacteria in the body are harmless due to the protection afforded by the immune system. These bacteria are known as commensal or "good" bacteria, because they perform some vital and useful functions in the human body, for example, *Escherichia coli* are found in the gut and play an important role in maintaining efficient digestion.[26] However, some species of bacteria are pathogenic and are capable of causing infectious diseases, including cholera, syphilis, anthrax, leprosy and bubonic plague. The pathogenic bacteria can be divided into two groups---opportunistic pathogens and primary pathogens. Opportunistic pathogens do not normally cause disease as the host immune system will prevent this from happening, but will if a patient has a compromised immune system, bacteria which are part of the natural flora e.g. *E. coli* are allowed to multiply and cause disease and therefore are considered opportunistic. The pathogens that are able to cause infection and disease in healthy individuals are recognised as primary pathogens.[27] Humans are most interested in the species of pathogenic bacteria which affect humans although humans and animals share a common susceptibility to certain pathogens. Pathogenic bacteria including *Streptococcus, Staphylococcus, Tuberculosis* and *Escherichia coli* are most studied by researchers, because these bacteria account for many illnesses and disease epidemics.

Infection during hospital infection, known as nosocomial infection, is a global concern[28] and has become far more dangerous with the emergence of antibiotic resistant strains of many pathogens, with the most notable being methicillin resistant *Staphylococcus aureus* (MRSA).[29-30] It is reported that at least half of all cases of nosocomial infections are associated with medical devices.[31] The medical consequences of device-related infections can be disastrous; they include potentially life-threatening systemic infections and device malfunction that may require device removal, often complicated by tissue destruction. As described bacteria can colonise many items prior to use and then inoculate a patient with the bacteria. Inoculation can also occur from a patient's skin or orifice during procedures, for example, nasogastric intubation may transfer bacteria occupying nasal cavity further into the patient which will allow colonisation of the mucosal membrane. Urinary catheters may also transfer bacteria from a patient's skin and allow migration from the urethral fissure toward the bladder causing consequent infections.[30] Sterilised surfaces may also be colonised by bacteria. When the nutrition requisite for cell proliferation is not present, the bacteria can depress metabolism and await inoculation to a host. This causes a biotransfer threat and generally occurs in hospitals (MRSA) and in the food industry (*Salmonella enterica*, *Escherichia coli*).[32] Urinary tract infection resulting from catheterization accounts for over 40% of all nosocomial infections. Removal and replacement of soiled catheters generally requires a further invasive procedure and expense.[33] *P. aeruginosa* (PAO1), *S. aureus* (MSSA 476) as pathogenic bacteria are used in this work and *E. coli* (DH5α) as a control system, hence the three species of bacteria will be presented in the thesis in chapter 2.

1.2.4 Pathogenic Toxins

It is known that pathogenic bacteria secrete an array of virulence factors such as lipases and toxins which cause local tissue breakdown, by damaging cell walls. This is illustrated in figure 1.3. Pathogenic bacteria cause harm to their eukaryotic hosts by secreting enzymes and toxins that damage cells and connective matrix material of the tissues. They include adhesins that allow them to attach to tissues and enzymes that degrade tissue matrix proteins and allow deep tissue penetration such as hyaluronidase

or lipase. Other virulence factors such as leukocidin, leukotoxin and staphylysin act as cytotoxins, directly killing host cells allowing further tissue invasion and suppressing their own immune destruction. Proteins such as coagulase and protein A further act to suppress the host immune system. It should be noted that the secretion of virulence factors can essentially alter the properties of the host environment which is common to all pathogenic bacteria. Knowledge of the enzymes and toxins secreted by specific pathogens and their mode of attachment onto eukaryotic cells provides an opportunity for detecting the presence of pathogens. For example, the lysis of red blood cells around bacterial colonies on agar plates has long been used as a clinical microbiology diagnostic for the detection of certain common human infections (such as *Streptococcus aureus* and *Staphylococcus*).

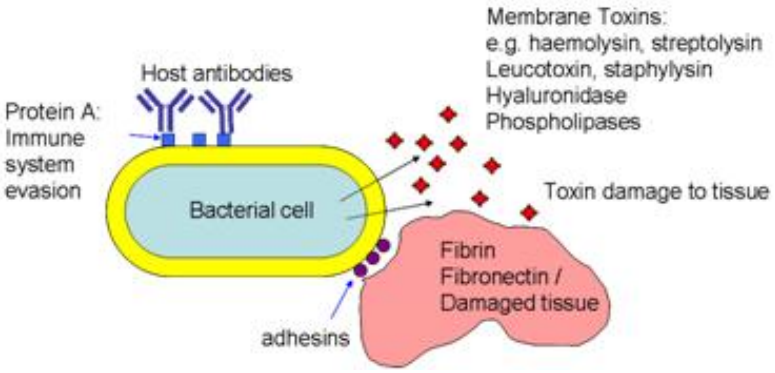

Figure 1.3: Schematic of array of membrane bound bacterial cell and secretion of proteins/toxins that pathogenic bacteria can deploy against healthy tissue.

1.2.4.1 Endotoxins

Endotoxins are a component of the outer membrane of the cell wall of gram-negative bacteria. They are associated with gram-negative bacteria whether the bacteria are pathogenic or non-pathogenic.[34] Endotoxins mainly refer to lipopolysaccharide (LPS) which is a part of outer membrane of gram negative bacteria such as *Escherichia coli, Salmonella, Shigella* etc. The typical molecular weight of LPS is about 10 kDa but can be up to 1000 kDa because they can form into aggregates. The role of endotoxins in the

outer membrane of bacteria is to act as a permeability barrier preventing large molecules and hydrophobic compounds from external environment. It also acts as a barrier to lysozyme and many antimicrobial agents. In addition, endotoxins may play a role as adhesins when they it colonise on the host. LPS consists of lipid A and a polysaccharide chain. Lipid A is responsible for causing toxic effect on host and polysaccharide is responsible for immunogenicity. Both lipid A and the polysaccharide side chains which are nontoxic but immunogenic portion of LPS are determinants of virulence in gram-negative bacteria.[35] LPS is responsible for a large number of clinical infections and even at low concentrations, LPS can cause extreme immune responses such as activation of inflammation and coagulation by the host.[36] Therefore, such immune reaction during the infection by gram-negative bacteria may cause toxic shock syndrome and even death of the host at high LPS concentrations.[37]

1.2.4.2 Exotoxins

Exotoxins are usually secreted by bacteria. They are released in soluble monomeric forms and act at a site away from bacterial growth. They can also be released by lysis of the bacterial cell. Exotoxins are usually proteins and rarely polypeptides. Proteins contain one or more polypeptides folded in a biologically functional way such as globular or fibrous form. Exotoxins can act enzymatically or through direct action with host cells and stimulate a variety of host responses.[38] Their actions against hosts are different depending upon the individual exotoxin. Some act as adhesins to colonise the host, while others act as invasins. Exotoxins are known to cause physiological and pathological damage to the host cells. Physiological damage refers to impairing particular functions of the host but without killing any cells e.g. cholera enterotoxin (Ctx) of *Vibrio cholera* promotes water and electrolyte secretion from enterocytes, causing diarrhea.[39] Some other exotoxins cause pathological damage to the host e.g. diphtheria toxins (Dtx) of *Corynebacterium diphtheria*[40] and exotoxin A of *Pseudomonas aeruginosa*. They cause the death of the target cell of the host by inhibiting protein synthesis. Some exotoxins have very specific cytotoxic activities and they only attack or

target specific cells. Other exotoxins produced by clinical pathogens such as *S. aureus* have broad cytotoxic effects.[41] These toxins have ability to damage the cell non-specifically and lead to apoptosis or necrosis.

1.2.4.3 Pore Forming Toxins (PFTs)

Pore-forming toxins belong to the group of protein exotoxins produced by pathogenic bacteria. The toxins can disrupt the selective influx and efflux of ions across the plasma membrane by inserting a transmembrane pore. At the molecular level, the toxins have an affinity to bind to membrane proteins, cholesterol or lipids to insert and form a pore to exert their virulent effects. Some toxins have a specific affinity to bind to cholesterol to insert and form a pore and this group of toxins is called cholesterol binding toxins (CBTs). Streptolysin of *Streptococcus pyogenes*, pneumolysin of *Streptococcus pneumoniae*, perfringolysin O of *Chlostridium perfringenes* and listeriolysin of *Listeria monocytogenes* belong to CBTs group. CBTs consist of three to four domains in their monomeric state and one of these domains is responsible for binding to cholesterol. Therefore the toxins are more likely to bind/insert to cholesterol-rich regions of the cell membrane and the resulting transmembrane pores are quite large with 24 to 48nm in diameter.[42] Some PFTs do not specifically bind to sites in the cell membrane. Monomer insertion with subsequent transformational changes results in hydrophobic pore formation. The PFT group is classified into two groups: α-PFTs and β-PFTs. The two groups are based on the differences in mechanisms of interaction with membrane.[43] α-PFTs insert helices into the membrane to form the pores while β-PFTs insert β-barrel in the membrane to form the β-barrel pores including aerolysin of *Aeromonas hydrophila*, α-toxin of *Clostridium septicum*, α-haemolysin of *S. aureus* and cytotoxin of *P. aeruginosa*.[44]

There are roughly two types of toxins: pore forming toxins and translocation toxins.[45] The pore forming toxins generally reside in the plasma membrane and form an ion channel conformation. The ion channel is mainly responsible for the toxicity either by

permeating through the membrane or by activating signal transduction pathways. The α-toxin of *S. aureus* and *E.coli* haemolysin are members of this family. The translocation toxins are known as "A-B type toxins" as they are made up of two subunits: the A domain carries the enzymatic property such as ribosylation (Diphtheria toxin, cholera toxin), adenyl cyclase (edema factor of *B. anthracis*) etc; [46] B domain binds to a receptor on a cell surface and plays an important role in translocation. These two domains are either connected to each other such as diphtheria toxin and cholera toxin or separated such as *B. anthracis* toxins.[47-48]

1.2.4.4 Exoenzymes

Exoenzymes, also known as extracellular enzymes, are secreted by many pathogenic bacteria and are associated with the process of cell degradation and invasion. Collagenase for example can break peptide bonds in collagen which is the supporting component of the extracellular matrix of eukaryotic cells.[49] Hyaluronidase degrades hyaluronic acid which is the anionic glycosaminoglycan found in connective, epithelial and neural tissues.[50] Some other enzymes such as phospholipases can recognise and degrade different types of phospholipids by hydrolysis. Different phospholipases recognise different sites of cleavage in different phospholipids (figure 1.5).

1.2.4.5 Superantigens

Some bacterial toxins can directly act on the T cells and trigger the immune system of the host. Several human diseases are associated with impairment of the immunologic functions of these cells by toxin. A large number of known and identified bacterial toxin superantigens belong to pyrogenic exotoxins which are produced by staphylococcal bacteria and streptococci. Their biological activities include potent stimulation of the immune system, pyrogenicity and enhancement of endotoxin shock. Superantigens have the ability to trigger the immune system and this immunostimulatory property is potent and triggered by extracellular binding of superantigens onto specific receptors of T-cells

and major histocompatibility molecules (MHC) which are expressed on the surface of antigen presenting cells.[51] The binding results in a massive proliferation of peripheral T cells followed by a massive release of cytokines from lymphocytes and monocytes. Cytokins are small proteins mainly responsible for cell signalling secreted by the glial cells of the nervous system and by the cells of the immune system. Over secretion of cytokines can trigger a dangerous syndrome called 'cytokine storm', which can cause several dangerous diseases such as toxic shock syndrome. The cytokines[52] are mediators for the hypotension, high fever, and diffuse erythematous rash which are characteristic of toxic-shock syndrome.[53]

1.2.5 Mode of Action of Bacterial Toxins

Many bacterial pathogens produce toxins which are considered as primary virulence factors. The mode of action of bacterial toxins depends on different toxins secreted by pathogens. The main barrier for the toxins to go through or interact with is the plasma membrane which is the primary defence of eukaryotic cells from the extracellular environment. Some toxins need to bind to cellular receptors on a membrane to exert their function and hence cause lysis; while some toxins need to insert into membranes to form a pore allowing water, ions, and small organic molecules pass through the membrane to cause the host cell death. In either case, toxins necessarily interact with the host cell membrane. Common modes of toxicity against the host cells include cell membrane damage, protein synthesis inhibition, pore formation, second messenger pathway activation and activation of immune response.[54]

1.2.5.1 Transmembrane Pore Formation

Membrane binding

The modes of interaction with target cells depend on different types of toxins. The mechanism of action of α-toxin secreted by *S. aureus* is detailed here as *S. aureus* is the bacterium that is used as a pathogenic model in the work. The dosage of α-toxin can result in two different modes of activity.[55] Low concentrations (< 50 mM) of toxin specifically bind to an unidentified cellular receptor and form the heptameric pore. This

pore allows the exchange of monovalent ions which results in DNA fragmentation and apoptosis.[56] Binding is saturable and displays an optimum at 22-26 ^{o}C. Higher concentrations (> 200nM) will result in the toxin absorbing nonspecifically in to the lipid bilayer and this accounts for its permeabilizing action on cells lacking the receptor (e.g. human erythrocytes) and on protein-free lipid bilayers (liposomes and planar lipid membranes). This will form large, Ca^{2+} permissive pores and result in massive necrosis and other secondary cellular reactions provoked by uncontrolled Ca^{2+} influx. [57]

Streptolysin O (SLO) secreted by streptococcal is a haemolytic exotoxin. SLO interacts primarily with cholesterol molecules in target bilayers.[58] The C-teminus plays a key role in binding.[59] In biology, C-terminus is the end of an amino acid chain which is terminated by a free carboxyl group (-COOH).

In contrast to α-toxin and SLO, it appears that HlyA does not interact with any specific acceptor molecule in target membranes. Binding is independent of the presence of proteins or cholesterol in the membranes. [60] In fact, the functional domain of HlyA has not been clearly identified. It is speculated that the hydrophobic sequence in HlyA forms at least part of the primary binding site and this domain possibly can spontaneously insert into lipid bilayers without any specific acceptor molecules.

Pore Formation

When bacterial toxins insert into a lipid membrane, toxins will generate hydrophobic domains to match the low polar character of the lipid acyl chains. The strategy is the oligomerization of toxin protomers to form partially or fully circularized protein complexes. This mechanism is applicable in the case of α-toxin [53] and SLO.[61] The energy required for pore formation depends on conformational changes in the toxin molecules themselves. It is proposed[62] that HlyA also forms oligomers in membranes but the detailed mechanism and supporting data are unknown. The mechanism of α-toxin formation has been studied in the greatest detail. The structure of the α-haemolysin heptameric complex which probably represents the pore has been studied by Song *et al.*[63] Each protomer mainly consists of a β-sheet structure. The heptameric complex has a mushroom shape of 100 Å in height and 100 Å in diameter, the stem of which forms the pore forming domain[59] (figure 1.4a). The structure is divided into three domains: the cap, the stem and the rim. The cap is composed of seven β-sandwiches,

interconnected by the first 18 N-terminal amino acids forming a latch, extending from one protomer to the next. The stem forms the true transmembrane channel. Each protomer contributes with two antiparallel β-strands. The rim interacts with lipid bilayer. Once the bulk of the oligomeric structure lies on the membrane surface, the portion will penetrate into the membrane and a series of changes will occur. The β-hairpin of the stem is quite small and can be fully internally hydrogen bonded. Within each strand, non polar and polar residues alternate which make the outside of the barrel hydrophobic and the inside channel hydrophilic, while the bottom of the rim is rich in aromatic residues with four tryptophans and two tyrosines per protomer, which are also important for membrane anchoring.

Once the pore is formed, only the stem inserts into the lipid matrix of the cell membrane while the cap heptamer stays above the membrane on the side where it is inserted. The channels have no control on transport of solutes, molecules etc and will cause lethal permeability changes in the membrane.

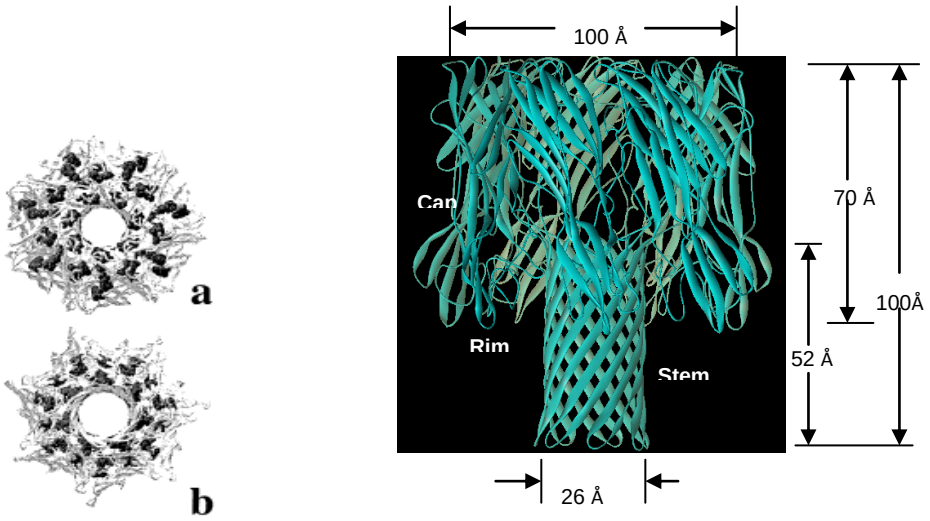

Figure 1.4: Ribbon diagram of the α-haemolysin of *S. aureus.*
Top/bottom (a,b) and lateral (c) views of the α-haemolysin oligomer.[58]

1.2.5.2 Lipid Damaging

Lipid damage can be caused either by some lipid-degrading extracellular enzymes or by endotoxins LPS. [47-48] The damage not only may result in the direct lysis of cells but also

can facilitate bacterial spread through tissues. Bacterial hyaluronidases, collagenases, and phospholipases are able to degrade cellular membranes. There are some examples of this type of toxin including α-toxin of *Chlostridium perfringens*, which possesses phospholipase C activity and clostridial collagenases.[51,64-66]

Phospholipases (PLs) are common extracellular enzymes produced by many human pathogenic bacteria.[67] PLs are highly site specific and they can bind to a wide range of lipids including phosphatidylcholine(PC), phosphatidylinositol(PI), phosphatidylethanol (PE), phosphatidylserine(PS), phosphatidylglycerol(PG), lysophosphatidylcholine(LPC), lysophosphatidylinositol(LPI) and sphingomyelin(SM).[57] Cellular damage caused by PLs is quite considerable because phospholipids are the main component of human cell membranes, constituting more than 75% of lipids (% mol) in human cells.[68] The mechanism is based on the sites of phospholipids at which particular PLs hydrolyse.(figure 1. 5)

There are four main categories, termed A, B, C and D, which are classified by different type of reaction they catalyse. Phospholipase A includes phospholipase A_1 (PLA_1) and phospholipase A_2 (PLA_2). PLA_1 and PLA_2 can recognise *sn*-1 and *sn*-2 acyl bonds of phospholipids respectively and hydrolyses the fatty acids.[69] Phospholipase A_2 is an enzyme which is present in the venom of the bees and viper snakes.[70] Phospholipase B (PLB) cleaves both *sn*-1 and *sn*-2 acyl chains. It is also known as a lysophospholipase. Phospholipase C (PLC) and phospholipase D (PLD) hydrolyse the bonds before and after the phosphate group respectively.[71] Lipid catalysed by PLC will release diacylglycerol and a phosphate-containing head group, while PLD breaks the lipid down to phosphatidic acid and an alcohol.[72]

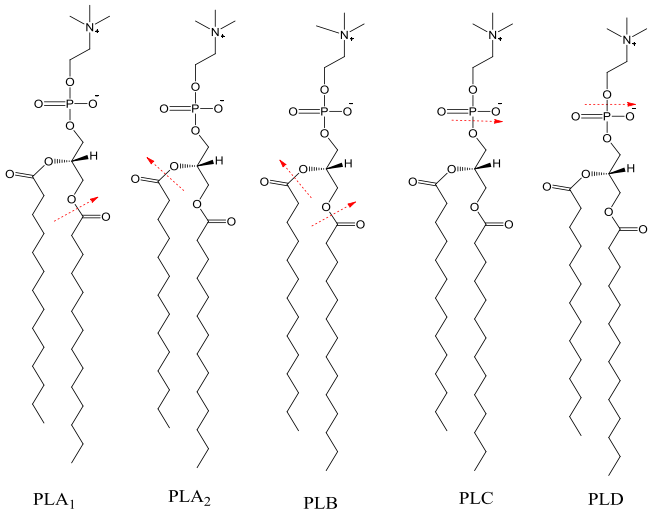

Figure 1.5: Cleavage sites of different phospholipases (shown with red dashed line)

1.2.5.3 Inhibition of Protein Synthesis

This group of toxins consists of A-B subunits: the A subunit is responsible for enzymatic activity, while the B subunit is designed to target a specific receptor on the host cell and then translocate the enzyme across the membrane to intracellular targets.[73] Subunit A enters the host cell either by pore forming or receptor-mediated endocytosis (RME). In the first mode of the action, subunit B binds to the specific receptor on the target cell and induces the formation of a pore where subunit A will translocate.[74] In the second mode, binding to a specific receptor on target cells triggers the formation of an endosome which is a process of an enclosed vesicle budding inward from the plasma membrane. Endosome carries the whole toxin and the change of pH in the cell will separate the subunits. Subunit A then reaches and inactivates internal targets.[54]

Corynebacterium diphtheriae is a human pathogen that generally colonises the human throat. Diphtheria toxin (DT) secreted by the bacterium is a potent toxin which is one of the most well studied and understood bacterial toxins.[75-76] The toxin can cause the disease diphtheria in humans by entering into the cell cytoplasm and inhibiting protein synthesis.[77] The DT catalytic domain belongs to a family of mono-ADP ribosyltransferases, which bind to NAD and transfer the ADP-ribose group to a specific residue on the target protein. The active site is conserved among the bacterial ADP-ribosylating toxins and forms the NAD-binding cavity which plays a major role in catalytic activity. The ADP-ribosylation of diphamide by DT prevents the binding of

eukaryotic elongation factor-2 (EF2) to tRNA, resulting in impaired protein synthesis.[78]

Pseudomonas exotoxin A (ExoA),[79] Shiga toxin (ST)[80] and *E. coli* verotoxin (VT) enter cells via the Golgi apparatus and the endoplasmic reticulum (ER). Exotoxin A uses as similar mechanism of action as DT does, while ST and VT impair ribosomal RNA function by cleaving an N-glycosidic bond in the 60S subunit. Pore forming toxin (PFT) such as *C. perfringens* enterotoxins (CPE) inhibit protein synthesis by inducing leakage of nucleotides, amino acids and other small molecules.

1.2.5.4 Activation of Secondary Messenger Pathways

Many bacterial toxins have the ability to kill the target cells indirectly by altering the function of a variety of cellular proteins. These toxins can activate and modify secondary messengers and result in the change of signal transduction pathways which play a key role in maintaining a variety of cellular functions.[81] Cholera toxin of *Vibrio cholerae*, heat-liable, heat-stable toxins and cytotoxic necrotizing factors (CNFs) of *E.coli* [82] and pertussis toxin of *Bordetella pertussis* all belong to this group of toxins. These toxins can affect the secondary messenger pathways and target guanine nucleotide-binding proteins (G-proteins) and Rho G-proteins.[83] The mechanism of action is similar to the toxins inhibiting protein synthesis. Both cholera and pertussis toxins utilise RME modes of translocation to enter the target cells. The cholera toxin is an oligomeric complex consisting of six protein subunits: a single copy of the A subunit which is an enzymatic part, and five copies of the B subunit, responsible for receptor binding.The five B-subunits form a five-membered ring, while subunit A carries enzymatic activity which ADP-ribosylates G proteins.[84] The pentameric part B of the toxin molecule binds to the targeted cells, while A subunit detaches from the pentameric part and enters the cell via receptor-mediated endocytosis. It ribosylates the Gs alpha subunit of the heterotrimeric G protein inside the cell, resulting in the production of cyclic adenosine monophosphate (cAMP). This leads to the secretion of fluid and electrolytes which will further cause serious disease such as diarrhea.

1.2.5.5 Inhibition of the Release of Neurotransmitters

Some toxins affect the nerve cells of peripheral nervous system (PNS) and central nervous system (CNS). This group of toxins is classified as neurotoxins and their modes of action include interfering with the ion transport function of many voltage gated ion channels and inhibiting the release of neurotransmitters of the nerve cells.[85]

1.2.6 Biofilms

A biofilm is a complex aggregation of microorganisms that can be attached to a non-living or living surface in the presence of sufficient nutrients.[86] More than one type of bacteria may be present in this sessile system and these adhered cells are usually embedded within a self-produced matrix of extracellular polymeric substance (EPS). Biofilm EPS is a polymeric conglomeration normally composed of extracellular DNA, proteins and polysaccharides. This matrix plays an important role in protecting the cells within it and facilitating communication among them through biochemical signals. Biofilms can form single-species films under certain conditions. However, biofilms often contain many different types of miroorganism, e.g. bacteria, archaea, protozoa, fungi and algae.

Biofilms are often characterised by surface attachment, structural heterogeneity, genetic diversity, and complex community interactions. Biofilms have altered phenotype and bacteria living in biofilms usually have different properties from planktonic microorganisms as the dense and protected environment of the films allow them to cooperate and interact in various ways. This leads to increased resistance to antimicrobial agents and the host's immune system.[87-88] In some cases, antibiotic resistance can be increased a thousandfold. [89]

1.2.6.1 Biofilm Formation

It was previously assumed that all bacteria are planktonic.[90] Microbial communities were found in the 1970s [91] and more work has been done to understand the mechanism of biofilm structure. Current understanding of biofilm formation is described as follows.[92-93]

Initially, free-floating microorganisms attach to a substrate through reversible attachment via van der Waals forces to condition the surface for further bacterial attachment.[90] The initial bacterial colonists can anchor themselves more permanently using cell adhesion structures such as pili [90] if the bacteria are not separated from the surface immediately. The early stage of biofilm formation is coordinated by unknown cues, bacteria use flagellar, twitching, and gliding motility mechanisms to grow together in nascent clusters.[94] Biofilms then grow by further addition of bacteria through more diverse adhesion sites and begin to build the matrix that holds the biofilm together. More bacteria either attach to the matrix or directly to earlier colonists. The cells are able to communicate through quorum sensing which is a process bacteria coordinate gene expression and communicate with each other based upon the density of their local population by using products such as *N*-acyl homoserine lactone (AHL) during this stage.

Biofilms then grow through the reproduction of bacteria and twitching motility. The final stage of biofilm formation is known as development. In this stage biofilms are established and may only change in shapes and sizes. [95] A schematic of biofilm formation is illustrated in figure 1.6.

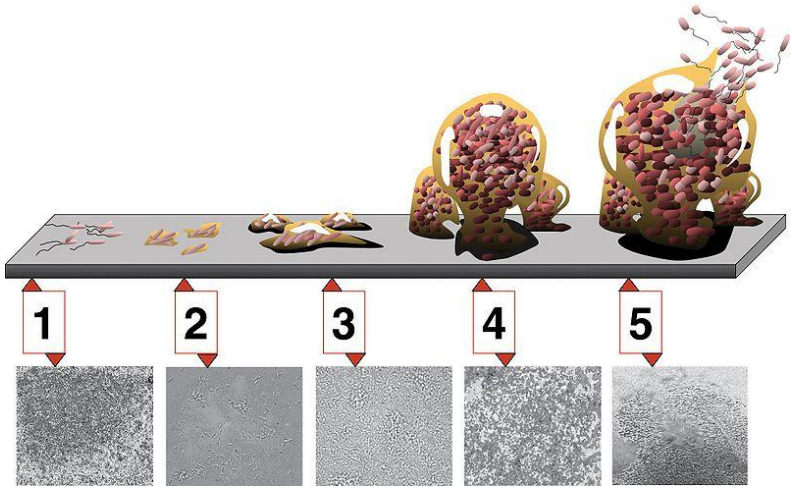

Figure 1.6: Stages of biofilm formation with corresponding photomicrographs.[96]
(1) initial reversible attachment via weak attractive forces; (2) irreversible attachment; (3) maturation: reproduction and recruitment of bacteria and production of exopolymers matrix; (4) maturation; (5) dispersion. (image credit: D. Davis)

1.2.6.2 Antimicrobial Resistance of Biofilms

Biofilms have proved to resist various antibiotics and human immune system responses.[97-98] Besides the familiar mechanisms of resistance such as efflux pumps, modifying enzymes, and target mutations, other possible factors may account for the protection of bacteria in a biofilm. Several defence mechanisms of bacterial communities are described as follows.[94]

The biofilm matrix can slow the diffusion of antibiotics, resulting in slow or incomplete penetration of the antibiotic into the biofilms.[99] Antibiotics that are absorbed into the biofilm matrix could also have a retarded penetration. This is might account for the slow penetration of aminoglycoside antibiotics.[100-101] The inherent negative charge in the biofilm matrix can bind to positively charged antibiotic ions.[102-103]

Bacteria living in biofilm structure are nutrient deficient and exist in a slow/non-growing or 'starved' state. This makes the bacteria communities not susceptible to antimicrobial agents.[104] Cell viabilities reduce from around 100% in the planktonic phase to around 10% in a biofilm.[104] However, slow growing *P. aeruginosa* cells have shown no greater resistance to antibiotics than do stationary phases of planktonic cells.[105] Experimental work has proved that the planktonic form of *P. aeruginosa* is less affected by antibiotics in the stationary phase compared to biofilm core cells.[106] The resistance to antibiotics in both stationary cells and biofilms is probably due to the presence of persister cells [96] which are a small subpopulation of microbial cells. The presence of persister cells can result in multidrug tolerance.[107]

Furthermore, the structural heterogeneity of biofilms ensures cells are in a variety of metabolic states and thus deny metabolically directed action. It is also possible that at least one species of bacteria living in biofilms are resistant to antibiotic attack. Therefore, the multicellular nature of biofilms provides dual defence methods to combat with the antimicrobial attack.[91]

Additionally, the altered chemical environment within biofilms may result in the antibiotic resistance of biofilm. Some studies have shown that oxygen in the surface layers of a biofilm can be completely consumed, causing an anaerobic environment in the deep layer of the biofilms.[108] Aminoglycoside antibiotics are less effective against

the same bacteria in anaerobic rather than in aerobic conditions. Alternatively, some local accumulation of acidic waste products may cause the changing of pH greater than 1 between the bulk fluid and the biofilm interior. This would cause the deactivation of an antibiotic.[108] In addition, the change of osmotic environment within biofilms which results in the induction of an osmotic stress response. This response could change the relative proportions of porins in a way and then reduces cell envelope permeability to antibiotics.[109]

1.2.6.3 Biofilm Related Infectious Diseases

Biofilms have been found to be related to a large variety of microbial infections in the body[110] such as urinary tract infections, middle-ear infections, formation of dental plaque,[111] gingivitis,[107] coating contact lenses,[112] etc. Most biofilms are comprised of a variety of organisms, i.e. polymicrobial. Biofilms are best known for their role in foreign device-related infections including infections of catheters and other biomaterials used in medicine. However, recent studies have shown that biofilms may impair wound healing and reduce topical antibacterial efficiency in the treatment of burn wound infection.[113-114] *Pseudomonas aeruginosa* is an environmental organism that regularly causes infections in burns and other wounds. The study of *P. aeruginosa* pathogenicity can explain the molecular mechanisms responsible for the switch from planktonic growth to a biofilm phenotype and the role of inter-bacterial communication in persistent disease.[115] Again, the increased resistance to antimicrobial agents and infections by biofilms make the research on biofilms extremely important for medical and clinical use.[108]

1.3 Pathogenesis of Burn Wound Infection

Not all of burn injuries will cause infection by pathogenic bacteria and the majority of burn injuries affect only the epidermis for example sun burn. However, the length of hospital stay, scarring, and pain will be increased when the open wounds are infected by pathogens. Human skin, as the first line of defense against invading microbes, is covered with a series of immune mediators which are able to clear invading bacteria and fungi.[16-117] Therefore, immune failure in a burn patient who has lost the skin barrier renders them vulnerable to bacterial infection. Bacteria can rapidly colonise open skin

wounds after burn injury even if burn wound surfaces are sterile immediately following thermal injury.[118-119] Microorganisms that colonise the burn wound originate from gastrointestinal and endogenous skin and also respiratory flora.[120-121] Gram-positive bacteria from patient's endogenous skin or external environment such as staphylococci, predominantly colonise the wound surface within the first 48 h unless specific topical antimicrobial agents are used for wound injury.[122] After an average of 5 to 7 days, these wounds are subsequently colonised with other microbes including gram-positive bacteria and gram-negative bacteria. Wound colonisation by yeast and fungi may occur later depending on whether broad-spectrum antibiotic therapy is used.[123-125]

Streptococcus pyogenes (beta-hemolytic streptococci) was once the most serious pathogen which can cause burn wound infections and was a major cause of death in severely burned patients. [126-127] With the introduction of penicillin G in the early 1950s, *Staphylococcus aureus* became the major pathogens which could result in severe wound infection. However, *Pseudomonas aeruginosa* from the patient's endogenous gastrointestinal flora or environmental source is the most common causes of wound infections in many burn wound centers.[128] *Pseudomonas aeruginosa* will be detailed in chapter 2. Table 1.1 shows the most common pathogenic bacteria colonising and infecting burn wounds.

Table 1.1: Lists of microorganisms responsible for causing burn wound infection [a]

Group	Species
Gram-positive organisms	*Staphylococcus aureus*
	Methicillin-resistant *S.aureus*
	Coagulase-negative staphylococci
	Enterococcus spp.
	Vancomycin-resistant enterococci
Gram-negative organisms	*Pseudomonas aeruginosa*
	Escherichia coli
	Klebsiella pneumoniae
	Serratia marcescens
	Enterobacter spp.
	Bacteroides spp.

Fungi	*Candida* spp. *Aspergillus* spp. *Fusarium* spp. *Alternaria* spp. *Rhizopus* spp. *Mucor* spp.
Viruses	Herpes simplex virus Cytomegalovirus Varicella-zoster virus

Data are from references 126, 129 and 130.

Antimicrobial resistance among a wide variety of human bacterial burn wound pathogens has been a major concern for many years and has had a negative effect on effective treatment of burn wound infections.[128,131] Hospitals often harbour multi-resistant strains of pathogens and microorganisms transmitted from the hospital environment tend to be more resistant to antimicrobial agents than those from patients' normal flora because of the transfer from patient to patient.[132-133] In addition, a high percentage of patient mortality and morbidity make MRSA, methicillin-resistant coagulase-negative *staphylococci*, vancomycin-resistant *enterococci*, and multiple resistant gram-negative bacteria with several types of beta-lactamases, including extended-spectrum beta-lactamases (ESBL), *ampC* beta-lactamases, and metallobeta-lactamases serious pathogens in hospitalised patients. β-lactamases are enzymes secreted by some bacteria and the enzymes are responsible for the resistance to various β-lactam antibiotics such as penicillin, methicillin and carbapenem. Data from Centre for Burn Treatment in Poland[134] show that both *Pseudomonas aeruginosa* and *Staphylococcus aureus* are the major strains isolated from burn wounds and are two major nosocomial pathogens to fight against.

1.4 Antimicrobial Agents Used for the Treatment of Burn Wound Infection

1.4.1 Introduction to Antimirobials

Current treatment for burn wound infections relies on the use of antimicrobials. The proper use of antimicrobial agents is a strategy to overcome the microbial invasion [135] of the host. Antimicrobial agents are molecules that are selectively toxic to microorganisms by interfering with essential microbial processes. This is due to the differences in cell membrane constituents and ribosome structure between the host and microbial cells. The presence of a microbial cell wall is usually a target for antimicrobial drug action. [136] (The description of the eukaryotic cell membrane will be presented in section 1.5) The different classes and mechanisms of actions are listed in table 1.2.

Table 1.2: Classes of antimicrobials and their mechanisms of action to the host [137]

Antibacterial	Mechanism
β – Lactams	Inhibit cell wall synthesis through inhibition of peptidoglycan crosslinking
Sulfonamides	Interfere with folic acid synthesis by competing with p-aminobenzoic acid
Macrolides	Inhibit protein synthesis by binding to 50S unit of ribosome
Chloramphenicol	Inhibit protein synthesis by binding to peptidyl transferase
Polypeptides	Disrupt cell membrane
Glycopeptides	Inhibit cell wall synthesis by binding to precursors
Aminoglycosides	Inhibit protein synthesis by binding to 30S

	unit of ribosome and distort membrane integrity through cationic character
Quinolones	Inhibit microbial topoisomerases, inhibits DNA relaxation and increases DNA breakage
Tetracyclines	Inhibit protein synthesis by binding to 30S unit of ribosome

Topical antimicrobials cover a wide range of compounds that are all applied directly onto the external site of infection in the form of creams. They are most commonly used for the treatment of bacterial infections. The ideal properties for an antimicrobial are listed below. So far, there is no antimicrobial agent available which possesses all of these properties: [138]

- Broad spectrum of activity
- Painless
- Long lasting
- Non-toxic
- Good eschar penetration
- Easy to apply
- No wound healing retardation
- Inexpensive
- Easy to store
- No systemic absorption

1.4.2 Topical Antimicrobial Agents

1.4.2.1 Silver Products

The use of topical chemotherapy has helped to improve the survival of patients with major burns and to minimise the incidence of burn wound sepsis, a main cause of mortality and morbidity in these patients. [139] One of the strategies for preventing bacterial infection is the use of metal antimicrobials, the most common of which is silver.[140] Siver has been known to possess bactericidal properties and silver compounds have been used for their medicinal properties for centuries as well.[141] Silver has been a viable treatment option for infections in burns, open wounds, and chronic ulcers. Several products incorporating silver have been used as topical antibacterial agents, such as

silver nitrate and silver sulphadiazine (SSD) Flammazine ™, (Smith & Nephew Health care Limited, Hull, Canada).[142] Acticoat ™ (Westaim Biomedical Inc., Fort Saskatchewan, Alberta, Canada) and Silverlon® (Argentum Medical, L.L.C., Lakemont, Georgia) are newly developed products which have a more controlled and prolonged release of nanocrystalline silver to the wound area. This mode of silver delivery allows the dressings to be changed with less frequency to reduce risk of nosocomial infection, cost of care, further tissue damage and patient discomfort.[10-11] Although silver products have been recognised as useful antibacterial agents for burn wound treatment, recent findings indicate that the compounds might delay the wound-healing process [12] and that silver may have serious cytotoxic activity on various host cells.[143]

Silver sulfadiazine (Ag-SD) has been clinically used as a standard treatment for burn wound infection over decades since silver sulfadiazine was first synthesized. Ag-SD was reported to be effective as a topical antimicrobial agent for the control of *Pseudomonas* infection in burns.[140] However, Cho Lee's[12] previous study showed the cyto-toxic effect of Ag-SD on HaCaT cells and delayed epithelisation process in a second-degree burn animal model.[144] Wound healing is a complex process involving several cell types including the processes of epithelisation and wound contraction, which is defined as closure of open wound by inward movement of the surrounding integument. [145] The process of re-epithelialization is generally keratinocyte dependent, while the process of contraction is fibroblast dependent. Therefore, impaired proliferation of these two cell types could lead to the delayed and complicated wound healing. [146] Thus, the use of Ag-SD is not recommended any more because of its reported wound healing inhibition.

1.4.2.2 Mafenide Acetate

Mafenide is a methylated sulphonamide available commercially as a 10% preparation in a water-soluble, hygroscopic cream base. It can interfere with the kidney's role in hydrogen ion excretion, resulting in metabolic acidosis. It has a large spectrum of activity against both the common gram-negative burn related pathogens such as *Pseudomonas aeruginosa* and the gram-positive pathogens.

Mafenide is usually used to treat the second and third degree burns and is not suitable to use as the first-line. [147] It should be reserved for infections that require rapid penetration

of the eschar for control and when other antimicrobials have failed. It may cause toxic effects and careful monitoring is necessary.[148] The agent is applied using open techniques. Mafenide can cause pain on application to partially burned areas, possibly because of its high osmolarity. It can also inhibit epithelial regeneration. Mafenide can be readily absorbed from burn wounds, so the actual therapeutic wound concentrations cannot be maintained unless the agent is reapplied.

1.4.2.3 Nitrofurazone

Nitrofurazone is another topical antimicrobial used in burn wound care. It inhibits bacterial enzymes and is used against *S. aureus*, *Streptococcus*, *E. coli*, *Clostridium perfringens*, *Enterobacter aerogenes*, and *Proteus* organisms. Nitrofurazone has a relatively more limited role in burn wound care and it is used as the treatment of second and third degree burns when resistance to other agents is a real or potential problem.

1.4.2.4 Povidone-Iodine

Povidone-iodine (PVP-I) is a complex of polyvinylpyrrolidone and iodine as an antiseptic for use on normal skin (e.g., surgical scrubs) and mucous membranes. Iodine has been broadly used for the treatment of skin infections and has been recognised as an effective broad-spectrum bactericide. This complex was then found to be less toxic and anti-bacterially effective in *vitro* tests.[149] The complex has a wide antimicrobial spectrum, but protein binding of iodine in the open wounds may result in decreased antimicrobial effect in *vivo*. The agent can be used with both the open and semiclosed techniques. It frequently causes pain on application to burned wound areas. This may be due to the acidic cream (pH 2.43) or to other side effects. It is also reported that povidone-iodine renal toxicity can result in lethal metabolic acidosis.[150]

1.4.2.5 Gentamicin Sulfate

Getamin sulphate is an aminoglycoside, bactericidal antibiotic used in the treatment of gram-negative infections, particularly those caused by *Pseudomonas*, and gram-positive

Staphylococcus.[151] Its mechanism of action is to disrupt bacterial protein synthesis. Although being gram-negative, *E. coli* shows some resistance to gentamicin. The use of gentamicin is not recommended in the treatment of *E. coli* infections. Therefore, the use of alternative broad-spectrum antibiotics has been increased, which may lead to the prevalence of antibiotic resistant bacterial infections by Gloden Staph and other so-called "superbugs". [137]

The drug is readily absorbed when applied to open wounds. Gentamicin is useful for invasive infection. It should be applied for brief periods to the smallest possible areas. The drug has some adverse effects including nephrotoxicity, auditory or vestibular ototoxicity and impairment of neuro muscular transmission and hypersensitivity reactions. Such toxicity remains a major problem in clinical use. [137] Therefore, blood levels of the drug should be carefully monitored. Superinfection with resistant bacterial strains will quickly occur with its protracted use.

1.4.2.6 Silver Nitrate Solution (0.5%)

Silver nitrate solution (0.5%) is an effective prophylactic agent for burns of less than 50% total surface area if properly used. [152] It can coagulate and precipitate bacterial proteins to inhibit bacterial growth. The diluted silver nitrate can be used in the treatment of common bacterial and fungal burn infections. Silver nitrate solution is not widely used clinically nowadays because it leaves black stains and has a limited scope of efficacy. In addition, silver compound probably inhibit tissue healing by several mechanisms and evidence suggests silver is cytotoxic.[143]

Silver nitrate solution is applied to thick cotton dressing (40-ply). These dressings must be wetted every 2 hours to ensure a constant source of silver ions at the wound site, the purpose of which is to prevent the wound from drying because the drying of the wound will lead to increased concentration of silver ions to injurious levels (>2%), and to minimise evaporative water loss and its attendant caloric requirement.[153]

1.4.2.7 Chlorhexidine

Chlorhexidine is a chemical antiseptic effective on both gram-positive and gram-negative bacteria.[154] It has both bactericidal and bacteriostatic mechanisms of action, the mechanism of action being membrane disruption.[155] Here the definition of bactericidal and bacteriostatic agents should be distinguished. Bactericidal agents kill bacteria and it includes disinfectans, antiseptics and antibiotis, whereas bacteriastatic agents interfere with the reproduction of bacteria and do not necessarily harm them. Chlorhexidine is harmful in high concentrations, but is used safely in low concentrations in many products including mouthwash and contact lens solution.

1.5 Biomembranes

1.5 .1 Basics of Lipid and Cell Membrane Structures

Cell membrane, which is also referred to as the plasma membrane, maintains a strictly balanced internal environment. Cells are surrounded by cell membranes. The major constituents of a cell membrane are amphiphilic biomolecules called phospholipids. Many different types of lipids, proteins, carbohydrates, cholesterols and all of their complexes are embedded in the lipid bilayer of cell membranes. All the constituents are held together by non-covalent, hydrophobic interactions within the cell membrane (figure 1.7). The type and composition of lipids, proteins, carbohydrates and cholesterols in cell membranes vary from cell to cell which depend on different properties of individual cells and the specialized functions that they perform. In most cell membranes, proteins constitute the largest fraction by weight and the ratio of lipid to protein is usually taken as an index of functional activity, comprising the higher ratio, the lower the activity and vice versa. In addition, the cell membrane is a platform for communication for inside and outside of the cells and involved in many cellular functional processes such as signal transduction, cell division and ion channel conductance.[156] Cellular organelles such as mitochondria, endoplasmic reticulum and Golgi complex (of the eukaryotic cell) are membrane-bound and all the intracellular

communications and the transport of components within the cell are also associated with the lipid bilayer membranes. Cell membrane becomes the primary target of the foreign invasions such as bacterial toxins and infection as it controls all possible means of access into the cell. [157] The compositional complexity and different varieties of membrane constituents make it a challenge to study, despite the detailed information on membrane-bound processes at the molecular level is crucial to understand the living organisms. This causes the development of simplified artificial model--lipid bilayers or lipid vesicles, comprising one or a few types of lipid molecules. The model lipid vesicles can mimic the cell membrane in several ways and allow the integration of membrane proteins by creating natural cellular environment, they allow not only the possibility to study the functional processes of cell membrane constituents but also become a potential future platform for biomolecular applications such as drug delivery. [158]

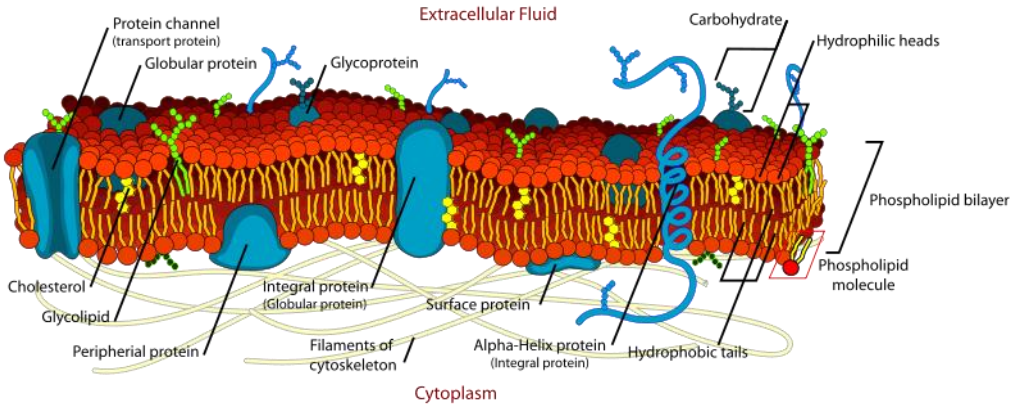

Figure 1.7: Basic construction of a typical eukaryotic cell membrane.
The phospholipid bilayer (shown in red) makes up the framework of the membrane. Cholesterol (yellow) fills any gap in the structure to aid in membrane strength and increase permeability to essential organic components

1.5.1.1 Glycerophospholipids

Glycerophospholipids are biological molecules which occur in all eukaryotic cells and are the most common membrane lipids. The 3 hydroxyl group of the glycerol is linked to a polar phosphate group and the 1 and 2 position hydroxyls linked to apolar acyl groups. The momenclature of glycerides is in terms of stereospecific numbering (*sn*), 1,2

di-myristoyl-*sn*-glycero-phosphatidylcholine, for example, is shown in figure 1.8. These glycerol esters are most abundant lipids in eukaryotic and most prokaryotic cellular membranes. Phosphatidylcholine is predominant in animals and phosphatidylethanolamine in bacteria. The length of the fatty acid tails can vary depending on different organisms but most commonly C16, C18 and C20. Incorporation of unsaturation in these fatty acids helps to increase fluidity of a membrane and the most common unsaturated tails are 18:1, 18:2, 18:3 and 20:4. The natural alkene bond in these fatty acids is *cis*- which causes disruption in the packing of fatty acid tails in a membrane resulting in less densely packed 'fluid' membrane. A combination of saturated and unsaturated fatty acid tails are incorporated into membranes to provide the optimal fluidity for that membranes function.[44] Due to their amphiphilic properties, phospholipids have ability to spontaneously form lipid bilayer (figure 1.8). This ability is resulting from the amphiphilic nature of phospholipids with a polar head and hydrophobic tails. The major driving force for this process is from the minimisation of unfavourable non-polar/polar interactions (fatty acid tails and water molecules) and the maximization of polar/polar solvent interactions (hydrogen bonding between the phosphate and head group regions and water molecules).

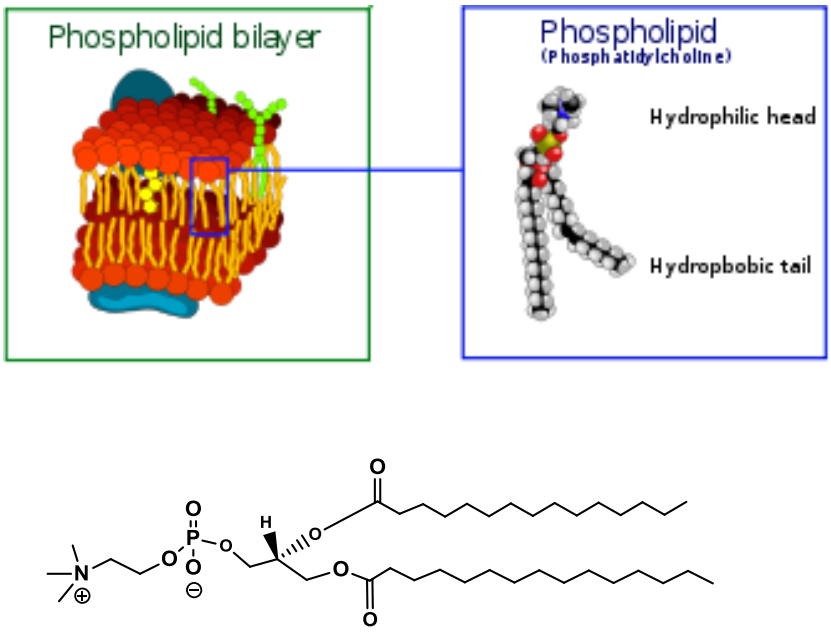

Figure 1.8: Lipid bilayer containing hydrophilic head and hydrophobic tail.
Below is one of the lipids commonly used throughout biological membranes and commercially available, 1,2-Dimyristoyl-*sn*-Glycero-3-Phosphocholine(DMPC)[159]

Because of the amphiphilic property of phospholipids, they have the ability to form supramolecular structures spontaneously *in vitro* such as micelles, vesicles or liposomes and crystalline structures. The liposome and lipid bilayer sheet are quite similar to that observed *in vivo* but much more basic. The bilayer is a way in which the lipids minimise their energy grouping hydrophobic tails together away from the water. This also provides separation of two volumes of water inside and outside of the liposome and either side of the bilayer sheet. The lipid bilayer sheet is useful for studying electrochemical responses across a membrane to stimuli interacting with the biomimetic lipid structure. Liposomes or vesicles not only provide this separation but they can encapsulate a different fluid inside the vesicles which can be used in drug delivery.

1.5.1.2 Membrane Fluidity

The interior of a lipid bilayer is usually highly fluid and in the liquid crystal state, hydrocarbon chains of phospholipids are disordered and in constant motion. At lower temperature, a membrane containing a single type of phospholipid undergoes phase transition to a crystalline state. Fatty acid tails are fully extended in this state, packing is highly ordered, and van der Waals interactions between adjacent chains are maximal

(figure 1.9). In addition, double bonds in fatty acid chains interfere with packing of lipids in the crystalline state and lower the phase transition temperature.

Figure 1.9: Structure of liquid-crystal phase of lipid bilayer

1.5.1.3 Cholesterol

Cholesterol is an important constituent of cell membranes. It has a rigid ring structure and a short branched hydrocarbon tail. Cholesterol is largely hydrophobic but it has one polar group, hydroxyl which makes it amphipathic. Cholesterol inserts into bilayer membranes with its hydroxyl group oriented toward the aqueous phase and its hydrophobic ring adjacent to fatty acid tails of phospholipids. The hydroxyl group of cholesterol forms hydrogen bonds with polar phospholipid head groups. Cholesterol plays a key role in maintaining the integrity of the lipid bilayer. The presence of cholesterol in a phospholipid membrane interferes with close packing of fatty acid tails in the crystal state. Interaction with relatively rigid cholesterol decreases the mobility of the hydrocarbon tails of phospholipids. Therefore, insertion of cholesterol inhibits transition to the crystalline state, for example, phospholipid membranes with a high concentration of cholesterol have a more tendency to stay in liquid crystalline state.

1.5.2 Description of the Background for Lipid Vesicles

Liposomes are microscopic vesicles, generally spherically shaped, which are formed from one or more lipid walls. The walls are prepared from lipid molecules, which have the tendency both to form bilayers and to minimise their surface area. The lipid molecules that make up a liposome have hydrophilic and lipophilic portions (figure 1.10). Upon exposure to an aqueous solution, the lipid molecules form a bilayer membrane wherein the lipid ends of the molecules in each layer are directed to the

centre of the membrane, and the opposing polar ends form the respective inner and outer surfaces of the bilayer membrane. Thus, each side of the membrane presents a hydrophilic surface while the interior of the membrane comprises a lipophilic medium.[160]

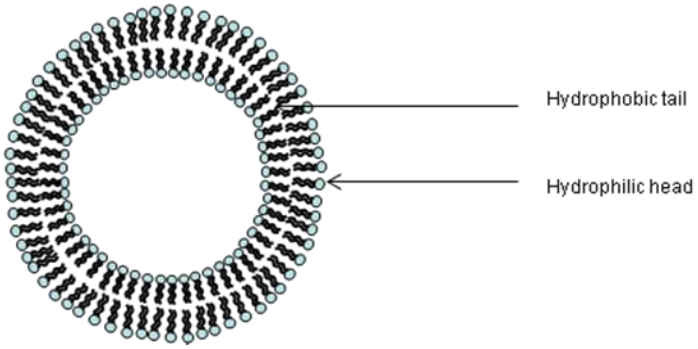

Figure 1.10: Basic structure of lipid vesicles with hydrophilic head and hydrophobic tail.

Liposomes can be divided into several categories based on their overall size and the nature of the lamellar structure. The classifications include small unilamellar vesicles (SUV), multilamellar vesicles (MLV) and large unilamellar vesicles (LUV) (also called as giant unilamellar vesicles, GUV). SUVs range in diameter from approximately twenty to fifty nanometres and consist of a single lipid bilayer surrounding an aqueous compartment. A characteristic of SUVs is that a large amount of the total lipid, about 70%, located in the outer layer of the bilayer. Among theses liposome, the most frequently encountered and easily prepared liposomes are the multilamellar vesicles. Where SUVs are single compartment vesicles of a fairly uniform size, MLVs vary greatly in diameter up to about 30,000 nanometers and are multicompartmental in their structure wherein the liposome bilayers are typically organised as closed concentric lamellae with an aqueous layer separation each lamellar from the next. Large unilamellar vesicles are so named because of their large diameter which ranges from about 600 nanometres to 30 microns.[161]

It is not common for SUV's to be used due to their thermodynamic instability. Their small size and high surface area are a driving force to coagulation, being only kinetically stable for a relatively short time. GUV's make good cellular approximation, and

functional molecules can be either embedded into their membrane architecture (such as cholesterol) or encapsulated inside the plasma membrane itself (including the compound in the buffer during the hydration phase).

1.5.3 Introduction to Polydiacetylene Vesicles

1.5.3.1 Polydiacetylene Vesicles

Polydiacetylene (PDA) is a conjugated polymer with optical properties that are usually used for the detection of biological molecules. Due to its unique colour changing properties upon stimulation, PDA based sensors for the detection of biologically species have been intensively studied.[162-164] Closely packed and properly designed certain diacetylenes can undergo polymerisation via a 1,4-addition reaction to form an ene-yne alternated polymer chain upon UV irradiation with 254 nm as shown in figure 1.11. The diacetylene polymerisation occurs only when the material is in a highly ordered state. It requires an optimal packing of the diacetylenic units to allow propagation of the linear chain polymerisation through the ordered phase. The packing of monomers in a crystalline lattice is determined by the side groups attached to the diacetylene units and therefore can be controlled by choosing the appropriated substituents or headgroups, in the case of lipids. [165-166] The resulting polydiacetlenes appear to be intense blue colour to the naked eyes. The blue-coloured polydiacetylenes can be prepared in form of liposomes in aqueous solutions or as thin films using Langmuir-Blodgett or Langmuir-Schaefer methods due to their amphiphilic properties. [167] The main advantage of polydiacetylenes as biosensors comes from the fact that a visible colour change from blue to red occur in response to a variety of environmental change (figure1.11B), such as temperature,[168-169] pH,[170] and ligand-receptor interactions[171-172] or mechanical stress. The mechanism of colour transition is not clear, but it has widely been accepted that colour change is associated with a conformational change of the polydiacetylene backbone. The polydiacetylene in its blue form has extended conjugation of *p*-orbital in the main chain of the polymers. The conjugated *p*-orbitals undergo distortion by environmental stimuli, which leads to a partial twist, decreasing the overlap of the *p*-orbital. Therefore, the blue colour of the polymers can gradually shift to the red colour irreversibly depending on the extent of the stress.

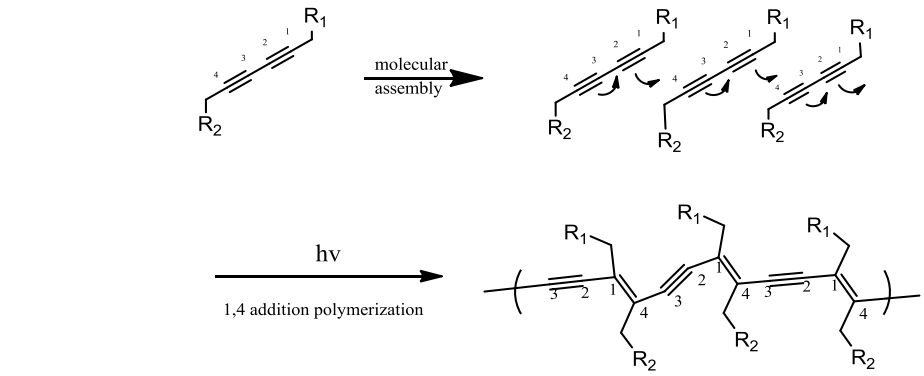

A

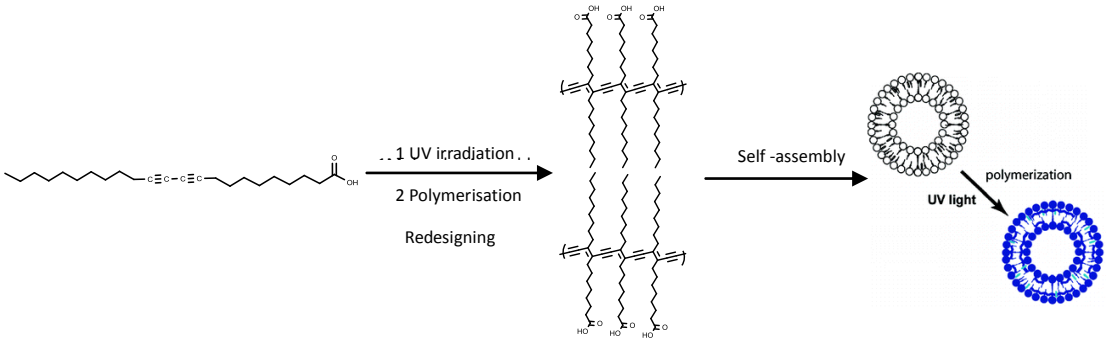

B

Figure 1.11: Schematic of polydiacetylene vesicle formation.
(A) Schematic representation of polymerisation of molecularly assembled functional diacetylenes by UV irradiation; (B) Schematic representation of the liposome prepared with 10, 12- tricosadiynoic acid (TCDA)

Diacetylene monomers for self-assembled materials consist of two parts: a polar headgroup and a hydrophobic tail containing the diacetylene moiety. Some representative monomers are shown in figure 1.12. The hydrophobic portion of the amphiphile is generally composed of a single alkyl chain, but can also have multiple chains with a diacetylene group in one or more chains. Each tail can be broken down into three parts: the diacetylene group, a spacer between diacetylene and the headgroup, and the terminal alkyl chain.[173] Each part of the diacetylene amphiphile plays an important role in deciding if the amphiphile can form self-assembled material or not. Headgroup chirality strongly influences colloidal structure; amphiphilic monomers with achiral headgroups usually form spherical liposomes, while chiral amphiphiles often form non-spherical structure such as helices and tubules. The number and the length of the tails influence the range of conditions under which an amphiphile will undergo self-assembly and the temperature of the melt transition (*Tm*) from 'crystalline' chain

packing to ‘liquid’ chain packing.

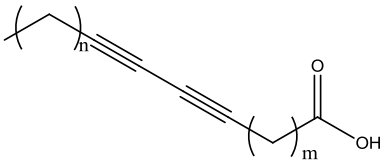

m, n	Abbreviation
0,15	2,4-HCDA
3,13	5,7-DCDA
4,12	6,8-DCDA
0,17	2,4-TRCDA
8,9	10,12- TRCDA
3,15	5,7 – TCDA
2,17	4,6 – PCDA

Figure 1.12: Diacetylene structures

1.5.3.2 Mixed Lipid/PDA Liposomes

One feature of PDA that makes it a promising biomimetic model is the rigid framework allowing incorporation of varied lipid constituents. Polydiacetylene vesicles are thermal stable at certain conditions after UV irradiation. This colorimetric platform consists of supramolecular aggregates of physiological lipid molecules such as DMPC embedded within a polydiacetylenic (PDA) lipid matrix (figure 1.13). One particularly important feature of lipid/PDA vesicle systems is the feasibility for incorporating a significant concentration of lipid constituents within the PDA matrix – up to 50% (mole ratio).[174] This construction is designed to better mimic the cell surface and is different from PDA systems both in structure and functionality. In fact, such mixed vesicle systems comprise distinct lipid domains embedded within the polymer framework that still retains its structural and chromatic properties.[175-176] Figure 1.13 presents a schematic description of lipid/PDA vesicles. Kolusheva[175] indicated that the lipids and polydiacteylene most likely form interspersed microscopic phases within the vesicles. The phospholipids incorporated in the PDA matrix adopt a bilayer structure, the dominant lipid organization within cellular membranes. The lipid components in the mixed vesicle system that form distinct bilayer domains are significant in the context of biological applications. Such vesicles could closely mimic the membrane surface of a cell. The utilisation of lipid/PDA vesicles for biological applications can be enhanced by incorporating within

the vesicles varied synthetic and natural phospholipids, glycolipids, lipopolysaccharides, cholesterol, or total membrane extracts, which can essentially mimic the lipid compositions of different membranes and cellular systems.[177]

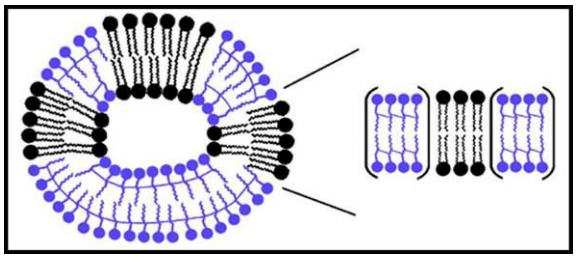

Figure 1.13: Structure of mixed lipid/PDA vesicle.
Blue part: cross-linked PDA bilayer; black part: lipid bilayer. [175]

1.6 Application of Liposomes --- As Drug Carriers

1.6.1 Lipid Vesicles/Liposomes

Antimicrobial treatment plays a major role in the treatment of patients' infection for decades. However, the failure of antimicrobial treatment is often encountered in the immunocompromised patients. There are several causes of failure of antimicrobial therapy including sub-effective drug concentrations at the infected site or the presence of barriers, low susceptibility of the microorganism to the applied antimicrobial agent, growing number of immunocompromised patients and sub-optimal treatment regimen because of unknown disease. A possible way to improve antimicrobial treatment is to formulate drugs into liposomes. Drug delivery could improve the therapeutic index by increasing control over the time, duration and site of drug action and by reducing side effects of potentially toxic antibiotics.[178-180] The ideal drug carrier should ensure the timely release of drug at the appropriate site and is neither toxic nor immunogenic, is biodegradable or easily excreted after action and is relatively cheap and stable upon storage. Liposomes possess many of these characteristics as described above.[181-182]

There have been several reports about the application of drug delivery based on liposomes.[183-184] These systems are known as nanocapsules and may include synthetic

elements to the leaflets. One example is the incorporation of polymers into the leaflets. Nanopartical systems responding to their local environments have been described with respect to certain applications. For example, a pH sensitive polymer-nanopartical which responds after the environment changes from pH 7.4 to pH 5; the polymers hydrolyse and the particles swell. The swelling compromises the membrane integrity and the encapsulated drug is then released, in this case paclitaxel, a chemotherapeutic agent used to indicate for lung cell carcinoma.[183] Another example is to use chitosan with the encapsulation of silver sulfadiazine. In this case the chitosan bursts and the antimicrobial is slowly released into the wound.[184] However, it is no longer advisable to use silver in such a way because recent research shows that to achieve a sufficiently antimicrobial environment a concentration of silver is required greater than the threshold for cytotoxicity.[12-13] The concept of encapsulating materials for the prevention of biofilm formation has been described, however, the use in wound dressings as an active response system was not addressed.[161] Liposome systems have shown to deliver drugs transdermally and to the lungs.[184-185] Liposomes *in vivo* have been shown to be less successful. They have to contend with the host immune systems which invariably recognise vesicles as a xenotopic entity.

1.6.2 Polydiacetylene Vesicles as Drug Carriers

The applications of liposomes for long-term, sustained release have been plagued by their insufficient morphological stability, susceptibility to acids, bases, or surfactants, and the resulting poor sustained- and controlled-released efficiency. Due to these issues, various polymerised vesicles with surfactant or lipid type have been investigated to overcome the instability problem.[186] The polymerised vesicles could maintain the shapes for an extended period of time, less susceptible to surfactant-induced disruption, and decrease the vesicle-vesicle fusion.[187]

Self-organised π-conjugated polydiacetylenes (PDA) are usually used as a platform for detection of biological analytes such as microorganisms, viruses and proteins. The

environmentally responsive chromic properties of the polymer, combined with self-assembled material formats, make these materials particularly attractive for biosensing applications. So far, the use of polydiacetylene vesicles alone or blended with liposome as drug carriers has rarely been studied. Compared with conventional liposomal formulations, polydiacetylene-phospholipid vesicles exhibit various advantages: (1) photoinduced polymerisation results in higher stability; (2) the conjugated backbone of polydiacetylene can be distorted upon exposure to pH, temperature and biorecognition, which can be used for stimuli-responsive drug controlled-release systems; (3) the degree of polymerisation along with the release of the entrapped drugs can be regulated by altering the proportion of diacetylene monomers.[188] Qin and his group developed partially polymerised liposomes composed of polydiacetylene lipids and saturated lipids.[189] The results showed that cross-linking of the diacetylene lipids prevents the drug leakage even at 40 ^{o}C for days and more than 70% of the encapsulated drugs can be instantaneously released by a laser that matches the plasmon resonance of the tethered gold nanoparticles on the liposomes.

1.7 Problem Statement & Aims

The re-emergence of bacterial infection of burn wound as a clinical problem in the late 20th century, after it was reportedly defeated by the widespread use of antibiotics, has triggered a growing interest in developing systems that either kill bacteria or prevent bacterial attachment and growth. Many bacteria can attach to surfaces, where they colonise and form complex communities (defined as biofilms) which are notoriously resistant to antibiotics. This has led to the development of antimicrobial coatings containing agents such as silver or quaternary ammonium cations (QCAs) that prevent or limit bacterial attachment and biofilm formation. However, it should be pointed out that there are some reports that the presence of silver ions in wounds can actively reduce wound healing, and that silver is cytotoxic at concentrations required for it to be an effective antimicrobial. Although they are functional in essence, they do not respond to their local environment, and operate whether bacteria are present or not. Therefore, there

is a need to develop a ‘smart’ wound dressing technology which can respond to the microbiological environment of the wound and give a colour response in the presence of pathogenic bacteria and will release an antimicrobial to kill/inhibit the growth of pathogenic bacteria only when required.

There are a number of drug delivery approaches that utilise nanocapsule technology. Vesicles have shown to be able to transfer drugs through skin [184] and to the lungs [190] as biomimetic model as their structure is similar to the structure of plasma membrane and they potentially have no harm to host cells. However, there are some critical issues for current liposomal carriers in clinical applications such as morphological instability, susceptibility to acids, bases, or surfactants, and the resulting poor sustained and controlled-release efficiency. In this work, a new liposomal system to achieve stability has been developed. The system is based on the polymerisable molecule, 10,12-tricosadiynoic acid (TCDA) (figure 1.11), in liposomes composed of phospholipids (DMPC,DMPE). The polymerisation of TCDA monomers occurs by UV irradiation, resulting in the formation of polydiacetylene-linkages. The focus of the stability study is to regulate the degree of polymerisation, hence the degree of stability of vesicle system by altering the TCDA proportion.

In this thesis, a microbiologically responsive nanocapsule system has been investigated for the potential use in burn wound dressings. Figure 1.14 outlines the experimental approach explored in this work. Two pathogenic bacteria have been used to be the agents of their own destruction by releasing toxins that rupture vesicles containing an antimicrobial agent and/or fluorescent dye. Non-pathogenic bacteria *E. coli* EH5α has been used for control system as it does not secrete any toxins. Pathogenic bacteria secrete membrane damaging toxins/enzymes that lyse the lipid membrane of vesicles which are attached to a treated surface. Antimicrobial agents and/or fluorescent dye will be released outside the vesicles to kill/inhibit bacteria growth. Meanwhile, vesicles conjugated fabrics will undergo a colour changing if a fluorescent dye is encapsulated inside.

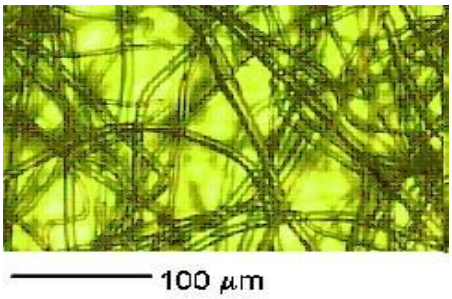

(a) Non-woven polypropylene textile material used in burn dressings: plasma/photografting modified the surface. Vesicles sprayed on and bound to fibers.

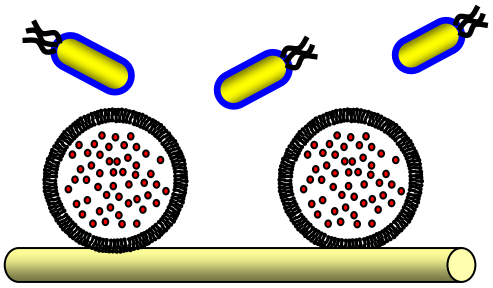

(b) Vesicles or partially polymerised vesicles attached to the modified surface covalently containing 'switched off' dye and antibiotic/antimicrobial.

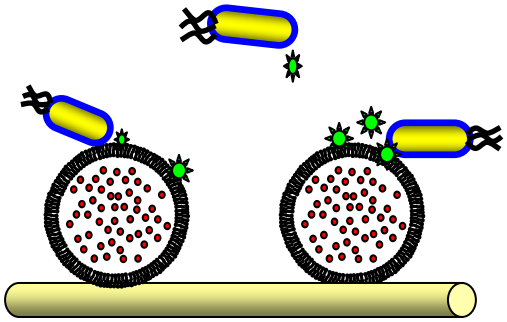

(c) Pathogenic bacteria secrete toxins and enzymes, some of which lead to lysis of vesicle wall.

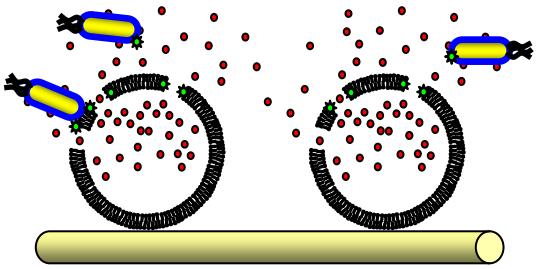

(d) Antimicrobial kills bacteria or encapsulated dye released

Figure 1.14: Schematic of responsive antimicrobial system showing an immobilised vesicle with encapsulated antimicrobial/fluorescent dyes.
Toxins secreted by pathogenic bacteria lyse the vesicle and release the antimicrobial, concomitantly killing the pathogenic bacteria.

1.8 References

1 UK Burn Injury Data 1986-2007. First Report of the Ibid www.ibid.org

2 National Burn Care Review. Standards and Strategies for Burn Care 2001.www.nbcg.nhs.uk/national-burn-care-review

3 Jenkins A.T.A., Young A., Smart dressings for the prevention of infection in paediatric burns patients, *Expert Rev. Anti Infect. Ther.*, 2010, *8*, 1-3.

4 Church D., Elsayed S., Reid O., Winston B., Lindsay R., Burn wound infections, *Clinical microbiology reviews*, 2006, *19*,403-434.

5 Mayhal C.G., The epidemiology of burn wound infections: then and now., *Clin. Infect. Dis.*,2003, *37*, 543-550.

6 Priti P., Patel M.D., *et al*. Topical antimicrobials in paediatric burn wound management. *J Craniofac Surg*., 2008, *19*,913-922.

7 Winter G.D., Nature, formation of the scab and the rate of epithelialization of superficial wounds in the skin of the young domestic pig, *Nature*, 1962, *193*, 293-294.

8 Carrougher G., Burn Wound Assessment and Topical Treatment, in Carrougher, G. (ed) *Burn Care and Therapy*, 1998, Mosby, Missouri, pp 133-165.

9 Pankhurst S., Pochkhanawala T., Wound Care, in Bosworth Bousfield, C. (ed) Burn Trauma Management & Nursing Care, 2002, 2nd edition, Whurr Publishers, London pp 81-108.

10 Richard J.W., Spencer B.A., McCoy L.F., Anticoat ™ versus Silverlon ®: the Truth, *J. Burns Surg Wound Care*, 2002,*1*, 11.

11 Sheridan R.L., Petras L., Lydon M.,Salvo P.M., Once-daily wound cleansing and dressing change: efficacy and cost, *J Burn Care Rehabil*, 1997, *18*, 139-140.

12 Cho Lee A.R., Leem H., Lee J., Park K.C., Reversal of silver sulfadiazine-impaired wound healing by epidermal growth factor, *Biomaterials*, 2005, *26*, 4670-4676.

13 Poon V.K.M., Burd A., In vitro cytotoxity of silver: implication for clinical wound care, *Burns*, 2004, *30*, 140-147.

14 Whitman W.B., Coleman D.C., Wiebe W.J., Prokaryotes: The unseen majority, *Proc. Nalt. Acad. Sci.* U.S.A., 1998, *95*, 6578-6583.

15 Hooper L.V., Gordon J.I., Commensal host-bacterial relationships in the gut, *Science*, 2001, *292*, 1115-1118.

16 Woese R.C., Kandler O., Wheelis M.L., Towards a natural system of organisms: proposal for the domains Archaea, Bacteria, and Eucarya, *Proc. Natl. Acad. Sci*.

U.S.A., 1990, *87*, 4576-4579.

17 Brock T.D., Madigan M.T., Martinko J.M., Parker J., Madigan M.T., Biology of microorganisms, 7th edition, Prentice-Hall, Inc.; Prentice-Hall, 1994.

18 Cabeen M., Jacobs-Wagner C., Bacterial cell shape, *Nat Rev Microbiol*., 2005, *3*, 601-610.

19 Young K., The selective value of bacterial shape, *Microbiol. Mol. Biol. Rev.*, 2006, *70*, 660-703.

20 Gram H.C., Über die isolierte Färbung der Schizomyceten in Schnitt- und Trockenpräparaten, *Fortschr. Med*., 1884, *2*, 185-189.

21 MacFarlane M.G., Knight B.C.J.G., The biochemistry of bacterial toxins: The lecithinase activity of Cl. Welchii toxins. *Biochem. J*., 1941, *35*, 884-902.

22 Hugenholtz P., Rogozin, Igor B., Grishin, Nick V., Tatusov, Roman L., Koonin, Eugene V., Exploring prokaryotic diversity in the genomic era, *Genome Biol*., 2002,3 (2): REVIEWS0003.

23 Walsh F., Amyes S., Microbiology and drug resistance mechanisms of fully resistant pathogens, *Curr. Opin. Microbiol*.,2004,*7*,439–744.

24 Image source: National Aeronautics and Space Administration-Locad Science

25 Sears C. L.,A dynamic partnership: celebrating our gut flora, *Anaerobe*, 2005, *11*, 247-251.

26 Lee P. S., Lee K. H., Escherichia coli---a model system that benifits from and contributes to the evolution of proteomics. Biotechnol Bioeng, 1999, *84*, 801-814.

27 Greenwood D., Slack R. C., Peutherer J. F., Medical Microbiology, CHURCHILL LIVINGSTONE 2006.

28 Emori T. G., Gaynes R.P., An overview of nosocomial infections, including the role of the microbiology laboratory, *Clin. Microbiol. Rev.*, 1993, *6*, 428-442.

29 Raad I., Hachem R., Zermeno A., Dumo M., Bodey G. P., In vitro antimicrobial efficacy of silver iontophoretic catheters , *Biomaterials*, 1996, *17*, 1055-1059.

30 Von Eiff C., Kohnen W., Becker K., Jansen B., Modern strategies in the prevention of implant-associated infections, *Int. J. Artif. Organs*, 2005, *28*, 1146-1156.

31 Richard M. J., Edwards J. R., Culver D.H., Gaynes R.P., Nosocomial infections in medical intensive care units in the United States National Nosocomial Infections Surveillance System. *Crit. Care Med*.1999, *27*, 887-892.

32 Verran J., Whitehead K., Factors affecting microbial adhesion to stainless steel and other materials used in medical devices,*Int. J. Artif. Organs*, 2005, *28*, 1138-1145.

33 Maki D.G., Tambyah P.A., Engineering out the risk for infection with urinary catheters, *Emerg. Infect. Dis*, 2001, *7*, 342-347.

34 Tzeng Y.L., Datta A., Kolli V.K., Carlson R.W., Stephens D.S., Endotoxin of Neisseria meningitidis composed only of intact lipid A: inactivation of the meningococcal 3-deoxy-D-manno-octulosonic acid transferase, *J. Bacteriol.*, 2002, *184*, 2379–2388.

35 Steward I., Schluter P.J., Shaw G.R., Cyanobacterial lipopolysaccharides and human health- a review, *Environmental Health: A Global Access Science Source*, 2006, *5*, 1-23.

36 Prof T., Fraser J.D., Bacterial superantigens, Clinical and Experimental Immunology, 2003,*133*, 299-306.

37 Kob M., Bacterial pyrogenic exotoxins as superantigens, *Clinical Microbiology Reviews*, 1995, *8*,411-426.

38 Information retrieved from Todar's textbook of online dictionary. http://textbookofbacteriology.net/proteintoxins.html

39 Sixma T.K., Pronk S.E., Kalk K.H., Wartna E.S., Van Zanten B.A.M., Witholt B., Hol W.G.J., Crystal structure of a cholera toxin-related heat-liable enterotoxin from *E.coli*, *Nature*, 1991, *351*,371-377.

40 Singh B.R., Li B., Read D., Botulinum versus tetanus neurotoxins: why is botulinum neurotoxin but not tetanus neurotoxin a food poison, *Toxicon,* 1995,*22*,1541-1547.

41 Bukowski M., Wladyka B., Dubin G., Exfoliative toxins of Staphylococcus aureus, *Toxins*, 2010,*2*, 1148-1165.

42 Gonzalez M.R., Bischofberger M., Pernot L., Van der Goot F.G., Freche B., Bacterial pore-forming toxins: the (w)hole story? *Cellular and Molecular Life Sciences*, 2008, *65*, 493-507.

43 Parker M.W., Feil S.C., Pore-forming protein toxins: from structure to function, *Progress in Biophysics and Molecular Biology,* 2005, *88*, 91-142.

44 Gennis R.B., Biomembranes: Molecular structure and function, Springer-Verlag, 1989.

45 Cabiaus V., Wolf C., Ruysschaert JM., International Journal of Biological Macromolecules, 1997, *21*, 285-298.

46 Olsnes S., Stenmark H., Moskaug JO., Madshus IH., Sandvig K., *Microb Pathog.*, 1990, *8*, 163-168.

47 Songer J.G., Bacterial phospholipases and their role in virulence, *Trends in*

Microbiology, 1997, *5*, 156-161.

48 Gupta R., Gupta N, Rathi P., Bacterial lipases: an overview of production, purification and biochemical properties, *Applied Microbiology and Biotechnology*, 2004, *64*, 763-781.

49 Goering R.V., Dockrell H.M. Zuckermann M., Wakelin D., Roitt I.M., Mims C., Chiodini P.L., Mim's medical microbiology, 4th Edition, Mosby Elisever Press, 2008.

50 Csoka A.B., Frost G.I., Stern R., The six hyaluronidase-like genes in the human and mouse genomes, *Matrix Biol.*, 2001,*20*,499-508.

51 Llewelyn M., Cohen J., Superantigens: Microbial agents that corrupt immunity, *Lancet Infect Dis.*2002, *2*, 156-162.

52 Alouf H.M., Carnoy C., Simonet M., Alouf J.E., Superantigen bacterial toxins: state of the art, *Toxicon*, 2001, *39*, 1691-1701.

53 Ulrich R.G., Bavari S., Olson M.A., Bacterial superantigens in human disease: structure, function and diversity, *Trends in Microbiology*, 1995, *3*, 463-468.

54 Schmitt C.K., Meysick K.C., O'Brien A.D., Bacterial toxins : friends or foes?, *Emerging Infectious Diseases*, 1999,*5*,224-234.

55 Hilderbrand A., Pohl M, Bhakdi S., *Staphylococcus aureus* α-toxin dual mechanisms of binding to target cells, *J. Biol. Chem.*, 1991, *266*,17195-17200.

56 Bantel H, Sinha B, Domschke W, Peters G, Schulze-Osthoff K, Jänicke RU , α-Toxin is a mediator of *Staphylococcus aureus*-induced cell death and activates caspases via the intrinsic death pathway independently of death receptor signaling, *J. Cell Biol, 2011*, 155, 637–48.

57 N.T.Thet, Modified tethered bilayer lipid membranes for detection of pathogenic bacterial toxins and characterisation of ion channels, PhD thesis, 2010.

58 Alouf J.E., Geoffrey C., The family of the antigenically related, cholesterol-binding ("sulphydryl-activated") cytolytic toxins. In: Alouf JE, Freer JH (ed) Sourcebook of bacterial protein toxins, 1991, Academic Press, New York London, pp 147-186.

59 Bhakdi S., Bayley H., Valeva A., Waleva A., Walker B., Weller U, Kehoe M., Palmer M., Staphylococcal alpha-toxin, streptolysin-O, and Escherichia coli haemolysin: prototypes of pore-forming bacterial cytolysins, *Arch Microbiol.*, 1996, *165*, 73-79.

60 Stanley P., Koronakis V., Hughes C., Acylation of Escherichia coli haemolysin: a unique protein lipidation mechanism underlying toxin function., *Microbiol. Mol. Biol. Rev.*, 1998, 62, *309-333*.

61 Bhakdi S., Tranum-Jensen J., Sziegoleit A., Mechanism of membrane damage by

streptolysin-O, *Infect Immun.*, 1985, *47*, 52-60.

62 Benz R., Schmid A., Wagner W., Goebel W., Pore formation by the Escherichia coli haemolysin: evidence for an association-dissociation equilibrium of the pore-forming aggregates. *Infect Immun.*, 1989, *57*, 887-895.

63 Song L., Hobaugh M.R., Shustak C., Cheley S., Bayley H., Gouaux J.E., Structure of staphylococcal alpha-haemolysin, a heptameric transmembrane pore., *Science*, 1996,*274*,1859.

64 Information retrieved from Wikipedia. http://en.wikipedia.org/wiki/Phospholipase_C

65 Lottenberg R, Minning-Wenz D, Boyle M.D., Capturing host plasmin(ogen): a common mechanism for invasive pathogens? *Trends Microbiol.* 1994, *2*, 20-24.

66 Harrington D.J., Bacterial collagenases and collagen-degrading enzymes and their potential role in human disease. *Infect. Immun*. 1996,*64*,1885-1891.

67 Christina R.H., Whitfield C., Lipopolysaccharide endotoxins, *Annual Review of Biochemistry*, 2002, *71*, 635-700.

68 Gennis R.B., Biomembranes: Molecular structure and function, Springer-Verlag, 1989.

69 Kuwabara Y., Maruyama M., Watanabe Y., Tanaka S., Takakuwa M., Tamai Y., Purification and some properties of membrane-bound phospholipase B from Torulaspora delbrueckii, *Journal of Biochemistry,* 1988, *104*, 236-241.

70 Vasudevan D.M., Sreekumari S., Textbook of biochemistry, 5th Edition.

71 Tiball R.W., Bacterial phospholipases C, *Microbiological Reviews*, 1993, *57*, 347-366.

72 McDermott M., Wakelam M.J.O., Morris A.J., Phospholipase D, *Biochemistry and Cell Biology*, 2004, *82*, 225-253.

73 Barth H., Aktories K., Popoff M.R., Stiles B.G., Binary bacterial toxins: Biochemistry, biology, and application of common Clostridium and Bacillus proteins, *Microbiology and Molecular Biology Reviews*, 2004, *68*, 373-402.

74 Pezard C., Berche P., Mock M., Contribution of individual toxin components to virulence of *Bacillus anthracis*, *Infection and Immunity*, 1991, *59*, 3472-3477.

75 Collier R.J., Diphtheria toxin: mode of action and structure, Bacteriological Reviews, 1965, 39, 54-85.

76 Brodsky W. A., Sadoff J.C., Durham J.H., Ehrenspeck G., Schachner M., Iglewski B. H., Effects of *Pseudomonas* toxin A, diphtheria toxin, and cholera toxin on

electrical characteristics of turtle bladder, *Proceedings of the National Academy of Sciences* U.S.A., 1979, *76*, 3562-3566.

77 Bell C.E., Eisenberg D., Crystal structure of diphtheria toxin bound to nicotinamide adenine dinucleotide, *Biochemistry,* 1996, *35*, 1137–1149.

78 Murphy J. R. (1996). Corynebacterium Diphtheriae*: Diphtheria Toxin Production* In: *Baron's Medical Microbiology* (Baron S *et al.*, eds.) *(4th ed.). Univ of Texas Medical Branch.*

79 Liu P.V., Extracellular toxins of *Pseudomonas aeruginosa*, *The journal of Infection Diseases*, 1974, *130*, S94-S99.

80 Endo Y., Tsurugi K., Yutsudo T., Takeda Y., Ogasawara T., Igarashi K., Site of action of a Vero toxin (VT2) from Escherichia coli O157: H7 and of Shiga toxin on eukaryotic ribosomes, *European Journal of Biochemistry*, 1988, *171*, 45-50.

81 Monick M.M., Huninghake G.W., Activation of second messenger pathways in alveolar macrophages by endotoxin, *European Respiratory Journal*, 2002, *20*, 210-222.

82 Sixma T.K., Pronk S.E., Kalk K.H., Wartna E.S., Van Zanten B.A.M., Witholt B., Hol W.G.J., Crystal structure of action and structure, *Bacteriological Reviews*, 1975, *39*, 54-85.

83 Aktories K., Rho proteins: targets for bacterial toxins, Trends in Microbiology, 1997, 5, 282-288.

84 De Haan L., Hirst T.R., Cholera toxin: a paradigm for multi-functional engagement of cellular mechanisms (Review), *Mol. Membr. Biol, 2004*, *21*, 77–92.

85 Popoff M. R., Poulain B., Bacterial toxins and the nervous system: neurotoxins and multipotential toxins interacting with neuronal cells, *Toxins*, 2010, *2*, 683-737.

86 Hall-Stoodley L., Costerton J.W., Stoodley P., Bacterial biofilms: from the natural environment to infectious diseases, *Nature Reviews. Microbiology*, 2004**,** *2*, 95–108.

87 Edwards R., Harding K.G., Bacterial and wound healing., *Curr. Opin. Infect. Dis*. 2004, *17,* 91-96.

88 Stoodley P., Sauer K., Davies D.G., Costerton J.W., Biofilms as complex differentiated communities, *Annu. Rev. Microbiol*., 2002, *56*, 187-209.

89 Stewart P. S., Costerton J.W., Antibiotic resistance of bacteria in biofilms, *Lancet*, 2001, *358*, 135–138.

90 O'Toole, G. A.;Kolter, R. Flagellar and twitching motility are necessary for *Pseudomonas aeruginosa* biofilm development,*Mol. Microbiol.*, 1998,*30*,295.

91 Costerton, J. W.; Stewart, P. S., Greenberg, E. P., Bacterial biofilms: A common cause of persistent infections, *Science,* 1999,*284*,1318-1322.

92 Ramsey, M. M.; Whiteley, M., *Pseudomonas aeruginosa* attachment and biofilm development in dynamic environments, *Mol. Microbiol.* 2004, *53*, 1075-1087.

93 Amano, A.; Nakagawa, I.; Hamada, Studying initial phase of biofilm formation: molecular interaction of host proteins and bacterial surface components. In *Biofilms*; Academic Press Inc: San Diego, 1999; Vol. 310, p 501.

94 Stewart P. S., Costerton J.W., Antibiotic resistance of bacteria in biofilms, *Lancet*, 2001, *358*,135-138.

95 DeBeer D., Stoodley P., Lewandowski Z., Effects of biofilm structures on oxygen distribution and mass transfer, *Biotech. Bioeng*., 1994, *43*, 1131-1138.

96 Monroe D., Looking for chinks in the armor of bacterial biofilms, *PLoS Biology*, 2007, *5*, 2458-2467.

97 Ceri, H., Olson, M. E., Stremick, C., Read, R. R., Morck, D., Buret, A., The Calgary Biofilm Device: new technology for rapid determination of antibiotic susceptibilities of bacterial biofilms, *J. Clin. Microbiol.* 1999, *37*, 177-1776.

98 Brown, M. R. W., Gilbert, P., Sensitivity of biofilms to antimicrobial agents, *Journal of Applied Bacteriology*, 1993, *74*, 87-97.

99 Davies, D., Understanding biofilm resistance to antibacterial agents. *Nat. Rev. Drug Discov.* 2003, *2*, 114-122.

100 Kumon H., Tomochika K., Matunaga T., Ogawa M., Ohmori H., A sandwich cup method for the penetration assay of antimicrobial agents through Pseudomonas exopolysaccharides. *Microbiol Immunol*, 1994, *38***,** 615–619.

101 Shigeta M., Tanaka G., Komatsuzawa H., Sugai M., Suginaka H., Usui T., Permeation of antimicrobial agents through *Pseudomonas aeruginosa* biofilms: a simple method, *Chemotherapy* 1997, *43*, 340–345.

102 Gordon C.A., Hodges N.A., Marriott C., Antibiotic interaction and diffusion through alginate and exopolysaccharide of cystic fibrosisderived *Pseudomonas aeruginosa*. *J Antimicrob Chemother*, 1988, *22*, 667–674.

103 Nichols W.W., Dorrington S.M., Slack M.P.E., Walmsley H.L. Inhibition of tobramycin diffusion by binding to alginate, *Antimicrob Agents Chemother.* 1988, *32*, 518–523.

104 Brown, M. R. W., Allison, D. G.,Gilbert P., Resistance of bacterial biofilms to antibiotics: a growth-rate related effect, *Journal of Antimicrobial Chemotherapy*

1988, *22*, 777-789.

105 Poering A. L., Lewis K., Biofilms and planktonic cells of *Pseudomonas aeruginosa* have similar resistance to killing by antimicrobials, *Journal of Bacteriology,* 2001, *183*, 6746–6751.

106 Brooum S., Liu S., Lewis K., A dose-response study of antibiotic resistance in Pseudomonas aeruginosa biofilms, *Antimicrob Agents Chemoter*, 2000, *44*, 640-646.

107 Bigger J. W., Treatment of staphylococcal infections with penicllin by intermittent sterilisation, *Lancet*, 1944, *244*, 497-500.

108 Tack K.J., Sabath L.D., Increased minimum inhibitory concentrations with anaerobiasis for tobramycin, gentamicin, and amikacin, compared to latamoxef, piperacillin, chloramphenicol, and clindamycin. *Chemotherapy*, 1985, *31*, 204–210.

109 Prigent-Combaret C., Vidal O., Dorel C., Lejeune P., Abiotic surface sensing and biofilm-dependent regulation of gene expression in *Escherichia coli*., *Bacteriol* 1999, *181*, 5993–6002.

110 Research on microbial biofilms (PA-03-047), NIH, National Heart, Lung, and Blood Institute. 2002-12-20.

111 Rogers A.H., Molecular Oral Microbiology, *Caister Academic Press*, 2008, pp. 65–108.

112 Imamura Y., Chandra J., Mukherjee P.K., *et al.* Fusarium and Candida albicans biofilms on soft contact lenses: model development, influence of lens type, and susceptibility to lens care Solutions, *Antimicrobial Agents and Chemotherapy* , 2008, *52*, 71–82.

113 Davis S.C., Ricotti C., Cazzaniga A., Welsh E., Eaglstein W.H., Mertz P.M., Microscopic and physiologic evidence for biofilm-associated wound colonisation in vivo, *Wound Repair and Regeneration*, 2008, *16* ,23–29.

114 Trafny E.A., Susceptibility of adherent organisms from *Pseudomonas aeruginosa* and *Staphylococcus aureus* strains isolated from burn wounds to antimicrobial agents. *Int J. Antimicrob. Agents*, 1998, *10*, 223-228.

115 Cornelis P., Pseudomonas: Genomics and Molecular Biology (1st ed.), *Caister Academic Press*, 2008, pp. 159–176.

116 Steinstraesser L., Oezdogan Y., Wang S.C. , Steinau H.U., Host defense peptides in burns. *Burns*, 2004, *30*, 619-727.

117 Nizet V., Ohtake T., Lauth X., Trowbridge J., Rudistill J., Dorschner R.A., Pestonjamasp V.,Piraino J., Huttner K., Gallo R.L., Innate antimicrobial peptide protects the skin from invasive bacterial infection. *Nature* 2001, *414*, 454-457.

118 Erol S., Altoparlak U., Akcay M.N., Celebi F.,Parlakm M.,Changes of microbial flora and wound colonisation in burned patients. *Burns*, 2004, *30*, 357-361.

119 Wysocki A.B., Evaluating and managing open skin wound: colonisation versus infection. *AACN Clin. Issues*, 2002, *13*, 382-397.

120 Barret J.P., Herndon D.N., Effects of burn wound excision on bacterial colonisation and invasion. *Plast. Reconstr. Surg*. 2003, *111*, 744-750.

121 Manson W.L., Klasen H.J., *Sauer* E.W., *Olieman* A., Selective intestinal decontamination for prevention of wound colonisation in severly burned patients:a retrospective analysis, *Burns*, *18*, 98-102.

122 Gibson C.D., Thompson W.C., The response of burn wound staphylococci to alternating programs of antibiotic therapy, *Antibiot. Annu.*,1995, *3*, 32-34.

123 Burdge J.J., Rea F., Ayers L., Noncandidal, fungal infections of the burn wound. *J. Burn Care Rehabil*.,1998, *9*,599-261.

124 Desai M.H., Herndon D.H., Eradication of Candida burn wound septicaemia in massively burned patients, *J. Trauma*, 1998, *28*, 140-145.

125 Ekenna O., Sherertz R.J., Bingham H., Natural history of bloodstream infections in a burn patient population : the importance of candidemia. *Am. J. Infect. Control*, 1993, *21*, 189-195.

126 Bang R.L., Gang R.K., Sanyal S.C., Mokaddas E.M., Lari A.R., Beta-haemolytic Streptococcus infection in burns. *Burns*, 1999, *25*, 242-246.

127 Lesseva M., Girgitzava B.P., Bojadjiev C., Beta-haemolytic streptococcal infections in burned patients. *Burns*, 1994, *20*, 422-425.

128 Altoparlak U.S., Akcay M.N., Celebi F., Kadanali A., The time-related changes of antimicrobial resistance patterns and predominant bacterial profiles of burn wounds and body flora of burned patients, *Burns*, 2004, *30*, 660-664.

129 Agnihotri N., Gupta V., Joshi R.M., Aerobic bacterial isolates from burn wound infections and their antibiograms—a five-year study, *Burns*, 2004, *30*, 241-243.

130 Church D., Elsayed S., Reid O., Winston B., Lindsay R., Burn wound infections, *Clinical Microbiology Reviews*, 2006, *19*, 403-434.

131 Clark N.M., Patterson J., Lynch J.P., Antimicrobial resistance among gram negative organisms in the intensive care unit, *Curr. Opin. Crit. Care*, 2003, *9*,

413-423.

132 Chitkara Y.K., Feierabend T.C., Endogenous and exogenous infection with *Pseudomonas aeruginosa* in a burns unit, *Int Surgery,* 1982, *66*, 237-240.

133 Hsueh P.R., Teng L.J., Yang P.C., Chen Y.C., Ho S.W., Luh K.T., Persistence of a multidrug-resistant *Pseudomonas aeruginosa* clone in an intensive care burn unit, *J. Clin Microbiol*, 1998, *36*, 1347-1351.

134 Bielecki P., Glik J., Kawecki M., Santos V.A.P.M., Towards understanding *Pseudomonas aeruginosa* burn wound infections by profiling gene expression, *Biotechnol. Lett.*, 2008, *30*, 777-790.

135 Bush K., Antimicrobial agents. *Curr. Opin. Chem. Biol*., 1997, 1, 169-175.

136 Schiffelers R.M., Bakker-Woudenberg I.A.J.M., Innovations in liposomal formulations for antimicrobial therap., *Expert Opin. Ther. Patents,* 2003, *13*, 1127-1140.

137 Moulds R.F., Jeyasingham M. S.,Gentamicin: a great way to start, *Australian Prescriber,* 2010, *33*, 134–135.

138 Noronha C., Almeida A., Local *burn* treatment--topical antimicrobial agents, *Annal. Burns Fire Disast.*, 2000, *13*, 216-219.

139 Fraser J.F., Cuttle L., Kempf, M., Kimble R.M., Cytotoxicity of topical antimicrobial agents used in burn wound in Australasia. *ANZ J. Surg,* 2004, *74*, 139-212.

140 Wright J.B., Hansen D.L.,Burrell R.E., The comparative efficacy of two antimicrobial barrier dressings: in vitro examination of two controlled release of silver dressings, *Wounds*, 1998, *10*, 179-188.

141 Fu-Ren F., Fan Allen J., Bard chemical, electrochemical gravimetric, and microscopic studies on antimicrobial silver films, *Phys Chem B* 2001, *106*, 279-287.

142 Monafo W.W., Freedman B., Topical therapy for burns, *Surg. Clin. North Am.*, 1998, *64*, 133-145.

143 Atiyeh B.S., Costagliola M., Hayek S.N., Dibo S.A., Effect of silver on burn wound infection control and healing: review of the literature, *Burns*, 2007, *33*, 139-148.

144 Cooper, M.L., Laxer J.A., and Hansbrough J.E., The cytotoxic effects of commonly used topical antimicrobial agents on human fibroblasts and keratinocytes. *J. Trauma.*, 1991, *31*, 775-782.

145 Leitch, I. O., Kucukcelebi, A., and Robson, M. C., Inhibition of wound contraction by topical antimicrobials. *Aust. N. Z. J. Surg.*1993, *63*, 289-293.

146 McCauley, R. L., Li, Y. Y., Poole, B., Evans, M. J., Robson, M.C., Heggers, J. P., Hemdon, D. N., Differential inhibition of human basal keratinocyte growth to silver sulfadiazine and mafenide acetate. *J. Surg. Res.*, 1992, *52*, 276-285.

147 Siuda J. F., Cihonski C. D., New compounds: carbamate derivatives of mafenide homosulfanilamide, *J. Pharm. Sci.*1972, *61***,** 1856–1857.

148 Monafo W.W., Avyazaian V.H., Topical therapy, *Surg. Clin. North Am.*, 1978, *58*, 1157-1171.

149 Shelanski H.A., *U.S. patent*. *2739922*, 1956.

150 Pietsch J. Meakins J.L., Complications of povidone-iodine absorption in topically treated burn patients, *Lancet*, 1976, *1*, 280-282.

151 Gentamicin: Drug Information Provided by Lexi-Comp: Merck Manual Professional

152 Moyer C.A., Treatment of large human burns with 0.5% silver nitrate solution, *Arch Surg*.,1965, *90*, 812-867.

153 Shuck J.M., Moncrief J. A., Monafo W.W., The management of burns: I. General considerations and the sulfamylon method. II. The silver nitrate method, *Curr Probl Surg*, 1969, *6*, 3-65.

154 The most common topical antimicrobials, *Care of the umbilical cord*. World Health Organization.1998.

155 Kuyyakanond T., Quesnel L.B., The mechanism of action of chlorhexidine, *FEMS Microbiol Lett.*, 1992, *79*,211–215.

156 Vaandrager A.B., Van der Wiel E., Hom M.L., Luthjens L.H. and de Jonge H.R. Heat-stable enterotoxin receptor/guanylyl cyclase C is an loigomer consisting of functionally distinct subunits, which are non-covalently linked in the intestine. *J. Biol. Chem*., 1992, *269*, 16409-16415.

157 V. Cabiaus, C. Wolff and J-, M.Ruysschaert, Interaction with a lipid membrane: a key step in bacterial toxins virulence, International Journal of Biological Macromolecules, 1997, *21*, 285-298.

158 Cornell B.A., Braach-Maksvytis V.L.B., King L.G., Osman P.D.J., Raguse B., Woeczorek L., Pace R.J., A biosensor that uses ion-channel switches.,*Nature*, 1997, *387*, 580-583.

159 Image retrieved from Webster online dictionary:

http://www.websters-online-dictionary.org/definitions/Cell%20membrane

160 Bangham, A.D. and Horne, R.W., Negative staining of phopholipids and their structured modification by surface active agents as observed in the electro microscope, *J. Mol. Biol*.1994, *8*, 660-668.

161 Tamilvanan S., Venkateshan N., Ludwig A., The potential of lipid- and polymer-based drug delivery carriers for eradicating biofilm consortia on device-related nosocomial infections, *J. Control. Release*, 2008, *128*, 2-22.

162 Okada S.Y., Jelinek R., Charych D., Induced color change of conjugated polymeric vesicles by interfacial catalysis of phospholipase A_2, *Angew. Chem. Int. Ed.*, 1999, *38*, 655-659.

163 Berman A., Ahn D.J., Lio A., Salmeron M., Reichert A., Charych D., Total alignment of calcite at acidic polydiacetylene films: cooperativity at the organic-inorganic nterface, *Science*, 1995, *269*, 515-518.

164 Kolusheva S., Shahal T., Jelinek R., Cation-selective color sensors composed of ionophore-phospholipid-polydiacetylene mixed vesicles, *J. Am. Chem. Soc*., 2000, *122*, 776-780.

165 Bloor D., Chance R.R., Polydiacetylenes synthesis, structure and electronic properties, Martinus Nijhoff Publishers: Dordrecht/Boston/Lancaster, 1985, 102.

166 Shostakovskii M.F., Bogdanova A.V., The chemistry of Diacetylenes, John Wiley & Sons: New York, Toronto, 1974.

167 Eun-Kyung J., Dong J.A., Jong-Man K., The fluorescent Polydiacetylene Liposomes, *Bull. Korean Chem. Soc.*, 2003, *24*, 667-668.

168 Beckham H.W., Rubner M.F., On the origin of thermochromism in cross-polymerised diacetylene- functionalized polyamides, *Macromolecules*, 1993, *26*, 5198-5201.

169 Hankin S.H.W., Downey M.J., Sandman D.J., On the structural origins of solid-state urethane polydiacetylene thermochromism-thermal and structural properties of ipudo monomer and polymer, *Polymer*, 1992, *33*, 5098-5101.

170 Cheng Q., Stevens R.C., Charge-induced chromatic transition of amino acid-derivatized polydiacetylene liposomes, *Langmuir*, 1998, *14*, 1974-1976.

171 Cheng Q., Stevens R.C., Coupling of an induced fit enzyme to polydiacetylene thin films: colorimetric detection of glucose, *Adv. Mater*. 1997, *9*, 481-483.

172 Cho J.T., Woo S.M., Ahn D.J., Ahn K.D., Lee H., Kim J.M., Cyclodextrin-induced color changes in polymerised diacetylene langmuir-schaefer films, *Chem. Lett*.,

2003, *32*, 282.

173 Reppy M.A., Pindzola B.A., Biosensing with polydiacetylene materials: structures, optical properties and applications, *Chem. Commun.*, 2007, *42*, 4317-4338.

174 Jelinek R., Kolusheva S., Biomolecular sensing with colorimetric vesicles, *Bulletin of the Israel Chemical Society*, 2008, *23*, 6-11.

175 Kolusheva S., Wachtel E., Jelinek R., Biomimetic lipid/polymer colorimetric membranes: molecular and cooperative properties, *J. Lpid Res.*, 2003, *44*, 65-71.

176 Jelinek R., Kolusheva S., Polymerised lipid vesicles as colorimetric biosensors for biotechnological applications, *Biotechnol. Adv.* 2001, *19*, 109-118.

177 Shai Y., Mechanism of the binding,insertion and destabilisation of phospholipid bilayer membranes by helical antimicrobial and cell non-selective membrane-lytic peptides, *Biochimica et Biophysica Acta*, 1999, *1462*, 55-70.

178 Schreier H., Preface, technology: physical, chemical and biological methods, Shreier H (Ed.), Marcel Dekker, New York, USA (2001): iii-ix

179 Duncan R, Where are we now and where are we going? *J. Drug Target*, 1997, *5*, 1-4.

180 Miller G., Breaking down barriers, *Science*, 2002, *297*, 1116-1118.

181 Brandl M., A technological approach. Biotechnol. Ann. Rev., 2001, *7*, 59-85.

182 Allen T.M., Opportunities in drug delivery, *Drugs*, 1997, *54*, 8-14.

183 Griset A.P., Walpole J., Liu R., Gaffey A., Colson Y.L., Grinstaff M.W., Expansile nanoparticles: synthesis, characterisation, and *in Vivo* efficacy of an acid-responsive polymeric drug delivery system, *J. Am. Chem. Soc.*, 2009, *131*, 2469-2471.

184 Bouwstra J.A., Honeywell-Nguyen P.L., Skin structure and mode of action of vesicles, *Adv. Drug Deliv. Rev.*, 2002, *54*, 41-55.

185 Lu B., Zhang J.Q., Yang H., Non phospholipid vesicles of carboplatin for lung targeting, *Drug Deliv.*, 2003, *10*, 87-94.

186 Fendler J.H., Polymerised surfactant aggregates: novel mem- brane mimetic systems, *Science*, 1984, *223*,888-894.

187 Sisson T.m., Lamparski H.G., Kollchens S., Elayadi A., O'Brien, D.F., Cross-linking polymerisations in two-dimensional assemblies, *Macromolecules*, 1996, *29*, 8321-8329.

188 Guo C.X., Liu S.Q., Jiang C., Li W.Y., Dai Z.F., A promising drug controlled-release system based on diacetylene phospholipid olymerized vesicles,

Langmuir, 2009, *25*, 13114-13119.

189 Qin G., Li Z., Xia R., Li F., O'Nell B.E., Goodwin J.T., Khant H.A., Chiu W., Li K.C., Partially polymerised liposomes: stable against leakage yet capable of instantaneous release for remote controlled drug delivery, *Nanotechnology*, 2011, *22*, 155605-155611.

190 Lu B., Zhang J.Q., Yang H., Lung-targeting microspheres of carboplatin, *Int. J. Pharm.*, 2003, *265*,1–11.

Chapter 2 Instrumentation and Theory

2.1 Fundamentals of Plasma Polymerisation and Surface Modification

Plasma polymerisation is a unique technique to fabricate thin polymer films (100 Å-1 μm) from a variety of organic and organometallic starting materials. Plasma polymerised films are highly crosslinked and therefore are insoluble, thermally stable, chemically inert and mechanically tough. In addition, such films are often highly coherent and adherent to a variety of substrates including conventional polymer, glass and metal surfaces. Due to excellent properties they have been used in last few years for a variety of applications such as permselective membranes,[1-2] protective coatings,[3] biomedical materials,[4] optical devices [5-7] and adhesion promoters[8], plasma polymerisation technique is employed in this work for surface modification, on which the vesicles can covalently bonded.

Low-pressure plasma polymerisation is an ultimately green process, in which a minimum amount of material is used and actually no effluent results from the process. Low-pressure plasma polymerisation is a useful and economical tool for nanofilm coatings which is quite friendly to the environment. It is reported that the functionalisation of solid surfaces for biocompatibilisation has been a challenging task for interdisciplinary research bordering between materials and life sciences. While plasma polymers have commonly been associated with protective coatings, diffusion barriers, optical applications, and abrasion resistance, more recently there has been increased interest in the chemistry of these coatings with the aim to maximise the retention of the functional groups present within the monomer structure.[9]

2.1.1 Main Sources of Gas Discharge Plasmas

The plasma state is a mixture of electrons, negatively and positively charged particles, and neutral atoms and molecules. Plasmas have been described as the fourth state of matter, which is more highly activated than in solid, liquid or gas state. Three factors are required for plasma generation: (1) an energy source for ionisation, (2) a pumping

system to maintain the plasma state; vacuum or atmospheric, (3) and a reaction chamber. This energy source can be used to initiate polymerisation. The mechanism of plasma polymerisation is complex and is not well understood.[10] However the use of plasma in this study is to deposit an activating layer of grafting compounds onto a fabric which means that the explicit processes of plasma initiated organic gas polymerisation is beyond the scope of this study.[11]

Plasma can also be created by other conditions by transferring power from an electric field to electrons or by applying intense heat to a state of matter.[1, 12-14] In most cases, a direct current (DC) glow discharge is attained by passing electric current through a gas under low pressure. The cathode is bombarded with positive ions, resulting in the generation of secondary electrons. These electrons are accelerated away from the cathode until they gain sufficient energy to ionise the gas molecules or atoms that collide with the electrons.

Another way to create glow discharge is by using alternating current. The frequency of alternation is important. At a low frequency, it can be regarded as a DC discharge with changing polarity. The positive ions become immobile upon increasing the frequency of the applied voltage since they can no longer follow the periodic changes in field polarity, and therefore respond to time-averaged fields. A frequency of about 50-100 kHz is sufficient to provide a continuous discharge. At radio frequency (r_f, 13.56 MHz), no contact between the electrodes and the plasma is required. The plasma can be initiated and sustained by external inductive electrodes.

2.1.2 The Plasma Polymerisation Mechanism

The concept of this polymerisation is that elemental reactions occurring in plasma polymerisation are the fragmentation of monomer molecules, the formation of active sites (radicals) from the monomer, and recombination of the activated fragments to form a polymer. H. Yasuda described this process as the rapid step growth of polymers due to fragmentation of monomers, which occurs in a glow discharge region.[1, 15-16] This process is attributed to the various types of collisions simultaneously or separately in the reaction chamber. The starting molecules for plasma polymerisation are not restricted to unsaturated compounds. Saturated compounds can also deposit plasma polymers. The

fragmentation of starting molecules in plasma is represented by two types of reactions, namely the elimination of the weakly bonded hydrogen atom and the scission of the C-C bond.

(a) Hydrogen elimination

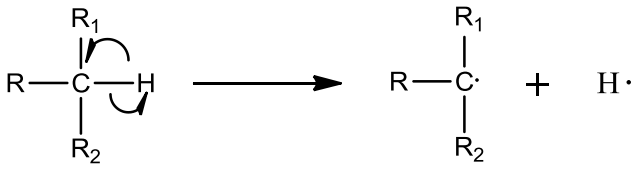

(b) C-C bond scission

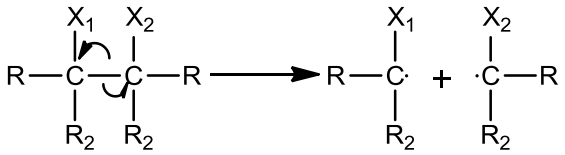

Hydrogen elimination is considered to contribute greatly to the polymer-forming process in plasma polymerisation. The gas phase of a closed system after plasma polymerisation of hydrocarbons is mainly composed of hydrogen as reported by Hillman and co-workers.[17]

Figure 2.1 shows an essential polymer forming process as proposed by H. Yasuda, which can be related to the elimination of hydrogen and scission of C-C bonds. When hydrogen atoms are eliminated from monomer molecules by plasma to form mono-radicals M_i ; and bi-radicals $\dot{M}_k$; and therefore, the addition of the radicals to monomer and the recombination between two radicals proceeds to make large molecules with or without radical. Mono-radicals $M_i \cdot$ add to the monomer to form a new radical M_j-M : Mono-radical $M_i \cdot$ may combine $M_j \cdot$ to form a neutral or stable molecules M_i-M_j. A bi-radical can also attack the monomer to form a new bi-radical $\dot{M}_k$-M ; or recombine with another bi-radical to form a new bi-radical $\dot{M}_k$-M_j : The new monomer M_i-M_j is activated by plasma to form mono- or bi-functional activated species. The cycle (i) is the repeated activation of the reaction products from mono-functional activated species, cycle (ii) shows the recombination of the mono and bi-radical to form larger radicals.

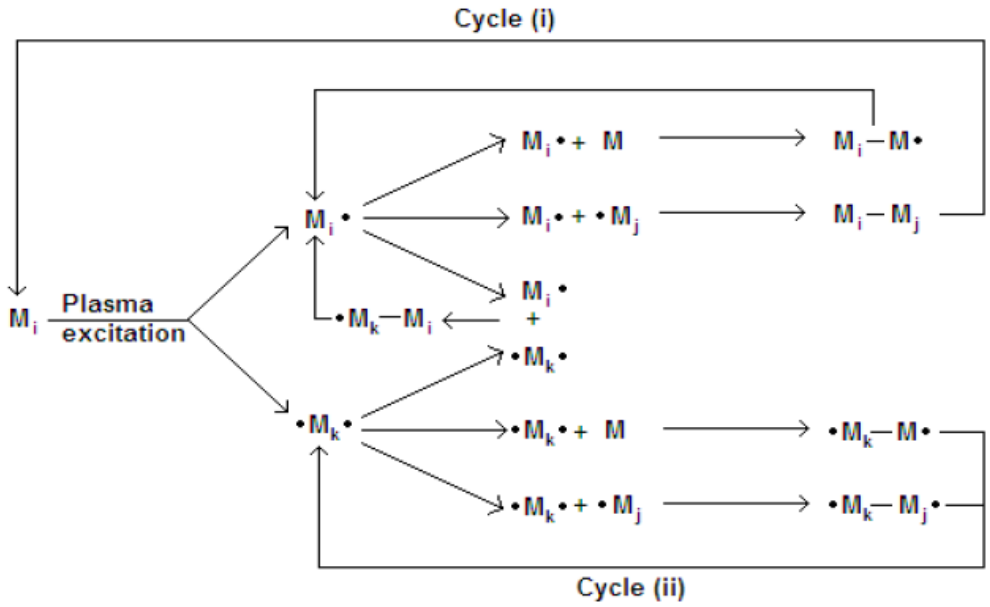

Figure 2.1: Overall plasma polymerisation mechanism showing a bi-cyclic step-growth.[4]

Plasma polymerisation in this work was done using a home-made reactor which belongs to the A.T.A.Jenkins research group at the University of Bath and can be seen in figure 2.2.

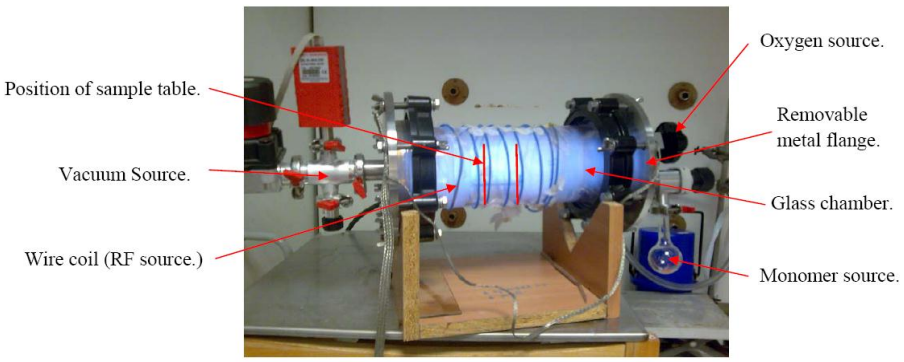

Figure 2.2: Home-made plasma reactor

The reactor is schematically represented by figure 2.3. The reaction chamber (centre) is kept under high vacuum (10^{-2} mbar), with organic vapour allowed to flow from the Youngs flask. The substrate is immobilised in the reaction chamber and the plasma is ignited using RF power via the copper wire wrapped around the chamber (blue). Oxygen may be supplied to etch substrates for cleaning purposes or to activate a surface prior to deposition.

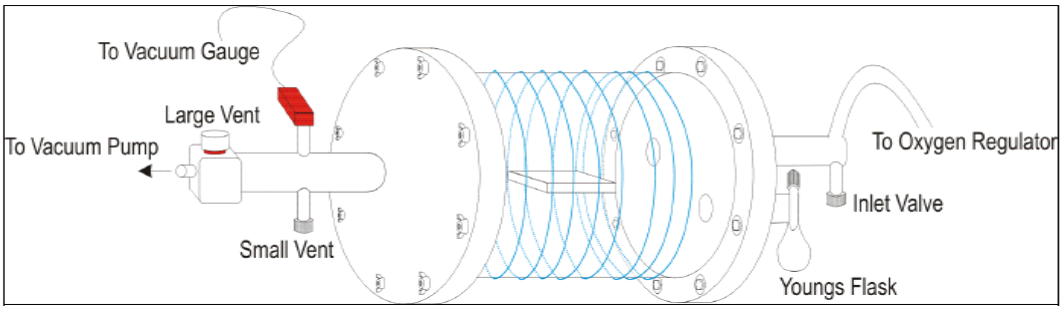

Figure 2.3: Diagram of a plasma reactor.

The Plasma Reactor can be used to form an oxygen plasma for cleaning gold electrode surfaces. The general procedure is detailed in the appendix. The reactor can also be used to oxidise a gold surface or to form polymers on a surface (the monomeric unit being introduced *via* the Young's Flask)

The structure of the deposition is determined by many factors. The input power can be oscillated on and off during deposition, thus a lower incidence of bombardment from ions and radiation provides an overall lower particle temperature. The off time cycle allows for recombination processes that are unavailable in the high energy continuous wave mode allowing more time for binding to substrates.[11, 18-19] The flow of the monomer from the Youngs flask to the reaction chamber also impacts on film chemistry. Homogenous films are obtained at higher flow rate (low pressure) and heterogeneous films with lower flow rate (high pressure). Flow rate can be calculated by measuring the change in pressure over a time when the vacuum chamber is isolated via equation 2.1. This equation also provides an indication of the volatility of a monomer. In addition some empirical parameters also have impacts on the film chemistry which include position in reactor, flow rate under the vacuum, volume of plasma glow and substrate temperature. It is found that positioning substrates downstream of the centre of the plasma glow allows better control of film chemistry.

$$\chi = \frac{dn}{dt} = \left(\frac{P_f - P_s}{\Delta t}\right)\left(\frac{V}{RT}\right) \qquad (2.1)$$

In this equation, χ is the flow rate in cm^3 sec^{-1} when Δt is time in seconds, V the volume (litres), R the gas constant, T temperature (K) and P_s and P_f are the start and final pressures (mbar).

2.1.3 Plasma Reactor

Home-made plasma reactor was used in this work with help from Dr. Stuart Fraser of the

University of Sheffield based on the design explained by Bullett et al [20] (figure 2.2).

The reactor comprises a Pyrex cylindrical tube, 30 cm long and 10 cm in diameter. The reactor had a round stainless steel flange at either end. Substrates were positioned at an optimised point for deposition according to the conditions and monomer used. The system was kept under vacuum by an Edwards RV5 pump (ca. 10^{-2}mbar). Gases for reactor cleaning or film tailoring (e.g. oxygen) were fed in via a gas control valve and monomer vapour allowed to flow from the Youngs tap. The rate of gases was controlled by adjustment of the tap and/or external heat applied to the monomer chamber. Power was supplied by a 13.56 MHz RF coaxial system and connected to the reactor via a coil of solid copper wire of 2 mm diameter and was earthed through the electrodes or vacuum line. A manual matching network was used to adjust input impedance so that maximum power was transferred from the generator to the load. The RF power supply was introduced in CW or pulse mode by using a pulse generator. An oscilloscope was used to alter the width and amplitude of the pulse which allows high levels of control over reaction conditions.

2.2 Fluorescence [21]

2.2.1 Principles of Fluorescence

Luminescence is the emission of light from any substance and is divided into two categories, fluorescence and phosphorescence. Both fluorescence and phosphorescence involve a transition from an electronically excited state to the ground state.[21] In a singlet excited state the excited electron has the opposite spin to an electron in the ground state orbital, therefore when the excited electron moves to the ground state the transition is spin allowed. Therefore these transitions occur rapidly (ca. 10^8 s^{-1}); this is fluorescence and has a life time of about 10 ns. In phosphorescence an electron is in an excited triplet state and has the same spin as an electron in the ground state orbital. The transition for the electron to move back to the ground state is spin forbidden and therefore occurs over a long time period (rate ca. 10^3-10^0 s^{-1}) with a life time of milliseconds to seconds. [21]

Fluorescence is a well described and exploited phenomenon. Fluorophores often exhibit strongly delocalised electrons in conjugated double bonds or aromatic systems. The

schematic Jablonski energy level diagram is the usual way to explain the absorption and emission of fluorescence and phosphorescence. A Jablonski diagram is shown in figure 2.4.

VR = Vibrational Relaxation
ISC = Inter System Crossing
IC = Internal Conversion

T = Triplet State
S = Singlet State

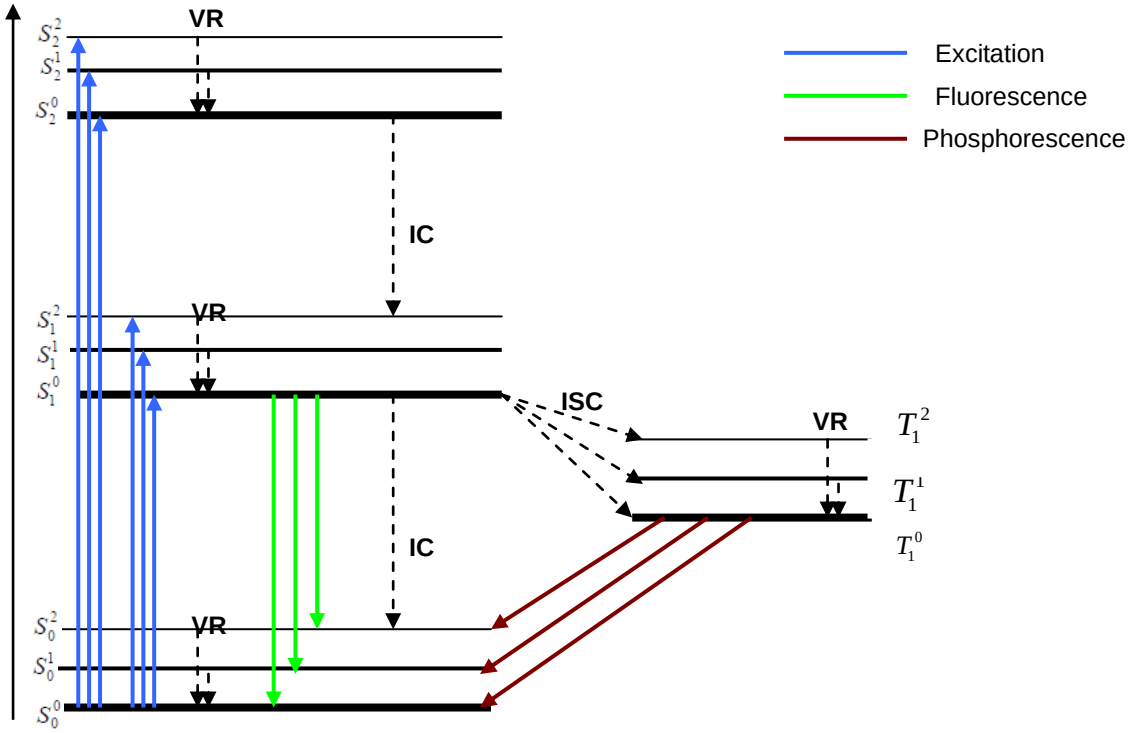

Figure 2.4: Excitation and relaxation of molecules due to absorption and emission of light.
Absorption of light is followed by vibrational relaxation (VR) or radiationless internal conversion (IC) between electronic states. The superscripts of the electronic states represent the vibrational quantum numbers of the various vibrational sublevels. Return to the ground state from S_1^0 can be proceed by internal conversion, fluorescence (F) or intersystem crossing to the lowest triplet state (T_1). The triplet state is deactivated by phosphorescence (P) or radiationless intersystem crossing.

Excitation of a fluorophore is induced by absorption of electromagnetic wave energy of specific quanta. An electron can be excited to the higher excited energy levels of S_1 or S_2 and rapidly relaxes and returns to the ground state (S). An electron at an excited state will undergo vibrational relaxation (VR) from a vibrational level returning to the lowest vibrational level within an exited state. This process is called internal conversion and is a

non radiative decay pathway. This process generally occurs in 10^{-12} s or less which is much more quickly than fluorescence (10^{-8} s). Therefore, fluorescence occurs from the lowest excited state (S_1^0) (Kasha's law). From this exited state (S_1^0) the molecule can decay to any of the vibrational states of the ground electronic state ($S_0^{1,2,3.....}$) by emitting photons at a rate of κ_F.

The transition between two states of the same spin multiplicity is a quantum mechanically allowed process and the rate of emission is typically high at $\tau\ 10^{-8}$ s. Stokes' shift, the spectra of fluorescence emission to a lower wavelength (red shift) relative to absorption, is a way to compare the difference between absorption and emission in energy. This shift can be explained by energy losses between the two processes due to the rapid internal conversion in the excited states (S_1, S_2) and the subsequent decay of the fluorophore to higher vibrational levels of S_0. The Stokes' shift allows differentiation between excitation and emission energies such that discrete wavelengths can be used to excite systems and measure emission allowing isolation of the emitted photons and exciting photons (figure 2.5).

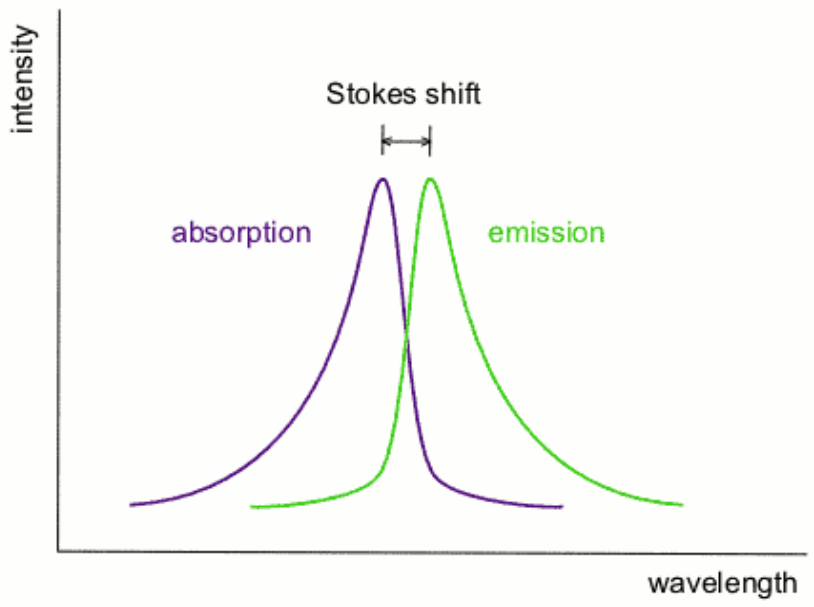

Figure 2.5: Spectra of Stokes' shift.

The peaks occur at the $S_0^x - S_1^y$ transition energies, the difference in energy illustrates the Stokes' shift of

a fluorophore. The specific transition between $S_0^0 - S_1^0$ would be expected to be at the same energy as no vibrational relaxation occurs. However if energy is lost due to solvent collisions and the surroundings, in the gas phases this energy difference is reduced. [21-22] (Image source is from free Wikipedia)

Generally the fluorescence emission spectrum appears to be a mirror picture of the absorption spectra due to the same transitions that are involved in both processes and the similarities among the vibrational levels of S_0 and S_1. However, exceptions do exist due to excited state reactions and geometric differences between electronic ground states and exited states. Kashsa's law explains this: all excitation from S_0^0 to any level greater than S_1^0 will decay extremely rapidly to S_1^0 and so all emission will occur from this level. Again there are some exceptions in molecules with different absorption/emission in different ionised forms. Some molecules also fluoresce from the S_2^0 state, but these molecules are rare and have not been found in biological systems.

Quantum yield and fluorescence lifetime are two main characteristics that describe a fluorophore. The quantum yield is defined as the ratio of emitted photons to the number of photons put into the system. Starting from the excited state S_1 the fluorophore can not only dissipate its energy by fluorescence emission with the rate κ_F, but several other radiationless decay channels can be found that lead to a depopulation of S_1. Electronic transition to triplet states by intersystem crossing (ISC) as well as quenching processes (κ_Q) and resonant energy transfer (κ_{ET}) result in a decrease of the fluorescence quantum yield, which is defined as in equation (2.2)

$$Q = \frac{\kappa_F}{\kappa_F + \kappa_0} \tag{2.2}$$

In this equation, Q is quantum yield, κ_F is the rate of fluorescence and κ_0 is the rate of internal conversion from the first electronic excited state to the ground state.

This is equivalent to the ratio of the number of emitted photons over absorbed ones. The rate constant κ_0 combines all possible radiationless decay channels including internal conversion losses (κ_{IC}).

$$\kappa_0 = \kappa_{ISC} + \kappa_{IC} + \kappa_Q + \kappa_{ET} \tag{2.3}$$

Fluorescence lifetime τ is defined as the average time that a molecule spends in the excited state before return to the ground state. The general value for this property is around 10ns.

$$\tau = \frac{1}{\kappa_F + \kappa_0} \tag{2.4}$$

In addition the environment of the fluorescent species such as polarity of the solvent or pH may influence intensity and the wavelength of emitted fluorescence. The interaction with the fluorophore's dipole and chemical reactions between the dye and solvent molecules such as hydrogen bonding, charge transfer and ionisation can also have impact on fluorescence intensity. The solvent effects are used to explore the environment in which the fluorophore exists particularly in complex biological systems. Some heavy atoms such as iodine and bromine can result in poor quantum yields. In the following section, quenching will be discussed.

2.2.2 Fluorescence Quenching

Fluorescence intensity can be reduced by a number of processes, for example complex formation, energy transfer, excited state reactions or collision of molecules. The energy that has been absorbed can be dissipated without fluorescence occurring. Such processes are called fluorescence quenching and can occur via multiple mechanisms. Collisional quenching occurs when the excited-state fluorophore is deactivated upon contacting with other molecules in solution, which is called quencher. Static quenching happens when the fluorophore and the quencher form a nonfluorescent complex through collisional quenching. The decrease in intensity is described by Stern-Volmer equation.

$$\frac{I_0}{I} = 1 + \kappa_Q \tau_0 [Q] = 1 + \kappa_D [Q] \tag{2.5}$$

In this equation, I and I_0 are the fluorescence intensities of the quenched and unquenched fluorophore respectively. κ_D is the Stern-Volmer quenching constant, κ_Q is the bimolecular quenching constant, τ_0 is the unquenched lifetime and $[Q]$ is concentration of quencher. Quenching data are usually plotted as I_0/I versus $[Q]$. The ratio of such value is expected to give a linear dependence. However, if a quencher forms a non fluorescent complex with fluorophore, this is known as static quenching. Deviations from linearity can be described by equation 2.6.

$$\frac{I_0}{I} = 1 + \kappa_S [Q] \tag{2.6}$$

In this expression, κ_S is the association constant for the fluorophore-quencher complex. Mechanisms of energy transfer, chemical reaction and oligomerisation can lead to quenching and the exact process varies between systems. For example, carboxyfluorescein which is used in the thesis will self quench at high concentrations.

2.3 Instrumentation for Characterisation and Visualisation of Vesicles

2.3.1 Fourier-transform Infra-red Spectroscopy

Following synthesis of plasma polymerisation in this work, identification of polymer composition is required. In this section, FT-IR will be employed to detect the characterisation of plasma deposition for pp-MA and to provide an evidence of vesicles attachment onto deposited films.

FTIR requires the change in dipole moment of a molecule upon vibration. The compound is recognised if an antisymmetric stretch occurs, or the bending of a bond results in departure of the dipole moment from zero. An infrared spectrum represents a fingerprint of a sample with absorption peaks which correspond to the frequencies of vibrations between the bonds of the atoms making up the material. Hence such bonds as N-H, C=O, C-N can be applied to use in functional group characterisation.

IR spectroscopy is based on specific absorption of a photon by photo-excitation. If a photon of infra-red radiation of frequency ν is absorbed which matches the separation in vibrational levels, the molecule is excited to a higher vibrational level. Bonds vibrate at certain energy and therefore an IR spectrum may be obtained by measuring percentage transmission or absorption of an IR beam against wavenumber after data processing (Fourier-transform). The chemical composition may then be determined by from this spectrum.[23-24] Therefore the frequency of the vibrations can be associated with a particular bond type. A Perkin-Elmer FT-IR spectrum 100 spectrometer with an ATR attachment was used during this work to indentify the covalent bond formation after vesicles attached to pp-MA modified non-woven polypropylene.

2.3.2 Fluorescent tagging

A fluorescent dye may be encapsulated in both phospholipid vesicles and polydiacetylene/phospholipid vesicles in order to identify their presence and/or their interaction with pathogenic bacteria over time. Such dyes utilise the principle of fluorescence which has been described in section 2.2.

2.3.2.1 Fluorescence Spectroscopy

A spectrofluorometer is an instrument which can both excite fluorophores and detect emission of fluorescence. The emission is normally recorded as the intensity versus wavelength which is called emission spectra. A sample is bombarded by a high intensity of light source which allows the maximum number of molecules to be in the excited state at any point in time. The light is passed through either a filter or a monochromator to select a fixed wavelength to use as the exciting light. The emission is collected at 90 degree to the exciting light and beam is then passed through either a filter or a monochromator before being detected. A BMG Labtech microplate reader was used as the spectrofluorometer in this work which is shown in figure 2.6. The multifunctional plate reader covers a full range of wavelength from 230 to 900 nm for both excitation and emission by integrating a high intensity xenon flash lamp. It can detect both fluorescence intensity and UV/Vis absorbance. The emission/excitation maximum for the fluorescence used in this work is 488/510 nm. This technique was employed for measuring vesicle leakage when bacteria were inoculated in vesicle solution

(self-quenched fluorescent dye encapsulated) in terms of fluorescence intensity increasing over time.

Figure 2.6: FLUOstar Omega microplate reader

2.3.2.2 Fluorescence Microscopy

Light microscopy can be adapted to utilise fluorescence in visual representation of cell viability. Ultraviolent is the light source in fluorescence microscopy. Fluorophores are excited similarly to fluorescence spectroscopy and emit photons which can be viewed optically. [25] The excitatory light is passed from above (or for inverted microscopes, from below), through the objective and then onto the specimen instead of passing it first through the specimen. The fluorescence in the specimen gives rise to emitted light which is focused to the detector by the same objective that is used for the excitation. A filter between the objective and the detector filters out the excitation light from fluorescent light. Since most of the excitatory light is transmitted through the specimen, only reflected excitatory light reaches the objective together with the emitted light and this method therefore gives an improved signal to noise ratio (figure 2.7). This method was used to take images of giant unilamellar vesicles attaching onto plasma- and non-treated surfaces post bacterial attachment. The fluorescence microscope used here was a Nikon eclipse TE2000-S epi-fluorescence microscope.

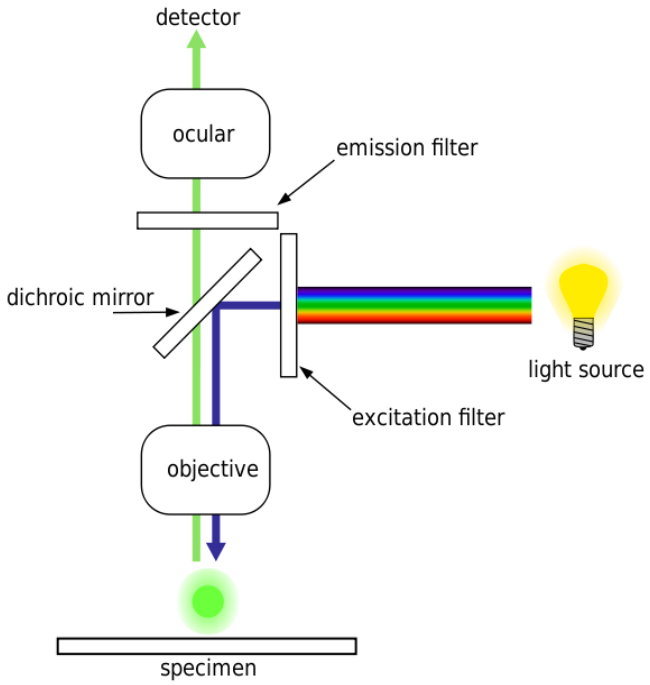

Figure 2.7: Schematic of fluorescence microscope [26]

2.3.3 Scanning Electron Microscopy (SEM)

The scanning electron microscope (SEM) was used to visualise the surface structure of the vesicle conjugated plasma deposited surface. SEM uses a focused beam of high-energy electrons to generate a number of signals at the surface of solid specimens. Theses signals result from interactions of the electron beam with atoms at or near the surface of the sample. These signals of interactions reveal information about the sample such as external morphology (texture), chemical composition, and other properties such as conductivity. Data are generally collected over a selected area of the surface of the sample. Areas ranging from approximately 1 cm to 5 microns in width can be imaged in a scanning mode with conventional SEM techniques which allows magnification ranging from 20 x up to 30,000 x and 50 to 100 nm in spatial resolution. [27-30]

There are many types of signals produced by an SEM such as secondary electrons, back-scattered electrons (BSE), characteristic X-rays, visible light (cathodoluminescence) and heat. Secondary electrons are the main means of viewing

images in SEM and can produce high resolution images of a surface sample which can reveal details less than 1 nm in size. The SEM micrographs can produce a characteristic three-dimensional appearance which provides a useful tool to understand the surface structure of a sample due to the very narrow electron beam, thus having a large depth of field. Back-scattered electrons (BSE) are beam electrons that are reflected from the sample by elastic scattering. The images produced by BSE can provide information about the distribution of different elements in the sample because the intensity of BSE signal is associated with atomic number (Z) of the sample. Therefore, BSE are often used in analytical SEM along with the spectra made from the characteristic X-rays. Characteristic X-rays are produced when the electron beam removes from the sample to an inner shell electron and cause a higher energy electron to fill the shell and release energy. X-rays are often used to identify the composition and measure the abundance of elements in the sample. [25] A scanning electron microscope (SM6480LV) was used in this work to explore the structure after polydiacetylene vesicles have been attached onto a pp-MA polypropylene surface. Diagrams of typical electron microscopes are detailed in figure 2.8.

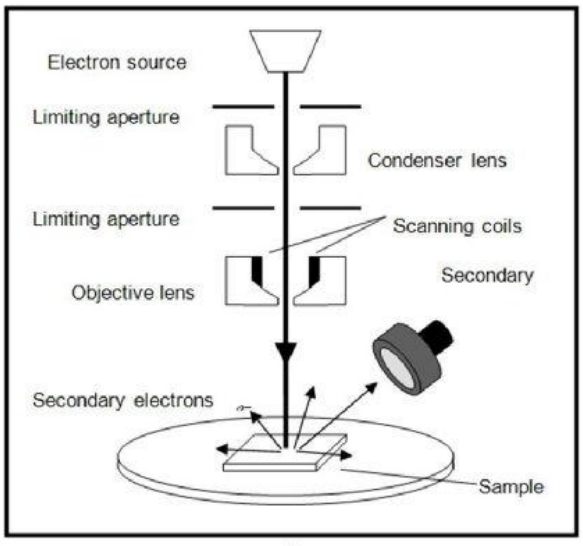

Figure 2.8: Schematic diagram of a SEM;
A vacuum source is generally provided to reduce the free path of electrons. The source of electrons is generally a tungsten filament or lanthanum hexaboride. Sample should be coated with an electrically conductive material e.g. gold.

2.3.4 UV-Vis Spectroscopy

UV-Vis spectroscopy refers to absorption spectroscopy or reflectance spectroscopy in the ultraviolet-visible spectral region. In this region of the electromagnetic spectrum, molecules will undergo electronic transitions from one energy level to higher energy level. When molecules are exposed to light having an energy which matches a possible electronic transition within the molecule, some of the light energy will be absorbed as the electron is promoted to a higher energy orbital. An optical spectrometer will record the wavelength at which absorption occurs with degree of absorption at specific wavelength. The resulting spectrum may be presented as a graph of transmittance ($T = I/I_0$) or absorbance ($A = \log I_0/I$) versus wavelength. If no absorption occurs, T=1.0 and A = 0. A corrected absorption value as the molar absorptivity is often used to compare the spectra of different compounds using Beer-Lambert law:

$$A = \log_{10} (I_0/I) = \varepsilon c L \quad (2.7)$$

(Where A = absorbance, I_0 = intensity of the incident light at a given wavelength, I = transmitted intensity, L = the length of light path through the sample in cm, c = the sample concentration in moles/litre, ε = molar absorptivity or extinction coefficient)

Molar absorptivity is a fundamental molecular property in a given solvent, at a particular temperature and pressure and is useful when comparing the spectra of different compounds and determining the relative strength of light absorbing functions (chromophores).

The spectrometer used in this work to determine the absorbance of conjugated polydiacetylene/phospholipid vesicles at specific wavelength was BMG Labtech microplate reader which has been introduced in section 2.3.2.1. This technique was also used to determine bacterial viability/growth in terms of optical density when they were inoculated in vesicle solution (antimicrobial/fluorescent dye encapsulated within the vesicles), which will be described in microbiological assay.

2.4 Microbiology

Microbiology refers to the study of organisms that are too small to be seen by naked eyes.[32] This includes eukaryotes such as fungi and protista, and prokaryotes, which are bacteria and archaea. Microbes can be grouped into three categories according to DNA

structure: Bacteria, Archaea, and Eukarya. The former two kingdoms have prokaryotic cell structure, which has been presented in previous chapter, the latter eukayotic cell structure having a more advanced form of cell. Three main methods for detecting bacterial growth will be presented in this section.

2.4.1 Bacteria Used in the Work

Pseudomonas aeruginosa (PAO1), *Staphylococcus aureus* (MSSA 476) are used in work and *Escherichia coli* (DH5α) as a control system, hence the three species of bacteria will be detailed in the thesis.

2.4.1.1 *Pseudomonas aeruginosa*

Pseudomonas aeruginosa (*P.aeruginosa*) is a gram-negative, aerobic rod measuring 0.5 to 0.8 μm by 1.5 to 3.0 μm which belongs to the family Pseudomonadaceae (figure 2.9). The bacterium is commonly found in soil and water, or regularly on the surfaces of plants or occasionally on the surfaces of animals. Typical Pseudomonas bacterium in nature is found in a biofilm which is attached to some surfaces or substrates, or in a planktonic form. This bacterium is quite tolerant to a wide range of physical conditions, including temperature, for example, its optimum temperature for growth is 37 degrees, and it is also able to grow at temperature as high as 42 degrees. In addition, it is resistant to high concentration of salts and dyes, weak antiseptics, and many commonly used antibiotics. *P. aeruginosa* isolates may produce three colony types according to published results. Natural isolates from soil or water generally produce a small, rough colony, while clinical samples generally produce one or another of two smooth colony types. One is a fried-egg appearance which is large, smooth, with flat edges and an elevated appearance; another type has a mucoid appearance which is generally from respiratory and urinary tract secretions. It is estimated that the smooth and mucoid colonies play a role in colonisation and virulence. *P.aeruginosa* produces a variety of pigments, including the fluorescent pigment pyoverdine, blue pigment pyocyanin, and red-brown pyorubin. Pyocyanin is produced a lot in media of low-iron content and functions in iron metabolism in the bacterium. Pyocyanin is also a characteristic of suppurative infections caused by *P. aeruginosa*.

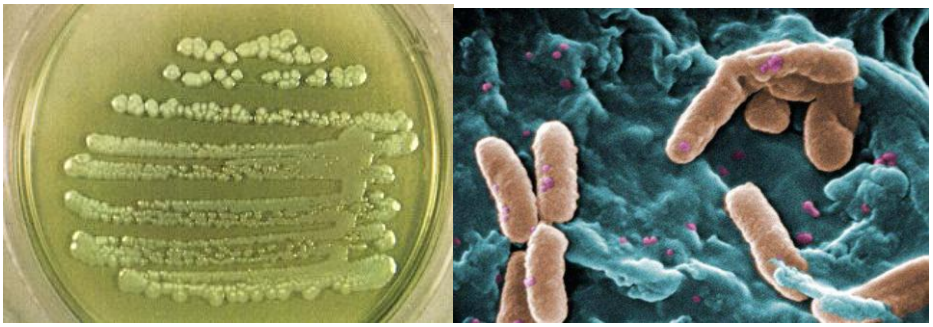

A B

Figure 2.9: *P. aeruginosa* colonies on an agar plate and its micrograph in SEM.
(A) *P.aeruginosa* colonies on agar; [33] (B): False colour SEM (9560 x) of *Pseudomonas aeruginosa* (Image Source: Carr J. H., in MRSA_PHIL #10046 and PAO1_PHIL#10043, Public Health Image Library.)

P. aeruginosa has been increasingly considered as an emerging opportunistic pathogen of clinical relevance. *Pseudomonas aeruginosa* is an opportunistic pathogen which means that it almost never infects uncompromised tissues, but it can cause infection if the tissue defenses are compromised in some manner. It generally causes urinary tract infections, respiratory system infections, dermatitis, soft tissue infections, bacteremia, bone and joint infections, gastrointestinal infections and systemic infections, especially in patients with severe burns and in cancer and AIDS patients who are immunosuppressed. It is found that almost one in ten hospital-acquired infections are from Pseudomonas, for example the infection is a serious problem in patients hospitalised with cancer, cystic fibrosis, and burns. This major nosocomial pathogen has a low antibiotic susceptibility and is intrinsically resistant to a great number of antibiotics including all penicillins with the exception of certain ureidopenicillins.[34] This resistance results from the action of multi drug efflux pumps with genetically encoded antibiotic resistance as well as the low permeability of the cellular envelope. *P. aeruginosa* also acquires resistance by the action of genetic mutation and horizontal gene transfer of antibiotic determinants. Biofilms of *P. aeruginosa* can cause chronic opportunistic infections. This kind of infection is a serious problem for medical care, particularly in immunocompromised patients and the elderly. The infection is hard to treat effectively with traditional antibiotic therapy because biofilms as presented above seem to protect these bacteria from adverse environmental factors. This will require better clinical management of chronically infected patients and should lead to the development of new drugs.[34]

P. aeruginosa (PAO1) is used in the study as the gram-negative model.

2.4.1.2 *Staphylococcus aureus*

Staphylococcus aureus (*S. aureus*) is a gram positive, facultative anaerobic and cluster –forming coccus (figure 2.10). *S. aureus* is nonmotile and non-spore forming, catalase and coagulase positive.[35] Typical colonies are yellow to golden yellow in colour. *S. aureus* can cause haemolysis when grown on blood agar plates.[35] Gram-positive means that the bacterium retains crystal violet dye because of its cell wall construction. This type of bacterium lacks the outer lipopolysaccharide wall which can be normally found in gram negative but has thicker peptidoglycan layer. *S. aureus* is mainly present in nasal passages and regularly can be found on skin surfaces, oral cavity and gastrointestinal tract. Although it is usually harmless at these sites, it may get into the body through breaks in the skin such as abrasions, cuts, wounds *et al.* and cause infection. Therefore, *S. aureus* is considered as an important nosocomial and community – acquired pathogen and is the most common cause of hospital acquired infection. It is responsible for a range of illnesses from skin infections (impetigo, boils and sores) to lethal infections such as cellulitis, meningitis, endocarditis, toxic shock syndrome (TSS) and bacteremia to name a few. Toxic shock syndrome is a severe systemic illness and a complication of burn injury. It is a rare but serious type of blood poisoning caused by toxin-producing Staphylococcus and Streptococcus bacteria. TSS has a high risk of patient mortality, particularly in paediatric patients. It is known that unrecognised and untreated TSS in paediatric burn patients can lead to extremely high mortality which is up to 15-20%.[36] Some strains of *S. aureus* are usually responsible for TSS because they produce exotoxin TSST-1 which is the causative agent of toxic shock syndrome.

The treatment for *S.aureus* infection is penicillin. However, most strains of *S. aureus* are now resistant to β-lactam antibiotics including penicillins, carbapenems and cephalosporins.[37] This is because *S. aureus* can produce a substance called "β-lactamase" which can degrade penicillin and destroy its antibacterial property. Following the introduction of methicillin (a new type of penicillin antibiotic which was not degraded by β-lactamase and was used as an effective antibiotic to treat infections), certain strains of *S. aureus* showed resistant to methicillin. These methicillin–resistant *S.aureus* became known as "MRSA" for short although methicillin is no longer

prescribed and have been replaced by fluocloxacillin, which is a better penicillin-type antibiotic that is also not affected by β-lactamase, and the term "MRSA" continues to be used. Figure 2.10 shows a colony of MRSA under scanning electron microscope and MRSA infection on a patient skin.

Methicillin susceptible *S. aureus* (MSSA 476) is used in the study as the gram positive model.

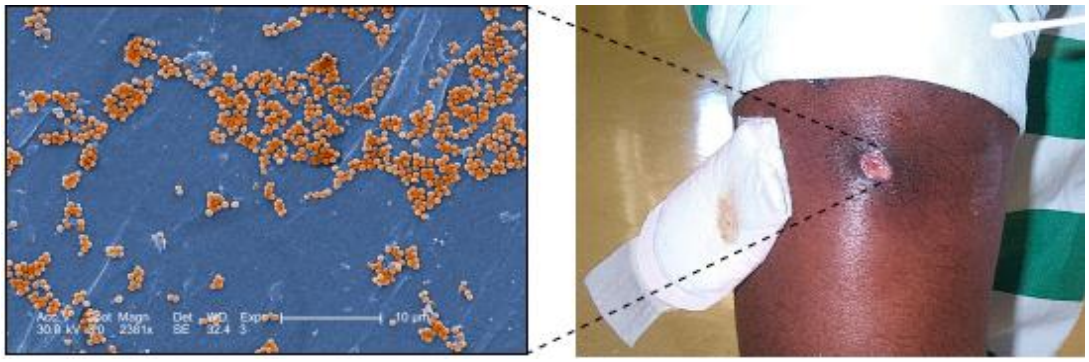

Figure 2.10: Micrograph of *S.aureus* in SEM and wound infection caused by MRSA.
Left: scanning electron micrograph (SEM) of a colony of MRSA magnified 2381 times. Right: an abscess is shown on the knee of a prison inmate caused by MRSA [38] (image source: Centre for Disease Control and Prevention, http://phil.cdc.gov/phil)

2.4.1.3 *Escherichia coli*

Escherichia coli (*E.coli*) is a gram-negative, non-sporulating, facultative anaerobic bacterium with an average size of 2 μm by 0.5 μm [39] (figure 2.11). The bacterium can survive on a wide variety of surfaces but is commonly found in the lower intestine of warm-blooded organisms in endotherms. Most of *E.coli* strains are harmless and they are a part of gut flora and can benefit their hosts by production of vitamin K and also they can prevent the establishment of pathogenic bacteria within the intestine.[40-41] However, some virulent strains of *E. coli* are responsible for a range of illnesses, such as gastroenteritis, urinary tract infections, and neonatal meningitis. In some cases, virulent strains can even cause haemolytic-uremic syndrome, peritonitis, mastitis, septicaemia and gram-negative pneumonia.[42] Pathogenic strain O157: H7 is notorious for causing serious and even life-threatening complications such as haemolytic-uremic syndrome. The mechanism of infection includes the common pilus attachment and then the release of a phage encoded shiga toxin which can induce a severe inflammatory response and haemolysis.[42-43]

It is comparatively simple to culture and manipulate the genetics of *E. coli* which makes it a popular prokaryotic gram negative model. *E. coli* DH5*α* is a non-pathogenic bacterium to normal healthy individuals and has been used in the laboratory for many years and most of its virulent factors have been removed, leaving no virulence factors. Therefore, *E. coli DH5α* is used in this work as non-pathogenic control bacteria.

Figure 2.11: False colour SEM (× 22,000) of hemorrhagic *E. coli* O256:H7 [43]

2.4.2 Methodology of Detection for Bacteria

Bacteria can be cultured in aqueous or solid media by inoculation of the media with a small amount of cells. Most bacteria have individually defined minimum, maximum and optimum growth temperatures which range from -10^{o} C to over 80^{o}C. The majority of pathogenic bacteria tend to have an optimum of 37^{o}C, or human body temperature. Equally, bacteria can grow in a range of oxygen concentrations, pH and water content. Also, bacteria can be tagged with a fluorescent dye in order to identify their presence and/or viability. Such dyes utilise the principle of fluorescence, which is evidenced by decay of short lived excited states in an atom or molecule through the emission of a photon.

2.4.2.1 Basics of Bacterial Growth

Bacteria grow to a fixed size and then reproduce by a process of binary fission, which is a form of asexual reproduction.[44] The nutrient and the temperature play an important

role in the growth and reproduction of a bacterium. Therefore, with sufficient nutrients and optimum temperature, bacteria can grow and reproduce very well. It is estimated that bacteria can grow and divide rapidly and bacterial populations can double as quickly as every 9.8 minutes under optimal conditions.[45] In laboratories, bacteria are generally grown or cultured using solid (agar plates or slopes) or stirred liquid medium (broth) in an incubator at 37 ^{o}C. Solid media such as agar plates are used to isolate pure cultures of a bacterial strain. Liquid growth media are used when large amount of cells are required. As bacteria reproduce, the resulting cells are genetically identical to their mother cells if no mutation occurs during growth.

Under ideal conditions, the growth of a population of bacteria occurs in several stages termed lag, log (exponential), stationary, and death. During the lag phase, active metabolic activity occurs involving synthesis of DNA and enzymes, but no growth. Geometric population growth occurs during the log or exponential phase, when metabolic activity is most intense and cell reproduction exceeds cell death. The measurement of an exponential bacterial growth curve in batch culture was traditionally a part of the training of all microbiologists; the basic method requires bacterial enumeration (cell counting) by direct and individual (microscopic, flow cytometry),[46] direct and bulk (biomass), indirect and individual (colony counting), or indirect and bulk (most probable number, turbidity, nutrient uptake) methods. Following the log phase, the growth rate slows and the production of new cells equals the rate of cell death. This period, known as the stationary phase, involves the establishment of an equilibrium in population numbers and a slowing of the metabolic activities of individual cells. The stationary phase reflects a change in growing condition such as a lack of nutrients and/or the accumulation of waste products. When the rate of cell deaths exceeds the number of new cells formed, the population equilibrium shifts to a net reduction in numbers and the population enters the death phase, or logarithmic decline phase (figure 2.12).

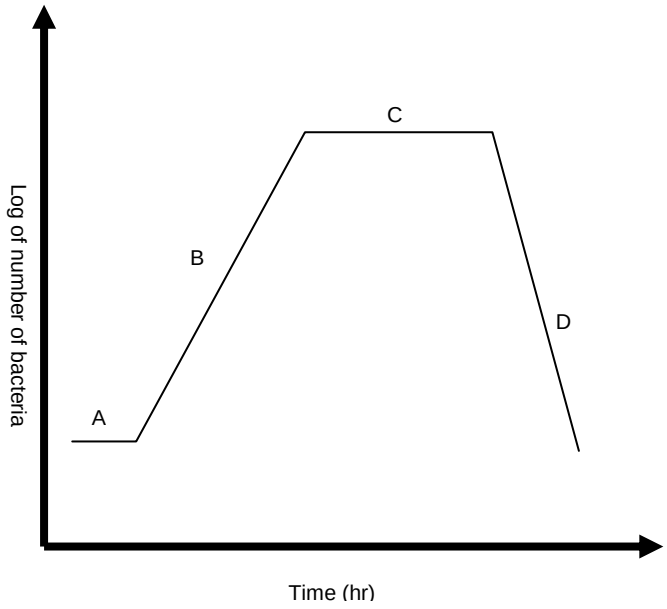

Figure 2.12: Foure stages of bacterial growth.
A: lag phase; B: log , or exponential growth phase; C: stationary phase; D: death, or logarithmic decline phase. [47]

2.4.2.2 Colony Counting

Plate counting is widely used and suitable for enumerating bacteria in appropriate media. Typically serial dilutions are prepared for each sample with vesicle solution (antimicrobial encapsulated) and several replicate plates are prepared from each dilution. Agar plate containing nutrients necessary for growth is used to allow bacterial growth to be monitored quantitatively in terms of growth colony counting followed incubation at an optimal growth temperature. After a strain-dependent period of time (usually 18h) visible cell colonies appear on the agar surface (figure 2.13). The visible cells correspond to an initial cell which has reproduced sufficiently. Although the labour required to prepare, inoculate, and count the plates are not insignificant, it is a relatively reliable way to estimate a quantity of bacteria which were present in the original solution, typically expressed as colony forming units per millilitre (CFU ml $^{-1}$).[32] This is the 'gold standard' of bacterial detection as it provides both an estimation of cell quantities and shows any contamination within the culture e.g. other micro-organisms.

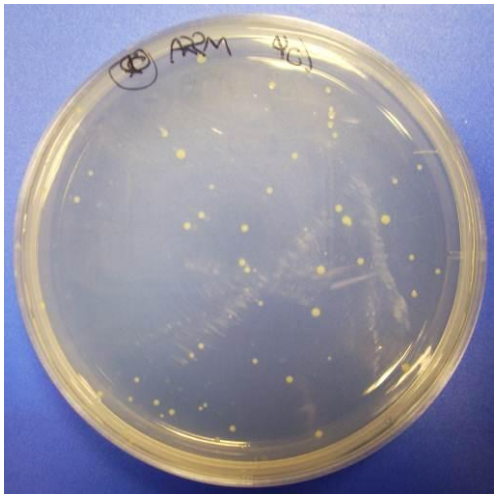

Figure 2.13: *S.aureus* (MSSA 476) colonies on an agar plate grown from individual cells

2.4.2.3 Solution Turbidity

Solution turbidity is a more straightforward but slightly more inaccurate and indirect way to determine cell quantification. Because cell reproduction results in a less transparent solution than pure media alone, the difference in light absorption can be measured and related back to the initial bacterial concentration.[36] This is normally measured by a UV-vis spectrophotometer, with the transmission of light through a known path length reduced by cells in terms of optical density reading (OD) for the sample which is shown in figure 2.14.

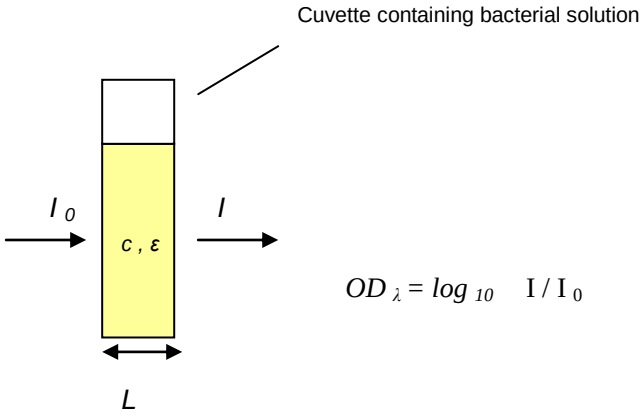

Figure 2.14: UV-vis measurement to determine the optical density of bacterial culture
where I_0 = incident beam intensity, I = transmitted beam intensity and wavelength of incident light (typically 600 nm).

Optical density can be associated with CFU mL^{-1} when the same bacterial solution is colony counted at various known dilution factors to yield a calibration plot. The calibration plot is used to determine the bacterial concentration at specific OD_{600}. The plot is highly strain specific. Therefore a calibration plot must be done for every single bacterial strain under particular experimental conditions. In addition the limit of detection of this method is in the range of 10^5-10^8 CFU mL^{-1} due to the fact that the light cannot pass through with large amount of bacterial cells. The UV-Vis spectrophotomer used in this work to determine the concentration of bacteria was FLUOstar Omega microplate reader which has been presented in 2.3.2.1.

2.4.2.4 Optical Density-CFU Relationship of Bacteria

The relationship between optical density at 600nm (OD_{600}) against CFU mL^{-1} is shown in figure 2.15 which elucidates the relationship as a quick reference for indentifying bacterial concentration. Such relationship only applies to the range of 10^5 -10^8 CFU mL^{-1} which has been explained in section 2.4.1.3.

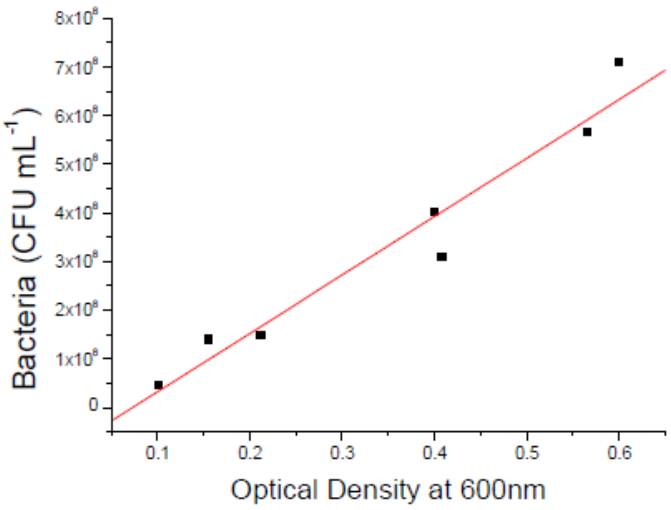

Figure 2.15: Optical density of *S. aureus* (MSSA 476) against the number of CFU mL^{-1} [48] (reproduced with permission from MPhil thesis of A. Loftus, 2010).

2.4.3 Sterilisation

The maintenance of sterile conditions is necessary to work safely with bacterial sample.

All work was carried out with Class II pathogens (MSSA 476, PAO1) in a class II safety cabinet in this work. Bleach or 70% alcohol was used to disinfect the surfaces outside of the cabinet.

Media and equipment were sterilised by the use of heat, which is in the form of an autoclave. Autoclaving is a decontamination process of materials at depressurised steam which must run at 121℃ and 15 psi for 15 minutes.[32] All pp-MA treated non-woven polypropylene samples were sterilised by using a quick and dry method of UV/ozone treatment as an ultraviolet light source can attack bacteria on contaminated surface by bombarding chemical bonds within the cell via high energy light.

2.4.4 Antimicrobial Evaluation Assays

In order to evaluate antimicrobial property of vesicles both in solutions and on surfaces, the methods used in this work were chosen according to their applicability and are presented here. All potential antimicrobials against a non-treatment control system must be carried out in this work.

2.4.4.1 Solution Assays

This assay would investigate the antimicrobial ability of vesicle solution if antimicrobials are encapsulated inside. A known concentration of bacteria (by measuring it optical density) mixing with antimicrobial vesicle solution was tested either in microplate reader overnight in terms of optical density at wavelength of 600 nm or through use of colony counting. Due to the high concentration of bacterial cells in some solutions, multiple dilutions are required when doing the colony counting.

2.4.4.2 Surface Assays ---JIS

The measurement of antimicrobial activity from vesicle modified nonwoven is based on using the Japanese Industry standard (JIS 1902) to determine antimicrobial efficacy on treated surface, the experimental procedure of which will be detailed in experimental section. Typically, the surface is lightly rinsed and votexed to remove surface-attached bacteria. These bacteria can then be assessed by colony counting.

2.4.4.3 Minimum Inhibitory Concentration Assays

This assay aims to determine the bacterial susceptibility to free antimicrobials in solution. The principle of such assay is that the lower MIC in mg mL^{-1} the more sensitive the bacterial isolate is to the antimicrobial. There are three general methods of determining MIC. Theses are the serial dilution, disc diffusion, and gradient diffusion methods. Serial dilution method is commonly used in laboratories. In this method, the antibiotic solution is diluted to various concentrations. The broth or agar containing the dilution multiples are then inoculated with bacterial isolated of interest and incubated overnight at 37 ℃. The broth dilution tubes or agar plates are then inspected to determine the lowest concentration of antibiotic that prevents of turbidity (dilution tubes) using UV-Vis spectrophotometer. The data reported by UV spectrophotometer will be plotted and the concentration of an antimicrobial can be determined constructing a dose-response curve. The common assessment is based on the ability of the antimicrobial to inhibit either 50% or 90% of bacterial cell growth compared to the control system.[49-50]

2.5 Estimation of Minimum Encapsulation Volume

In this work, vesicles are used as antimicrobial/fluorescence carriers for killing/detecting the presence of pathogenic bacteria. The estimated concentration of encapsulated dye/antimicrobial should be taken into consideration to ensure appropriate concentration of fluorescent dye/antimicrobials encapsulated in the vesicles to kill/inhibit the growth of bacteria. The assumption is on the basis of estimating the total internal volume of vesicles when all the vesicles are ruptured in solution. The most straightforward way to measure this is to consider a uniform size population of vesicles sphere with an outer diameter and an inner diameter. Due to the size differences, the GUVs and polydiacetylene vesicles is discussed separately.

2.5.1 Structure and Organisation of Lipid Bilayer

Lipid bilayers consist of two single-molecule layers of an amphiphilic substance. Lipid bilayers are held together by non-covalent forces. This is because lipids can self-assemble into this structure due to hydrophobic effect, which creates an

energetically unfavourable interaction between the hydrophobic chains and surrounding aqueous medium.

Lipid bilayers consist of several chemical regions across its bilayer arrangement. Hydrophilic headgroup which is located on either side of the bilayer is the first region. This region is completely hydrated and is typically around 0.8-0.9 nm thick. In phospholipid bilayers the phosphate group is located within this hydrated region and is approximately 0.5 nm outside the hydrophobic core.[51] The hydrated region can be extended much further in some cases when larger proteins or a longer sugar chain are grafted onto the region, for instance the lipopolysaccharide coat on a bacterial outer membrane.[52] Such grafted substance can help maintain an aqueous layer around the bacteria to prevent dehydration. The intermediate region is next to the hydrated headgroup and is partially hydrated. This region is approximately 0.3 nm thick.[53-54] The length of hydrophobic region of bilayer varies with chain length and temperature, especially near a phase transition.[55-57] The hydrophobic part of the bilayer is approximately 3-4 nm thick. A schematic structure of a typical lipid bilayer with three chemical regions is shown in figure 2.16.

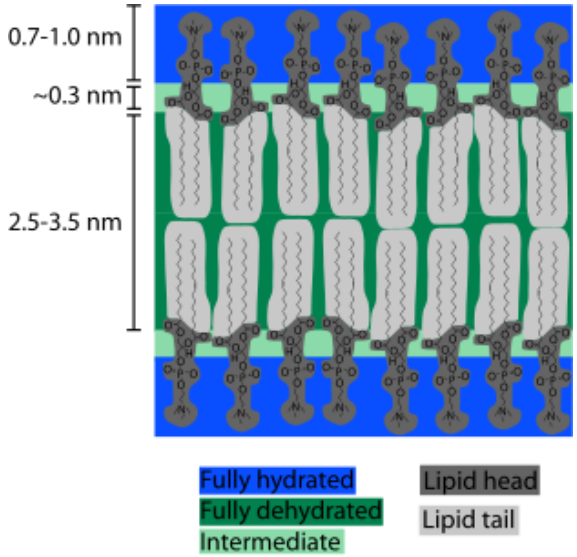

Figure 2.16: A typical lipid bilayer with several chemical regions.
There are three distinct regions: a fully hydrated phosphate group in phospholipids; a partially hydrated intermediate region; a completely dehydrated region of alkane tails.
(Image source is from free Wikipedia: http://en.wikipedia.org/wiki/Lipid_bilayer)

2.5.2 GUVs

GUVs were formed based on rotary evaporation and thus the sizes of vesicles are much larger than that of polydiacetylene vesicles which was made by the extrusion method. The assumption of outer diameter and inner diameter should be taken into account in order to calculate the total encapsulation volume. The assumption of outer diameter is 1 μm and this was measured by fluorescence microscopy. To estimate the diameter of inner sphere, the approximate length of lipid bilayer should be considered. The length of lipid bilayer is assumed to be 5 nm in this work [58] based on the discussion of section 2.5.1. The diameter of inner sphere can be calculated to be 990 nm (figure 2. 17).

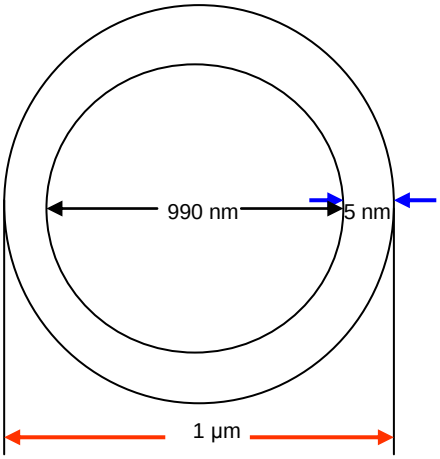

Figure 2.17: Simplified vesicles with estimation of inner and outer diameter.

If an average lipid head group area of 60Å ^{2} is assumed,[59] and the lipids are highly packed in a bilayer configuration,[60] the number of lipids in one vesicle with internal volume can be calculated. The detailed estimation of volume calculation is presented as follows:

Outer diameter: 1000 nm
Area of outer sphere = $4 \pi r^2 = 3.14 \times 10^{-12}$ m^2
Inner diameter: 990 nm

Area of inner sphere = $4 \pi r^2 = 3.08 \times 10^{-12}$ m^2

Area of a DMPC head group = $60 Å^2 = 6 \times 10^{-19} m^2$

Number of lipids:

Outer sphere = area of outer sphere/area of a DMPC head group = 5233333 lipids

Inner sphere = area of inner sphere/ area of a DMPC head group = 5133333 lipids

Total number of lipids in one vesicle = 5233333 + 5133333 = 1.04×10^7 lipids/ vesicle

Total number of vesicles per mL

In GUVs: 0.041g DMPC was used to form GUVs = 6.05×10^{-5} moles (Mr_{DMPC} = 677.93 g/mol)

Total number of lipid molecules

= moles of DMPC formed in the vesicles x $N_A = 3.64 \times 10^{19}$

Total number of vesicles = total number of lipids in GUVs solution / number of lipids in one vesicle = 3.5×10^{12} in experiment (6.65 mL)

Number of vesicles per mL = total number of vesicles/ experiment (6.65 mL) = 5.26×10^{11} vesicles/mL

Total encapsulated volume

Volume encapsulated in one vesicle = $(4/3)\pi r^3 = 5.08 \times 10^{-15}$ m^3

Total encapsulated volume in 6.65 mL = volume in one vesicle x total number of vesicles = 2.67 mL

The encapsulated volume per mL = 400 μL

2.5.3 Polydiacetylene Vesicles

Polydiacetylene vesicles were formed by the extrusion method with 100 nm pore size of polycarbonate filters. The size of resulting vesicles were quite uniform with outer diameter of 110 nm and an inner diameter 100 nm assuming a bilayer thickness of 5 nm. Therefore, the encapsulated volume in polydiacetylene vesicles can be considered in the same manner as the GUVs did.

Outer diameter: 110 nm

Area of outer sphere = $4 \pi r^2 = 3.80 \times 10^{-14}$ m^2

Inner diameter: 100 nm

Area of inner sphere = $4 \pi r^2 = 3.14 \times 10^{-14}$ m^2

Area of a DMPC head group = $60 Å^2 = 6 \times 10^{-19}$ m^2

Number of lipids:

Outer sphere = area of outer sphere/area of a DMPC head group = 63333 lipids

Inner sphere = area of inner sphere/ area of a DMPC head group = 52333 lipids

Total number of lipids in one vesicle = 63333 + 52333 = 1.15×10^5 lipids/vesicle

Total number of vesicles per mL

In polydiacetylene vesicles: 30 mol% TCDA for example: approximate 3.26 mg DMPC was used to form 30 mol% TCDA vesicles= 4.81×10^{-6} moles (Mr_{DMPC} = 677.93 g/mol)

Total number of lipid molecules

= moles of DMPC formed in the vesicles x $N_A = 2.90 \times 10^{19}$

Total number of vesicles = total number of lipids in GUVs solution / number of lipids in one vesicle = 2.52×10^{14} vesicles in experiment (5 mL)

Number of vesicles per mL = total number of vesicles/ experiment (5mL) = 5.04×10^{13} vesicles/mL

Total encapsulated volume

Volume encapsulated in one vesicle = $(4/3)\pi r^3 = 5.24 \times 10^{-22}$ m^3

Total encapsulated volume in 5mL = volume in one vesicle x total number of vesicles = 1.32×10^{-1} mL

The encapsulated volume per mL = 2.64×10^{-2} mL = 26.4 μL

2.6 References:

1 Yasuda, H, Plasma Polymerisation. Academic Press: New York, London, 1985.

2 Hinman P.V, Bell A.T, Shen M., Composite reverse osmosis membranes prepared by plasma polymerisation of allylamine. Evaluation of membrane performance for the treatment of washwater and its components, *J. Appl. Polym. Sci.,* 1979, *23*, 3651-3656.

3 Cho D.L, Yamada H, *Proceedings of the ACS Division of Polymeric Materials* 1987, *57*, 599.

4 Yasuda H., Gazicki M., Biomedical applications of plasma polymerisation and plasma treatment of polymer surfaces., *Biomaterials,* 1982, *3*, 68-77.

5 Morita S, Tamano J, Yasuda M, Iedo M, Morita S, Yoneda K, Ishibashi S., *Thin Solid Films* 1981, *83*, 189-194.

6 Osada Y, Mizumoto A, Tsuruta H, J. Macromo. *Sci. Chem. A* 1987, *3&4,* 403-413.

7 Tien P.K, Smotinski G, Martin R., Thin organosilicon films for integrated optics, *J. Appl. Optics*, 1972, *11*, 637-642.

8 Moshonov A, Avni Y., The use of acetylene glow discharge for improving adhesive bonding of polymeric films, *J. Appl. Polym. Sci*., 1980, *25*, 771-781.

9 Jenkins A.T.A, Hu J, Wang Y.Z, Schiller S., Foerch R., Knoll, W., Pulsed plasma deposited maleic anhydride thin films as supports for lipid bilayers, *Langmuir*, 2000,*16*, 6381-6384.

10 Inagaki N., Plasma Surface Modifacation and Plasma Polymerisation, Technomi, Lancaster, PV, USA, 1996.

11 Jenkins A.T.A., Hu J., Wang Y.Z., Schiller S., Foerch R. and Knoll W., Pulsed plasma deposited maleic anhydride thin films as supports for lipid bilayers, *Langmuir*, 2000, *16*, 6381-6384.

12 Hudis, M, Techniques and Applications of Plasma Chemistry, John Wiley: New York, 1974.

13 Chan, C.M, Ko, T.M, Hiraoka, H., Polymer surface modification by plasmas and photons. *Surface Science Report*, 1996, *24*, 3-54.

14 Yasuda, H.K, Some important aspects of plasma polymerisation, *Plasma Process & Polymers*, 2005, *2*, 293-304.

15 Wertheimer, M.T.,Thomas, H.R., Perri, M.J., Klemberg Sapieha J.E., Martinu L., Plasmas and polymers: From laboratory to large scale commercialization, *Pure and*

Applied Chemistry 1996, *68*, 1047-1053.

16 Kurosawa S., Choi B.G., Park J.W., Aizawa H., Shim K.B., Yamamoto K., Synthesis and characterisation of plasma-polymerised hexamethyldisiloxane films, *Thin Solid Films* 2006, *506*, 176-179.

17 Yasuda, H, Bumgarner, M.O, Hillman, J.J., Polymerisation of organic compounds in an electrodeless glow discharge. IV. Hydrocarbons in a closed system, *Appl. Polym Sci*., 1975, *19*, 531-543.

18 Ryan M.E., Hynes A.M., Badyal P.S., Pulsed Plasma Polymerisation of Maleic Anhydride, *Chem. Mat.*, 1996, *8*, 37-42.

19 Savage C.R., Timmons R.B., Lin J.W., Molecular control of surface film compositions via pulsed radio-frequency plasma deposition of perfluoropropylene oxide, *Chem. Mat.*, 1991, *3*, 575-577.

20 Bullett, N. A., Whittle, J. D., Short, R. D., Douglas C. W. I., Adsorption of immunoglobulin G to plasma-*co*-polymer surfaces of acrylic acid and 1,7-octadiene, *J. Mater. Chem.* 2003, *13*, 1546-1553.

21 Lakowics J.R., Principles of Fluorescence Spectroscopy. 2nd Edition ed. 1999, New York: Kluwer Academic/Plenum Plublishers.

22 Lakowicz, J.R., Principles of Fluorescence Spectroscopy, Plenum Press, New York, 1983.

23 Shriver, D. F.; Atkins, P. W. *Inorganic chemistry*; 3rd ed.; Oxford University Press, 1999.

24 Ebsworth, E. A. V.; Rankin, D. W. H.; Cradock, S. *Structural methods in inorganic chemistry*; Blackwell, 1991

25 Nicklin, J.; Graeme-Cook, K.; Killington, R. *Microbiology*; 2nd ed., BIOS scientific, 2002.

26 Image Source is from free Wikipedia: http://en.wikipedia.org/wiki/File:FluorescenceFilters_2008-09-28.svg

27 Goldstein J., Scanning electron microscopy and X-ray microanalysis, Kluwer Adacemic/Plenum Publishers, 2003.

28 Reimer, L., Scanning electron microscopy: physics of image formation and microanalysis. Springer,1998.

29 Egerton, R. F., Physical principles of electron microscopy: an introduction to TEM, SEM, and AEM. Springer,2005.

30 Clarke, A. R., Microscopy techniques for materials science. CRC Press (electronic

resource), 2002.

31 Image Source: Department of Physics, The University of Warwick: http://www2.warwick.ac.uk/fac/sci/physics/postgraduate/current/regs/mpags/ex5/techniques/structural/sem3/

32 Nicklin, J.; Graeme-Cook, K.; Killington, R. *Microbiology*; 2nd ed.; BIOS scientific, 2002.

33 Image Source: Todar's Online Textbook of Bacteriology: http://www.textbookofbacteriology.net/pseudomonas.html

34 Cornelis P., Pseudomonas: Genomics and Molecular Biology, Caister Academic Press, 2008.

35 Ryan K.J., Ray C.G. (2004). *Sherris Medical Microbiology* (4th ed.). McGraw Hill. Hiramatsu K.A.N., Dissemination in Japanese hospitals of strains of *Staphylococcus aureus* heterogenously resistant to vancomycin. *Lancet* , 1997, 350, 1670-1673.

36 Grundmann H., Aires-De-Sousa M., Boyce J., Tiemersma E., *Emergence and resurgence* of methicillin-*resistant Staphylococcus aureus* as a public-health threat, *Lancet*, 2006, *368*, 874-885.

37 Centre for Disease Control and Prevention, http://phil.cdc.gov/phil

38 Kubitschek H. E., Cell volume increase in *Escherichia coli* after shifts to richer media, *J. Bacteriol.*, 1990, *172*, 94-101.

39 Hudault S., Guignot J., Servin A.L., *Escherichia coli* strains colonising the gastrointestinal tract protect germfree mice against *Salmonella typhimurium* infection, *Gut*, 2001, *49*, 47–55.

40 Reid G., Howard J., Gan B.S., Can bacterial interference prevent infection? , *Trends Microbiol.*, 2001, *9*, 424–8.

41 Todar, K., Pathogenic *E. coli*., *Online Textbook of Bacteriology*, University of Wisconsin–Madison Department of Bacteriology. http://www.textbookofbacteriology.net/e.coli.html. Retrieved 2007-11-30.

42 Rendon M. A., Saldana Z., Erdem A. L., Monteiro-Neto V., Vazquez J.B., Kaper J., Puente L., Giron J.A., Commensal and pathogenic *Escherichia coli* use a common pilus adherence factor for epithelial cell colonisation, *Proc. Natl. Acad. Sci.* U.S.A., 2007, *104*,10637-10642.

43 England N.M 2nd Edition Dec, 2010.

44 Koch A., Control of the bacterial cell cycle by cytoplasmic growth, *Crit Rev Microbiol*, 2002, *28*, 61-71.

45 Eagon R.G., Pseudomonas natriegens, a marine bacterium with a generation time of less than 10 minutes, *J. Bacteriol.*, 1962, *83*, 736-737.

46 Skarstad K., Steen H.B., Boye E., Cell cycle parameters of slowly growing *Escherichia coli* B/r studied by flow cytometry. *J. Bacteriol.*, 1983, *154*, 656–62.

47 Information retrieved from Wikipedia http://en.wikipedia.org/wiki/Bacterial_growth

48 Loftus A., Autoresponsive and selective nanocapsules for infection indication and initial treatment, Mphil Thesis, 2010.

49 NIH Chemical Genomics Center // Assay Guidance // Assay Guidance Manual // Assay Operations for SAR Support

50 Information retrieved from the website: http://www.unmc.edu/Pharmacology/receptortutorial/competition/IC50.htm

51 Nagle J.F., Tristram-Nagle S., Structure of lipid bilayers, *Biochim. Biophys. Acta*, 2000, *1469*, 159–195.

52 Parker J, Madigan M.T., Brock T.D., Martinko J.M., *Brock biology of microorganisms* (10th ed.). Englewood Cliffs, N.J: Prentice Hall, 2003.

53 Marsh D., Polarity and permeation profiles in lipid membranes, *Proc. Natl. Acad. Sci. U.S.A.*, 2001, *98*, 7777–7782.

54 Marsh D., Membrane water-penetration profiles from spin labels, *Eur. Biophys. J.*, 2002, *31*, 559–562.

55 Lewis B.A., Engelman D. M., Lipid bilayer thickness varies linearly with acyl chain length in fluid phosphatidylcholine vesicles, *J. Mol. Biol.* 1983, *166*, 211–217.

56 Rawicz W., Olbrich K.C., McIntosh T., Needham D., Evans E., Effect of chain length and unsaturation on elasticity of lipid bilayers, *Biophys. J.* 2000, *79*, 328-329.

57 Trauble H., Haynes D.H., The volume change in lipid bilayer lamellae at the crystalline-liquid crystalline phase transition, *Chem. Phys. Lipids*, 1971, *7*, 324–335.

58 Kalb E., Frey S., Tamm L. K., Formation of supported planar bilayers by fusion of *vesicles* to *supported* phospholipid monolayers, *Biochm. Biophys. Acta.*, 1992, *1103*, 307-316.

59 Jenkins A. T. A., Olds J. A., Electrochemical measurement of the interaction of *Crotalus adamanteus* venom with DMPC vesicles, *Chem. Commun.*, 2004, 2106-2107.

60 Kucerka N., Kiselev A., Balgavy P., Determination of bilayer thickness and lipid surface area in unilamellar dimyristoylphosphatidylcholine vesicles from

small-angle neutron scattering curves: a comparison of evaluation methods, *Eur. Biophys. J.*, 2004, *33*, 328-334.

Chapter 3 Experimental Methods

In this chapter, a detailed description of the establishment, optimisation and development of the experimental set-up are presented. The different experimental procedures for the formation of nanocapsules (GUVs and PDA vesicles) with fluorescent dye/antimicrobial are presented, followed by a description of the experimental methods employed.

3.1 Material Science

3.1.1 Synthesis and Purification of Giant Unilamellar Vesicles

All chemical used in this work were purchased from Sigma-Aldrich, UK, and not purified further. The 1,2-dimyristoyl-*sn*-Glycero-3-phosphocholine (DMPC) and 1,2-dimyristoyl-*sn*-Glycero-3-phosphoethanolamine (DMPE) lipid were purchased from Avanti Polar Lipids, USA. Sephadex columns of NAP-10 and NAP-25 for vesicle purification were purchased from GE Health Care.

3.1.1.1 Formation of GUVs

Aqueous bulk solutions were prepared before vesicle synthesis for encapsulation purpose. A bulk solution was prepared containing one of fluorescein, sodium azide or gentamicin sulphate. Carboxyfluorescein was encapsulated in the GUVs to detect the purification efficiency between NAP-10 and NAP-25 in the later work. The compositions are shown in table 3.1.

Table 3.1: Encapsulated agents used in this work and the concentration prepared in different buffer systems

Compound	Buffer	Concentration	Structure /Formula
Sodium Azide	Tris-HCl (0.05M, pH 7.4)	15 mg mL^{-1}	NaN_3
Gentamicin Sulfate	Phosphate Buffered Saline	5 mg mL^{-1}	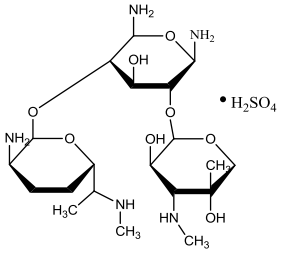
Fluorescein	Tri-HCl (0.05M, pH 7.4)	0.25 mM	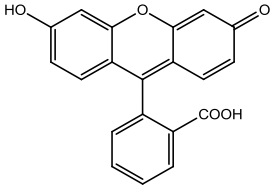
5(6)-carboxyfluorescein	HEPES (composition is detailed in Table 3.7	50 mM	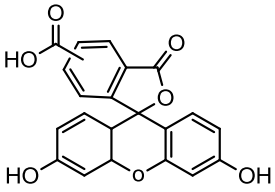

The encapsulated concentration of gentamicin sulfate varies according to different vesicle system.

GUVs were synthesised according to the work of Moscho et al: [1] The mixture of 0.041g of DMPC and 0.002g of DMPE with 0.013g cholesterol was added to a vial with 1mL chloroform (Fischer). A 200µL aliquot of this solution was added to a 50mL round-bottomed flask containing 980µL chloroform and 150µL methanol (Fisher). To a clean vessel, 6650 µL aqueous bulk was carefully added into the flask along the sides of the glass wall. The resultant mixture was rotary-evaporated for 2 minutes at 40 ℃. Two major boiling events were noticed to occur (the first due to the chloroform, the second due to the methanol). After 2 minutes, the liquid in the round-bottom flask was observed

to be a faint milky-white opalescent fluid which contained GUVs in high yield (which was the GUV stock solution). When not in use, the GUV solution was kept sealed in a refrigerator for no longer than a week. They were sonicated and briefly vortexed each time before use.

3.1.1.2 Purification of Giant Unilamellar Vesicles (GUVs)

There is a specific eluent buffer for each aqueous bulk. The eluent buffers are shown in table 3.2:

Table 3.2: Eluent buffer systems for different encapsulating compounds

1 Eluent Buffer for Sodium Azide (50 mL)

Constituent	Concentration
Tris-HCl (pH 7.4)	0.05 M

2 Eluent Buffer for Gentamicin Sulfate (50 mL)

Constituent	Amount
Phosphate Buffered Saline	0.25 Tablet

3 Eluent Buffer for fluorescein (50 mL)

Constituent	Amount
Tris-HCl (pH 7.4)	0.05M

In this work, two types of columns were used for the purification of vesicle solution. These were GE healthcare NAP-10 and NAP-25 sephadex columns which were used based on size exclusion. These are disposable columns prepacked with Sephadex G-25 DNA grade and require only gravity to run. NAP-10 columns were mainly used for the purification of giant unilamellar vesicles and NAP-25 for polydiacetylene/phospholipid vesicles. The only difference between the columns is that NAP-25 columns allow greater volume to be purified. The columns were secured in a clamp stand and the storage

solution was drained. Excess buffer was passed through the column in order to equilibrate it. Once the equilibration buffer had drained from the column, the sample was then placed in the reservoir and allowed to load onto the column. Once the sample was loaded onto the column the eluent buffer (same composition as the equilibration buffer) was added to the reservoir and collection of the chromatographic eluent began. The purified vesicle solution was collected either in 15 mL plastic tubes or a 96 well microtiter plate, into each well 4 drops (approx 155 µL) were collected. The purified vesicle solution was kept in refrigerator at 4 ^{o}C for further use. The information of the columns is shown below in table 3.3.

Table 3.3: Description of two types of columns used in the purification of vesicles including the parameters for sample and eluent volumes

Columns	Equilibration volume(mL)	Sample volume(mL)	Eluent (mL)
NAP-10	10	0.5	2
NAP-25	15	2	2.5-3

In this work, 5(6)-carboxyfluorescein was encapsulated in giant unilamellar vesicles to investigate the better purification system. The bulk solution and eluent buffer system for carboxyfluorescein are shown in table 3.7 and 3.8.

3.1.2 Synthesis and Purification of Polydiacetylene/Phospholipid Vesicles

3.1.2.1 Preparation of Stock Lipid Solution (SLS)

Before vesicle synthesis, the lipids DMPC and DMPE, diacetylene monomers TCDA, cholesterol was first separately dissolved in 1mL chloroform and stored in glass vials at -20 ^{o}C for further use. The compositions of the stock lipid solution (SLS) are shown in table 3.4.

Table 3.4: Vesicle stock solutions

Compound	Mr (g mol $^{-1}$)	Mass (mg)	Concentration (mol L $^{-1}$)
TCDA	346.55	35	0.11
DMPC	677.93	73	0.11
DMPE	635.85	18	0.03
Cholesterol	386.65	39	0.10

3.1.2.2 Compositions of Phospholipid/PDA Vesicles

TCDA stabilised vesicles with varying TCDA concentrations were formed referred to table 3.5

Table 3.5: Constituents of 20,30,40,50,60 mol % TCDA vesicles

mol% TCDA	TCDA (µL)	DMPC (µL)	DMPE(µL)	Cholesterol(µL)
20	20	58	2	20
30	30	48	2	20
40	40	38	2	20
50	50	28	2	20
60	60	18	2	20

3.1.2.3 Synthesis of Polydiacetylene/Phospholipid vesicles

As previously described, aqueous bulk solutions were prepared before vesicle synthesis for encapsulation purpose. A bulk solution for such system was prepared containing one of carboxyfluorescein, gentamicin sulphate, silver nitrate, chlorhexidine. The compositions are shown in table 3.6. The composition of aqueous bulk solution for carboxyfluorescein is listed separately due to the complexity of the constituent of the buffer system.

Table 3.6: Compositions of aqueous bulk solution for encapsulation, solvent is distilled water

Compound	Buffer	Concentration	Structure /Formula
Silver Nitrate	Distilled water	1 mg mL^{-1}	$AgNO_3$
Gentamicin Sulfate	Phosphate Buffered Saline	1 mg mL^{-1}	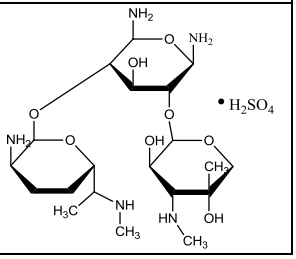

Chlorhexidin	Distilled water	1 mg mL^{-1}	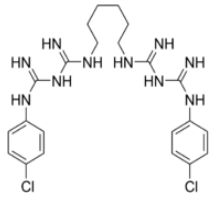
5(6)-carboxyfluorescein	HEPES(composition will be detailed in table 3.7	50 mM	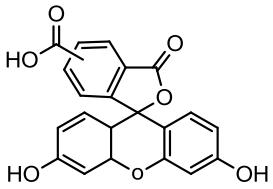

Table 3.7: Composition of aqueous bulk solution system for 5(6)-carboxyfluorescein (50mM) in 50mL

Constituent	Mass(mg)
HEPES	119.2
NaCl	29.2
NaOH	170.0
EDTA	14.2
5(6)-carboxyfluorescein	938.5

The vesicle system comprises 20 mol% cholesterol, 2 mol% 1,2-dimyristoyl-*sn*-glycero-3-phosphatidylethanolamine (DMPE) and various fractions of 1,2-dimyristoyl-*sn*-glycero-3-phosphatidylcholine (DMPC) and 10, 12-tricosadiynoic acid (TCDA). Lipids, cholesterol and TCDA were mixed in chloroform, dried under nitrogen. Following evaporation, 5 mL HEPES buffer (pH 7.4) containing 5(6)-carboxyfluorescein/antimicrobials was added and votexed vigorously. The suspension was then heated up at 75 ℃ to ensure all lipids were mixed well due to different phase transition temperatures of the different lipids. The resultant vesicle solution was then subjected to freeze-thaw cycles at least 3 times to enhance encapsulation efficiency if any drugs/dyes are encapsulated within the vesicles. The resultant vesicle solution was cooled at 4 ℃ overnight to allow lipid head groups to hydrate and for membrane components to separate into phase domains.

3.1.2.4 Polymerisation

The vesicles were then purified using NAP-25 columns to separate non-encapsulated dye/antimicrobials from vesicles before being exposed to UV light (254 nm) for a total of 60 seconds from a high intensity of UV source (Hamamatsu photonics). Overnight hydrated un-polymerised vesicle solution in quartz cuvette (1 mL) was irradiated by hard UV point by point with each point of 10-second irradiation (totally three points per side) (Figure 3.1B). The partially polymerised vesicle solution was then mixed well and subjected to UV radiation in the same manner, each point with 10 second of irradiation. The resultant vesicle solution was votexed again and kept in regrigerator at 4 ^{o}C prior to use for no longer than 1 month. The detailed procedure is shown in figure 3.1A.

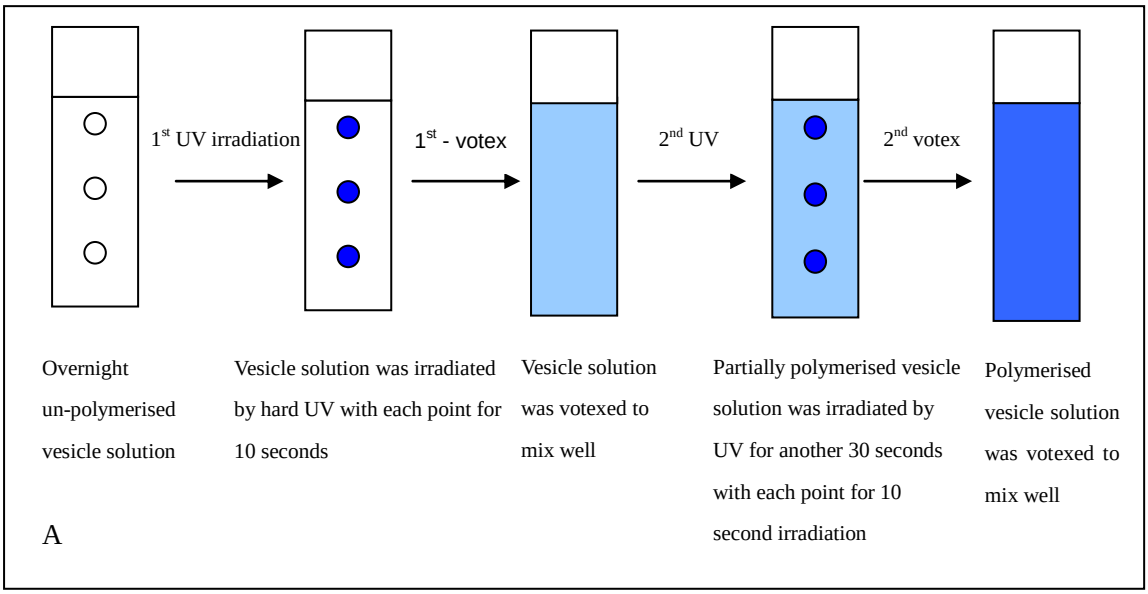

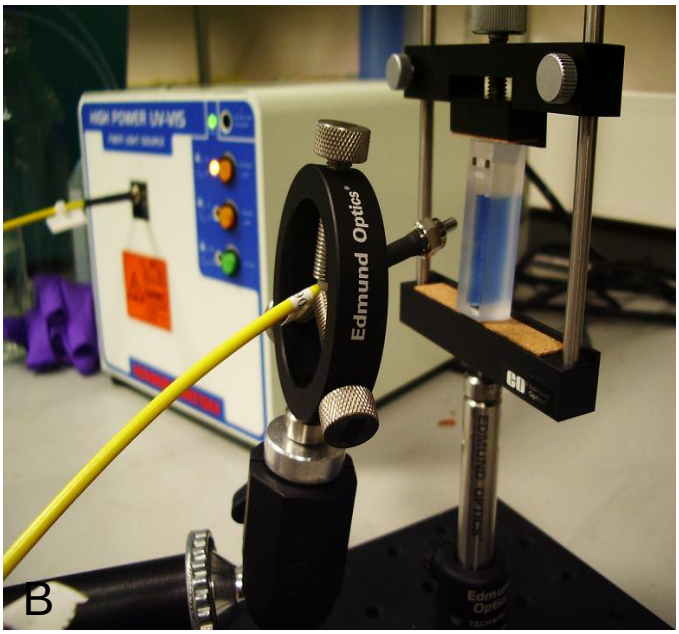

Figure 3.1: Details of polymerisation of polydiacetylene/phospholipid vesicle induced by UV irradiation and experimental setup in the A.T.A.Jenkins group.
(A) procedure of how the polymerised vesicles form under UV irradiation by giving a colour transition from transparent to blue depending upon different concentrations of diacetylene monomer incorporation.; (B) Experimental setup: a quartz cuvette containing vesicle solution was stabilised by a stabilizer and was irradiated by hard UV light point by point for total 1 minute to form blue coloured polymerised vesicle solution.

3.1.2.5 Purification of Phospholipid/PDA Vesicles

Vesicles were purified using illustra ^{TM} NAP-25 columns to remove un-encapsulated carboxyfluorescein/antimicrobials. The procedure of purification has been detailed in section 3.1.1.2. The eluent buffer for 5(6)-carboxyfluorescein is shown in table3.8.

Table 3.8: Eluent buffer (pH 7.4) for 50mM 5(6)-carboxyfluorescein (50 mL)

Constituent	Mass (mg)
HEPES	310
NaCl	76
NaOH	702
EDTA	37

3.2 Physical Science

3.2.1 Characterisation of Chromatic Property for Phospholipid/TCDA vesicles

UV-Vis spectroscopy used here was to detect the colorimetric properties of phospholipid/TCDA vesicles. Samples were prepared at a concentration of 0.1 mM total lipid. The blank system was HEPES buffer (eluent buffer system which can be referred to table3.8). Samples with various concentrations of TCDA were measured at room temperature using the Thermos Helios Gamma single beam spectrophotometer, with a 1 cm optical path cell.

Quantification of the extent of the blue-red colour transition is given by the colorimetric response (% CR), which is defined as follows:

$$PB = A_{blue} / (A_{blue} + A_{red}) \quad (3.1)$$

$$\%CR = [(PB_0 - PB_I) / PB_0] \times 100\% \quad (3.2)$$

In these two equations, A is the absorbance measured at either ‘blue’ component (640

nm) or the 'red' component (500 nm) of the visible spectrum. PB_0 is the value of the control sample. PB_I is the value of the vesicle solution after appearance of the colour change.

3.2.2 Colorimetric Detection of Bacteria-Vesicle Interactions

This measurement was carried out in 96-well plate. The absorbance of vesicle solution was measured using a BMG Labtech fluorostar microplate reader in absorbance mode at 600nm for 1 cm path length before addition of bacteria as the control system. A 190 µL vesicle solution was added to 10 µL of overnight cultured bacteria (10^6 CFU mL^{-1}) and was incubated at 37 ^oC overnight. The absorbance spectrum was then recorded after leaving overnight.

3.2.3 Carboxyfluorescein Fluorescence – Concentration Analysis

5(6)-carboxyfluorescein was dissolved in HEPES buffer (eluent buffer system table 3.9) at a concentration of 95 mM, which is a concentration above the threshold of concentration induced self-quenching. A factor of 10 serial dilutions was made and each diluted solution (200 µL) was placed in a Costar 96-well plate and analysed for fluorescence intensity with excitation at 485nm and emission at 520 nm by using a BMG Labtech fluorostar fluorimeter. The resultant figure was then plotted with fluorescence intensity versus various concentrations of carboxyfluorescein containing unquenched and quenched concentrations. The result is shown in figure 5.9. The HEPES buffer system for dissolving carboxyfluorescein to make a concentration of 95 mM is listed in table 3.9. All the measurments were measured at room temperature.

Table 3.9: HEPES buffer system for 95mM carboxyfluorescein

Constituent	Mass (mg)
HEPES	119.2
NaCl	29.2
NaOH	511.5

EDTA	14.2
5(6)-carboxyfluorescein	1784.6

3.2.4 Carboxyfluorescein Photobleach Analysis

The experiments were carried out in a Costar 96-well plate reader to detect the fluorescence intensity after photobleach by hard UV source. All the samples were placed in a quartz cuvette for UV irradiation. Carboxyfluorescein samples (1 mL) dissolved in appropriate HEPES buffer with the concentrations of 50 mM, 500 μM, 50 μM were exposed to UV radiation using Hamamatsu UV-Vis Fiber Light Source L10290 fibre optic for 10 minutes. The way of irridating the sample is similar to the vesicle polymerisation. The UV fiber source was pointed one side of the quartz cuvette (1 min/side) and was then mixed well. This was done for at least 10 times for total 10 min. The fluorescence would be identical to a control sample (before UV irradiation) if the radiation had no effect on the samples. All measurements were measured at room temperature.

3.2.5 Stability Study of Phospholipid/PDA Vesicles–Dehydration & Rehydration Assay

The measurement aims to find out the optimal vesicle system which could survive in dry condition. 50 μL of polymerised vesicle solution containing self-quenched carboxyfluorescein with varying concentrations of TCDA (0, 10, 20, 30, 40, 50, 60 mol%) was placed in a Costar 96-well plate. The plate was then dried in a Class II flow hood for 24 hours. After overnight the dehydrated vesicles were then rehydrated with appropriate HEPES buffer (pH 7.4, eluent buffer system) and the 96-well plate was then measured in a fluorostar fluorimeter with exciting light at 485 nm, and emission at 520 nm to measure the fluorescence intensity of the rehydrated vesicles. Vesicles with more diacetylene incorporation would retain their structures and will not lose their whole payload of fluorescence. All experiments were repeated 3 times for a given set of conditions and all the mearsuments were measured at room temperature.

3.2.6 Sensitivity Study of Phospholipid/PDA Vesicles to Lytic Agents

In order to ascertain the sensitivity of vesicles with varying molar concentrations of TCDA to lytic agents, a set of compounds were selected and assessed for their ability to disrupt lipid bilayers. Triton X-100 was used as the positive control in experiments, which can cause total lysis of the bilayer membrane of vesicles. These compounds are listed in table 3.10.

Table 3.10: List of lytic agents for their ability to lyse vesicle membrane and hence release the contents

Compound	Concentration
Triton X-100	1/10 (distilled water)
Phospholipase A_2	0.1mg mL^{-1}
α-Haemolysin	0.1mg mL^{-1}

The first measurement was based on fluorescence intensity measurments of different concentrations of TCDA vesicles after lysis by Trition X-100.The measurement was placed on a Costar 96-well plate using a BMG Labtech fluorimeter with exciting light at 485nm and emission light at 520nm. 100 μL vesicle solutions with various TCDA concentrations (0%, 10%, 20%, 25%, 30%, 40%, 50%, 60%, 100%) were measured in the fluorimeter for 5.5 hours. The plate was then taken out of the fluorimeter and 20 μL of Triton was added into each well containing different concentrations of TCDA vesicles. The plate was put the fluorimeter to measure the fluorescence release overnight.

Phospholipase A_2 used in this work was purchased Sigma Aldrich and is extracted from honey been venom as the lyophilized powder of 600-2400 units/mg protein. Haemolysin and PLA_2 was dissolved in PBS buffer with a concentration of 0.1 mg/ mL and freezing below -8 ^oC before use. All the experiments were carried out in a Costar 96-well. Vesicles with TCDA concentrations of 0%, 20%, 30%, 40% (100 μL) were measured in the 96-well plate in terms of fluorescence intensity before the lysis by the lytic agents listed above. After that an aliquot of 20 μL of each of the compounds (Triton, PLA_2,

α-Haemolysin) was transferred to wells containing 100 μL of freshly made vesicle solution with different TCDA concentrations of 0%, 20%，30%，40%. 0% TCDA vesicle was used as a positive control system to give an indication of maximum fluorescence after lysis by Triton. The plate was then measured in a fluorostar plate reading fluorimeter with exciting light at 485 nm, and emission at 520 nm. All experiments were repeated 3 times for a given set of conditions and all measurements were measured at room temperature.

3.2.7 Plasma Polymerisation

Plasma reactor was employed here to deposit a thin film of maleic anhydride as supports for both GUVs and PDA vesicles. The aim is to immobilise the vesicles onto various textiles such as glass slide, non-woven polypropylene or polystyrene petri dishes and thus vesicles are attached onto pp-MA treated surface via covalent bonding.

The use of the reactor for plasma polymerisation required loading of substrate to the main chamber, then adding monomer to the Young's flask. The detailed procedure can be seen in the appendix. In brief, the chamber was evacuated, allowed to reach a suitable base pressure, the monomer tap was opened and either continuous wave or pulse plasma was ignited using the radio frequency source. Pulse plasma deposition was operated using the standard monomer deposition procedure. Duty cycles of 1/40 (T= 41ms) were employed by altering on/off times on the oscilloscope to give an equivalent input power of 1.2W at a peak power of 50W. 100 mg maleic anhydride powder was loaded in the Young's flask and was freeze-dried three times just prior to deposition to remove adsorbed water and then deposited using low power 1/40 at 50W input power to afford a high retention of anhydride and ring structure in the deposited film.

3.3 Microbiological Assays

All microbiological work was undertaken in Class II flow hood in the Department of Chemicstry, the University of Bath. Safety precautions should be taken when working

with microbes including lab coat, gloves and use of a flow hood. Prior to flow hood use, the interior was sterilised with 70% ethanol. All equipment used for contact with microbes (e.g. pipette tips, tubes) was either pre-sterilised or autoclaved at 121 ℃.

3.3.1 Bacterial Culture

Three strains of *S.aureus* (MSSA 476), *P. aeruginosa* (PAO1), and *E. coli* DH5α were used as model microorganisms. Cultures were prepared by inoculation of an agar plate with desired bacteria using a sterile loop and incubated at 37 ℃ for 48 hours to allow growth. A single colony was transferred from the stock plate to 10 mL of LB/TSB broth and was incubated overnight (18 h) at 37^{o}C with shaking at 200 rpm to agitate growth by using aseptic technique. Also, a negative control of LB/TSB was set up to check for contamination. The overnight cultures are in the static phase of bacteria growth. 100 µL of the overnight culture was re-suspended in 10 mL of clean LB/TSB and incubated at 37^{o}C for 4 hours. The re-suspended culture was in the exponential phase in which virulence factors were produced by pathogenic bacteria. This procedure is called sub-culture. The sub-cultured bacteria were used in experiments unless otherwise stated. Tryptic soya broth (TSB) was used as medium to grow *S .aureus* (MSSA 476) in the late period of the work as it provided greater environment for MSSA 476 growth and more toxins could be produced by MSSA 476 when grown in TSB.

3.3.2 MIC Assays

Culture Preparation:

The three strains of bacteria were grown overnight in 10 mL LB, 37 ^{o}C, 200 rpm. A total of 100 µL of the overnight culture was subcultured in 10 mL of LB, 37 ^{o}C, 200 rpm and grown to exponential phase (OD_{600} = 0.3-0.4).

Assay Method:

MICs of four different compounds were determined in this work: sodium azide, gentamicin sulphate, silver nitrate and chlorhexidine. An initial dilution series of these

test compounds were made up in distilled water over a suitable concentration range by serial dilution.

Initially, a range-finding test was performed with 1 replicate that tested 8 different concentrations (e.g. 1/10 dilutions from 0.1 μg mL^{-1} to 10 mg mL^{-1}) to gauge a rough indication of sensitivity to the compound. Triplicates using a narrow range of concentrations were then performed once a good indication of range finding test has been confirmed. The serial dilutions of concentrations should contain the concentrations which show no effect on growth through to total inhibition of growth. 9.7 mL LB was then transferred to clean, sterile glass universals and 200 μl of antimicrobial at varying concentrations were followed to add to LB medium. 100 μl of fresh sub-culture were then added to each glass universal. Also, a negative control was set up only to check for contamination. The cultures were grown with shaking 200 rpm at 37 ^{o}C overnight (16-18 h). The OD_{600} of the cultures was measured by using UV-Vis spectroscopy. Results of this assay provided an estimation for the minimum concentration required to inhibit bacterial growth. Each parallel experiment was carried out in triplicate.

3.3.3 Antimicrobial Analysis

3.3.3.1 Colony Counting

Three strains of bacteria were grown and sub-cultured as described in MIC assay. 100μL of bacteria at a concentration of ca. 10^{9} CFU mL^{-1} in LB was added to a suspension of 900 μL of GUVs. Every 20 min, the bacteria concentration was determined by standard plating assays and colony counting. The bacteria solution containing vesicles (antimicrobial inside) was made 10-fold serial dilutions. After overnight incubation, colonies were then counted and scaled up (multiplied by 10 x dilution factor) to give an estimation of viable cell count, in terms of colony-forming units per millilitre (CFU mL^{-1})

The number of colonies was determined by the equation:

CFU/ mL = CFU/plate x dilution factor x 10 (to get back to 1 mL) (3.3)

Bacteria colonies, theoretically originating from a single bacterial cell termed 'colony forming unit' (CFU), were counted and the original bacterial concentration determined.

3.3.3.2 Solution Turbidity Assay

The assay was performed on a 96 well plate using a BMG Labtech fluorostar plate in absorbance mode with a software correction factor to plot absorbance data at 600 nm for 1 cm path length. A 10 µL vesicle solution was added to 190 µL of bacteria (10^5 CFU mL^{-1}) in LB culture media or Tryptic Soy Broth on a 96 well plate, allowing all experiments to be repeated 3 times for a given set of conditions. The plate was incubated at 37 ^oC and shaken before measurement. The optical density was recorded over time.

3.3.3.3 JIS Assays –Antimicrobial Test on Modified Surface

The assay was based on the Japanese Industry Standard (JIS 1902) for determination of the antimicrobial efficacy of fabrics. Maleic anhydride was plasma deposited onto non-woven polypropylene, which were subsequently cut into four pieces of 2 cm x 2 cm squares; the pp-MA treated fabrics were then immersed into the vesicle solution for 1 h and were then rinsed with appropriate buffer (the buffer system applied here depending on different compounds encapsulated within vesicles) to remove non-binded vesicles from the surface and the samples were then inoculated with 200 µL of a culture of concentration 10^5 CFU mL^{-1} in LB with exponential phase. pp-MA treated fabrics were used as control systems and were sterilised by UV exposure and were treated in an identical way. The fabric squares were either incubated at 37 ^oC for 4 hours or analysed immediately to determine the concentration of adherent bacteria. The negative for growth controls was analysed immediately after inoculation. The treated samples and further controls were incubated for 4 hours for further analysis.

After 4 hour period, the fabrics were rinsed in physiological saline (0.9% NaCl w/v), placed in 5 mL of physiological saline and vigorously vortexed for 5 x 5 s to remove the adherent bacteria. The saline/bacterial solution was then spread on LB agar to obtain

proper concentrations: 1.5 x 10^{-2}, 2.5 x 10^{-3}, 1.25 x 10^{-4}, 6.25 x 10^{-6}, 3.125 x 10^{-7}. These six concentrations were made by a serial dilution with 20 dilution factor. Each concentration of saline/bacteria was spread to an LB agar plate. The plates were then incubated at 37 ^{o}C overnight. The colonies were then counted after following day and the number of colony forming units (cfu) per millilitre (concentration) was then determined.

3.3.4 Fluorescence Response Assay ---Pathogenicity Assay in Suspension

The basis of the detection assay is that at high concentration, carboxyfluorescein is non-fluorescent. Following breakdown of the lipid vesicle containers by bacterial toxins, the dye becomes diuted and 'switches on'. Experiments were performed on a 96-well plate using a BMG Labtech fluorostar plate reading fluorimeter. A 150 μL vesicle solution was added to 50 μL of bacteria with starting concentration of 10^{5} CFU mL $^{-1}$ on a 96 well plate. *S.aureus* (MSSA 476) was grown in TSB medium, while *P.aeruginosa* (PAO1) and *E.coli* (DH5α) were grown in LB medium. All experiments were repeated 6 times for a given set of conditions. The dye was excited with light at 485 nm, and emission measured at 520 nm. Plates were incubated at 37 ^{o} C and shaken every 30 seconds for 2 seconds prior to measurement. Fluorescence was recorded every 4 minutes and plotted both vs. time and as a histogram at a fixed time point, showing both the absolute value of fluorescence and increase following addition of Triton X-100 to lyse the vesicles.

3.4 Attachment of Vesicles to Treated Fabrics

Vesicles can be attached on various treated fabrics. Pulse plasma polymerised deposition is the most commonly used in the thesis for attaching vesicles via covalent bonding. Poly (acrylic acid) photochemically grafted non-woven polypropylene was given from Dr Thet Naing Tun, in the Jenkins' group. Vesicles are attached to these fabrics via hydrogen bonding. Hydrogels were used or incorporated in the modified surface in order to improve the hydrophilicity of the surface hence maintain vesicles intact and stable for

long term use.

3.4.1 Pulse Plasma Polymerisation

Polymers were deposited onto several substrates including polystyrene petri-dishes, and non-woven polypropylene fabrics (purchased from Boots, the chemist). Preparation of polymeric surfaces for the acceptance of plasma films or for use as controls in microbiological assays was achieved using either oxygen plasma or UV/O_3 treatment.

Freshly prepared pp-MA modified nonwoven polypropylene fabrics, polystyrene Petri dishes were removed from the reactor and immediately placed in 2 mL of vesicle suspension. The substrates were left for 1 hour to allow formation of amide linkages three times in PBS buffer (GUVs) or appropriate HEPES eluent buffer (PDA vesicles) to remove most non-covalently bound vesicles. The vesicle bound surfaces were then used for FT-IR analysis.

3.4.1.1 Pathogenicity Assay on pp-MA Treated Fabrics

Vesicle modified non-woven polypropylene fabrics were cut into 3 cm x 6 cm. The experiment was carried out in petri dishes and each sample was placed in one petri dish. 200 μL sub-cultured bacteria (two pathogenic strains *P.aeruginosa* and *S.aureus* and one non-pathogenic strain *E.coli* DH5α) with an initial concentration of 10^5 CFU mL^{-1} were inoculated on vesicle modified pp-MA non-woven polypropylene. *E.coli* DH5α was used as a control system. The bacterial bound fabrics were incubated at 37^{o}C overnight. The photograph was taken under a low power UV lamp the following day. All experiments were repeated 3 times for a given set of conditions.

3.4.2 Surface Photografting of Poly (acrylic acid) on Non-woven Polypropylene

The Poly (acrylic acid) photochemically grafted non-woven polypropylene was offered

by Dr. Thet Naing Tun of the Jenkins' group. The detailed procedure will not be shown here. Generally, the non-woven polypropylene was primed with the photo-initiator BP to provide high concentrations of photo-initiator. The systems were then dried and monomer solution was then loaded onto the primed surface and temporarily sealed with adhesive tapes. The treated non-woven polypropylene was then exposed to UV radiation for 20 minutes. After UV exposure the monomer solution was flushed out and the system was thoroughly rinsed prior to use. 100 µL of vesicle solution was then placed on the treated fabric for further use.

3.4.2.1 Pathogenicity Assay on UV-Induced PAA Grafed Non-woven Polypropylene

Vesicle modified UV induced PAA grafted non-woven polypropylene fabrics were cut into 3 cm x 3cm. The experiment was carried out in petri dishes and each sample was placed in one petri dish. 100 µL sub-cultured bacteria (two pathogenic strains *P.aeruginosa* and *S.aureus* and one non-pathogenic strain *E.coli* DH5α) with an initial concentration of 10^5 CFU mL^{-1} were inoculated on vesicle modified fabrics. *E.coli* DH5α was used as a control system. The bacterial bound fabrics were incubated at 37^oC. The photograph was taken under a low power UV lamp after 4 hours. The plates were then put back in the incubator and measured overning. All experiments were repeated 3 times for a given set of conditions.

3.4.3 Gelatine

Pork gelatine sheets were used in this work and purchased from AB World Foods. Gelatine sheets were hydrated using appropriate HEPES buffer (eluent buffer for carboxyfluorescein) prior to use. The vesicle solution with total 100 µL was then placed on hydrated gelatine sheets. Double layered sheets were most commonly used with vesicles sandwiched between the two sheets in order to maintain a moist environment. Vesicle solution was generally placed on hydrogels by transferring one drop (20 µL) five times to different distributed locations on the fabrics as shown in figure 3.2.

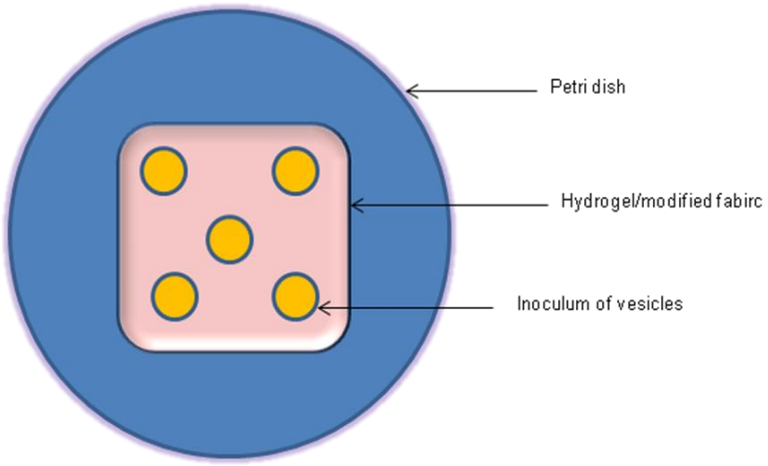

Figure 3.2: Representation of the positions that vesicles were placed

3.4.4 Collagen Grafted pp-MA Non-woven Polypropylene

Collagen solution used in this work was made by mixing 0.2 g gelatine (Sigma-Aldrich) and 0.05 g Catrix® in 5 mL appropriated HEPES buffer (pH 7.4). Catrix® is collagen based powder for use in wound management and was purchased from Cranage Healthcare.

Vesicle mediated pp-MA fabrics were immersed in the collagen solution for 1 hour to ensure high concentrations of grafted collagen. Double layered sheets were most commonly used to maintain vesicles intact and stable.

3.4.4.1 Pathogenicity Assay on Collagen Grafted pp-MA Non-woven Polypropylene

The modified fabrics were cut into 3 cm x 3 cm and the pathogenicity test on the non-woven polypropylene is referred to section 3.4.1.1.

3.5 Visualisation of Vesicles

Vesicles (fluorescent dye encapsulated inside) or the interaction of vesicles and bacteria can be visualised either by microscopy or under low power UV light.

3.5.1 Visualisation of GUVs with bacteria by Using Fluorescent Microscopy

Plasma polymer (maleic anhydride) was deposited onto petri dishes before visualisation under microscope. The treated petri dishes were sterilised by exposing to UV/O_3. The GUVs containing fluorescein were subsequently attached onto the pp-MA treated petri dishes. The GUVs were imaged using a Nikon eclipse TE2000-S epi-fluorescence microscope followed by the inoculation of 200 μL of bacteria (ca. 10^9 CFU mL^{-1}) onto the vesicles attached surfaces.

3.5.2 Visualisation of Phospholipid/PDA Vesicles on pp-MA Treated Fabrics by Scanning Electron Microscopy

SEM images of phospholipid/TCDA vesicles on pp-MA treated non-woven polypropylene were obtained using JEOL JSM-6480LV scanning electron microscope. A drop of vesicle solution to be tested was applied to a 1 x1 cm pp-MA modified non-woven polypropylene and the tested system was then placed in dessicator overnight for drying and was vacuum-coated with gold the following day prior to use.

3.6 References:

1 Moscho A., Orwar O., Chiu D. T., Modi B. P., Zara R. N., Rapid preparation of giant unilamellar vesicles, *Proc. Natl. Acad. Sci.* U.S.A. 1996, *93*, 11443-11447.

Chapter 4 Giant Unilamellar Vesicles as Response System for Killing/Inhibiting Growth of Pathogenic Bacteria

In the previous chapters, the instrumentation and experimental were described which laid a foundation for the following evaluation of responsive nanocapsule system. This chapter presents an initial microbiologically responsive nanocapsule system, giant unilamellar vesicles covalently attached to plasma polymerised maleic anhydride (pp-MA) modified non-woven polypropylene. The system shows that pathogenic bacteria can be used to be the agents of their own destruction by releasing toxins that degrade or damage vesicles containing an antimicrobial agent. This is shown for two strains of pathogenic bacteria, *P. aeruginosa* (PAO1) and *S. aureus* (MSSA 476). A non-pathogenic strain of *E. coli* (DH5α) was used as the control system. Antimicrobial assays (solution assay and JIS) show that antimicrobial GUVs have the ability to kill pathogenic bacteria.

This chapter is organised as follows: In section 4.1, the compositions of vesicles and their theory of formation and purification are described. The phase transition temperature of different phospholipids is also detailed. In section 4.2, a novel method for attaching GUVs onto pp-MA treated non-woven polypropylene is presented. Section 4.3 outlines vesicles antimicrobial efficacy containing an antimicrobial both in suspension and on pp-MA modified fabrics using Japanese Industry Standard (JIS 1902). Section 4.4 further investigates vesicle lysis by bacteria by using fluorescence microscopy. Finally, section 4.5 concludes the chapter and summarises the key findings.

4.1 Formation and Purification of GUVs

4.1.1 Materials

Giant unilamellar vesicle in this work is a hybrid composed of two types of lipids and cholesterol. The main functions of these three constituents are described as follows.

4.1.1.1 DMPC

1,2-dimyristoyl-*sn*-glycero-phosphocholine (DMPC) is a phospholipid which is a major component in animal cell membranes. The primary role of phosphatidylcholine (PC) is to provide a structural framework for the membrane and maintain the permeability barrier. It also plays a role in membrane mediated cell signalling. The lipid has four distinct regions which are anchor, spacer, linkage and lipid tails (figure 4.1). Anchor unit is made of a quaternary ammonium salt containing the *N*, *N*, *N*-trimethylethanolammonium cation. The spacer unit consists of phosphate group which provides an aqueous space. The linkage is actually a glycerol which one of hydroxyls is linked to a polar phosphate-containing group and the other two hydroxyls are linked to hydrophobic fatty acid chains. The chemical structure of DMPC is represented in figure 4.1.

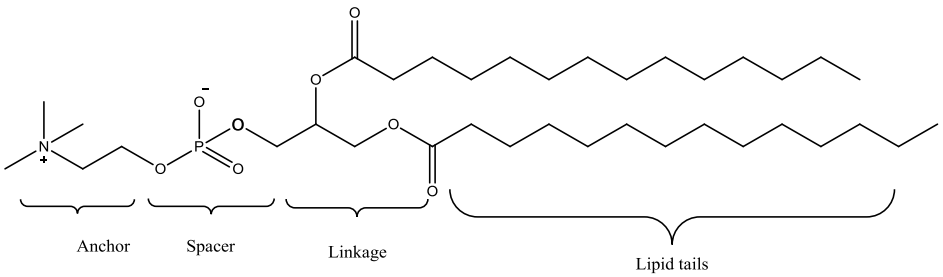

Figure 4.1: Chemical structure of 1,2-dimyristoyl-*sn*-glycero-phosphocholine. (DMPC, $C_{36}H_{72}NO_8P$, PC: (14:0/14:0), mw: 677.933, T_m: 23 ^oC).
The charged polar groups and lipophilic hydrophobic tails are situated away from each other allowing supramolecular interaction of polar and apolar moieties.

4.1.1.2 DMPE

1,2-dimyristoyl-*sn*-Glycero-phosphoethanolamine (DMPE) is normally present in bacterial membranes. Similarly, DMPE contains four different moieties which are anchor, spacer, linkage and hydrophobic tails. The only difference of DMPE is that the phosphate group is linked to ethanolamine as indicated in figure 4.2**.** The anchor part (ethanolamine) plays a major role in immobilisation of the lipid vesicles by anchoring onto plasma treated surface via covalent bonding which will be described in section 4.3.

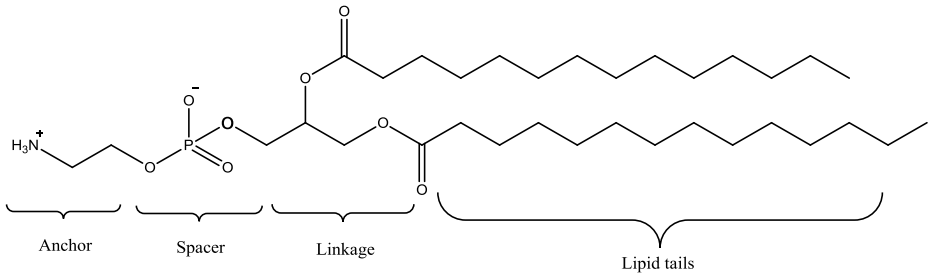

Figure 4.2: Chemical structure of 1,2-dimyristoyl-*sn*-glycero-phosphoethanolamine.(DMPE, $C_{33}H_{66}NO_8P$, PE: (14:0/14:0), mw: 635.853, T_m:50 ^oC).
The charged polar groups and lipophilic hydrophobic tails are situated away from each other allowing supramolecular interaction of polar and apolar moieties.

4.1.1.3 Cholesterol

Cholesterol is the major sterol found in animal cell membranes which regulates membrane permeability and fluidity over a wide range of temperatures. It also plays a role in facilitating cell signalling. Cholesterol is a compact, rigid hydrophobic molecule with a polar hydroxyl group. The hydroxyl group interacts with the polar head group of the membrane phospholipids and phingolipids, the bulky steroid and the hydrocarbon chain are embedded in the membrane which aligns the fatty acid chain of the lipids (figure 4.3). Cholesterol makes up approximately 20% of the cell membrane's mass.[1] Therefore, cholesterol was used to incorporate into lipid bilayer with 23 w% of the whole lipids due to two reasons. Firstly, incorporation of 20% cholesterol into lipid bilayers makes the whole vesicle more biomimetic as natural eukaryotic cell membranes consisting of cholesterol.[2] Secondly, cholesterol used here can improve the stability of

GUVs at room temperature as it helps maintain liquid crystalline phase of lipid bilayers and prevent extremes—whether too fluid, or too firm—in the consistency of the membrane. Cholesterol also has some effects on bacterial toxins in direct or indirect ways as some of toxins secreted by bacteria may recognise the presence of cholesterol on cell membrane e.g. cholesterol binding toxins (CBTs).

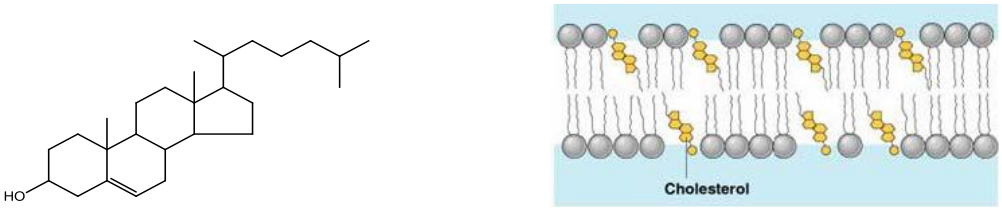

Figure 4.3：Chemical structure of cholesterol ($C_{27}H_{46}O$，mw:386.65) and interaction of cholesterol and lipid bilayers.
Cholesterol disrupts long range order which prevents solid phase and enhances short range order which increases short acyl chain order in fluid phase.

4.1.1.4 Temperature Effect on Lipid Membranes

Lipids in bilayer membranes undergo different phase transition in response to temperature change. This transition exhibits the change from the gel state ("solid") to the liquid crystalline state ("fluid") as surrounding temperature increases. In the gel state, the saturated extended acyl chains are closely packed and stabilised by van der Vaals forces. As a result, lipids are almost locked in the bilayer membrane with minimum lateral movement thus it is relatively unsusceptible to outer environmental changes. In the liquid crystalline phase, the acyl chains have less attractive forces on each other and able to diffuse laterally and freely at higher temperature. This provides a lipid bilayer with sufficient fluidity in the liquid crystalline phase. The phase transition temperature (T_m) is at which a lipid changes state from gel phase to liquid crystalline phase. It is evident that T_m increases with increasing chain length and decreases with increasing unsaturation. This is due to more thermal energy being required to disrupt more extensive contact areas with longer chains. The kink introduced into long hydrocarbon

chains disrupt this order and thus destabilises the gel phase so less thermal energy is required for unsaturated hydrocarbon chains. Table 4.1 shows the T_m of phosphatidylcholine as a function of tail length and number of double bonds.

Table 4.1： Phase transition temperature with different tail length and number of double bonds[2].

Number of carbon atoms in lipid tails	Number of double bonds	Phase transition temperature (T_m in ^{o} C)
12	0	-1
14	0	23
16	0	41
18	0	55
18	1	1
18	2	-53
20	0	66
22	0	75

Lipids employed in this work are DMPC and DMPE with 14 carbon atoms in each hydrophobic region. The use of mixture of DMPC and DMPE improves the biomimetic property of lipid membrane. In addition the mixture of phospholipids in vesicles would not exhibit a simple "melting" point. The T_m of DMPC and DMPE are 23 ^{o} C and 50 ^{o} C, respectively. The difference of transition temperature of these lipids results from differences of head groups. Phosphatidylethanolamine (PE) creates a more viscous lipid membrane compared to phosphatidylcholine (PC), thus more heat will be required to melt PE compared to the same chain length of PC. It is concluded that the mixture of lipids is mostly in the liquid crystalline phase at room temperature as only a small amount of DMPE is incorporated in the lipid bilayer in this work. The insertion of cholesterol further improves the stability of lipid bilayer which provides both firmness and fluidity in lipid bilayers. Therefore, the GUVs are maintained in a sufficiently fluid phase for proper insertion by pathogens and their functions as drug carriers.

4.1.2 Mechanism of GUVs Formation

The method of making vesicles used here is based on reference 4, the procedure of which requires only standard laboratory apparatus. The GUVs made were around 1 μm in diameter that in addition to having high encapsulation efficiencies also can be viewed by a light microscope. The process of vesicle formation is presented as follows: initially, an ordered monolayer of phospholipids is formed at the interface between the two phases (figure 4.4A). In this interfacial region, the polar head groups are located in the aqueous phase, whereas the fatty acid chains are present in the organic layer. When the organic phase is evaporated under reduced pressure, these ordered structures are ruptured into fragments and forced into the aqueous phase; some fragments are transported by air bubbles (figure 4.4B and C). Subsequently, these phospholipid monolayer fragments fuse into bilayer fragments (figure 4.4E). Alternatively, phospholipid bilayer fragments are formed from micellar structures containing the organic solvent (figure 4.4D), and as the evaporation progresses, the entrapped liquid (organic phase) will undergo a phase transition into a gas, and the micellar structures will collapse, yielding bilayer phospholipid fragments (figure 4.4E). These fragments will then spontaneously undergo self-closure into unilamellar vesicles (figure 4.4F).

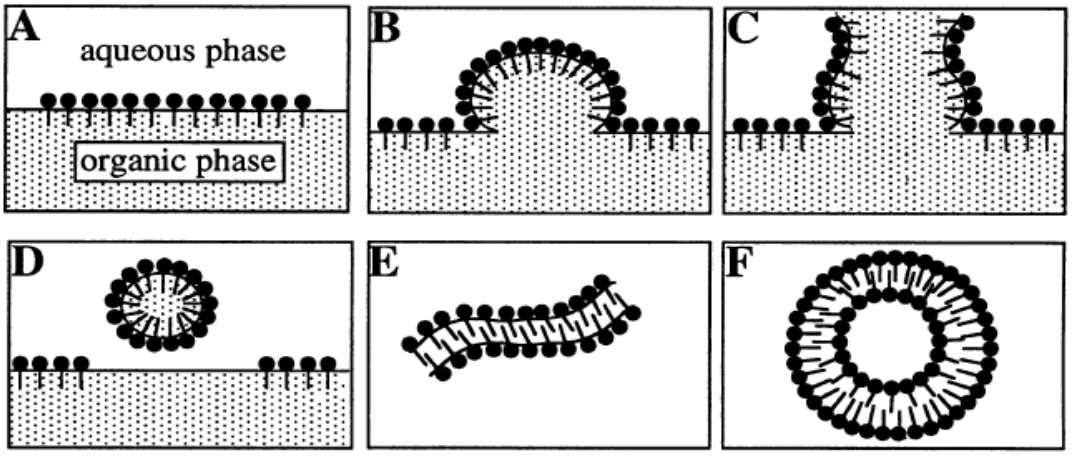

Figure 4.4: Diagram of the suggested mechanism of GUVs formation.
Initially there is an ordered monolayer of phospholipids at the interface between an aqueous and an organic phase (A). During evaporation, bubbles form (B) that rupture the phopholipid film into fragments (C). The resulting phospholipid monolayer fragments fuse to bilayers (E), which spontaneously vesiculate (F). An alternative way for the formation of bilayer phospholipid fragments (D) involves micellar structures having entrapped liquid organic solvent. [4] (pictures are reproduced with permission from reference 4)

4.1.3 Purification of GUVs

Once vesicles are formed, it is necessary to remove all non encapsulated fluorescent dye or antimicrobial agents from the system before it can be used in the further study. In order to suspend the vesicles in 'clean' non fluorescent/bacterial buffer, chromatography was used to separate the aqueous bulk from the vesicles. The purification is based on size exclusion chromatography and due to the size of vesicles (around 1 μm of diameter) it can be inferred that the vesicles will elute from the column before the free fluorescein/antimicrobials. Figure 4.5 shows the typical traces of the NAP-10 column system used on fluorophore containing vesicles. All freshly made vesicles were purified in the same way in terms of chromatography. In the case of undetectable (non-fluorophore containing antimicrobials agents) vesicles the elution time is inferred to be the same as those for fluorescent vesicles and double filtration has to be applied when antimicrobials are encapsulated in the vesicles in order to obtain pure vesicles.

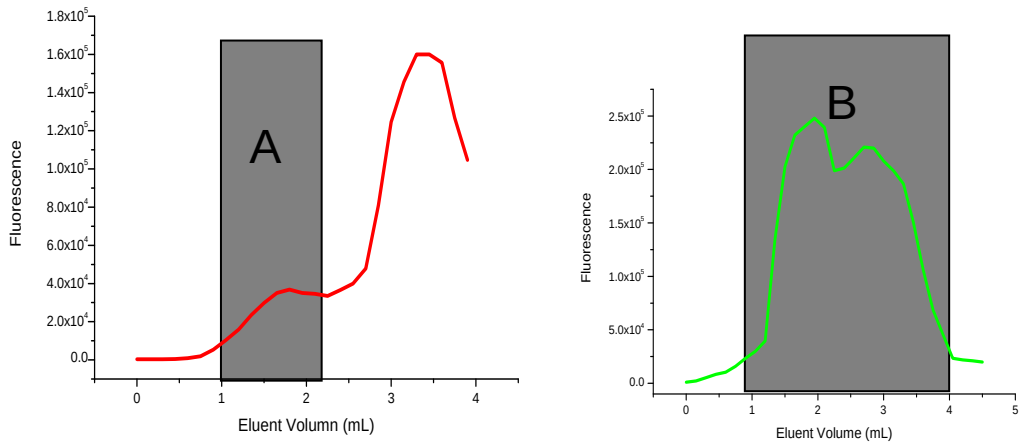

Figure 4.5: Typical traces of NAP-10 column used on 5(6)-carboxyfluorescein containing vesicles. Grey boxes show the wells which were used for further purification (A) or selection for use in experiments (B). Reduction in fluorescence of carboxyfluorescein was due to the fact that relatively high concentration of carboxyfluorescein can quench itself in a range of concentrations (the concentration effect of carboxyfluorescein will be described in chapter 5)

NAP-25 columns became available until late in the work of GUVs and were mainly used to purify vesicles from unencapsulated fluorophore/antimicrobials. The volume of sephadex gel is greater in NAP-25 columns compared to NAP-10 and therefore the transverse area of the column allows greater differentiation of elution times. Figure 4.6 shows the trace graph of NAP-25 and indicates purification by NAP-25 yielded an optimal separation. The differentiation in elution of vesicles and free carboxyfluorescein is apparent as seen in the graph. The selected well are indicated by the grey box and other remarkable events are labelled as well. The double peak shows clear separation in the selected wells due to size distribution. From the graph the low fluorescence peak indicates elution of pure vesicles with carboxyfluorescein inside, whereas a high fluorescence indicates free unencapsulated carboxyfluorescein. The reduction in fluorescence in later wells results from the elution of high concentration of carboxyfluorescein causing itself quenching.

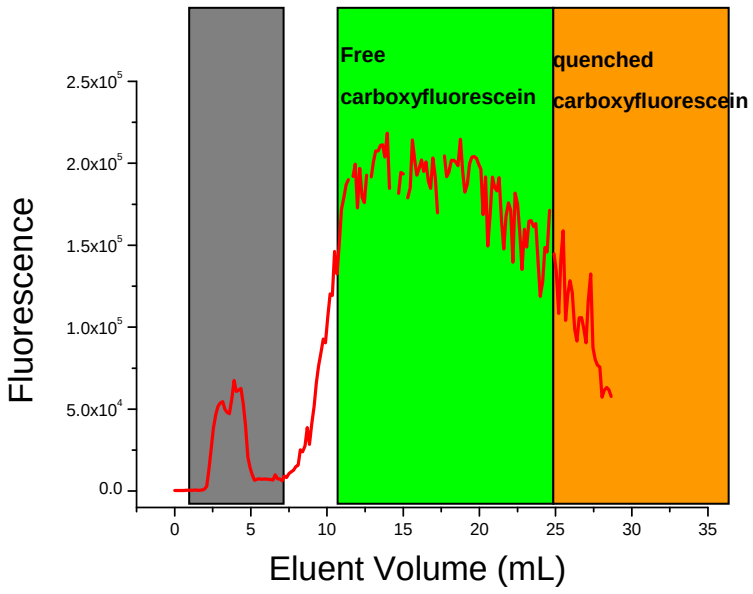

Figure 4.6: Fluorescence intensity change of eluent using NAP-25 column.

This concentration effect can be also mirrored by visual colour of the solution of 5(6)-carboxyfluorescein in figure 4.7. The solution becomes more orange with increased elution volume. The concentration effect on fluorescence intensity only applies in carboxyfluorescein in aqueous bulk.

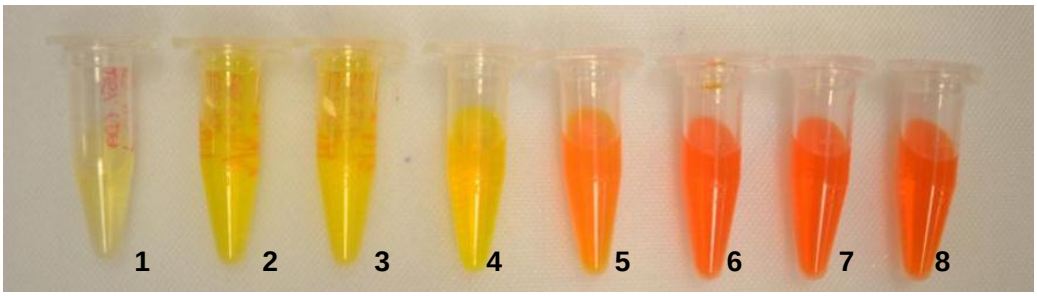

Figure 4.7: Visual images of eluate from NAP-25 column.
5(6)-carboxyfluorescein vesicles were eluted as a yellow eluate in vial 1, 2, 3. Eluent buffer mixed with pure vesicles were in vial 1, whereas some free carboxyfluorescein mixed with pure vesicles were in vial 4. Therefore, pure vesicles were collected from vial 2 and 3 to reduce contamination with free carboxyfluorescein.[5]

4.2 Surface Design – Pulsed Plasma Deposited Maleic Anhydride Thin Films as Supports for Vesicles

The utility of vesicles as encapsulation vehicles for antimicrobial agents in wound dressings requires that they can be attached to fabric. The vesicles can either be immobilised to fabrics via electrostatic or covalent bonding. Nonwoven fabrics and plasma have been of great interest recently. Plasma polymerisation allows fabrics functional with a large variety of physicochemical properties such as anti-soiling, increased hydrophobicity which repels bacteria, preventing attachment and subsequent colonisation. Organometalics have been used to be deposited creating an antimicrobial coating which is toxic to *P. aeruginosa* and *S. aureus.*[6] Maleic anhydride is of particular interest for the synthesis of functional organic thin films because of the double bond and the reactive anhydride group. In the case of maleic anhydride pulsed plasma polymerisation (PPP), anhydride functionality incorporation is favoured at short on-times and long off-times[6]. The proposed reaction mechanism for PPP using maleic anhydride as a model is summarised in figure 4.8. Indeed, the reaction is generated during the on-time by radical step-growth as described above, the polymer is deposited then a chain-growth mechanism takes over during the off-time.

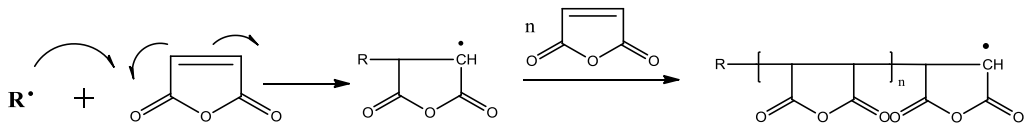

Figure 4.8: Chain growth of a polymer growth during the pulsed off period of PPP

In low power pulsed condition, an open film with retention of the anhydride hetero ring structure has been observed.[6] This ring can undergo nucleophilic attack, a freshly polymerised film left in water results in hydrolysis and formation of carboxylic acid moieties.[7] Free amines can attack the ring system forming amides. Free amine moieties in a supramolecular structure such as a vesicle can be used to tether the whole

suprastructure to the treated fabric via an amide link.[8] The vesicle based on amine attack on the hetero ring is schematically shown in figure 4.9.

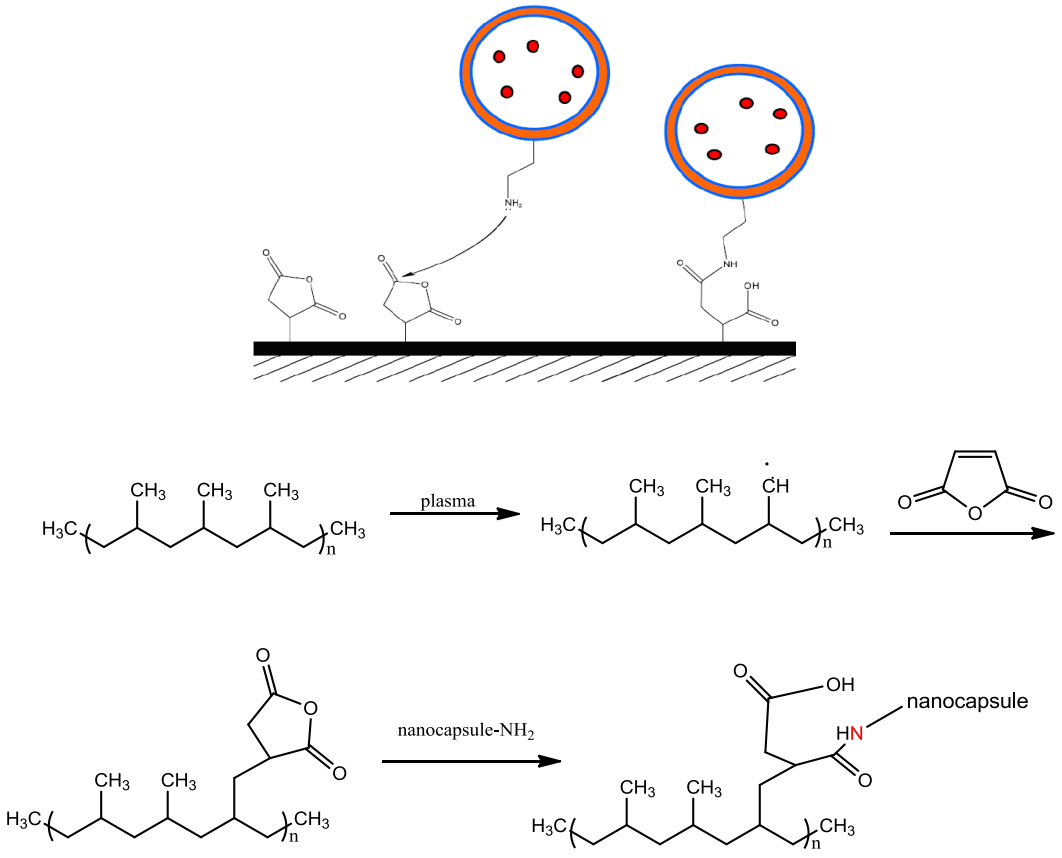

Figure 4.9: Schematic diagram & simplified reaction showing GUVs attached to pp-MA treated non-woven polypropylene via amide bond.
Maleic anhydride is grafted to a non-woven polypropylene. The free amine moiety of a phosphoethanolamine (2 mol %) can initiate a nucleophilic attack on the hetero ring forming an amide linkage.

4.2.1 Chemical Structural Characterisation for Plasma Polymerised Maleic Anhydride

The FT-IR spectrum of the pulsed plasma polymerised maleic anhydride using a plasma ON/OFF ratio of 1/40 (ms/ms) shows the film contains both anhydride structures around 1780 and 1860 cm^{-1}, as well as the structures representative of carboxyl groups around 1730 cm^{-1}. Figure 4.8 shows the typical anhydride group of pp-MA deposited on glass slides. Interestingly, the pp-MA was not stable enough after overnight at room

temperature when exposed to queous solution as can be seen from figure 4.10. The shoulder peak at 1860 cm^{-1} disappeared which clearly suggests loss of the anhydride structure (1780 and 1860 cm^{-1}) accompanied by the appearance of a broad band at around 1700 cm^{-1} due to the hydrolysis of anhydride bond and the formation of -COOH. Therefore, the pp-MA treated fabrics should be kept in plasma chamber under vacuum condition if it is not in use.

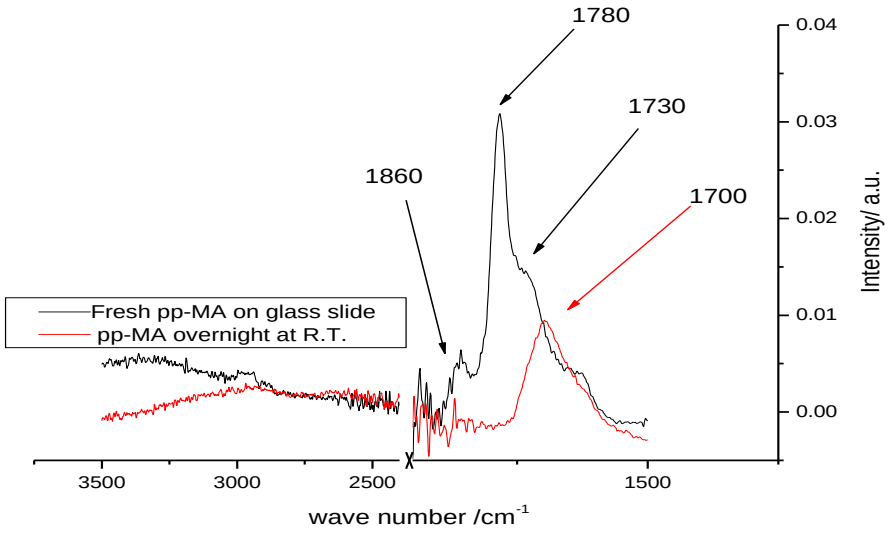

Figure 4.10: FT-IR spectra of pulsed plasma-polymerised maleic anhydride. Fresh pp-MA is shown in black and overnight pp-MA at room temperature shown in red.

4.2.2 Chemical Characterisation for Vesicles Attachment to pp-MA Non-woven Polypropylene

Any surface can be treated by plasma polymerisation. Non-woven polypropylene sheets purchased from Boots, the chemist, were used as a substrate for vesicle attachment since such non-woven polymers are used extensively in wound dressings, hygiene articles etc. FTIR spectra (figure 4.11) show the C-H bond expected for polypropylene. The plasma polymerised maleic anhydride deposited fabrics shows typical anhydride group at 1780 and 1850 cm^{-1}. Attachment of vesicles to the pp-MA nonwoven shows a strong, broad adsorption at 1630 cm^{-1}, which primarily results from ester C=O in the fatty acid chains of the phospholipids (both PC and PE) and amide C=O in the reacted MA only contributed to a fraction of the peak at 1637 cm^{-1}.

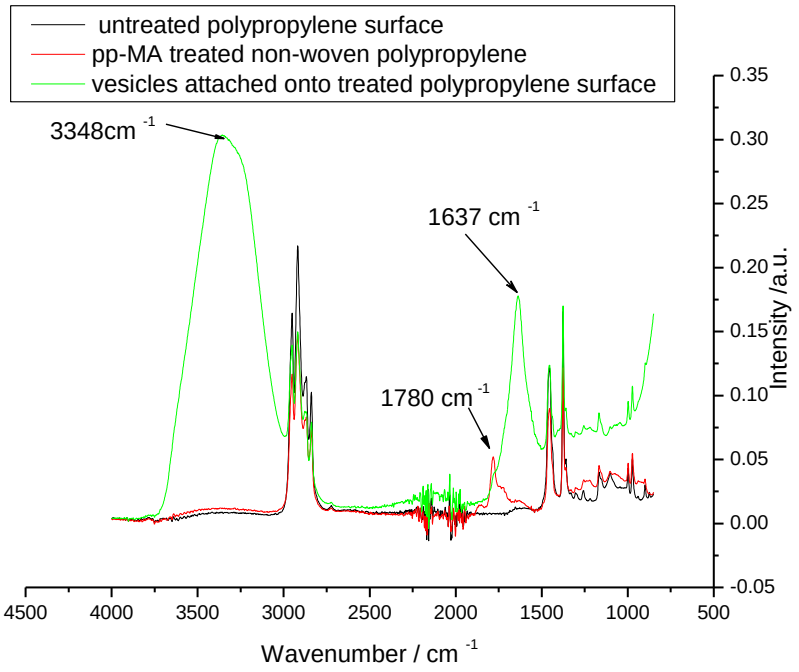

Figure 4.11: FTIR data for vesicles attachment onto treated non-woven polypropylene.
Black, standard polypropylene fabric; Red: non-woven polypropylene was modified with plasma polymerised maleic anhydride and shows anhydride group; Green: modified non-woven fabric was immersed in pure vesicles containing DMPE vesicle solution with amide bond formation around 1637 cm^{-1}.

4.3 Antimicrobial Activity Measurement of GUVs

In this study, antimicrobial efficacy of GUVs was evaluated both in suspension and on modified pp-MA non-woven polypropylene. Sodium azide was initially encapsulated in the vesicles as the released antimicrobial to kill/inhibit bacteria. The viable bacterial population in terms of CFU mL^{-1} or optical density was then plotted versus time. Bacterial susceptibility to antimicrobials was measured before antimicrobial test to obtain the information about the MIC_{50}.

4.3.1 Antimicrobials Studied in this Work for killing Bacteria

4.3.1.1 Sodium Azide

Sodium azide (NaN_3) is commonly used as biocide in hospitals or laboratories. Sodium azide inhibits cytochrome oxidase by binding irreversibly to the heme cofactor

in a process similar to the action of carbon monoxide. The compound is toxic and it may cause serious effects on humans such as convulsions, low blood pressure, low heart rate, loss of consciousness, lung injury and respiratory failure and even lead to death[9].

4.3.1.2 Gentamicin Sulfate

Gentamincin sulphate has been described in section 1.4.2.5.

4.3.2 Pathogens Studied in This Work

Bacteria studied in this work are specific strains of pathogens belongs to gram-positive *S. aureus* and gram-negative *P. aeruginosa*. These bacteria are generally present on human body in normal conditions but responsible for causing a wide range of infectious diseases ranging from minor skin infections to some life-threatening diseases such as toxic shock syndrome (TSS). *S. aureus* (MSSA 476) and *P. aeruginosa* (PAO1) were used as model pathogens in the work as they secrete a large variety of toxins which has been described in chapter 2 to cause destruction of membranes of vesicles. *E.coli* (DH5α) was chosen as control system as most of toxic genes has been removed from this strain and thus it doesn't secrete toxins to lyse vesicles.

4.3.2.1 *In-Vitro* Haemolysis Test

Pathogenicity assay on blood agar plate (figure 4.12) illustrates the lysis of haemoglobin around colonies of pathogenic bacteria *S. aureus* (MSSA 476) and *P. aeruginosa* (PAO1) as they secrete a wide range of toxins, while *E.coli* (DH5α) does not produce any toxins hence does not cause haemolysis on the blood agar plate.

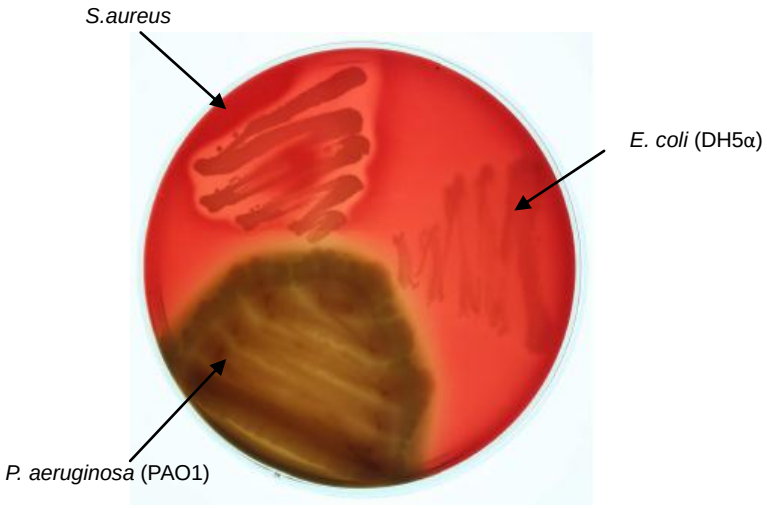

Figure 4.12: Blood agar plate showing the lysis of haemoglobin around colonies of typical pathogenic bacteria

S. aureus (MSSA 476) and *P. aeruginosa* (PAO1). *E. coli* (DH5 α) is a control system as it does not secrete toxins and it does not cause haemolysis; The photograph was taken by Dr. Geraldine Mulley from Department of Biology and Biochemistry, University of Bath, UK.

4.3.3 Determination of Bacterial Susceptibility

4.3.3.1 Minimum Inhibitory Concentration (MIC_{50})

The minimum inhibitory concentrations to kill 50% of the bacterial population (MIC_{50}) of sodium azide and gentamicin sulfate against the three bacterial strains, *S. aureus* (MSSA 476), *P. aeruginosa* (PAO1), and *E. coli* (DH5α) were determined. Initially, a range-finding test was performed to gauge a rough indication of sensitivity to sodium azide and gentamicin sulphate. Table 4.2 and 4.3 show the concentrations of sodium azide and gentamincin sulphate separately and at which bacterial growth was inhibited.

Table 4.2: Range finding test of NaN_3 against three strains of bacteria (where '+' is positive growth and '-' indicates no growth.)

NaN_3 (mg mL^{-1})	*E.coli* DH5α	*P.aeruginosa* (PAO1)	*S.aureus* (MSSA 476)
0	+	+	+
0.0001	+	+	+
0.001	+	+	+
0.01	+	+	+
0.1	-	-	+
1	-	-	-

Table 4.3: Range finding test of gentamicin sulphate against three strains of bacteria (where '+' is positive growth and '-' indicates no growth)

Gentamicin sulphate(mg mL^{-1})	*E.coli* DH5α	*P.aeruginosa* (PAO1)	*S.aureus* (MSSA 476)
0.00001	+	+	+
0.0001	+	+	+
0.001	+	+	+
0.01	-	-	+
0.1	-	-	-
1	-	-	-

The results of range finding test indicate at which range of concentration, the antimicrobial started to inhibit bacterial growth. Triplicates with a narrow range of concentrations were performed once a good indication of range finding test has been confirmed. The experiments of narrow range of concentrations of both sodium azide and gentamicin sufate against three bacterial strains were further performed on a fluorostar fluorimeter in absorbance mode at 600 nm. The concentrations of sodium azide and gentamicin sulfate to inhibit the three strains of bacteria are shown as follows:

- *E.coli* DH5α : 0.01 -0.1 mg/mL NaN_3 ;
- 0.001-0.01 mg/mL gentamicin sulphate
- *P.aeruginosa* PAO1 : 0.01-0.1 mg/mL NaN_3
- 0.001-0.1 mg/mL gentamicin sulphate
- *S.aureus* MSSA 476 : 0.1- 1 mg/mL NaN_3

- 0.01-0.1 mg/mL gentamicin sulphate

Based on the range of concentrations analysed above, the value of optical density dependent on varying concentrations of the three bacterial strains was then plotted, as presented in figure 4.13.

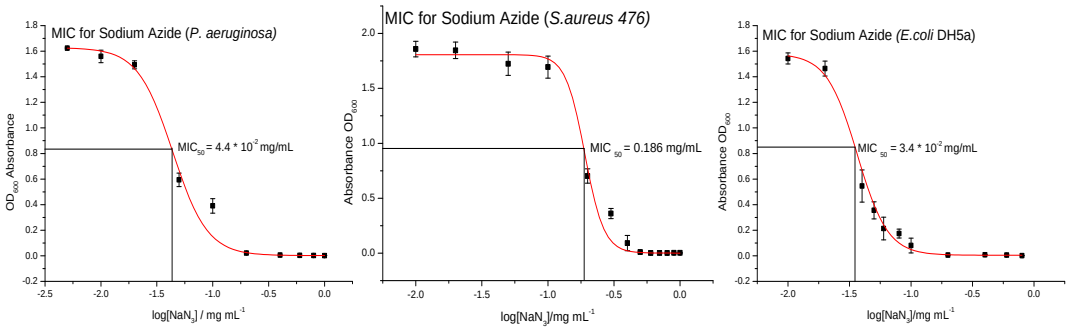

Sodium azide

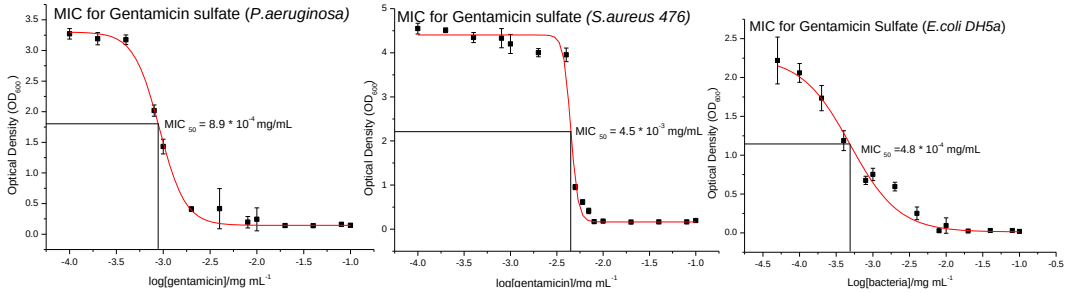

Gentamicin sulfate

Figure 4.13: MIC_{50} of sodium azide and gentamicin sulfate against the three strains of bacteria.
The shapes of bacterial optical density-antimicrobials (sodium azide and gentamicin sulfate) graphs give a clue that at which concentration of bacteria starts to respond to sodium azide/gentamicin sulfate and at which concentration of bacteria would be completely inhibited by these antimicrobials. The error bars represent standard deviations based on three measurements of each sample.

Minimum inhibitory concentrations were observed for sodium azide and gentamicin sulfate in solution. These are summarised in table 4.4. From the table, it can be observed that *E.coli* DH5α shows the most sensitive strain to both sodium azide and gentamicin sulfate meaning that more *E.coli* DH5α would be killed in comparison with

P.aeruginosa PAO1 and *S.aureus* MSSA 476 with same concentration of these antimicrobials. In both cases, *S.aureus* MSSA was relatively less sensitive to both antimicrobials. Also of interest was a much lower MIC for gentamicin versus the three strains than sodium azide which was around 100 times less than observed for sodium azide.

Figure 4.13 shows that *P. aeruginosa* started to respond (declines in concentration) to sodium azide and gentamicin sulfate at concentrations of 20 μg mL^{-1}, 0.6 μg mL^{-1} and was almost completely inhibited at concentrations of 200 μg mL^{-1}, 3 μg mL^{-1}; *S. aureus* showed that it became sensitive to sodium azide at 100 μg mL^{-1} and need 500 μg mL^{-1} for complete inhibition, whereas *S. aureus* started to respond to gentamicin sulfate at 3 μg mL^{-1} and was completely inhibited at a concentration of 7 μg mL^{-1}; *E.coli* (DH5α) showed most sensitive to both antimicrobials from both graphs and the table listed. The MIC provides information for the further studies especially for the study of antimicrobial measurement of vesicles containing various antimicrobial agents.

Table 4.4: MICs determined for sodium azide and gentamicin sulfate versus three strains of bacteria

Antimicrobials	*P.aeruginosa*PAO1 MIC_{50}(mg mL^{-1})	*S. aureus* MSSA 476 MIC_{50}(mg mL^{-1})	*E.coli* (DH5α) MIC_{50}(mg mL^{-1})
Sodium Azide	4.4×10^{-2}	1.9×10^{-1}	3.4×10^{-2}
Gentamicin Sulfate	8.9×10^{-4}	4.5×10^{-3}	4.8×10^{-4}

4.3.3.2 Minimum Encapsulation Concentration

In order to avoid any ineffective antimicrobial activity of releasing antimicrobials to bulk solution, the minimum encapsulation concentration should be estimated. The idea is on the basis of total internal encapsulation volume in section 2.5 and results of MIC_{50} in section 4.3.3.1.

Sodium Azide:

Total internal volume of GUVs per mL :

400 μL (the calculation is referred to section 2.5)

The highest concentration of NaN_3 needed to inhibit 50% of the three strains:

0.19 mg mL^{-1}

The highest concentration of NaN_3 which can kill/inhibit 100% of the three strains:

0.5 mg mL^{-1}

The minimum concentration of NaN_3 to be encapsulated within vesicles:

0.5 / 0.4 = 1.25 mg mL^{-1}

Therefore, the calculated concentration of NaN_3 is 1.25 mg mL^{-1}. A preliminary concentration of 15 mg mL^{-1} NaN_3 was encapsulated within vesicles to ensure a high encapsulated concentration thus can totally inhibit the two strains of pathogenic bacteria. Calculations were assumed that 100% of sodium azide was encapsulated and all vesicles had a uniform size, which in reality is not the case.

The minimum encapsulation concentration for gentamicin sulfate was calculated in the same manner. The calculated concentration is 0.025 mg mL^{-1}. A preliminary concentration of 5 mg mL^{-1} gentamicin sulfate was encapsulated within vesicles in order to ensure a high encapsulated concentration.

4.3.4 Solution Assay

4.3.4.1 Time Resolved Bacterial Killing by Sodium Azide Vesicles

Measurments of the bacterial mediated vesicle lysis and subsequent self-destruction were based on using conventional plate counting method to obtain the viable bacterial population every 20 minute. Figure 4.14 is the plot that viable cells of bacteria in terms of colony forming unit per millilitre over 4 hours. The graph shows a decrease in the concentration of viable *P. aeruginosa* and *S. aureus* over 4 h. *P. aeruginosa* was reduced in concentration at a rate of 0.12 $CFUm^{-1}$ min^{-1}, while the concentration of *S. aureus*

was decreased at a rate of 0.03 $CFUm^{-1}$ min^{-1}. The shape of the bacterial optical density versus sodium azide concentration graphs (figure 4.13) provides a clue to this behaviour. *P.aeruginosa* showed more susceptible to sodium azide in comparison with *S. aureus* shown on table 4.4. The rate at which *P. aeruginosa* was inhibited would be greater than *S. aureus* at low concentrations of sodium azide, if sodium azide was being slowly released at a constant rate in both cases. This difference in rate appeared to superficially correlate with the difference in MIC of the two bacteria. However, other factors which affect the rate of concentration decrease should also be taken into account such as the expression levels of virulence factors which lyse the vesicles from the two bacterial strains, which are not known.

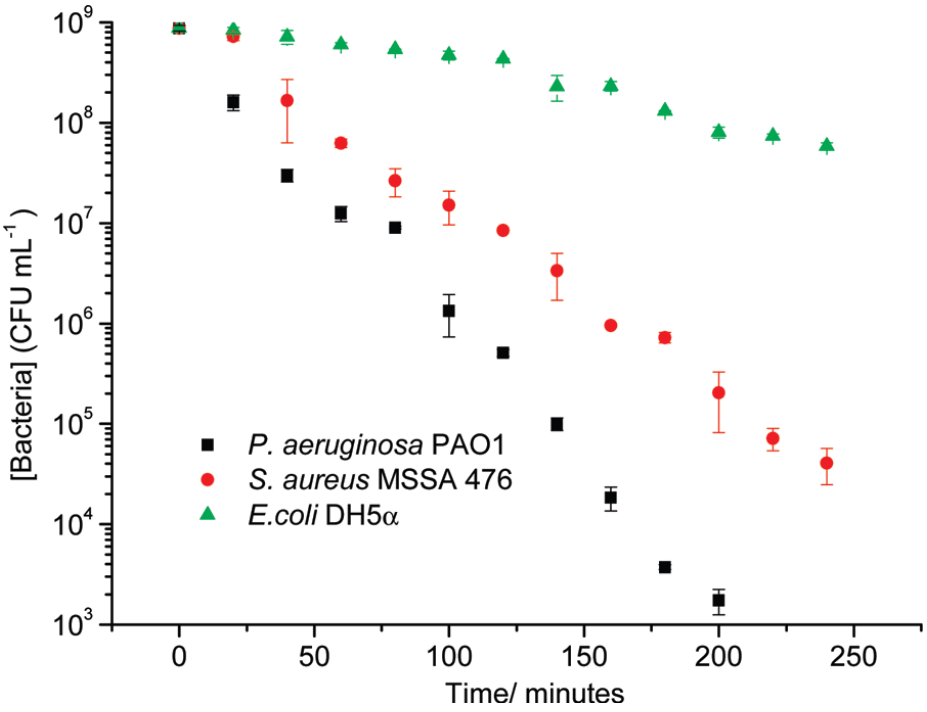

Figure 4.14: Reduction in the number of viable bacteria (CFU mL^{-1}) following exposure to vesicles containing sodium azide in aqueous suspension, over a 4 h period.
The strains tested were the pathogenic *P. aeruginosa* PAO1 and *S. aureus* MSSA 476 and the nonpathogenic *E. coli* DH5α. Error bars represent standand deviation based on three measurements of each sample.

In contrast, there was a much lower decrease in the number of *E. coli*, despite this strain being the most sensitive to sodium azide. Therefore, it can be concluded that the

pathogenic bacteria are rapidly killed/inhibited by sodium azide released from the vesicles, which are specifically lysed by membrane-damaging toxins produced by the pathogenic strains.

4.3.4.2 Time Resolved Bacterial Killing by Gentamicin Sulfate Vesicles

In this part of study, gentamicin sulfate was encapsulated in the vesicles which are lysed by toxins secreted by two pathogenic bacterial strains. The assay was based upon using a BMG Labtech plate reader. The resulting graphs shown in figure 4.15 are the viable number of bacteria in terms of optical density versus time. Vesicles containing gentamicin sulfate were incubated overnight in the presence of pathogenic strains *P. aeruginosa* and *S. aureus* and non-pathogenic *E. coli* DH5α. Inhibition of growth should be seen in *P. aeruginosa* PAO1 and *S. aureus* MSSA 476 as the virulent factors secreted by these two strains make a contribution to the lysis of vesicles. *E.coli* DH5α as a negative control should show a normal growth curve.

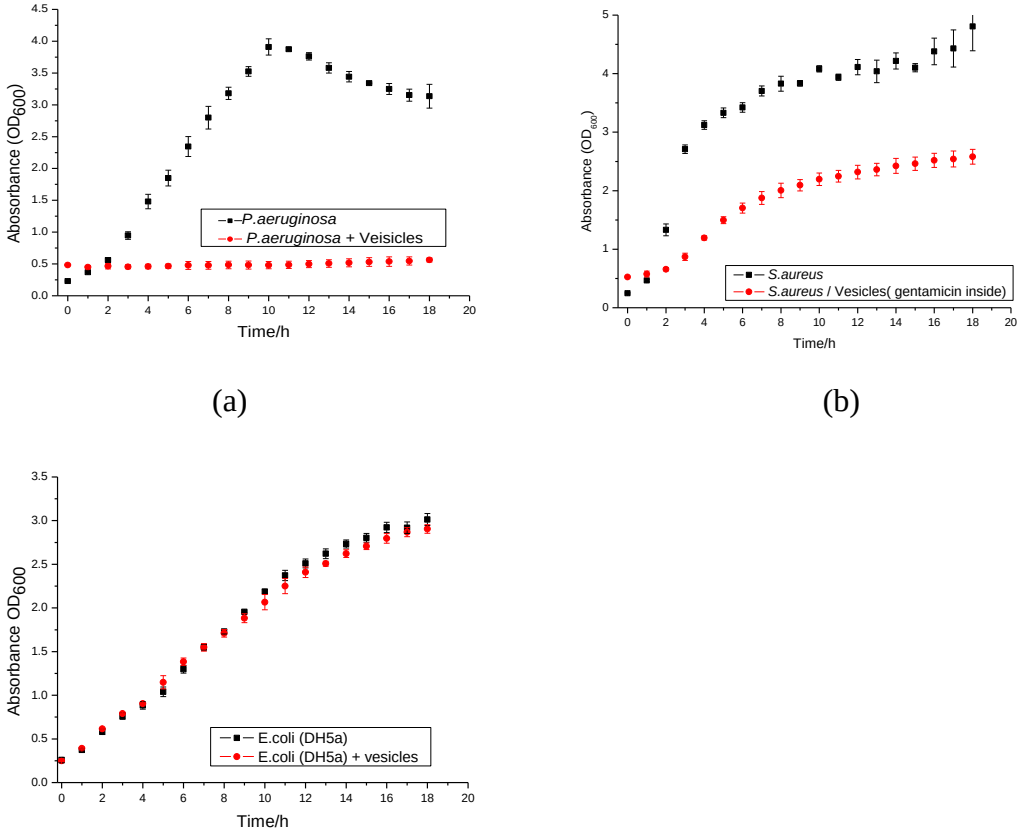

Figure 4.15: Time-course of viable number of pathogenic and non-pathogenic bacteria with GUVs containing gentamicin sulfate.

a) *P.aeruginosa* (PAO1) was incubated with GUVs overnight. Black squares show normal growth curve of *P.aeruginosa* PAO1; Red squares show *P.aeruginosa* PAO1 was completely inhibited/killed by gentamicin sulfate released from the GUVs after overnight; b) *S. aureus* (MSSA 476) was incubated with GUVs overnight. Black: growth curve of *S.aureus* MSSA 476; Red: The number of viable of *S.aureus* MSSA 476 was decreased by inhibition of getamicin sulfate; c) *E.coli* (DH5α) shows identical growth curve after it was incubated with GUVs after overnight. Error bars represent standard deviations based on three measurements of each sample.

The graphs confirm that *P. aeruginosa* PAO1 and *S. aureus* MSSA 476 were inhibited/killed by gentamicin sulfate released from GUVs as these two pathogenic strains secrete a large variety of virulent factors such as phospholipase, exotoxin A by *P.aeruginosa* and α-haemolysin, leucocidin by *S. aureus*. From the graphs, *P. aeruginosa* PAO1 was completely inhibited/killed by gentamicin sulfate released from GUVs overnight, while *S. aureus* MSSA 476 showing much lower decease with GUVs after overnight. The difference in the rate of the viable number decreasing between these two

strains is due to the difference of sensitivity to gentamicin sulphate of these two strains (MIC data) and mechanism of interaction between toxins and membrane of vesicles. Similarly to sodium azide, *S. aureus* MSSA 476 shows less sensitivity to gentamicin sulfate which is about 10 times higher than *P. aeruginosa* PAO1. The rate at which *P. aeruginosa* was inhibited would be greater than *S.aureus* at low concentrations of gentamicin sulphate. In addition, the graph further confirms the description that gentamicin is used particularly to treat the infection caused by gram-negative organisms.[10] Furthermore, due to the different modes of action of virulent factors secreted by these two strains, the different ways of lysing membrane of vesicles should also be taken into consideration. Chapter 1 describes the main toxins secreted by *P. aeruginosa* and *S. aureus* which would make a contribution to the destruction of vesicles. The possible reason is that phospholipase C secreted by *P. aeruginosa* lyses the membrane of a vesicle and would make the whole shell of the vesicle rupture which leads to the encapsulated antimicrobials released to the external solution immediately, whilst α-haemolysin secreted by *S.aureus* is a pore-forming toxin which would create many holes to insert into the membrane of the vesicles and thus the encapsulated antimicrobials would be released gradually to the external environment.

In contrast, the viable numbers of *E. coli* DH5α with vesicles exhibit indentical growth curve although this strain shows the most sensitive to gentamicin sulfate. Therefore, it can be concluded that the pathogenic bacteria are inhibited/killed by getamicin sulfate released from the GUVs as they produce membrane-damaging toxins which will lead to the lysis of vesicles.

4.3.5 Fabric Assay Japanse Industry Standard (JIS)

Having successfully immobilised vesicles on the pp-MA modified nonwoven polypropylene, this part of the study will investigate the antimicrobial performance of the modified fabrics against the two pathogenic bacteria (*P. aeruginosa* PAO1 and *S. aureus* MSSA 476) and a nonpathogenic control *E.coli* DH5α. The control provides

important information on whether the fundamental hypothesis is correct: pathogenic bacteria lyse the vesicles and ensure their self-destruction, but nonpathogenic bacteria are largely unaffected.

The antimicrobial performance of the vesicles containing sodium azide attached to fabrics was initially tested using the methodology described in experimental section. Other antimicrobials such as gentamicin sulfate, silver nitrate, chlorhexidine encapsulated within vesicles were also tested using JIS which will be demonstrated in chapter 7. The results in figure 4.16 show that the vesicle modified nonwoven fabric completely inhibits/kills both pathogenic bacteria *P. aeruginosa* PAO1 and *S. aureus* MSSA 476, while the nonpathogenic *E. coli* DH5α colonised the vesicle-modified fabric to almost the same extent as the non-modified control because it does not secrete membrane damaging toxins. There was a decrease in the number of *E .coli* DH5α due to some passive leakage of sodium azide which limited the growth of *E. coli* to an extent. Therefore the *E.coli* control is useful as a measure of the 'leakiness' of vesicles containing sodium azide.

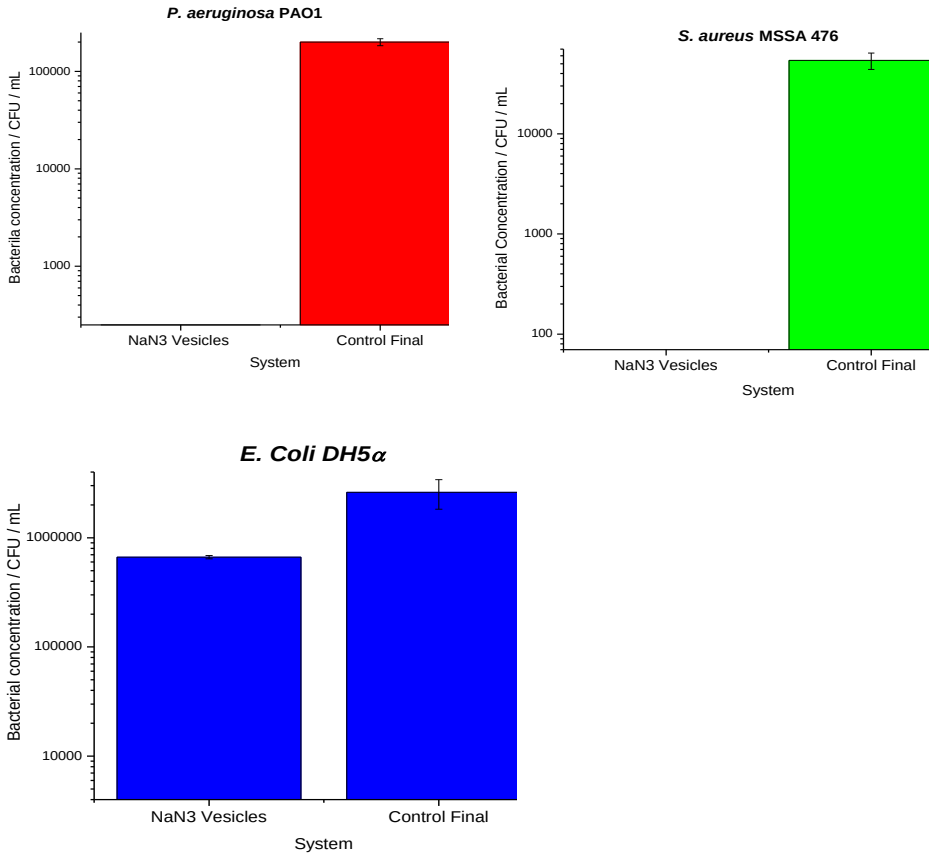

Figure 4.16: JIS results of lipid vesicles (containing sodium azide) against three strains of bacteria. The figures show persistence and growth of two pathogenic (*S. aureus* MSSA 476 and *P. aeruginosa* PAO1) and one nonpathogenic (*E. coli* DH5α) strains of bacteria on fabric modified with vesicles containing sodium azide (NaN_3 vesicles) in comparison to nonmodified, UV sterilised nonwoven (control), over a 4 h period. The pathogenic bacteria secrete membrane damaging toxins which lyse the vesicles, releasing sodium azide at a concentration that inhibits bacterial growth, with total clearing of *S. aureus* and 2 CFU mL^{-1} of *P. aeruginosa* being measured after 4 h. Error bars represent standard deviations based on six measurements of each sample.

4.4 Visualisation of Vesicle Lysis by Bacteria under Fluorescence Microscopy

The main advantage of GUVs is that their sizes are relatively large which can be easily visualised, especially if containing a water-soluble dye such as fluorescein. Fluorescence microscopy was used in this work to provide further confirmation of the hypothesis that the pathogenic bacteria lyse vesicles, while the nonpathogenic strain does not. The results in figure 4.17 show individual immobilised vesicles on pp-MA modified Petri

dishes, and subsequent lysis on addition of *P .aeruginosa* and *S. aureus. E. coli* DH5α as a control system did not lose fluorescence, meaning that the *E.coli* DH5α does not secrete membrane damaging toxins. Interestingly, there are some differences in the images of the vesicles being lysed by *P .aeruginosa* compared with *S. aureus*. *P. aeruginosa* appears to have caused the vesicle to initially swell before loosing its encapsulated dye; the vesicles exposed to *S. aureus* gradually lost fluorescence intensity, but in a way of slow release of dye rather than swelling. This difference could relate to the differences in the modes of action of the different virulent factors secreted by *P. aeruginosa* compared to *S. aureus*.

0 minutes	20 minutes	80 minutes	120 minutes
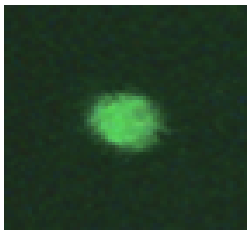	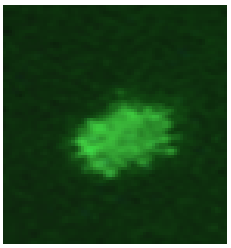	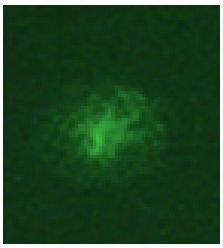	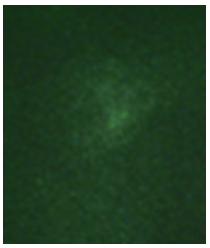
P.aeruginosa **PAO1**			
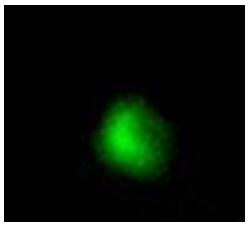	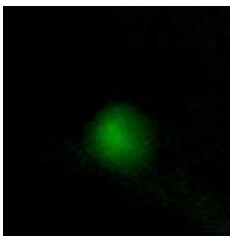	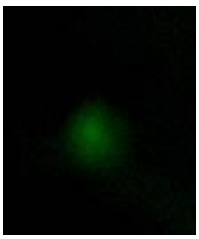	
S. aureus **MSSA 476**			
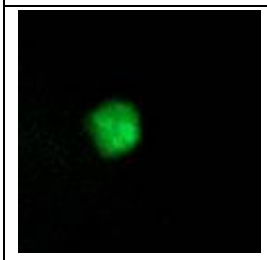		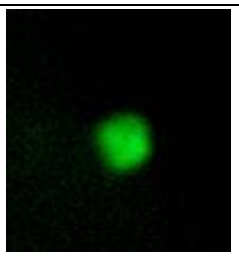	
E. Coli **DH5α**			

Figure 4.17: Fluorescence imaging of surface attached vesicles exposed to the three strains of bacteria. Box width 60 μm.

4.5 Conclusion

In this chapter, an initial microbiologically responsive nanocapsule system for controlling bacterial growth and infection has been presented. The synthesis of GUVs is relatively easy to manipulate: incorporation of cholesterol in the vesicle system provides

vesicles stability at room temperature as well as renders vesicles biomimetic; DMPE provides an anchoring site---ethanolamine which would make a contribution to the immobilisation of vesicles onto plasma pp-MA treated fabrics. The purification of vesicles using NAP-10 and NAP-25 and the efficiency of purification of these two columns were also demonstrated. Vesicle immobilisation has been addressed by using plasma polymerised maleic anhydride deposited onto nonwoven. FT-IR data further proves the successful attachment of vesicles to treated fabrics. The GUVs containing antimicrobial agents have the ability to inhibit/kill pathogenic bacteria and are not affected by non-pathogenic bacteria. These assays were carried out both in suspension and on pp-MA treated fabrics. Two different methods of measuring viable number of bacteria against vesicles over time were carried out in this chapter in terms of conventional plate counting methodology and optical density. Further microscopy images prove the hypothesis---pathogenic bacteria can damage the membrane of vesicles to cause the vesicles lysis, while non-pathogenic bacteria are not affected by vesicles because they do not secrete virulent factors.

In the case of purification, NAP-10 columns were mainly used in this work to purify GUVs and double filtration was applied to encapsulated antimicrobial agents in order to obtain pure vesicle solution. NAP-25 became available later in the work and was mainly used for the purification of phospholipid/PDA vesicles. However, GUVs were used for evaluating the efficiency of these two columns by encapsulating carboxyfluorescein (self-quenching at high concentration) and NAP-25 was confirmed to be used for the further study due to its greater volume capacity and low cost compared to NAP-10 columns.

However, the GUVs have some problems for long term use such as susceptibility to surfactants, morphological instability and entrapped drug leakage over time. Therefore, it is unlikely, for example, that GUVs would be used in a final product. The ultimate aim of this work is to attempt to construct a ‘smart’ wound dressing system that only releases an encapsulated antimicrobial agent in the presence of pathogenic bacteria, while not

responding to commensal/harmless bacteria. Furthermore, the system would minimise the pressure of selected antibiotic resistance by ensuring antibiotics are released only in response to pathogenic bacteria and would prolong the efficacy and shelf life of the encapsulated antimicrobial.[11] Also, a simple colorimetric or fluorimetric response could be built into the system to provide an early warning of wound infection for patients or clinicians. Important problems regarding vesicle stability, tuning of response, manufacturability, and immunological response remain to be solved. However, this chapter of study provides the possibility of building a prototype of wound dressing for detecting/killing pathogenic bacteria. Partially polymerised acetylene fatty acid/phospholipid vesicles as an alternative to improve the stability of vesicles will be presented in detail in next chapters. Furthermore, the study of tuning of fluorescence response will also be demonstrated in next chapter.

4.6 References

1 Alberts, et al., *Molecular Biology of the Cell: Fourth Edition*, New York: Garland *Science*, 2002, 588.

2 Genis R.B., Biomembranes: Molecular structure and function, Spring-Verlag, 1989.

3 Wan et al., Biochemistry 47, 2008.

4 Moscho A., Orwar O., Chiu D. T., Modi B. P., Zara R. N., Rapid preparation of giant unilamellar vesicles, *Proc. Natl. Acad. Sci*.U.S.A. 1996, *93*, 11443-11447.

5 Bean J., Development of antimicrobial encapsulated lipid vesicles for use in 'smart' burn wound dressings**,** MChem Thesis, 2011.

6 Poulter N., Munoz-Berbel X., Johnson A.L., Dowling A.J., Waterfield N., Jenkins A.T.A.,An organo-silver compound that shows antimicrobial activity against *Pseudomonas aeruginosa* as a monomer and plasma deposited film, *Chem. Commun.*, 2009, 7312-7314.

7 Liu S., Vareiro M., Fraser S., Jenkins A.T.A., Control of Attachment of Bovine Serum Albumin to Pulse Plasma-Polymerised Maleic Anhydride by Variation of Pulse Conditions, *Langmuir*, 2005, *21*, 8572-8575.

8 Schiller S., Hu J., Jenkins A.T.A., Timmons R.B., Sanchez-Estrada F.S., Knoll W., Forch R.,Chemical structure and properties of plasma-polymerised maleic anhydride films, *Chem. Mat.*, 2002, *14*, 235-242.

9 Mallinckrodt Baker, Inc. (2008-11-21); information retrieved from Wiki

10 Moulds, Robert, Jeyasingham, Melanie, Gentamicin: a great way to start, *Australian Prescriber*, 2010, *33*, 134–135.

11 Hecker M.T., Aron D.C., Patel N. P., Lehmann M. K., Donskey C. J., Unnecessary use of antimicrobials in hospitalised patients: current patterns of misuse with an emphasis on the antianaerobic spectrum of activity, *Arch. Intern. Med*., 2003, *163*, 972-978.

Chapter 5 Study of Partially Polymerised Polydiacetylene/Phospholipid Vesicles Based Upon Construction of a Fluorescence Sensing System

The previous chapter was devoted to constructing a new microbiologically responsive system for detecting and killing bacteria. The present chapter is based on the idea of improving the stability of such a system by insertion of diacetylene fatty acids within the lipid vesicles and polymerising. Such a sensing system might be robust enough for clinical use. As stated previously, burns and wounds are particularly susceptible to bacterial infection especially in young children. Wound swabs, microbiological cultures and/or other related tests used to diagnose infection often do not provide clinicians with the timely guidance they require which result in inaccurate diagnoses based on the child's clinical condition alone. Therefore, there is a clinical requirement to diagnose infection at early stages and preferably, without the removal of adherent dressings. A wound dressing designed to change colour can indicate the change in microbiological state, allowing for rapid intervention. A fluorescence sensing system was constructed based upon the dilution of a self-quenching fluorescent dye. Carboxyfluorescein was used as a dye and was encapsulated within vesicles. The basis of this idea is that at high concentration, carboxyfluorescein is non-fluorescent; following breakdown of the lipid vesicle containers by bacterial toxins, the dye becomes diluted and "switches on".

The reminder of the chapter is organised as follows: in section 5.1, the methods to stabilise phospholipid vesicles by using photo-polymerisable fatty acid moieties are presented. In section 5.2, the study of colorimetric property is discussed by using UV-vis spectroscopy. A fluorescence sensing system using self-quenching carboxyfluorescein within vesicles has been discussed in section 5.3. Section 5.4 elaborates on the study of stability and sensitivity of such system by incorporating different molar concentration of

TCDA. Section 5.5 further exploits the vesicles' response to pathogenic bacteria while not responding to non-pathogenic bacteria by using encapsulating carboxyfluorescein within vesicles. Section 5.6 concludes the chapter and summarises the key findings.

5.1 Formation and Purification of TCDA/phospholipid Vesicles

5.1.1 Materials

TCDA/phospholipid vesicle in this work is a hybrid which is composed of two types of lipids, cholesterol, and self-assembled diacetylene monomers. DMPC, DMPE, cholesterol have been described in section 4.1.1 and will not be discussed here. The main functions of TCDA are described as follows.

5.1.1.1 TCDA

10, 12-tricosadiynoic acid is a type of diacetylene monomers (figure 5.1A). It is composed of two different parts: a polar head group and a hydrophobic tail with diacetylene moiety. The TCDA is a self-assembly material when it is exposed to aqueous solution. The diacetylene will undergo 1,4-addition under UV irradiation(figure 5.1B) to form a cross-linked polymer. The detailed scheme of how they form polymerised vesicles has been introduced in chapter 1.

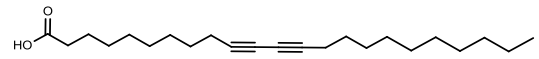

(A)

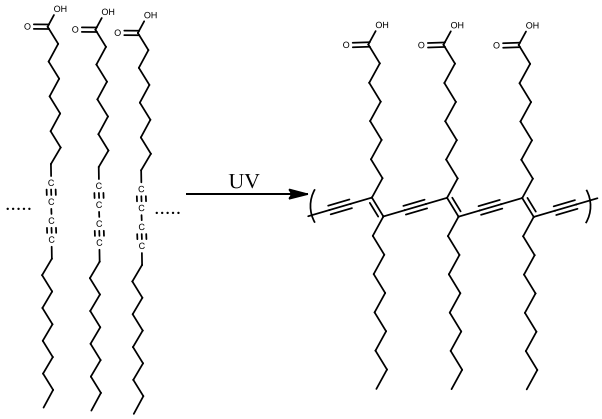

(B)

Figure 5.1: Chemical structure and polymerisation of 10, 12 - tricosadiynoic acid.
A) Chemical structure of 10, 12-tricosadiynoic acid (TCDA, $C_{23}H_{38}O_2$, mw: 346.55, mp: 56-60 ^oC); B) Organisation of the polymerised backbone from the diynoic acid monomers after UV irradiation.

5.1.1.2 Structure and Phase Separation

The vesicle system consists of a mixed assembly of membrane lipids and other membrane constituents such as cholesterol, combined with polymerised diacetylenic lipids which are called PDA. Lipid/TCDA mixed vesicles are generally prepared by mixing the lipids and diacetylene monomers in appropriate molar ratios.The resultant lipid/TCDA vesicles exhibit a blue colour after photo-polymerisation due to the conjugated backbone of the PDA polymer. The study of the colorimetric properties will be described in section 5.2. Furthermore, such vesicular aggregates have been shown to undergo distinct blue-red colorimetric changes owing to conformational transitions in the conjugated (ene-yne) polymer backbone, induced by external structural perturbations.[1] It is shown that the lipids and PDA part are interspersed within the mixed assemblies and they are likely to form distinct domains[1] (figure 5.2).Such organisation and association would assist the stability and sensitivity by adjusting the molar

concentrations of the TCDA part.

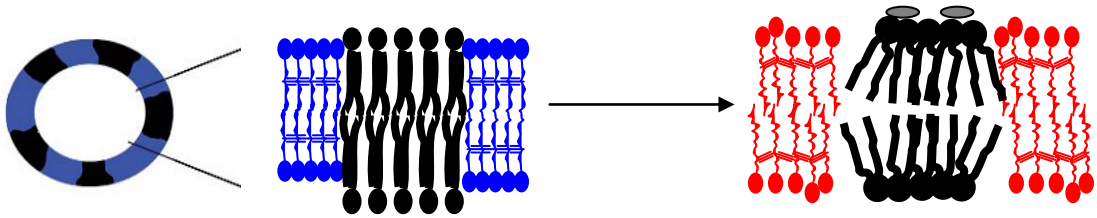

Figure 5.2: Organisation of phospholipid/TCDA vesicles and their colorimetric sensing. Structural/colorimetric transformations of PDA (blue part) can be induced by external molecules (grey part) which interact with the lipid bilayer domains (black part). [2]

5.1.1.3 Temperature Effect of TCDA on Mixed Vesicle System

Temperature plays an important role in determining the stability and sensitivity of vesicle systems as described in section 4.1.1.4. The vesicle system becomes leaky if it is in its liquid crystalline phase; the system lacks sensitivity which makes it impossible to be lysed by virulent factors if it is all in the gel phase. In this work, various concentrations of TCDA from 5 mol% up to 60 mol% have been incorporated into the phospholipid part to find out the optimal system which can be sensitive to toxins as well as be stable enough for the long term. Most of the lipid mixtures would be in liquid crystalline phase with small amount of TCDA incorporation at room temperature. The concept is to produce a 'hard' polymerised TCDA shell which contains patches of liquid crystalline phospholipid. Furthermore, the insertion of cholesterol further improves the stability of the lipid bilayer and provides both firmness and fluidity in lipid bilayers. Therefore, the TCDA/phospholipid vesicles are maintained in a sufficiently fluid phase by insertion of appropriate molar concentration of TCDA into the bilayer moiety. Such functionality is suitable to be used as drug carriers at 37 ^{o}C as all microbiological work was carried out at 37^{o}C for optimal growth of bacteria.

5.1.2 Vesicle Formation and Polymerisability

Lipid extrusion was used here for the synthesis of phospholipid/TCDA vesicles to obtain uniform size distributions and the detailed procedure has been presented in the experimental section. In the case of polydiacetylene vesicle formation, the lipids must hydrate and organise into the correct packing and orientation to undergo the 1,4-addition to form conjugated polymer. The resultant vesicle solution exhibits a colour transition from transparent to blue. Therefore, the polymerisation reaction itself and the optical detection of the blue colour provide indirect evidence of an ordered lipid assembly. Vesicle formation can be determined by scanning electron microscope which is shown in figure 5.3. The image shows vesicles with relatively uniform size distributions. Vesicles were extruded by using 100 nm of pore size. Vesicle used here was composed of 10 mol% TCDA and the SEM study was conducted after 1 week of vesicle formation. Therefore, the diameter of resultant vesicles was around 150 nm due to the some degree of vesicle-vesicle fusion. This is because that vesicle growth could, in principle, occur by the incorporation of free amphiphilic molecules or micelles, or through vesicle-vesicle fusion.

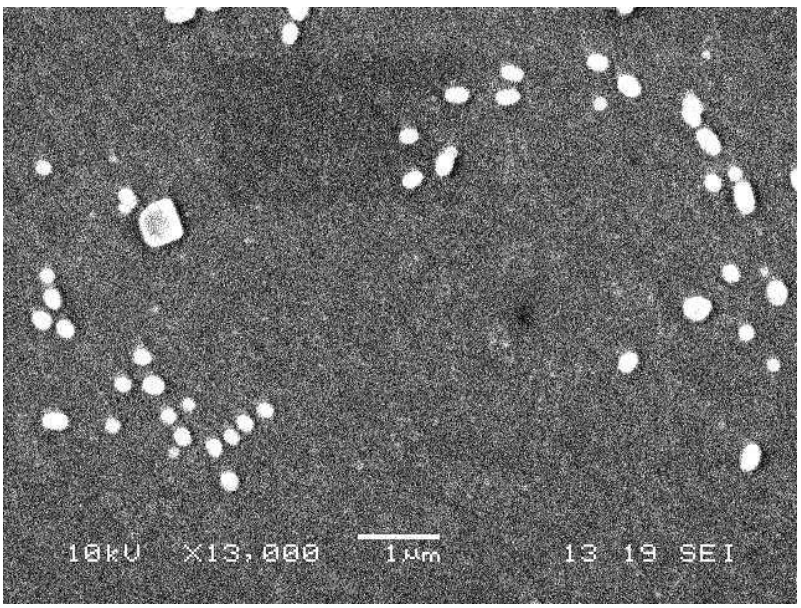

Figure 5.3: SEM image of phoshpolipid/TCDA vesicles composed of 10 mol% TCDA, 20 mol% cholesterol, 2 mol% DMPE and 68 mol% DMPC.
The average partical size is approximately 150 nm.

5.1.3 Purification of Phospholipid/TCDA Vesicles

TCDA/phospholipid vesicles were purified in the same manner using NAP-25 columns purchased from GE Healthcare. The detailed study of purification has been described in section 4.1.3.

5.2 Study of Colorimetric Property of Polydiacetylene/Phospholipid Vesicles

One of the most interesting aspects of polydiacetylene chemistry is the colour and chromism of the materials. This can be ascribed to many factors such as the original packing state of the monomers and the exposure of the polymeric moiety to environmental perturbations such as heat (thermochromism),[3-5] mechanical stress (mechanochromism),[6-7] or solvent (solvatochromism).[6,8]

The colorimetric property of vesicles assembly constructed from phospholipid molecules and conjugated polydiacetylene was studied here. UV-Vis spectroscopy was applied to characterise their chromatic property and their contributions to the observed blue-to-red colour transitions.

5.2.1 UV-Vis Spectra of Vesicles Depending upon the Molar Ratios of Lipid-PDA

The mixed vesicle system shows color transition from colorless to blue after photo-polymerisation because of conjugation of TCDA. Figure 5.4 shows a photograph depicting the appearance and UV-Vis spectra of aqueous solutions of vesicles with different molar ratios of DMPC and TCDA at 640nm. The figure clearly shows that the intensity of the blue color and the corresponding absorbance spectrum are closely related to the DMPC-TCDA ratio within the vesicles. The visual image also shows that the extent of color changing strongly depends upon the ratios of the lipids-TCDA. Indeed, the formation of vesicles with relatively high mol% of DMPC yields completely colorless vesicles (figure5.4b10%). The dependence of colorimetric property of the

vesicles upon the DMPC-TCDA molar ratio indicates that the two components are interspersed and they do not form two separate vesicle phases in solution. It can be explained that the similar conjugation and blue appearance of the solutions would be observed if they form two distinct vesicle solutions. However, such result is not observed here. Furthermore, the optical detection of the blue colour for the diacetylene system can provide direct evidence of the polymerisation of diacetylenic lipids.

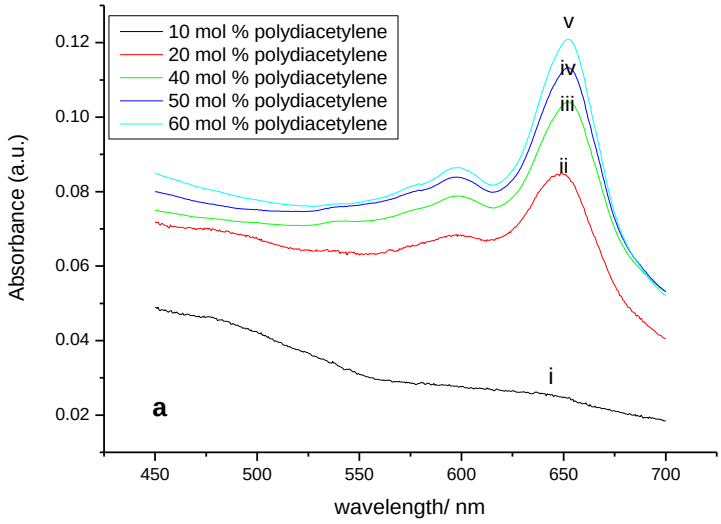

.

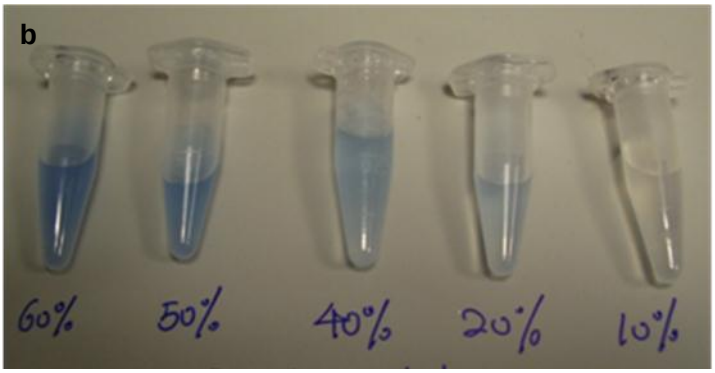

Figure 5.4: Colorimetric properties of phospholipid/TCDA vesicles after UV irradiation.
(a) Visible absorption spectra of phospholipid/TCDA vesicle solution irradiated with UV light and plots of absorption at 640 nm; (b) Photograph depicting the appearance of vesicles with different mol % of polydiacetylene (PDA).

5.2.2 Thermochromic Property of Phospholipid/PDA Vesicles

This part of the study investigates the temperature effect upon the chromatic properties of the vesicles. The colour transition of the vesicles was monitored by visible absorption spectroscopy with peaks within the range of 620-640 nm (PDA blue phase) and 490-540 nm (PDA red phase). The blue to red transition is associated with a conformational change of the polydiacetylene backbone from planar to nonplanar.[9] It is proposed that the acetylenic backbone converts to the butatrienic form, as shown in figure 5.5.

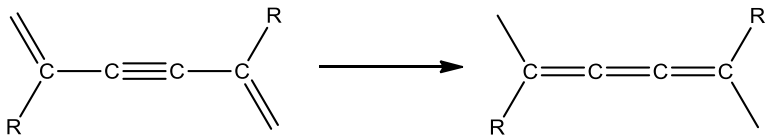

Figure 5.5: The transition of backbone structures of polydiacetylene from planar to nonplanar

Vesicles with 40 mol % TCDA were formed in this experiment which is due to the reason that low concentration of TCDA (10, 20, 30 mol% TCDA) would lead to undetectable colour change. To evaluate the colour changes, colorimetric response was defined as the relative change in "percent blue" for the vesicle preparation. PB_0, the initial percent blue, is defined as:

$$PB_0 = A_{blue} / (A_{blue} + A_{red}) \times 100\% \quad (5.1)$$

In this expression, A is the absorbance at the wavelength of either the blue or red form. The colorimetric response gives the percent conversion to the red form at a given temperature, which is defined as:

$$CR = (PB_0 - PB_I)/PB_0 \times 100\% \quad (5.2)$$

The resulting plot was the extent of blue-red colour transition (CR %) of vesicle samples as a function of temperature.

Figure 5.6 shows the dependence of colorimetric and dynamical properties of different compositions of vesicles upon temperature. The percentage of colorimetric transition (CR) was induced by temperature. Higher CR value indicates more colour transitions, for example, more reddish appearance of the solution was observed. The photograph insert above shows the colour change of vesicles (DMPC/DMPE/Cholesterol/TCDA) was induced by heating the solution from 20 ^{o}C to 40 ^{o}C. At various points in between, the vesicle solution takes on a purple to pink colour compared to the initial faint blue. The graph also shows that the lipid composition affects the thermal sensitivity of the vesicles. From the data, the DMPC/DMPE/TCDA assemblies undergo stronger blue-red transitions as compared with DMPC/DMPE/Cholesterol/TCDA vesicles. This is due to the fact that the presence of cholesterol increases rigidity of the colorimetric membrane bilayer. Therefore, it can reduce its temperature sensitivity. Again, incorporation of cholesterol into the lipid membrane is necessary because the chromatic property of the vesicles would interfere with fluorimetric response if a fluorescent dye encapsulated within vesicles and probably have a negative effect on the fluorimetric response of the vesicle system. Therefore, 20 mol% cholesterol was used here for stabilising vesicle system as well as for reducing PDA vesicles' temperature sensitivity.

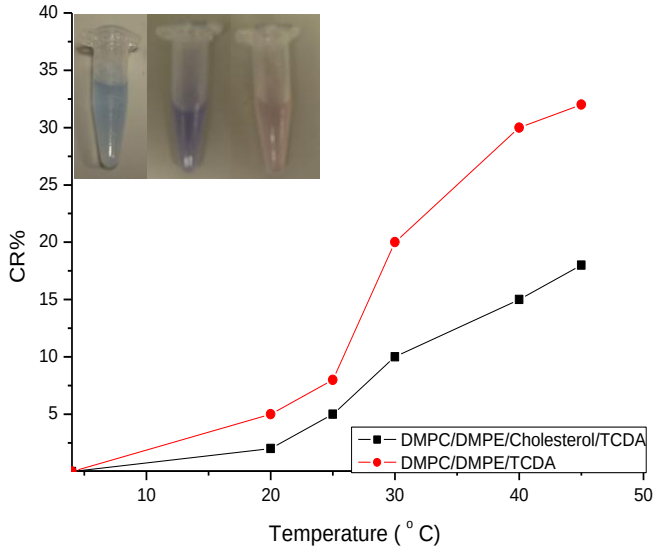

Figure 5.6: Graph of colorimetric response (CR) calculated from the visible absorption spectra of DMPC/DMPE/ 40 mol % TCDA and DMPC/DMPE/Cholesterol/40 mol % TCDA as a function of the solution temperature.

The insert photograph showing plastic tubes containing the vesicle solution (DMPC/DMPE/TCDA/Cholesterol) before heating, at room temperature (faint blue), at 30 ^{o}C (purple) and at 40 ^{o} C (pink)

5.2.3 Colorimetric Detection of Bacteria-Vesicle Interactions

Several reports have demonstrated that lipid/PDA vesicles undergo colour transitions upon binding of bacteria or antimicrobial peptides.[1, 10] This part of the study investigated the colorimetric transition of the vesicles with addition of bacteria and the differentiation of colour response between pathogenic bacteria and non-pathogenic bacteria. *P. aeruginosa* (PAO1) and *S. aureus* (MSSA 476) as the pathogenic model and *E.coli* (DH5α) as the non-toxic model were cultured with phospholipid/TCDA vesicles at 37 ^{o}C. It was speculated that the colour changes could yield distinct colours by binding different bacteria which would be an indication of differentiating pathogenic and non-pathogenic bacteria: the binding of *P.aeruginosa* PAO1 and *S.aureus* MSSA 476 would undergo a stronger colour transition. Unfortunately, UV-visible spectra and the photographs insert (figure 5.7) show no distinct colour is observed, suggesting the colorimetric transition of such vesicle system is not affected by different types of

bacteria. The photographs show that the vesicles undergo stronger colour transition in comparison with the photograph in figure 5.6 at relatively similar condition (37 ^{o}C), which suggest the colorimetric transition is affected by more than one factor. The transition is mainly ascribed to the interaction between vesicles and compounds/agents (either toxic or non-toxic) produced by bacteria. Such a property is not appropriate to be used in the further experiments as it affects the fluorescence sensing system if any fluorescent dye is encapsulated in the vesicles. The optimal way to reduce such colorimetric response is to form vesicles with a small amount of TCDA as well as retaining sensitivity and stability which is quite controversial and complicated.

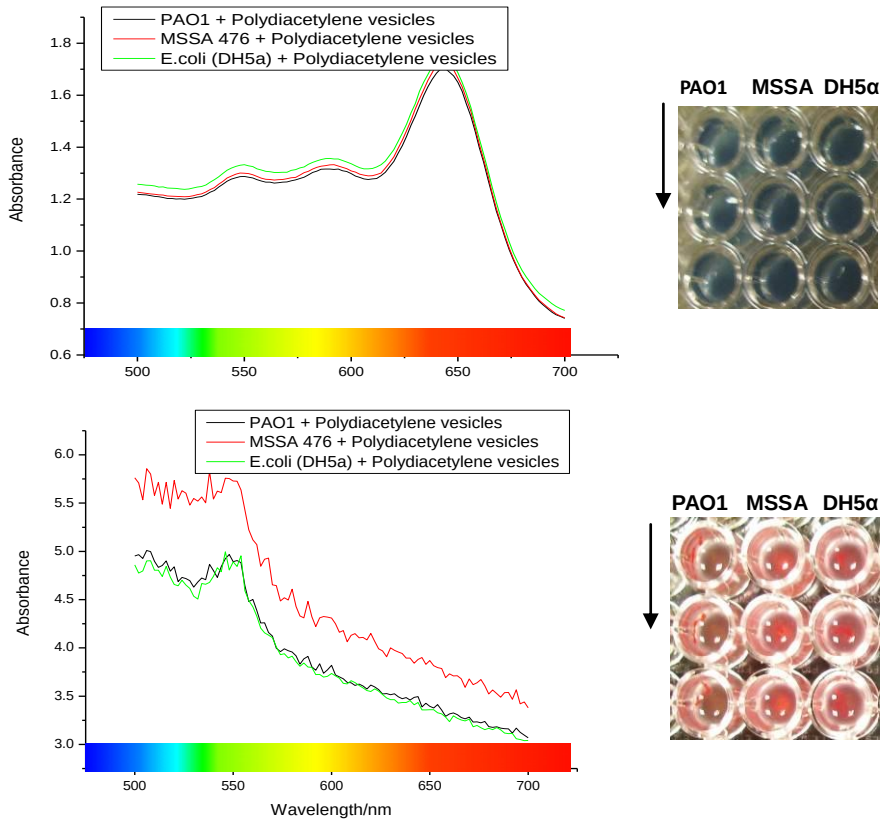

Figure 5.7: UV-Vis absorption spectra showing colour transitions of vesicles (DMPC/DMPE/Cholesterol/ 40 mol % TCDA) induced by three strains of bacteria.
Photographs insert showing the appearance of colours before and after addition of bacteria; left: *P. aeruginosa*; middle: *S. aureus* (MSSA 476); right: *E. coli* (DH5α)

5.3 Fluorescence Sensing System

This part of the study explores the ideal fluorescence sensing system based on the use of

self-quenched 5(6)-carboxyfluorescein. Carboxyfluorescein offers advantages for its use as a probe because it is easy to use, non-toxic, and self-quenching dependent upon concentration. In addition carboxyfluorescein has been reported to leak out of the cell less than fluorescein.[11] Such advantage may overcome the problem of a continuous background fluorescence production. The use of such a system is on the basis that carboxyfluorescein is self-quenched within the vesicle and prior to release; following release, and subsequent dilution in the wound environment, the dye ' switches on' , becoming fluorescent.

5.3.1 Preparatory Work

Figure 5.8 is the image of the vesicle system (with carboxyfluorescein encapsulated inside) in both pre lysis and post lysis forms. It shows that a system that releases a quenched probe which is activated by dilution in the external solution. Such a system aims to be influenced by biological aspects and analysed by its ability to react to a microbiological environment.

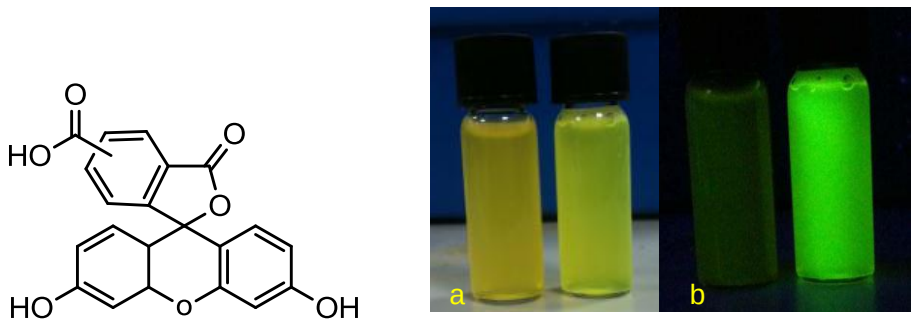

Figure 5.8: Chemical structure of 5(6)-carboxyfluorescein and images of the system in its pre-lysis (on left of frame) and post lysis (on right of frame) forms by Triton.
(a) The image is under ambient lighting; the colour change is obvious from orange to green after lysis by Triton; (b) The image was taken under a low power (8W) long wavelength UV lamp at 365 nm illumination; right side shows obvious fluorescent colour change after lysis by Triton and self-quenched fluorescence by dilution in the bulk solution.

It is concluded that the sensing system constructed here could be used as a tool to

selectively sense pathogenic bacteria, while not responding to non-pathogenic bacteria. The next part of the study investigates the concentration effect of carboxyfluorescein and the influence of UV irradiation on photobleach of such systems. Actual assessment of such theoretical systems will be discussed in next sections. 5(6)-carboxyfluorescein is most commonly used for the fluorescence sensing detection in the thesis.

5.3.2 Carboxyfluorescein Fluorescence – Concentration Analysis

In order to find at which range of concentration, carboxyfluorescein begins to self quench, the study of various concentrations of carboxyfluorescein in HEPES buffer solution versus fluorescence intensity was analysed. Figure 5.9 shows the fluorescence intensity of 5(6)-carboxyfluorescein against varying concentrations. The graph indicates the concentration at which self quenching begins to occur. It suggests that carboxyfluorescein has dose response behaviour at low concentration (< 9Mm); the fluorescence intensity is dramatically decreased when the concentration is above 9 mM. It is suggested that in carboxyfluorescein solutions, the fluorescence lifetime decreased drastically as concentration changes over the narrow range 20-50mM which is due to the energy transfer to dimers.[11] The quenched concentration of 50 mM is most commonly used in this work and as shown here up to a 10^5 dilution will provide an increase in fluorescence.

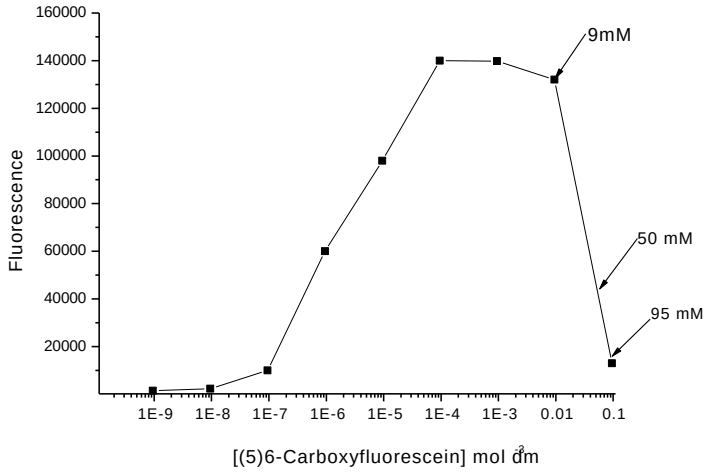

Figure 5.9: Graph showing self-quenching behaviour depending upon varying concentrations. The concentration at which self-quenching occurs is when the concentration higher than 9 mM.

5.3.3 Calculation of Fluorescence Release from Vesicles After Total Lysis

The change in concentration of fluorescent probe can be estimated when all the vesicles are ruptured. The most straightforward way to do this is to consider total internal volume of the vesicles which has been based upon a uniform size population of vesicle spheres with an outer diameter of 110 nm and an inner diameter 100 nm. Such a calculation has been detailed in section 2.5.2. Detailed calculation is shown as follows: 30 mol% TCDA/Phospholipids is used here as an example.

The calculated value of internal volume of phospholipid/30 mol% TCDA vesicles is 132 μL in total 5 mL. Given that the initial encapsulated concentration of carboxyfluorescein is 50 mM, it can be calculated that the final concentration of carboxyfluorescein is around 1.32 mM when it is released to bulk solution (5 mL). Such a value is almost 35 times lower than initial concentration which yields a fluorescent colour change exposed to low power UV illumination. The calculation of internal volume of phospholipid/ polydiacetylene vesicles is described in section 2.5.2.

5.3.4 Carboxyfluorescein Fluorescence – Photobleach Analysis by UV Irradiation

Carboxyfluorescein used in this work was subject to a great deal of irradiation with UV light, for example in the use of hard UV irradiation for polymerisation of diacetylene monomers (TCDA) which have been incorporated into the lipid vesicles. This assay aimed to explore the detrimental influence of UV irradiation on carboxyfluorescein. To evaluate the detrimental affect of UV irradiation on the fluorophore, free carboxyfluorescein with both quenched and un-quenched concentrations was exposed to UV irradiation using Hamamatsu UV-Vis Fiber Source L10290 fibir optic with the irradiation time of 10 minutes. Table 5.1 shows the resulting fluorescence intensity before and after UV irradiation. The table shows that the UV irradiation has no effect on the fluorophore. It is estimated that irradiation may have greater effect on a quenched 50mM sample than on unquenched 500 μM and 50 μM samples.

Table 5.1: Fluorescence intensity of three difference concentrations of 5(6)-carboxyfluorescein before and after irradiation; hard UV was used to irradiate for 5 minutes.

Concentration	Control Fluorescence (non irradiated sample diluted to 50 µM)	Fluorescence after UV irradiation (irradiated samples diluted to 50 µM)	Normalised Response
50 mM	17865	16932	0.9479
500 µM	215322	211544	0.9825
50 µM	247411	238713	0.9648

5.4 Study of Vesicle Stability and Sensitivity

This part of the study looked at producing relatively stable lipid vesicles which would survive attachment to fabric, part drying and re-hydration, but still respond to pathogenic bacteria by breaking apart and releasing their payload, a fluorescent dye (carboxyfluorescein). Both studies were based upon the use of self-quenched carboxyfluorescein encapsulated within vesicles. Two main toxins used in this work are described as follows.

5.4.1 Alpha-Haemolysin (α-HL) and Phospholipase A_2 (PLA_2)

α-Haemolysin belongs to the family of pore-forming toxins. The proteins are secreated by human pathogen: *S. aureus*. The description of such toxin has been discussed in chapter 1.

PLA_2 can target various phospholipids and exert its function. The phospholipids include PC, PE, PI and PS. It hydrolyses fatty acids by cleaving *sn*-2 acyl bonds of phospholipids.[12]

5.4.2 Stability Study

The stability of the vesicles is a key concern in lipid-vesicle-based sensor systems, both within an aqueous environment and following drying and re-hydration. A number of vesicle stabilisation approaches have been reported in the literature, including the use of

sugars and photo-polymerisable lipids.[13] This work was followed on from the work of Kouschevra *et al* using acetylenic tricosadiynoic acid (TCDA). [14]

Initial experiments studied the effect of the mol % of the photo-polymerisable fatty acid TCDA on the stability of vesicles following partial drying for 48h and re-hydration in appropriate buffer. (Figure 5.10)

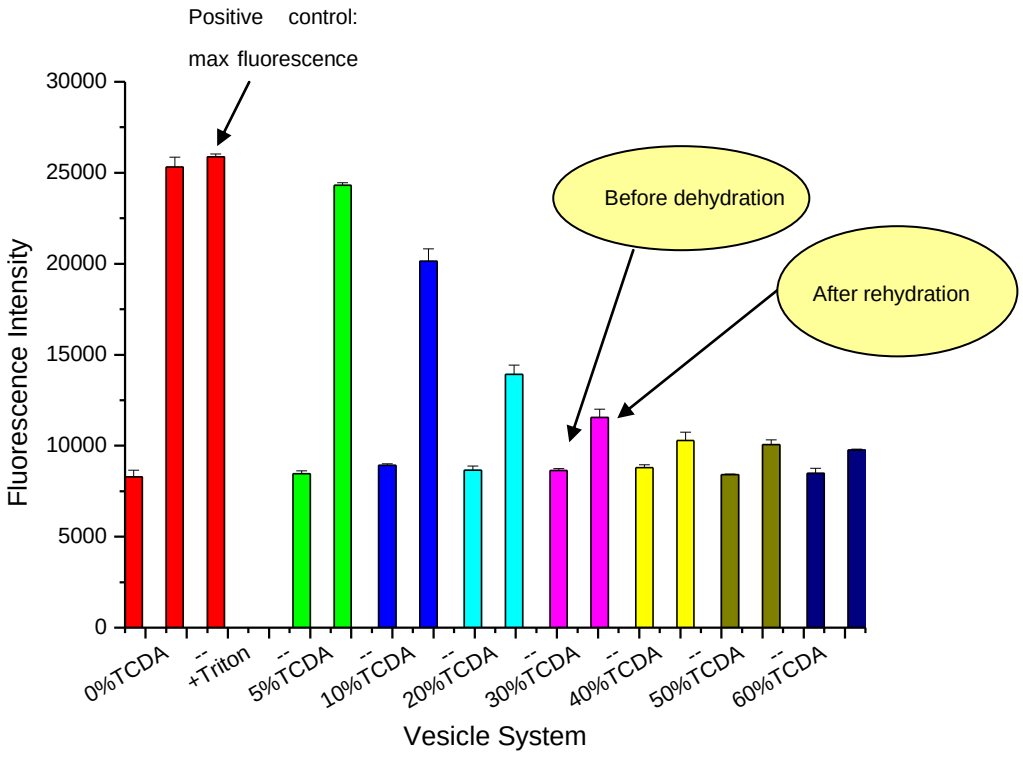

Figure 5.10: Graph showing study of vesicle stability
changes in the initial fluorescence of vesicles (left bar or pair) and fluorescence increase following partial drying and rehydration in HEPES buffer (pH 7.4, carboxyfluorescein eluent buffer system) (right bar) as a function of TCDA mol% in vesicles.Error bars represent standard deviations based on three measurements.

The dehydration-rehydration graph shows that incorporation of diacetylene part (TCDA) does stabilise lipid vesicles: higher concentration of TCDA incorporated into the lipid part, smaller increase in fluorescence on re-hydration. Total lysis of lipid vesicles (0 % TCDA) by Triton indicates the expected fluorescence if all vesicles are lysed. Loss of fluorescence is decreased by incorporation into more concentration of TCDA. This suggests that the vesicles retain their structure over the drying/rehydration cycle, with

TCDA concentration ≥ 30 mol %.

5.4.3 Sensitivity Study

This part of the study explored vesicle sensitivity to lysing agents: detergents and toxins with varying concentrations of TCDA. Figure 5.11A is the plot of vesicle lysis by detergent: Triton X-100 versus time. There is a clear decrease in fluorescence with higher concentration of TCDA incorporation. It is therefore concluded that an over-abundance of TCDA in the membrane may lower the sensitivity of the vesicle to lytic agents. It is also likely that large amount of TCDA may alter the vesicle size and shape such that they cannot carry a sufficient fluorescent payload. At hour-15, fluorescence intensity was increased faster between 0 mol% TCDA and 30 mol% TCDA vesicles, compared to the range of 40 mol% - 100 mol% with gradual increase of fluorescence intensity and following a relative no release of fluorescence intensity after hour-16. This is possibly due to the relative rigid shell of vesicle in 40%, 50%, 60% and 100% and therefore small/no release of fluorescent dye iduced by Triton. Figure 5.11B shows the sensitive response of vesicles by two types of lytic toxins and triton as a function of mol% TCDA. The plot indicates that as the TCDA concentration increases from 0 to 40%, the fluorescent increase upon lysis by Triton, haemolysin or PLA_2 decreases from a four-fold increase at 20% TCDA to a less than two-fold increase at 40% TCDA.

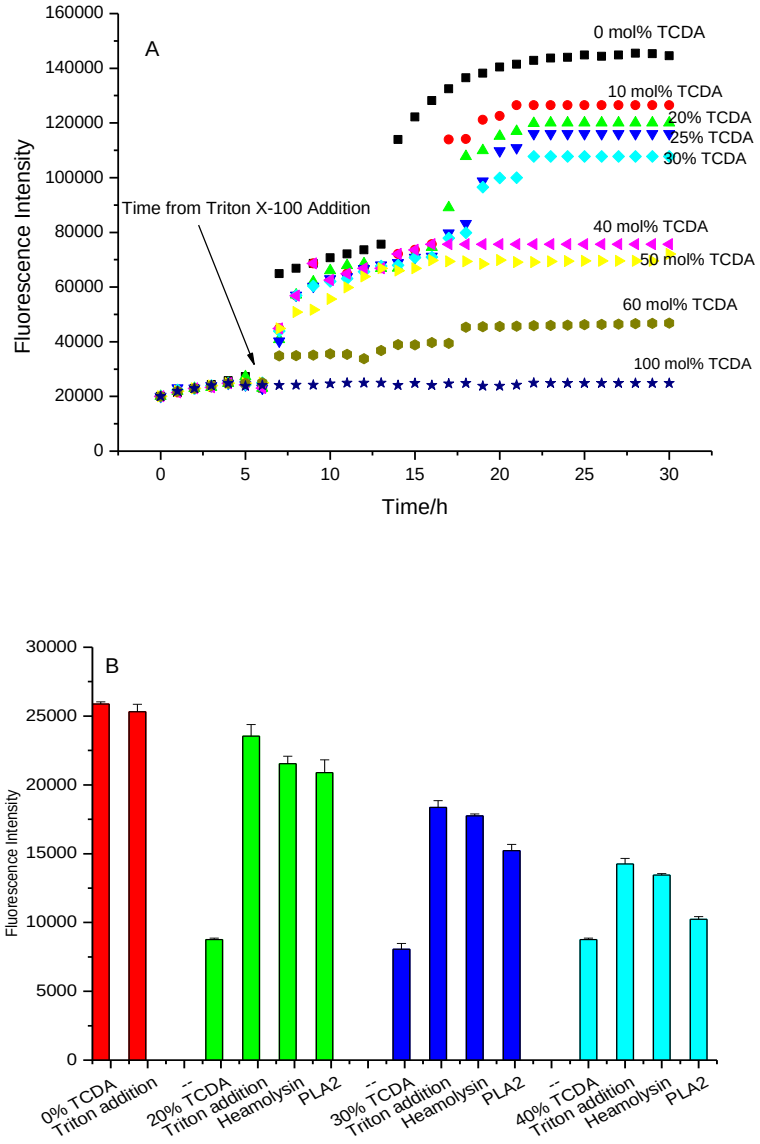

Figure 5.11: Graphs of vesicle sensitivity to lytic agents.
(A) the graph showing vesicle sensitivity to Triton as a function of TCDA mol%; (B) graph showing vesicle sensitivity to Triton, α-haemolysin and phospholipase A_2 (PLA_2) as a function of TCDA mol % , the 0 % TCDA gives the maximum fluorescence change possible for full lysis in absence of TCDA. For each system, the greater change in fluorescence on adding lytic toxin, the higher the sensitivity. Error bars in figure B represent standard deviations based on three mearsuements of each sample.

5.4.4 Summary

TCDA improves the stability of the vesicles, but negatively affects the sensitivity of vesicles. The vesicle system is relatively OK up to 30 mol% TCDA. The results from

figure 5.10, combined with figure 5.11, indicate that such vesicle system can relatively retain both stability and sensitivity between the ranges of 20 mol %-30mol % of TCDA. Therefore, such range of TCDA vesicle was chosen as an optimal system to be commonly used in the further study including construction of prototype which will be discussed in chapter 6.

5.5 Pathogenicity Assay in Suspension

The sensitivity of the vesicles to bacteria and their ability to discriminate between the non-pathogenic *E. coli* strain from the two pathogenic strains (*P. aeruginosa* PAO1 and *S. aureus* MSSA 476) was tested here. This part of work studied the fluorescence release from vesicles with varying mol% TCDA as bacteria grow and release toxins. All the experiments were performed on vesicles suspended in buffer/ bacterial growth medium. (TSB for *S. aureus*; LB for *P. aeruginosa* and *E.coli*)

Figure 5.12 demonstrates that the vesicles only responded to the two pathogenic species of bacteria as they grow (*S. aureus* and *P. aeruginosa*), but not to the non-pathogenic *E.coli*. Although the graph for the *E.coli* (a) (b) shows a slight increase in fluorescence intensity in comparison with the control system (vesicles suspended in buffer). This is due to the passive leakage because only small amount of TCDA are incorporated within the phospholipid vesicles. Therefore, such a system would lack relative rigidity and renders the vesicle system leaky. Although graphs (c) and (d) demonstrate that vesicles still respond to pathogenic strains (*S. aureus, P aeruginosa*), there is a decrease in fluorescence intensity with more mol% TCDA incorporated within the lipid bilayer, suggesting vesicles are gradually losing their sensitivity to toxins produced by pathogenic strains with more TCDA incorporation. In addition, *P. aeruginosa* grown with 50 mol% TCDA/lipid vesicles in LB medium shows a 5-fold decrease in fluorescence in comparison with its growing with 30 mol % TCDA/lipid vesicles as shown in figure (a). Interestingly, it seems that *S. aureus* is either more virulent, or secretes more toxins during its exponential growth phase when grown in TSB medium.

The four graphs show that toxins produced by *S.aureus* can cause more release of fluorescence from vesicles compared to *P.aeruginosa*.

The pathogenicity assay further proves that vesicles can still retain their stability and sensitivity when the TCDA concentration is in the range of 25% - 30%. However, there was still some degree of passive leakage of encapsulated contents from the vesicles, as presented in figure 5.10 (a), (b). Higher concentration of TCDA can significantly stabilise vesicles and showed no significant leakage of carboxyfluorescein from the vesicles, as shown in figure 5.10 (c) and (d). Overall, the TCDA concentration for optimum stability was chosen as 30% in this work; this provides stability without comprising flexibility.

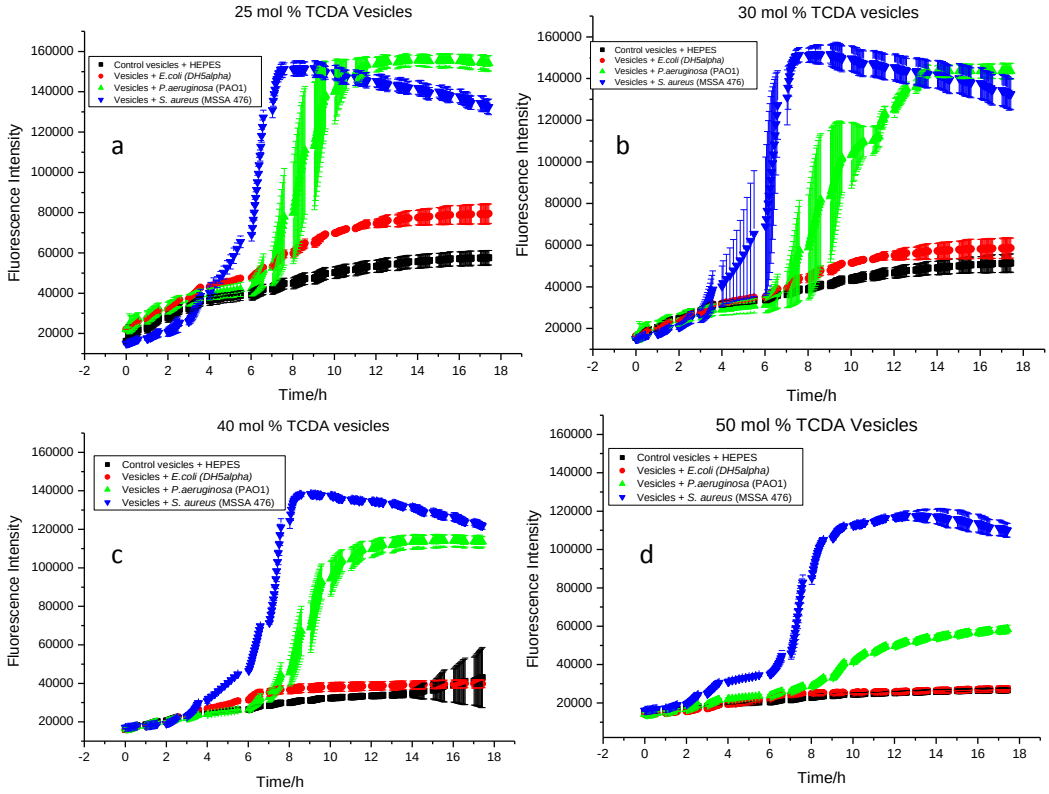

Figure 5.12: Time course of the kinetics of the interaction of bacteria with phospholipid/TCDA vesicles. Toxins secreted by *P.aeruginosa* PAO1 and *S. aureus* MSSA 476 (OD = 0.01) induces permeabilisation of different concentration of TCDA/PC vesicles at pH7.4 as revealed by the increase of fluorescence of 5(6)-carboxyfluorescein when this is released into the external solution; *E. coli* (DH5a) as control did not permeabilise vesicles as they do not secrete any lysing toxins or enzyme. MSSA476 was cultured in TSB medium which seems to secrete more virulent toxins to cause leakage of membrane of vesicles. More concentrated TCDA is incorporated in the mixture, more cross linked vesicles and hence the more stable

the system. Error bars represent standard deviations based on three measurements of each sample.

Figure 5.13 shows the similar results of fluorescence release from vesicles as bacteria grow and release toxins. The only difference between the two graphs is the medium for growing *S. aureus*; TSB medium was used as growing medium for *S. aureus* in (a), while LB medium was used in (b). In fact LB broth has been commonly used in all microbiologically related assays. Later, TSB was found to be an optimum culture medium for growing *S. aureus* as MSSA 476 is either more virulent, or secretes more toxins during its exponential growth phase in TSB medium than in LB medium. This is proved by the pathogenicity assay**.** Figure 5.13 (a) shows that *S. aureus* can secrete more virulent toxins and the graph shows more significant increase in fluorescence in comparison with (b). Therefore, TSB was chosen as the growth medium for *S. aureus* in this experiment.

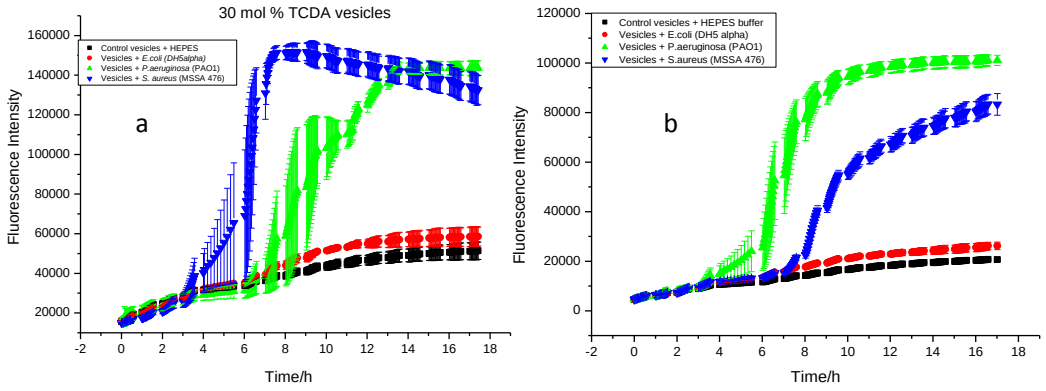

Figure 5.13: Similar graphs showing fluorescence release from vesicles (30 mol % TCDA/lipid vesicles) as bacteria grow in different media.
S.aureus MSSA 476 grown in TSB medium and other two strains grown in LB medium; (b) three strains all grown in LB medium. The graph suggests *S.aureus* is either more toxic or secretes more virulent toxins when grown in TSB medium. Error bars represent standard deviations based on three measurements of each sample.

5.6 Conclusion

In this chapter, a new methodology of detecting the microbiological state of wound dressing in terms of fluorescent indication has been developed. And a new stabilised vesicle system has been developed by inserting diacetylene monomers within the phospholipid bilayer. Such nanocapsule systems obtain chromatic properties due to the

conjugated structure and can undergo colorimetric transition under external stress including interaction of bacteria and lipid bilayers, or temperature increase. It is known that more conjugated component will yield a stronger colorimetric transition. Such property may interfere with fluorescence measurement if carboxyfluorescein is encapsulated within vesicles. Further stability/sensitivity tests suggest that the optimal vesicle system is around 30 mol% TCDA. Such a range of vesicles would not yield strong colour after UV irradiation and thus would not affect the further test of fluorescence sensing measurement in suspension which can be seen in figure 5.12 and 5.13. The pathogenicity assay further proves that such vesicle system can respond to pathogenic strains (*P.aeruginosa* PAO1 and *S. aureus* MSSA 476) and not respond to non-pathogenic strains (*E.coli* DH5 α). Both stability/sensitivity and pathogenicity tests demonstrate that a relatively stable vesicle system can be fabricated using an optimum concentration of TCDA as a stabiliser. The next chapter is to build up a simple prototype dressing to examine whether vesicle modified fabric would be sufficiently sensitive to pathogenic bacteria and to give a visual response under weak UV light, whilst not responding to non-pathogenic *E. coli*. In addition vesicles with 30 mol % TCDA are relatively more resistant to damage resulting from partial drying than in the absence of TCDA, but will not survive in a completely dry environment. Therefore the next part of study will also investigate to construct various prototypes to maintain vesicles stability and intact as well as assist wound healing.

5.7 References:

1 Ringsdorf H., Scholesterolarb B., Venzmer J., Molecular architecture and function of polymeric oriented systems: models for the study of organization, surface recognition, and dynamics of biomembranes *Angew. Chem. Int. Ed. Engl.* 1988, *27*, 113-158.

2 Jelinek R., Kolusheva S., Biomolecular Sensing with colorimetric vesicles, *Bulletin of the Israel Chemical Society*, 2008, *23*, 6-11.

3 Kuriyama K., Kikuchi H., Kajiyama T., Chromatic phase of polydiacetylene Langmuir-Blodgett film, *Langmuir*, 1998, *14*, 1130-1138.

4 Deckert A.A., Horne J.C., Valentine B., Kiernan L., Fallon L., Effects of molecular area on the polymerisation and thermochromism of Langmuir-Blodgett Films of Cd^{2+} salts of 5,7-diacetylenes studied using UV-Visible Spectroscopy, *Langmuir*, 1995, *11*, 643.

5 Hankin S.H.W., Downey M.J., Sandman D.J., On the structural origins of solid-state urethane polydiacetylene thermochromism-thermal and structural-properties of ipudo monomer and polymer, *Polymer*, 1992, 33, 5098.

6 Hammond P.T., Nallicheri R.A., Rubner M.F., *Mater.* An examination of the strain-induced orientation of hard segment domains in 4,4′-methylenebis(phenyl isocyanate)-based polyurethane-diacetylene segmented copolymers, *Sci. Eng*., 1990, *126*, 281.

7 Rubner M.F., Novel optical properties of polyurethane-diacetylene segmented copolymers, *Macromolecules* 1986, *19*, 2129.

8 Batchelder D.N., Colour and chromism of conjugated polymers, *Contemp. Phys*. 1988, *29*, 3.

9 Okada S. Peng S., Spevak W., Charych D., Colour and chromism of polydiacetylene vesicles , *Acc. Chem. Res.*, 1998, *31*, 229-239.

10 Ma Z., Li J., Liu M., Cao J., Zou Z., Tu J., Jiang L., Colorimetric Detection of Escherichia coli by Polydiacetylene Vesicles Functionalized with Glycolipid, *J. Am. Chem. Soc*., 1998, *120*, 12678-12679.

11 Chen R.F., Knutson J.R.,Mechanism of fluorescence concentration quenching of carboxyfluorescein in liposomes: energy transfer to nonfluorescent dimers., *Anal. Biochem.*,1988, *172*, 61-77.

12 Kuwabara Y., Maruyama M., Watanabe Y., Tanaka S., Takakuwa M., Tamai Y.,

Purification and some properties of membrane-bound phospholipase B from Torulaspora delbrueckii, *Journal of Biochemistry*, 1988, *104*, 236-241.

13 Yavlovich A, Singh A, Blumenthal R, Puri A., A novel class of photo-triggerable liposomes containing DPPC:DC(8,9)PC as vehicles for delivery of doxorubcin to cells, *Biochim Biophys Acta.*, 2011, *1808*, 117-26.

14 Kolusheva S., Shahal T., Jelinek R., Peptide−Membrane interactions studied by a new phospholipid/polydiacetylene colorimetric vesicle assay, *Biochemistry*, 2000, *39*, 15851-15859.

Chapter 6 Construction of a Prototype for Stabilising Vesicles and Assisting Wound Healing

While the previous chapter was devoted to the development of a new nanocapsule system which can detect the presence of pathogenic bacteria by utilising the self-quenching of carboxyfluorescein, the present chapter describes the construction of a simple prototype to maintain the vesicle intact as well as maintain a moist environment in order to assist wound healing. In this chapter, various methods including plasma-polymerised maleic anhydride and photo-polymerisation of poly (acrylic acid) grafted onto non-woven polypropylene have been discussed for stabilising vesicles. Following measurements were carried out to examine whether vesicle-modified fabric would be sufficiently sensitive to pathogenic bacteria to give a visual response, while not responding to non-pathogenic *E. coli*. In section 6.4, a simple prototype was constructed by utilising a hydrogel in order to maintain vesicle stability and to maintain a moist environment for assisting wound healing. Stability tests of prototypes were then studied for further research.

6.1 Construction of Wound Dressing

The wound dressing is based on the principle of creating and maintaining a moist wound environment. Characteristics of an ideal dressing are described as follows: [1]

1) Capable of maintaining a moist environment at the wound site while removing excess exudate
2) Non-toxic and non-allergenic
3) Capable of protecting the wound from further trauma
4) Can be removed without causing trauma to the wound
5) Impermeable to bacteria
6) Thermally insulating
7) Allows gaseous exchange

8) Comfortable and pain relief
9) Require only infrequent changes
10) Cost effective

Therefore, the construction of wound dressings should meet the standards of the above requirements. A bilaminar wound dressing is composed of an outer semi-permeable membrane and an inner three-dimensional matrix of a fabric or a sponge to constitute an ideal structure that promotes wound healing.[2] The outer membrane normally controls release of moisture vapour, provides an effective barrier to water or wound exudate, and protects the wound surface from bacterial invasion; inner matrix encourages adherence by tissue growth into the matrix. This project aims to develop a biosynthetic wound dressing with a drug delivery capability as well as a visual response in the presence of pathogenic bacteria. This medicated wound dressing is composed of several sheets modified with non-woven polypropylene fabrics and vesicle (containing antimicrobials/fluorescent dyes) which are laminated with hydrogel layer by layer. This structure of the proposed inner membrane is shown in figure 6.1.

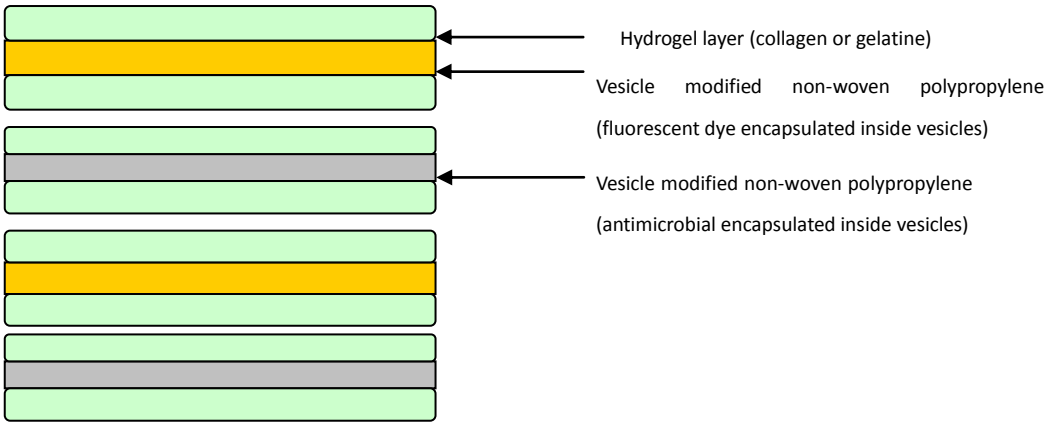

Figure 6.1: Schematic representation of the hydrogel-vesicle modified fabric-hydrogel construction.

6.2 Pulsed Plasma Deposited Maleic Anhydride Thin Films as Supports for Vesicles

The attachment of giant unilamellar vesicles containing DMPE lipids, using plasma deposited maleic anhydride, has been discussed in chapter 4. This part of the work follows on the use of pulsed plasma deposited maleic anhydride on polypropylene fabric with retention of the anhydride group functionality. Following film deposition, the fabric was immersed in an aqueous suspension of the lipid vesicles allowing formation of amide linkages between the anhydride group and amine functionality on PE lipids. Vesicle mediated pp-MA fabrics could be considered as a middle layer of wound dressing.

6.2.1 FT-IR for Surface Characterisation

Figure 6.2 is the FT-IR graph showing vesicles has been successfully attached onto pp-MA polypropylene. Similar graph shows an expected anhydride group at 1780 cm^{-1} on pp-MA polypropylene nonwoven. Following vesicles attachment, a strong and broad absorption at 1643 cm^{-1} suggests an amide bond formation, which primarily results from ester C=O bond from phospholipids and TCDA and a fraction of the peak results from amide C=O in the reacted maleic anhydride.

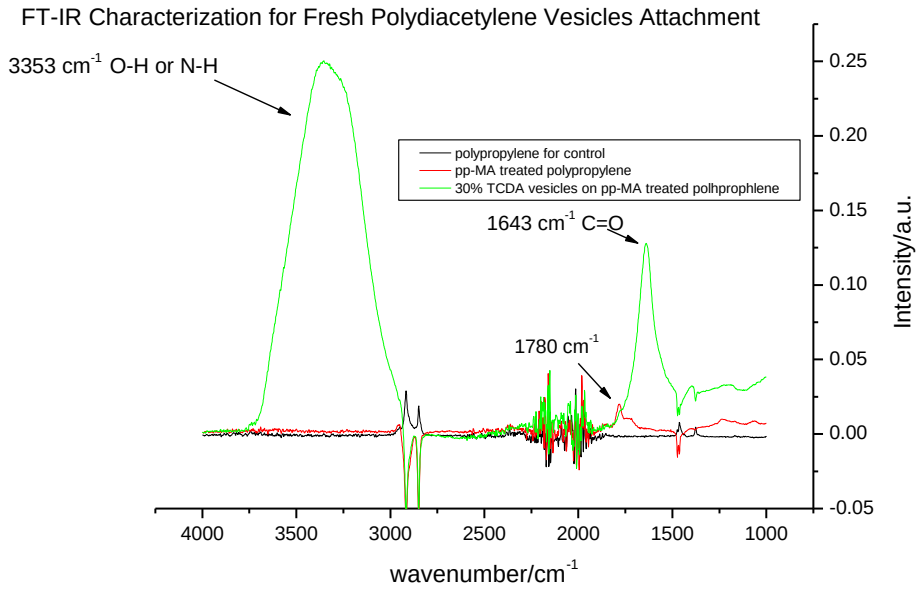

Figure 6.2: FT-IR data showing vesicles attachment onto treated non-woven polypropylene.
Black, standard polypropylene fabric; Red: non-woven polypropylene was modified with plasma polymerised maleic anhydride and shows anhydride group; Green: modified non-woven fabric was immersed in pure vesicles containing DMPE vesicle solution with amide bond formation around 1643 cm^{-1}.

6.2.2 SEM for Analysis of Vesicle Modified Surface

Scanning electron microscopy was used here to observe the surface morphologies of the vesicle modified non-woven polypropylene, which was deposited with a thin film of plasma polymerised maleic anhydride before vesicle attachment, as presented in figure 6.3. The regions are labelled at the top right corner of each image. SEM image in figure 6.3 A depicts a single fibre of polypropylene which was purchased from Boots, the chemist. Such non-woven polypropylene has been coated with unknown materials in order to improve its hydrophilicity before purchase. The surface of polypropylene was not further treated and was directly used in the experiment for plasma polymerisation. Figure 6.3 B represents appearance of the polypropylene deposited with a thin film of plasma polymerised maleic anhydride. The figure reveals that the cross-linked polymers are randomly coated on the surface and thus make the surface quite rough compared to non-treated polypropylene(A). Figure 6.3 C&D show the images of phospholipids/TCDA vesicles attached on the pp-MA treated non-woven polypropylene.

The vesicle mediated surface was rinsed with an appropriate buffer and then was imaged under SEM for visualisation. The freshly prepared vesicles are shown in C and D with a size range of hundreds of nanometres. Most of vesicles have irregular shapes with round edges. The variability in vesicle shapes is possibly due to incorporation of diacetylene part into lipid moiety and membrane crystallisation of PDA part at room temperature. The figures reveal that vesicles only exist on the region where the pp-MA is deposited.

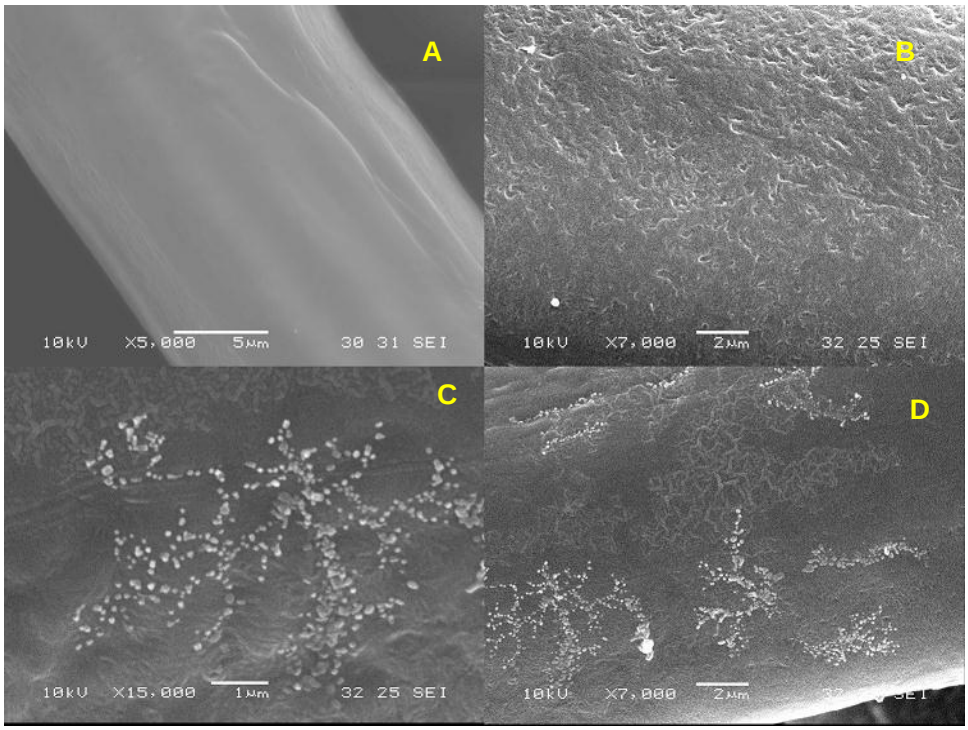

Figure 6.3: SEM images, recorded with JEM-6480LV scanning electron microscope
A) image of a single fibre of polypropylene; B) microscopic image of the surface of pp-MA treated non-woven polypropylene; C) surface of vesicles attached onto the pp-MA treated fabrics with magnification of 15,000; (D) surface of vesicles attached onto pp-MA treated fabrics with magnification of 7,000. vesicle composition: 48 mol % DMPC/2 mol% DMPE/20 % Cholesterol/ 30 mol% TCDA; plasma parameter: pulse 10/40ms, 30 min.

Figure 6.4 further illustrates the overview of the images of vesicles attached to the non-woven polypropylene coated with plasma polymerised maleic anhydride. The fibres of polypropylene shown here are coated with pp-MA almost everywhere. Therefore, vesicles can be attached onto treated area almost everywhere, suggesting more payloads could be encapsulated within vesicles, which would improve the efficiency of

fluorescent sensing detection and/or their antimicrobial properties.

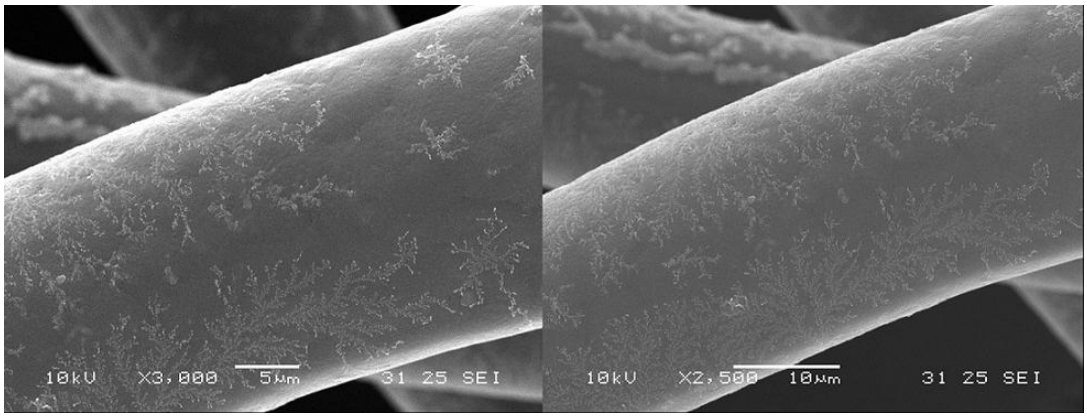

Figure 6.4: SEM images of vesicles on non-woven polypropylene deposited with plasma polymerised maleic anhydride, recorded with JEM-6480LV scanning electron microscope.
Vesicle composition: 48 mol % DMPC/2 mol% DMPE/20 % Cholesterol/ 30 mol% TCDA; plasma parameter: pulse 10/40ms, 30 min.

6.2.3 Attachment of Vesicles to Fabric and Stability /Response Testing

Figure 5.10 and 5.11 show vesicle stability before/after part dry and sensitivity to lytic agents on pp-MA modified non-woven fabrics. The results of the figures prove that vesicles can obtain both relative stability and sensitivity by selecting appropriate molar concentration of TCDA. This negative correlation with respect to TCDA concentration can be visually observed on vesicles attached via pulse plasma deposited maleic anhydride thin films on non-woven polypropylene fabric (figure 6.5). Figure 6.5 shows a visual response that correlates with the measurements in figure 5.10 and figure 5.11 B : too low a TCDA concentration results in the vesicles not being stable to partial drying (0, 5, 10%); too high a concentration of TCDA results in vesicles not being sensitive to lysis by Triton (50 and 60%). Therefore, the optimum TCDA concentration for stable and sensitive vesicles appears to be between 20 and 30%, as presented in figure 6.5.

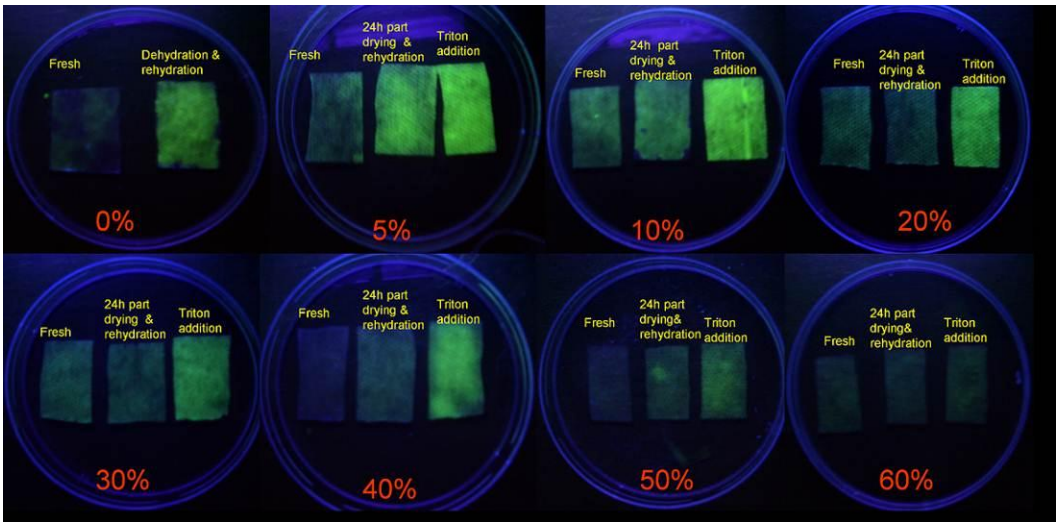

Figure 6.5: Polypropylene modified with vesicles containing initially self-quenched carboxyfluorescein (left-hand swatch) and switching on of fluorescence of dye following either vesicle destruction following part drying or direct lysis by Triton, as a function of mol % TCDA. plasma parameter: pulse 10/40ms, 30 min.

The parallel experiment (vesicle containing self-queched carboxyfluorescein in appropriate HEPES buffer) was carried out in a 96-well plate under a low power UV lamp. The visual colour of fluorescence in the plate is shown in figure 6.6. Each sample in triplicate further shows that a higher concentration of TCDA stabilises the vesicle structure, with progressively smaller increases in fluorescence on re-hydration.

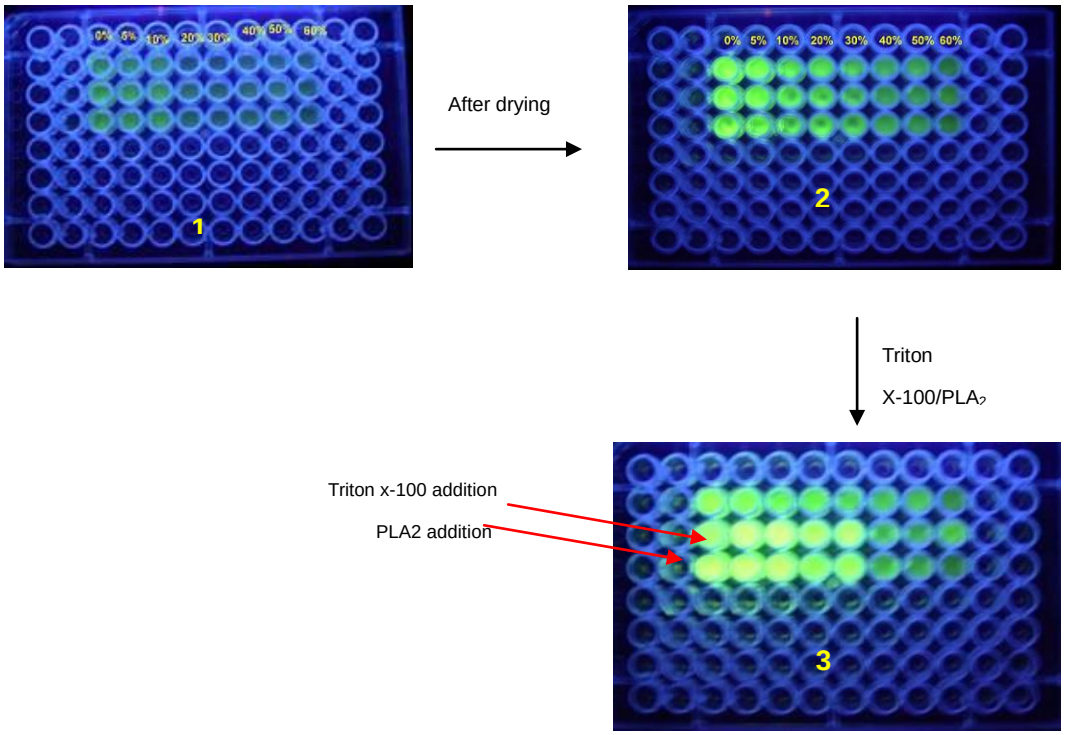

Figure 6.6: Fluorescent images of vesicles in 96-well plate.
Vesicles containing initially self-quenched carboxyfluorescein (Plate 1) in HEPES buffer solution and switching on of fluorescent dye following vesicle destruction by doing dehydration in class II flow hood for 24 hours and rehydration by appropriate HEPES buffer (Plate 2) and following lysis by Triton and phospholipase A_2, as a function of mol% TCDA.

The results shown in figure 6.5 and 6.6 demonstrate that a relatively stable vesicle system can be fabricated using an optimum concentration of TCDA as a stabiliser. This part of the study tested the response of the optimised (in terms of sensitivity and stability) vesicle system bound to pp-MA treated fabrics to strains of the test bacteria. Figure 6.7 shows the image of optimised vesicles (30 mol% TCDA) attached onto pp-MA treated non-woven fabrics responding to three strains of bacteria. The vesicles did not respond to non-pathogenic bacteria *E.coli* and only responded to pathogenic strains: *P.aeruginosa* PAO1 and *S.aureus* MSSA 476 as expected. This experiment, using pulse-plasma-deposited maleic anhydride to bind the vesicles to the fabric, and to create a thin hydrogel film, gave a clear indication that a fabric could be produced that exhibited a fluorescent response to pathogenic bacteria.

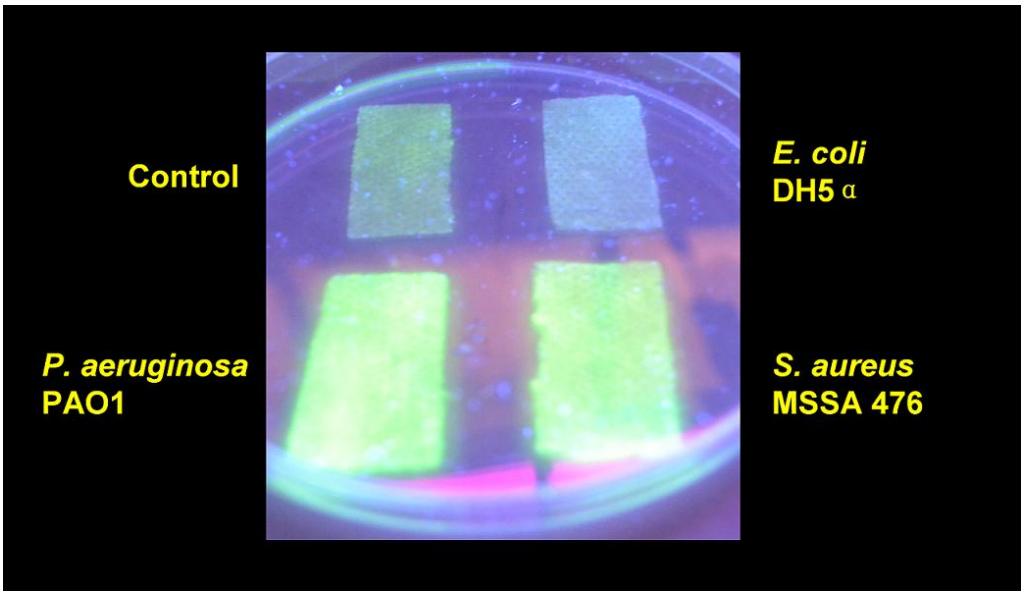

Figure 6.7: A crude 'proof of principle' prototype: response of modified fabric following overnight growth of bacteria on polypropylene fabric with 30 mol% TCDA vesicles.

6.3 Graft Polymerisation of Poly(acrylic acid) onto Non-woven Polypropylene

This part of study looked at using alternative for attaching vesicles via hydrogen bond. Such fabrics were kindly offered by Dr. Thet Naing Tun, Department of Chemistry, University of Bath, UK. Non-woven polypropylene was surface-modified by photo-induced graft polymerisation of poly (acrylic acid) or PAA by utilising benzophenone as a photo initiator to improve the hydrophilicity of the fabrics. Vesicles were then attached onto modified non-woven polypropylene via hydrogen bonding due to negatively charged carboxylic acid functional groups on grated surface in grafted chains. The advantages of photo-grafting of polymerisation are: 1) photochemically produced triplet states of carbonyl compounds can abstract hydrogen atoms from almost all polymers so that polymerisation can occur; 2) high density and localisation of reactive chains onto the surface; 3) low cost and simplicity.[3] Surface characterisation and wettability of surface have been studied by Dr. Thet Naing Tun and will not be detailed here. The schematic diagram for the process of surface graft polymerisation of PAA onto non-woven polypropylene is shown in figure 6.8.

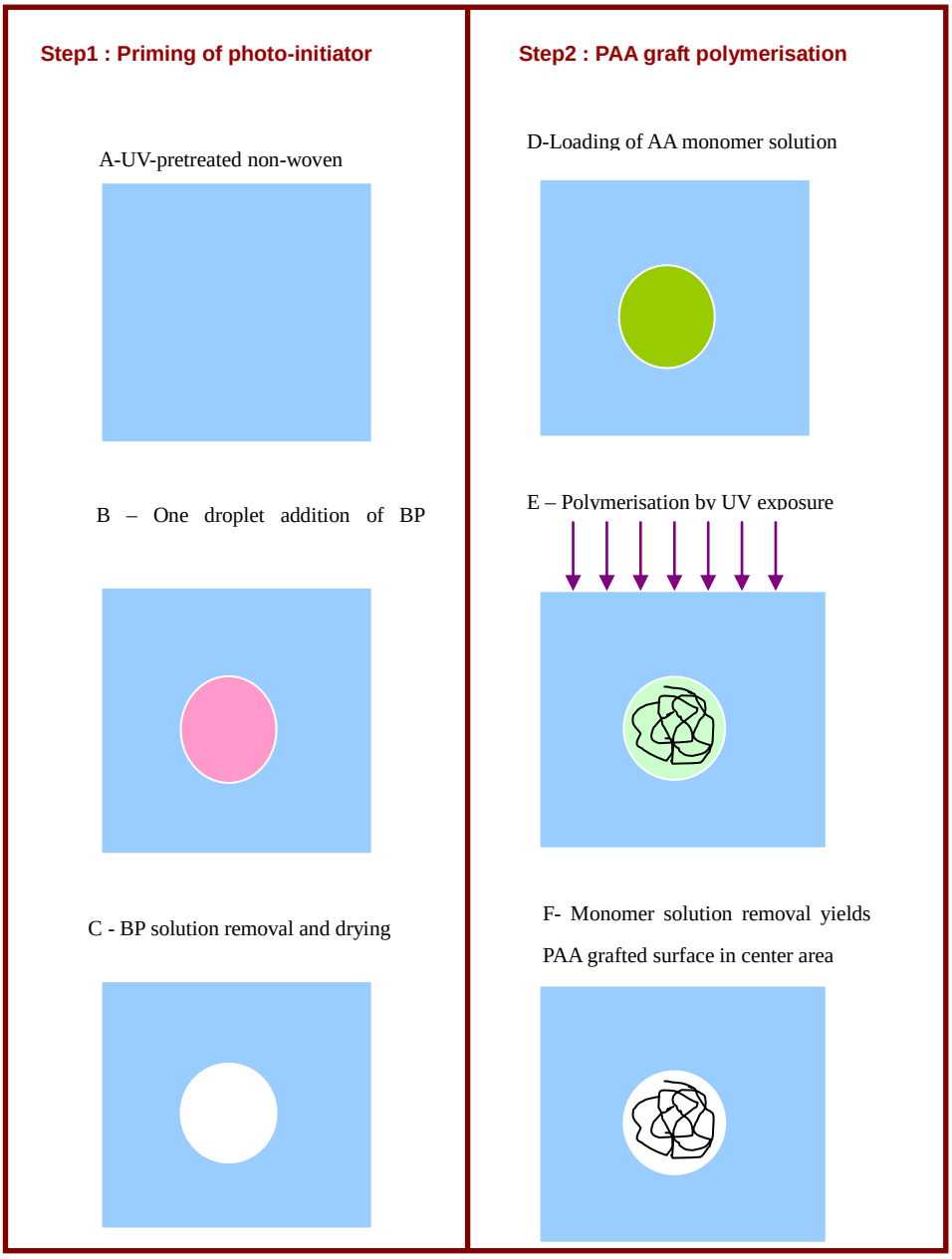
Step1 : Priming of photo-initiator
A-UV-pretreated non-woven
B – One droplet addition of BP
C - BP solution removal and drying
Step2 : PAA graft polymerisation
D-Loading of AA monomer solution
E – Polymerisation by UV exposure
F- Monomer solution removal yields
PAA grafted surface in center area

A

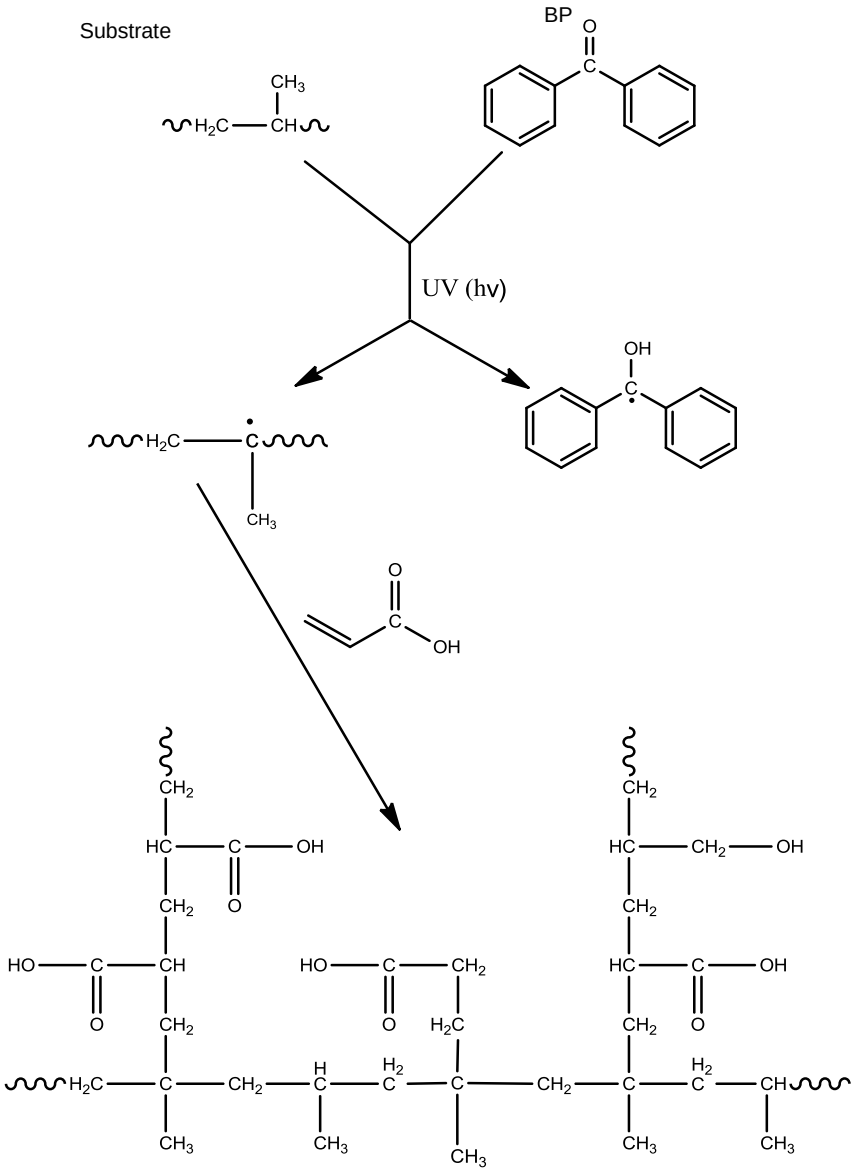

Figure 6.8: Schematic representation of UV-induc B ft polymerisation of poly (acrylic acid) on non-woven polypropylene.
(A) Process of UV induced chemical modification of non-woven polypropylene with acrylic acids as grafting agents. BP: benzophenone; (B) General scheme for the UV-induced modification of non-woven polypropylene.

Vesicle treated fabrics were incubated with the three strains of bacteria to examine whether the modified non-woven polypropylene responded to pathogenic bacteria *P.aeruginosa* (PAO1) and *S. aureus* (MSSA 476) and caused switch on of fluorescence of encapsulated carboxyfluorescein. The visual response was photographed under low power of UV light, as presented in figure 6.9 (B). Control system (vesicle on modified

surface) did not cause any fluorescence release overnight, indicating that vesicles were stable at least for 16 hours at 37 ^{o}C, which can be seen from control system. *P.aeruginosa* PAO1 and *S.aureus* MSSA 476 caused significant switch on of fluorescence overnight. It is apparent that *P.aeruginosa* PAO1 caused more dye leakage from vesicles in comparison with *S.aureus* MSSA 476 when these two strains are all grown in LB medium.The possible reason is because either more toxins or more virulent toxins were produced by *P.aeruginosa* PAO1. Furthermore, the rate of switch on of fluorescence in *P.aeruginosa* PAO1 was faster in comparison with *S.aureus* MSSA 476, which can be concluded from the image that more fluorescence was released after 4 h in *P.aeruginosa* PAO1 than in *S.aureus* MSSA 476. In addition differences in the mode of action of these two pathogenic strains resulted in the difference in diffusion of fluorescence. *E.coli* DH5α as control system showed almost no fluorescence release compared to the two strains of pathogenic bacteria.

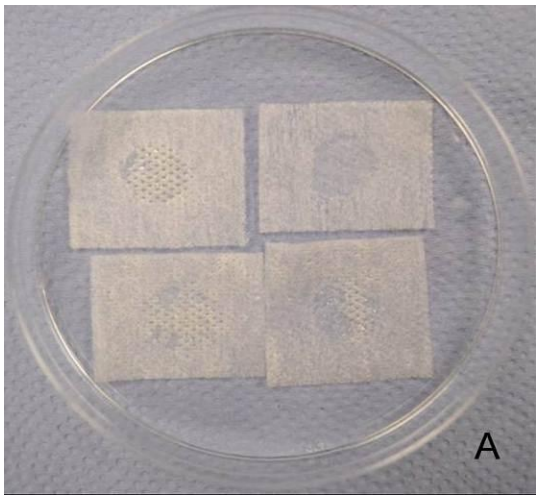

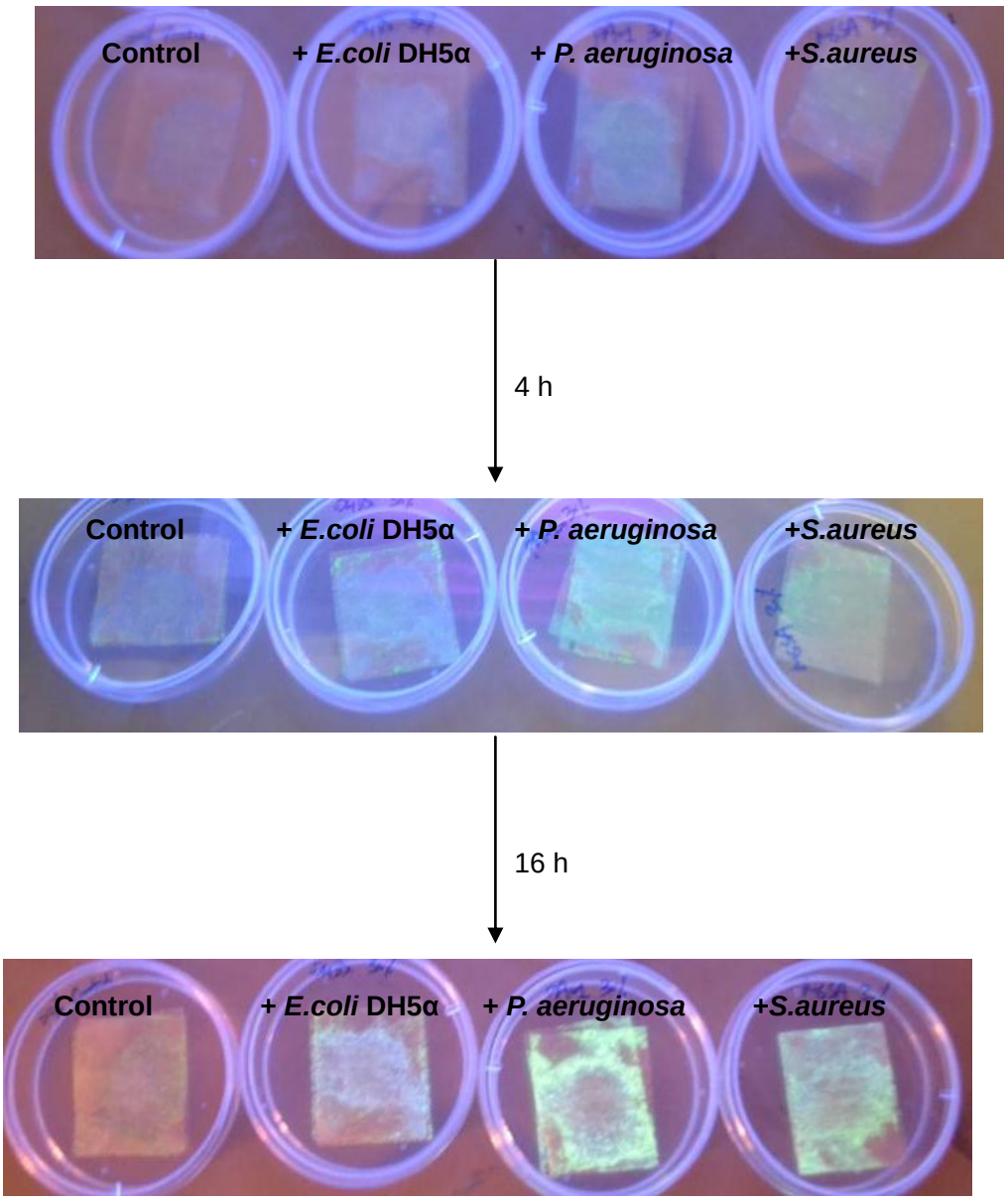

B

Figure 6.9: Images of photo-grafting polymerisation of PAA on non-woven polypropylene in the central area with a diameter of 1 cm and fluorescence response induced by toxins secreted by pathogenic bacteria (PAO1 and MSSA 476) after 4h and overnight.
A) freshly made photo-grafting polymerisation of PAA on non-woven polypropylene in central area (diameter: 1 cm); B) vesicles (30 mol % TCDA) attached onto the modified surface by hydrogen bond due to negatively charged carboxylic acid groups from grafted polymers and induced by toxins and following the switch on of fluorescence of carboxyfluorescein. The fabrics were incubated at 37 ^{o}C and were photographed under low power UV light after 4 h and 16h, respectively.

Here the fluorescence response experiment only confirms the efficiency of such modified fabrics and thus such a system is considered as an alternative for further prototype construction. The photo-grafted polymerisation onto non-woven

polypropylene as a simple prototype is currently being studied in the Jenkin's group, Department of Chemistry, University of Bath, UK.

6.4 A Simple Prototype Construction

The prototype constructed in this work was an initial trial to investigate its stability and efficiency of response to pathogenic bacteria which could be applied for further application of wound dressing. Although the relatively stable and sensitive vesicle system has been proved to be efficient in responding to pathogenic bacteria in section 6.2 and 6.3, the vesicles are not able to survive in 100% dry condition. Furthermore, a moist environment allows the optimum environment for healing based on the work of Winter (1962).[4] Most wound dressings nowadays have been designed to allow 'moist healing' to prevent dehydration and help protect and maintain temperature. Therefore, the most appropriate dressing designed in this work should maintain a moist environment at the wound surface without causing maceration of the surrounding skin as well as maintain vesicles intact and stable for long term use. The requirements of the prototype constructed in this work should be: 1) maintain the stability of vesicles; 2) stable at least for several days both at room temperature and 37 ^{o}C which is the optimum temperature for cellular activity and division; 3) promote wound healing.

6.4.1 Gelatine as Supports for Stabilising Vesicles

Gelatine is a mixture of peptides and proteins produced by partial hydrolysis of collagen. It is mainly used as a gelling agent in food, cosmetic manufacturing and pharmaceuticals.[5] Gelatine is a hydrolysed form of collagen, therefore it can aid wound healing as well as improve vesicle stability by incorporating gelatine in the prototype. The proposed prototype here is shown in figure 6.10.

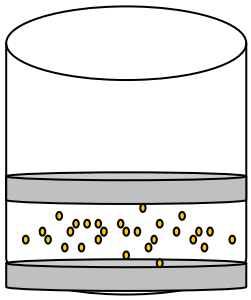

Figure 6.10: Schematic of simple prototype in single vial of 96-well plate, phospholipid/PDA vesicles (30 mol% TCDA) containing self-quenched carboxyfluorescein sandwiched between two hydrolysed gelatine sheets.

Relatively stable phospholipids/PDA vesicles were sandwiched between two gelatine sheets in order to maintain their stability and a moist environment. The experiment was carried out in 96-well plate and was sealed with transparent adhesive tapes when not in use. The stability was tested in terms of fluorescence released from vesicles each day. The stability data are shown in figure 6.11. The result shows that vesicles remain intact and stable in gelatines for almost 1 month at room temperature. The fluorescence intensity was 5-fold increase by the lysis of Triton. The photographs insert shows a visual image of vesicles between in gelatine sheets. No additional fluorescence was observed until the system was lysed by Triton. All measurements were carried out at room temperatures. Parallel experiment was carried out at 37 ^{o}C in order to measure the stability of the prototype at higher temperature. Unfortunately, gelatine sheets were melted at 37^{o}C thus they were not able to maintain vesicles intact and stable at 37 ^{o} C. Such data are not available to show here.

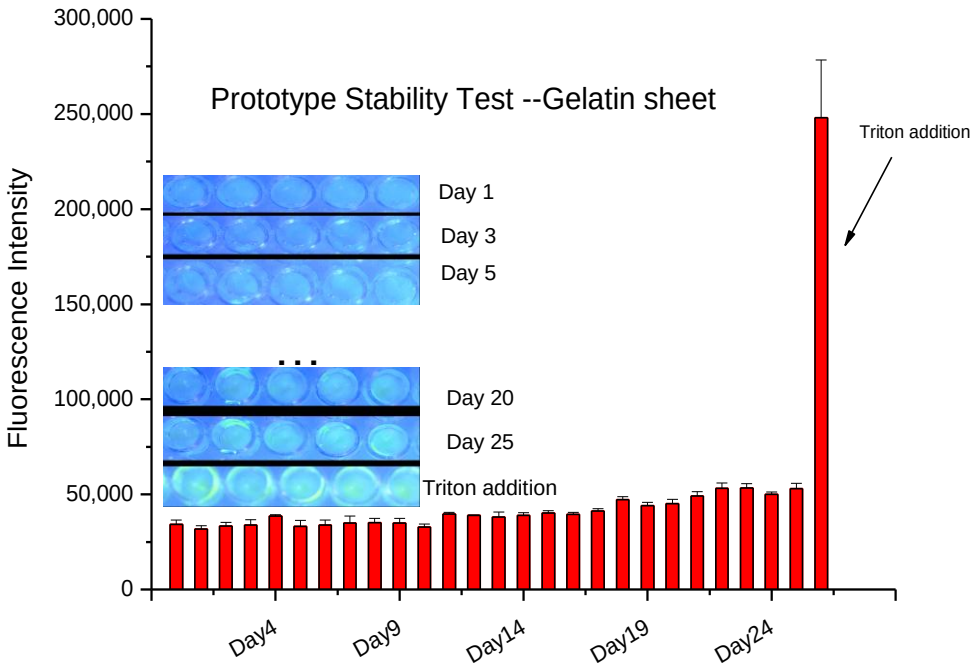

Figure 6.11: Graph showing stability test of phospholipids/PDA vesicles (30 mol% TCDA) in gelatine sheets for 25 days and significant fluorescence increase after lysis by Triton.
Photographs inserted are the images taken under low power UV light at room temperature. Error bars represent standard deviations based on three measurements of each sample.

6.4.2 Plasma Polymerised Maleic Anhydride Deposited onto Non-woven Polypropylene and Following Subsequent Grafting of Collagen onto Polymer Films

6.4.2.1 Stability Study of Collagen Grafted pp-MA Non-woven Polypropylene

This part of the study follows on the work of section 6.2 and investigated the stability of the prototype which is pp-MA modified surface coated with collagen solution. The pp-MA deposited non-woven polypropylene was dip coated in the collagen solution to improve the hydrophilicity of the whole surface and thus maintain vesicles intact and stable. Vesicles were sandwiched between two modified sheets, as presented in figure 6.12

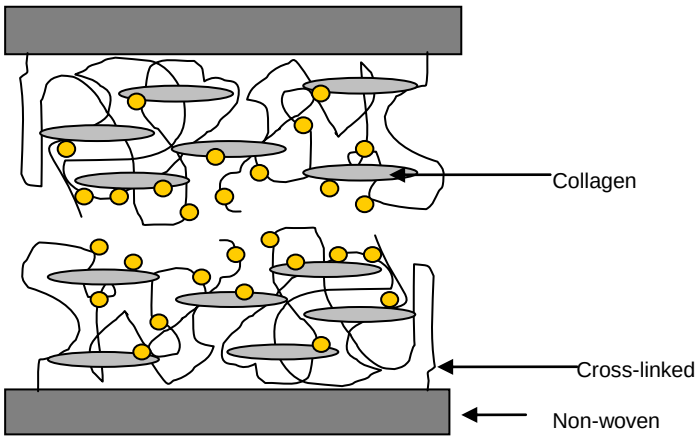

Figure 6.12: Schematic diagram of prototype construction: pp-MA modified non-woven polypropylene was dip coated in collagen solution, with vesicles containing self-quenched carboxyfluorescein following attached onto collagen grafted pp-MA surface.
The layout of such prototype was then placed in 96-well plate for stability test in terms of fluorescence release from vesicles.

The graph for the stability test at room temperature is shown in figure 6.13. The prototype was very stable for 25 days until lysis by Triton and did not show any change in fluorescence intensity on the histogram in comparison with figure 6.11, indicating that collagen grafted pp-MA non-woven polypropylene could provide an optimal environment to maintain vesicles intact and stability for long term use, possibly resulting from the covalent binding between vesicles and pp-MA treated surface and following the immersion of collagen solution which enhances the surface hydrophilicity. The stability test was only tested for 25 days at room temperature, whereas the prototype is assumed to be stable for more than 1 month as inferred from the graph.

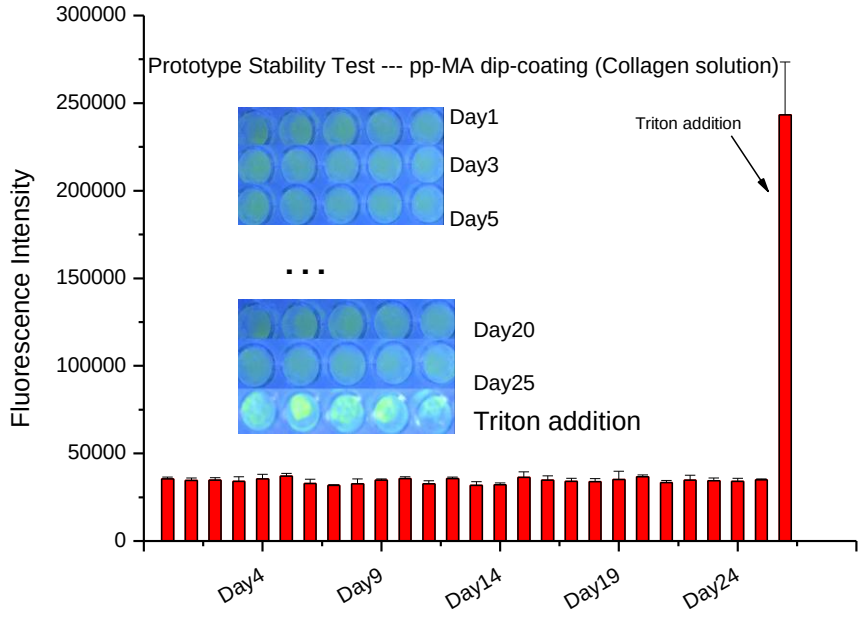

Figure 6.13: Graph showing stability test of phospholipids/PDA vesicles (30 mol% TCDA) sandwiched in collagen grafted pp-MA non-woven polypropylene for 25 days and significant fluorescence increase after lysis by Triton.

Photographs insert are the images taken under low power UV light. The images depict no release of fluorescent dye until the lysis by Triton addition. All measurements were carried out at room temperature. Error bars represent standard deviations based on three measurements of each sample.

A parallel experiment was carried out at 37 ^{o}C. The result indicated that such a prototype was not as stable as it was at room temperature, which is shown in figure 6.14. The data show progressively smaller increase for the first two days. A significant increase in fluorescence occurred from day-3 which is almost 5 times higher than the fresh system. It is possible that such a system would not carry a sufficient fluorescent payload in the process of time. Therefore, such system can retain its functionality for 1 or 2 days for responding to pathogenic bacteria otherwise it would interfere with fluorescence sensing result. It is probably because that water evaporated from the surface of the modified fabrics (water was primarily from the collagen solution) due to the continuous heat in the incubator, resulting in the total dry condition of the treated fabrics in the process of time. It is known that vesicles comprising phospholipids are not

able to survive in total dry conditions. This will lead to vesicle rupture and leakage of the fluorescent dye. Photographs insert here are in agreement with the graph, although the differences of increase in fluorescence were not clearly seen in the process of time.

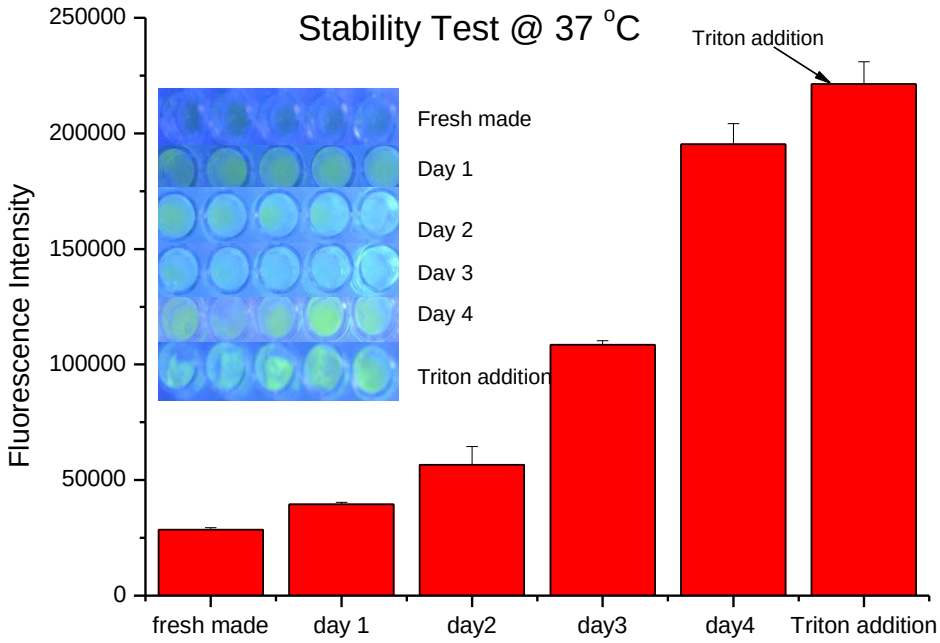

Figure 6.14: Graph showing stability test of phospholipids/PDA vesicles (30mol% TCDA) sandwiched in collagen grafted pp-MA non-woven polypropylene at 37 °C and fluorescence increase after lysis by Triton.

Photographs insert are the images taken under low power UV light. The images depict gradual increase in fluorescence in process of time. All measurements were carried out at 37 °C. Error bars represent standard deviations based on three measurements of each sample.

6.4.2.2 Pathogenicity Assay on Collagen Grafted pp-MA Non-woven Polypropylene

This part of the work investigated whether the simple prototype constructed here responds to pathogenic bacteria *S.aureus* (MSSA 476) and *P.aeruginosa* (PAO1), while not responding to non-pathogenic bacteria *E.coli* (DH5α). Given that the system is only stable for 1 or 2 days at 37 °C, such pathogenicity measurement is possible to be carried out in incubator at 37 ° C for 16 hours. The result shown in figure 6.15 indicates that

such a system effectively responds to pathogenic bacteria. It is illustrated that the vesicles can be coated on to a fabric and are sensitive to pathogenic bacteria when dispersed in broth, 'switching on' as the bacteria grow, as shown in figure 6.15 B**.**

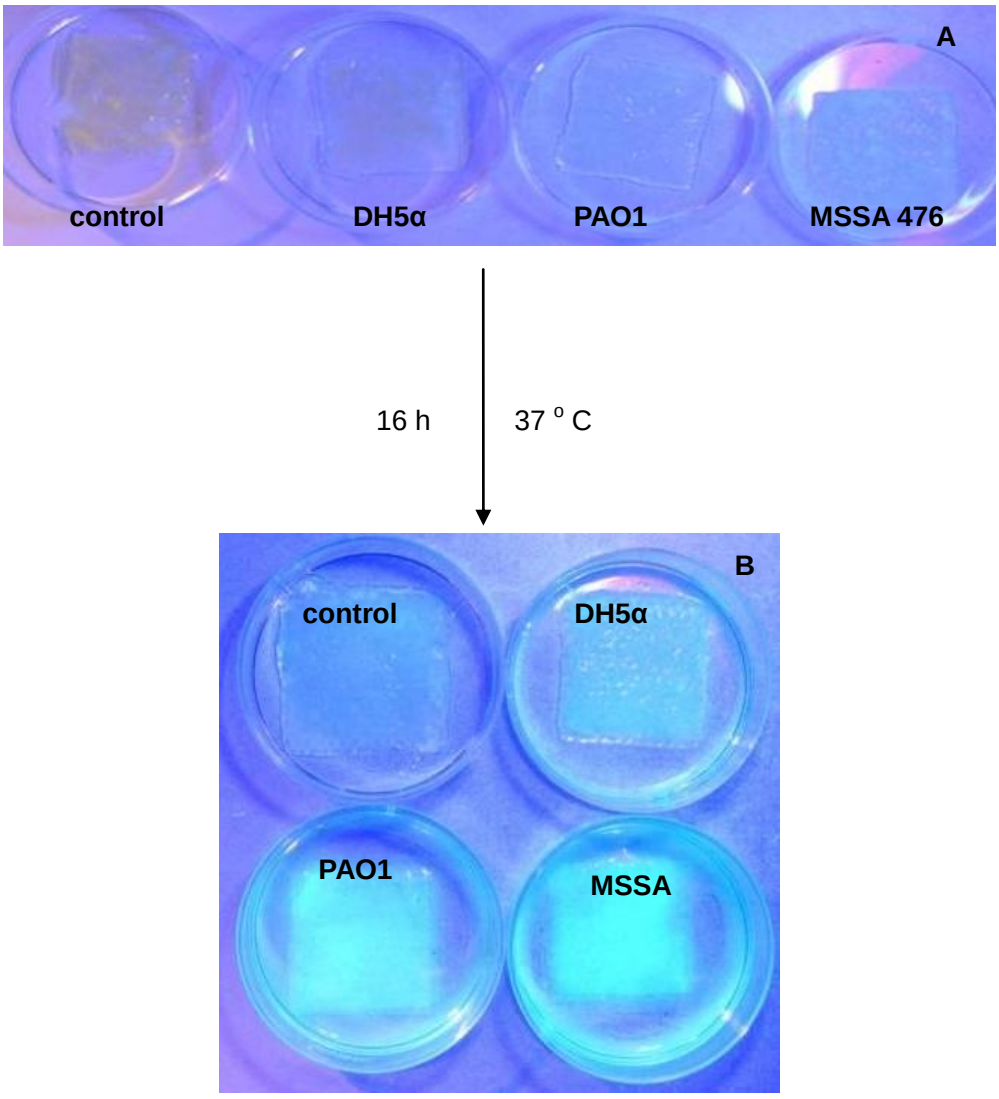

Figure 6.15: Simple prototype dressings: fluorescence response of modified fabric following overnight growth of bacteria on polypropylene fabric with 30 mol % TCDA vesicles.

6.5 Conclusion

In this chapter, three methods to stabilise phospholipid/PDA vesicles have been described including fabrics modified with plasma polymerised maleic anhydride, photo-grafting of polymerisation and gelatin sheets. Vesicles are attached on these

modified surfaces via covalent bond, hydrogen bond or electrostatic interaction. Furthermore, a prototype detection system for pathogenic bacteria on a simple model wound dressing is shown. The stability result of gelatin shows that gelatin is melted when temperature increases, indicating that it is not suitable in the use of wound dressings at relatively high temperature. Although the results of stability and pathogenicity indicate that pp-MA modified surface with grafted collagen so far has been considered as a good system for stabilising vesicles. However, such system is not as stable as expected for long term use at 37 ^{o}C. Various alternatives e.g. commercial and laboratory synthesised hydrogels which can replace such system for long term use especially at 37 ^{o}C is currently being studied in Jenkins' group.

Many factors have been recognised to reduce or delay wound healing including moist environment, pH changing on the surface of injured wound, temperature, and individual differences, etc. These factors should also be taken into account when constructing a prototype. More measurements are being studied in Jenkin's group such as the stability tests of prototypes in different pH and temperatures.

It is confirmed that the designed simple prototype can selectively respond to pathogenic bacteria by releasing fluorescent dye from vesicles to the external environment which provides an indication for clinical monitoring whether the wound is infected by bacteria or not. The ultimate aim of this work is to attempt to engineer a 'smart' wound dressing system that not only shows color change in the presence of pathogenic bacteria, without responding to commensal/harmless bacteria but also releases an encapsulated antimicrobial agent in the presence of pathogenic bacteria to inhibit/kill pathogenic bacteria. Chapter 7 represents antimicrobial property of vesicle modified pp-MA fabrics.

6.6 References

1 Jones V. Grey J.E., Harding K.G., *The ABC of wound healing*, *BMJ*, 2006, *332*, 777-780.

2 Kuroyanagi Y, Shiraishi A, Shirasaki Y, Nakakita N, Yasutomi Y, Takano Y, Shioya N., Development of a new wound dressing with antimicrobial delivery capability. *Repair Regen.*,1996, *2*, 122-129.

3 Uyama Y., Kato K., Ikada Y., Surface modification of polymers by grafting, *Advances in Polymer Science*, 1998, *137*, 1-39.

4 Winter G.D. Formation of a scab and the rate of epithelialization of superficial wounds in the skin of the young domestic pig. *Nature*, 1962, *193*, 293-34.

5 Ward, A.G.; Courts, A, The Science and Technology of Gelatin. *New York: Academic Press, 1997.*

Chapter 7 Development of Antimicrobial Property for Phospholipid/PDA Vesicles

Besides the property of colour response in the presence of pathogenic bacteria, construction of a 'smart' wound dressing requires that such nanocapsule system also has ability of killing/inhibiting bacterial growth if the infection occurs. This part of study looked at three types of topical antimicrobials which were encapsulated in the vesicles to make vesicle antimicrobial. The antimicrobial performances of vesicles were detected both in suspension and on plasma polymerised maleic anhydride deposited non-woven polypropylene.

The structure of this chapter is organised as follows: section 7.1 outlines a type of antimicrobial—silver nitrate encapsulated within vesicles. The antimicrobial efficacy of vesicles was evaluated both in suspension and on pp-MA modified non-woven polypropylene. The MIC_{50} of the pathogenic bacteria *P. aeruginosa* (PAO1) and *S. aureus* (MSSA 476) and non-pathogenic bacterial strain *E. coli* (DH5α) have been studied in this section in order to understand the susceptibility of the three strains to silver nitrate. Section 7.2 and 7.3 investigates antimicrobial efficacy containing gentamicin sulphate and chlorhexidine both in suspension and on pp-MA modified fabrics using JIS. The final part of this chapter concludes the chapter and summarises the key findings.

7.1 Silver Nitrate

Silver nitrate as the first antimicrobial was chosen to be used in this study. It has some issues with staining problems as stated in chapter 1. However, $AgNO_3$ is still a potent topical antimicrobial with high efficiency on a relatively wide range of bacterial infection. By utilising vesicles, cytotoxicity issues would be minimised due to a far lower concentration of silver nitrate released from vesicles and only when necessary.

7.1.1 Determination of Bacterial Susceptibility (MIC_{50})

The minimum inhibitory concentration to kill 50% of the bacterial population (MIC_{50}) of $AgNO_3$ against the three bacterial strains, *S. aureus* (MSSA 46), *P. aeruginosa* (PAO1), and *E. coli* (DH5α) was determined. Initially, a range-finding test was performed to gauge a rough indication of sensitivity to $AgNO_3$. Table 7.1 shows the concentrations of $AgNO_3$ and at which bacterial growth was inhibited.

Table 7.1: Range finding test of $AgNO_3$ against three strains of bacteria (where '+' is positive growth and '-' indicated no growth)

$AgNO_3$ (mg mL^{-1})	*E.coli* DH5α	*P.aeruginosa* (PAO1)	*S.aureus* (MSSA 476)
0.000001	+	+	+
0.00001	+	+	+
0.0001	+	+	+
0.001	+	+	+
0.01	-	-	+
0.1	-	-	-
1	-	-	-

The results of the range finding test indicates at which range of concentration $AgNO_3$ started to inhibit growth of bacteria. Triplicates with a narrow range of concentrations were then performed once a good indication of range finding test has been confirmed. The experiments over a narrow range of concentrations of $AgNO_3$ against three bacterial strains were further performed on a BMG Labtech fluorimeter in absorbance mode at 600 nm. The concentrations of $AgNO_3$ to inhibit the three strains of bacteria are shown as follows:

- *E.coli* DH5α : 0.001-0.01mg/mL $AgNO_3$
- *P.aeruginosa* PAO1 : 0.001-0.01mg/mL $AgNO_3$
- *S.aureus* MSSA 476 : 0.01-0.1 mg/mL $AgNO_3$

Based on the range of concentrations analysed above, final optical density for varying concentrations were measured after overnight and plotted against log([$AgNO_3$]), as presented in figure 7.1. These graphs were used to determine the value of MIC_{50} for *E. coli* DH5α, *P. aeruginosa* PAO1 and *S. aureus* MSSA 476.

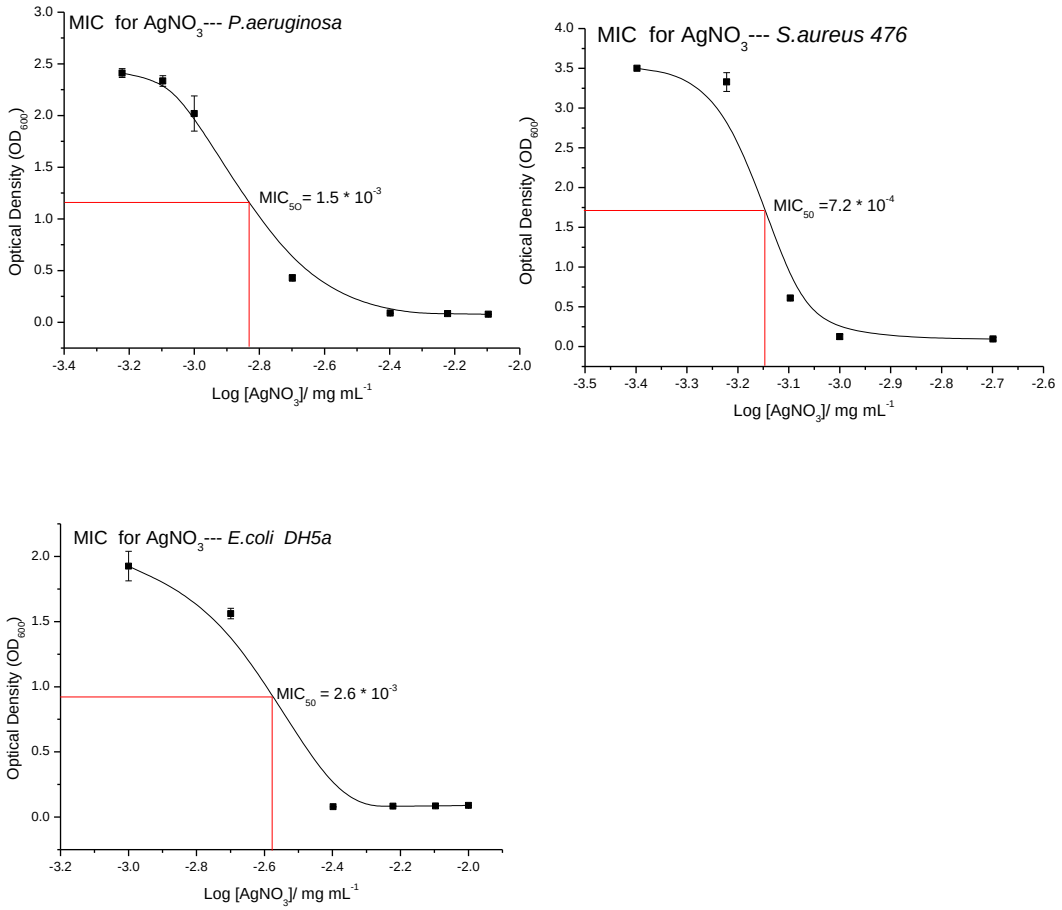

Figure 7.1: MIC_{50} of silver nitrate to the three strains of bacteria. The shapes of bacterial optical density-antimicrobials graphs give a clue that at which concentration of bacteria starts to respond to $AgNO_3$ and at which concentration of bacteria would be completely inhibited by the antimicrobial. Error bars represent standard deviations based on three measurements of each sample.

The minimum inhibitory concentrations of $AgNO_3$ versus three strains of bacteria were tested in solution and are summarised in table 7.2.

Table 7.2: Summary of MIC_{50} of $AgNO_3$ versus three bacterial strains

Antimicrobials	*P.aeruginosa*PAO1 MIC_{50}(mg mL^{-1})	*S. aureus* MSSA 476 MIC_{50}(mg mL^{-1})	*E.coli* (DH5α) MIC_{50}(mg mL^{-1})
$AgNO_3$	1.5×10^{-3}	7.2×10^{-4}	2.6×10^{-3}

From the table, it can be observed that *S. aureus* MSSA 476 showed the most sensitive

to $AgNO_3$, indicating that more *S. aureus* MSSA 476 would be killed compared to *P. aeruginosa* PAO1 and *E. coli* DH5α using same concentration of $AgNO_3$, whereas *E. coli* DH5α showed the lest susceptible to $AgNO_3$. The result of $AgNO_3$ was contrary to previous MIC_{50} data of both gentamicin sulfate and sodium azide. Figure 7.1 shows that *P. aeruginosa* PAO1 started to respond (declines in concentration) to $AgNO_3$ at the concentration of 0.76 μg mL^{-1} and was almost completely inhibited at concentration of 4 μg mL^{-1}; *S. aureus* MSSA 476 started to respond to $AgNO_3$ at the concentration of 0.5 μg mL^{-1} and was completely inhibited at the concentration of 1 mg mL^{-1}; *E. coli* DH5α became sensitive to $AgNO_3$ at 1 mg mL^{-1} and need 5 mg mL^{-1} for complete inhibition. The MIC results provide the information for the minimum encapsulation concentration of antimicrobials to be encapsulated within vesicles for antimicrobial test.

7.1.2 Minimum Encapsulation Concentration

MIC provides information for the further studies of antimicrobial measurement of vesicles and the calculation of minimum concentration of $AgNO_3$ should be encapsulated within the vesicles given that total volume of vesicles has been known. The minimum concentration of $AgNO_3$ to be encapsulated within vesicles is calculated as follows:

Total encapsulated volume per mL:

2.64×10^{-2} mL

The highest concentration of $AgNO_3$ to inhibit 50% of the three strains:

2.6×10^{-3} mg mL^{-1}

Therefore, the highest concentration of $AgNO_3$ which can completely kill/inhibit the three strains:

5.26×10^{-3} mg mL^{-1}

The minimum concentration of $AgNO_3$ to be encapsulated within vesicles:

$5.26 \times 10^{-3} / 2.64 \times 10^{-2} = 0.199$ mg mL^{-1}

Therefore, the calculated concentration of $AgNO_3$ is 0.199 mg mL^{-1}. A preliminary concentration of 2 mg mL^{-1} $AgNO_3$ was encapsulated within vesicles to ensure a high

encapsulated concentration thus can totally inhibit the two strains of pathogenic bacteria. Calculations were assumed 100% was encapsulated and all vesicles had a uniform size, which in reality may not be the case.

Another issue that needs to be considered is that $AgNO_3$ is photosensitive and the possibility of exposure cannot be eliminated although all precautions to keep samples away from light were taken. Exposure of $AgNO_3$ solution to light could cause any $AgNO_3$ to precipitate out. Therefore, a relatively low concentration of $AgNO_3$ encapsulated within vesicles indicates that $AgNO_3$ would be more soluble in solution and less photosensitive.

7.1.3 Antimicrobial Activity of Vesicles Containing $AgNO_3$ in Suspension

Measurements of vesicle ($AgNO_3$ encapsulated inside) lysis and subsequent self-destruction by toxins secreted from pathogenic bacteria were based on assessing viable numbers of bacteria by using BMG Labtech fluorimeter in absorbance mode at 600 nm. Vesicles with varying molar concentrations of TCDA (25%, 30%, 40%) were incubated overnight in the presence of *P. aeruginosa* PAO1, *S. aureus* MSSA 476, *E. coli* DH5α alongside negative and positive controls. Pure LB medium was used to determine contamination and pure bacterial solution was used to detect bacterial standard growth curve. Figure 7.2 shows the resulting bacterial growth in terms of colony forming units (CFU mL^{-1}) versus time.

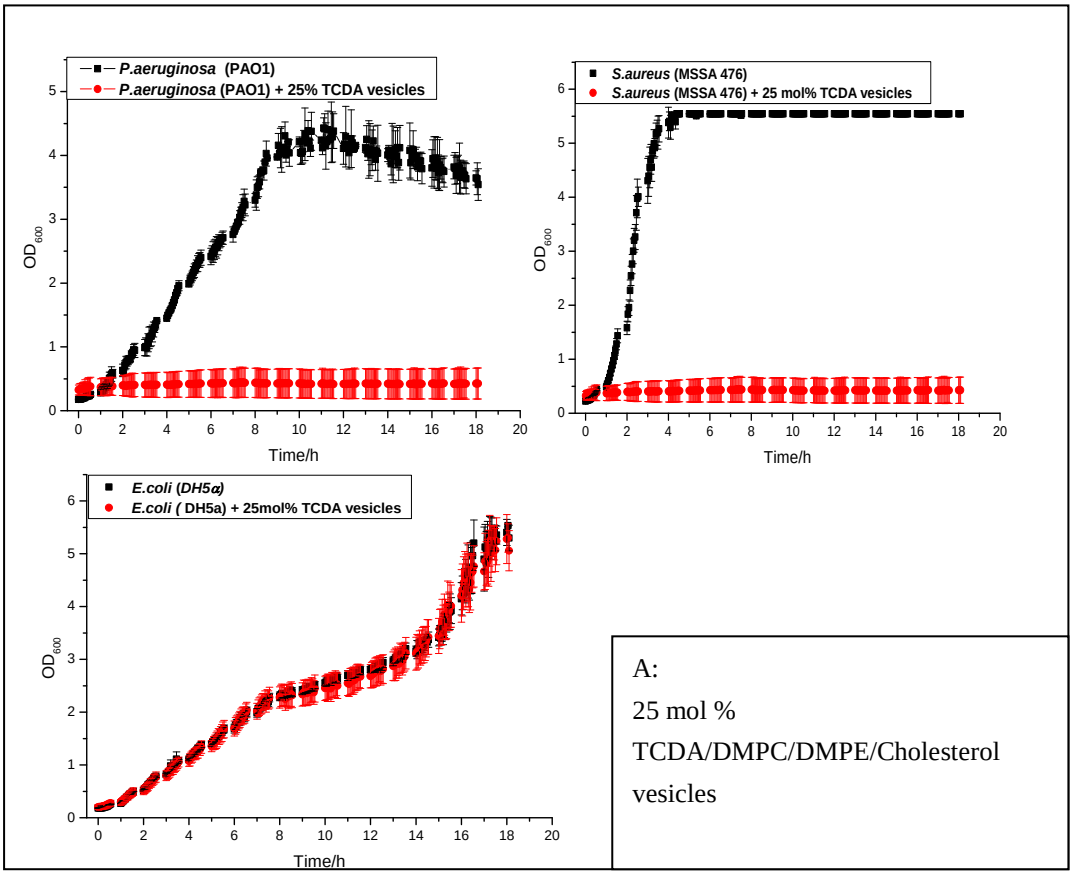

A:
25 mol %
TCDA/DMPC/DMPE/Cholesterol
vesicles

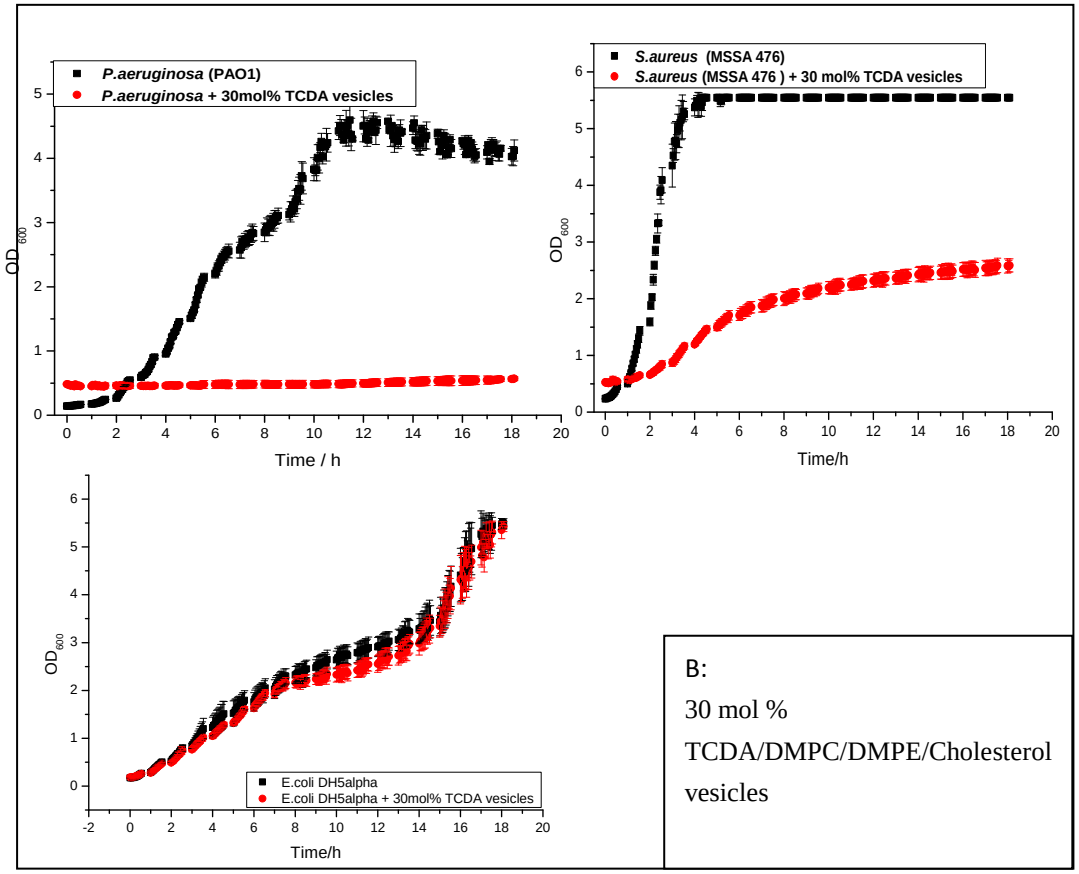

B:
30 mol %
TCDA/DMPC/DMPE/Cholesterol
vesicles

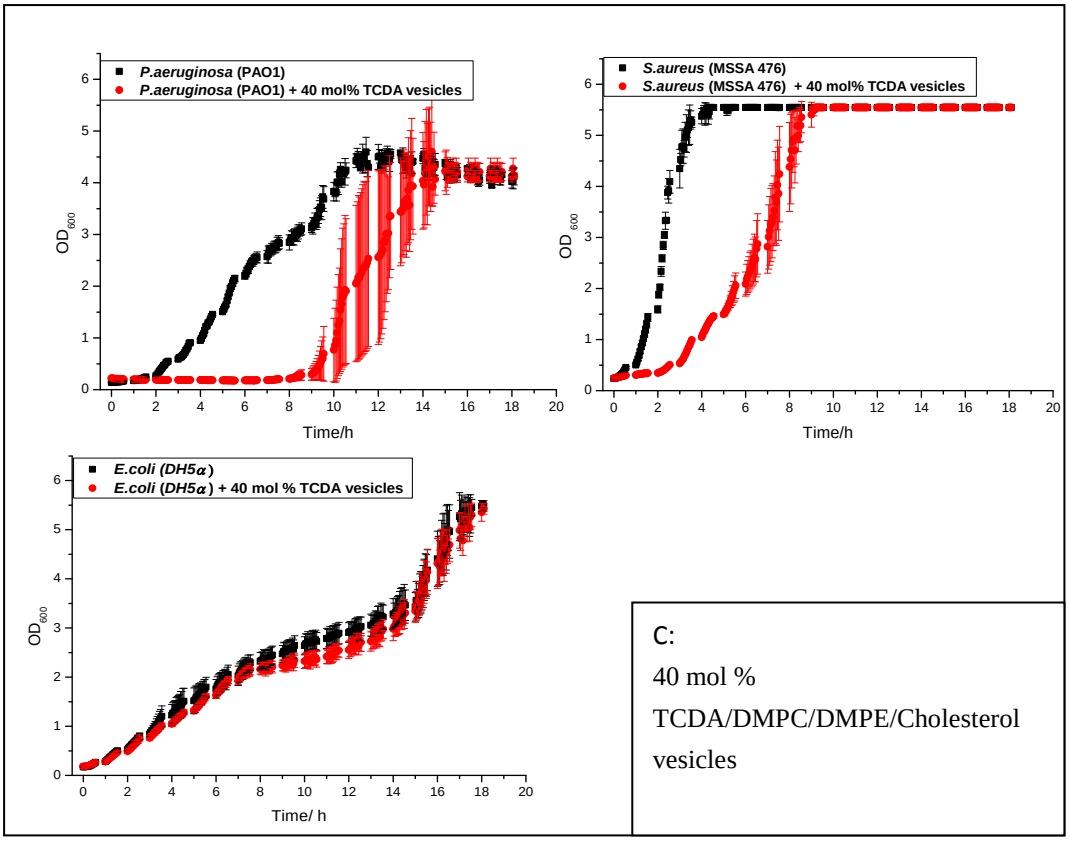

Figure 7.2: Time course of viable numbers of pathogenic and non-pathogenic bacteria incubated with phospholipid/PDA vesicles containing $AgNO_3$.

A: Three strains of bacteria incubated with 25mol%TCDA vesicles. Black squares show normal growth curve of three strains of bacteria. *P. aeruginosa* PAO1 and *S. aureus* MSSA 476 were completely inhibited/killed by $AgNO_3$ released from vesicles. B: Three strains of bacteria incubated with 30mol%TCDA vesicles. Black squares show normal growth curve of three strains of bacteria. *P. aeruginosa* PAO1 was completely killed/inhibited by $AgNO_3$ released from vesicles; *S. aureus* MSSA 476 was partially inhibited by $AgNO_3$ and showed growth eventually after overnight; C: Three strains of bacteria incubated with 40mol%TCDA vesicles. Black squares show normal growth curve of three strains of bacteria. Both *P. aeruginosa* PAO1 and *S. aureus* MSSA 476 show a retard of growth overnight. The difference in rate of growth in *P. aeruginosa* PAO1 and *S. aureus* MSSA 476 suggests the difference of susceptibility to $AgNO_3$ and the differences in the mode of action of these two bacterial strains. High error bars in graph c (P.aeruginosa with vesicles) was possibly due to the contamination of the bacteria. Error bars represent standard deviations based on three measurements per experiement.

As can be seen from the figure, black curves are all standard growth curves of three strains of bacteria. Vesicle samples all showed a standard growth curve when incubated with *E. coli* DH5α, indicating that vesicles were not ruptured by *E. coli* DH5α as it does not secrete any toxic/lytic agents. In *P. aeruginosa* PAO1, inhibition of growth was observed compared to the standard growth curve (black), meaning that vesicles were

lysed by toxins produced by *P. aeruginosa* PAO1 and thus antimicrobials released from vesicles killed/inhibited *P. aeruginosa* PAO1. Interestingly, *P. aeruginosa* PAO1 was completely killed/inhibited by $AgNO_3$ released from the vesicles in the beginning in 25 %, 30% TCDA vesicles, whereas *P. aeruginosa* PAO1 was inhibited in the beginning and then started to grow from hour-9 in 40% TCDA vesicles, meaning that the concentration of $AgNO_3$ released from vesicles was not sufficient to kill/inhibit *P. aeruginosa* PAO1 in 40% TCDA vesicles. This is due to the fact that the system is more stable with higher concentration of TCDA incorporated within lipid bilayer, making it difficult to be lysed by toxins/enzymes. Similarly, *S. aureus* MSSA also shows a large inhibition of growth compared to the standard growth curve (black). *S. aureus* MSSA shows a small growth after overnight in 30% TCDA vesicles compared to the complete inhibition/killing in *P. aeruginosa* PAO1, which negatively correlates the results of MIC_{50}. This is possibly because *P. aeruginosa* PAO1 is either more virulent or secretes more toxins during its exponential growth phase than *S. aureus* MSSA 476. Therefore, more $AgNO_3$ will be released from vesicles during lysis of vesicles by toxins/enzymes secreted by *P.aeruginosa*. In 40% TCDA vesicles, both *P.aeruginosa* PAO1 and *S. aureus* MSSA476 were inhibited in the beginning and started to grow. The rate at which *S. aureus* MSSA476 started to grow was faster than *P. aeruginosa* PAO1, which also negatively correlates with the result of $MIC_{50.}$ The results further confirm that TCDA does stabilise vesicles, making it difficult to be lysed by pathogenic bacteria with a higher concentration of TCDA.

7.1.4 Antimicrobial Activity on Vesicle Modified Fabrics ---JIS

Having successfully confirmed the antimicrobial property of vesicles ($AgNO_3$ inside) in suspension, this part of the study investigated the antimicrobial performance of vesicles on pp-MA modified plasma non-woven polypropylene against the two pathogenic bacterial strains *P.aeruginosa* PAO1 and *S. aureus* MSSA 576 and a non-pathogenic control *E. coli* DH5α. A concentration of 2 mg mL^{-1} $AgNO_3$ encapsulated within 30 mol% TCDA vesicles was first used to ensure a high encapsulated concentration. Agar

plates containing physiological saline samples of each fabric were cultured in incubator overnight and then each separate colony should be counted. It is important to dilute each sample appropriately as highly concentrated sample can cause a large number of colonies to grow, resulting in difficulty in counting accurately and increasing the risk of colonies merging and no longer being isolated. The number of viable bacterial colonies is calculated in terms of colony forming unit.

The antimicrobial performance of the $AgNO_3$ containing vesicles attached to fabrics was tested using the JIS methodology which has been described in the experimental section. The results in figure 7.3 show that test samples had a significant reduction in the number of viable bacteria after 4 hours, as the two pathogenic strains were able to lyse vesicles by producing toxins, resulting in the release of antimicrobial $AgNO_3$ to kill/inhibit bacteria. In *E. coli* DH5α, the test fabric samples show a similar number of viable cells compared to control fabric samples (with no vesicles). It is suggested that the growth of *E. coli* DH5α was not affected by $AgNO_3$ vesicles on modified fabric. The results are positively correlated with the results performed in suspension and are in agreement with the proposed hypothesis: pathogenic bacteria lyse the vesicles and ensure their self-destruction, but non-pathogenic bacteria are largely unaffected.

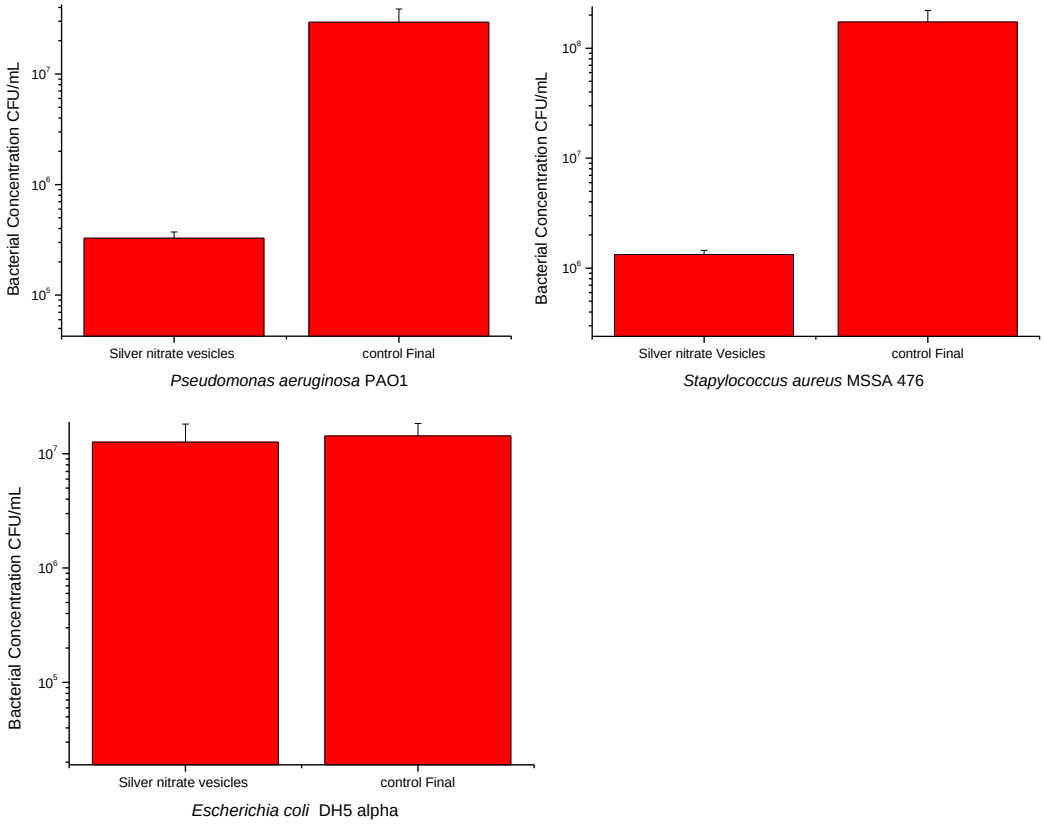

Figure 7.3: JIS result of TCDA vesicle (containing $AgNO_3$) bound to pp-MA nonwoven polypropylene against three strains of bacteria.

Graphs show persistence and growth of two pathogenic bacteria: *S. aureus* MSSA 476 and *P. aeruginosa* PAO1 and one non-pathogenic strain *E.coli* DH5α on fabric modified with vesicles containing $AgNO_3$ in comparison to non-modified, UV sterilised nonwoven PP (control), over a 4 h period. The pathogenic bacteria secrete membrane damaging toxins which lyse the vesicles, releasing $AgNO_3$ at a concentration that inhibit bacterial growth, with 4.6 x 10^5 CFU mL^{-1} of *P. aeruginosa* PAO1 and 5.3 x 10^5 CFU mL^{-1} of *S. aureus* MSSA 476 being measured after 4 h. Error bars represent standand deviations based on six measurements of each sample.

7.2 Gentamicin Sulfate

Gentamicin is a common aminoglycoside antimicrobial which inhibits bacterial protein synthesis. It is bactericidal instead of bacteriostatic. Gentamincin sulphate is a very expensive compound purchased from Sigma-Aldrich. It was used sparingly and in low concentrations due to toxicity and bacterial resistance issues.

7.2.1 Determination of Bacterial Susceptibility (MIC_{50})

The range finding test and MIC_{50} results has been discussed in 4.3.3 and will not be detailed here. Table 7.3 lists the MIC_{50} of the three strains of bacteria.

Table 7.3: Summary of MIC_{50} of gentamicin sulphate versus three bacterial strains

Antimicrobials	*P.aeruginosa* PAO1 MIC_{50}(mg mL^{-1})	*S. aureus* MSSA 476 MIC_{50}(mg mL^{-1})	*E.coli* (DH5α) MIC_{50}(mg mL^{-1})
Gentamicin Sulfate	8.9×10^{-4}	4.5×10^{-3}	4.8×10^{-4}

7.2.2 Minimum Encapsulation Concentration

The minimum encapsulation concentration is 0.034 mg mL^{-1} and a preliminary concentration of 5 mg mL^{-1} was encapsulated within vesicles to ensure a high encapsulation in order to completely inhibit the two strains of pathogenic bacteria. The details of calculation are referred to section 4.3.3.2.

7.2.3 Antimicrobial Activity of Vesicles Containing Gentamicin Sulphate in Suspension

Initially, 5mg mL^{-1} gentamicin sulphate was encapsulated within vesicles. Antimicrobial performance of vesicles containing gentamicin sulphate in the presence of three strains of bacteria (*E. coli* DH5α as control, *P. aeruginosa* PAO1 and *S. aureus* MSSA 476 as pathogenic strains) was measured in BMG Labtech fluorimeter in absorbance mode at 600 nm. Pure broth was set up to detect contamination and pure bacterial solution to detect the standard growth curve. Figure 7.4 shows the result of bacteria incubated with vesicles with 25%, 30%, 40% TCDA (containing gentamicin sulphate) overnight.

The results show that *E. coli* DH5α had no effect on the lysis of vesicles and thus was not killed/inhibited by the antimicrobial released by vesicles. All vesicle samples showed a standard growth curve when incubated with *E. coli* DH5α. In *P. aeruginosa* PAO1 and *S. aureus* MSSA 476, the growth was completely inhibited by gentamicin

sulphate in 25%, 30%, 40% TCDA vesicles, indicating that gentamicin was released through the lysis of vesicles. In addition, the shape of inhibition curve in gentamincin sulphate was different from $AgNO_3$, ($AgNO_3$ showed a retard in growth with higher concentration of TCDA). This is probably because too high a concentration of gentamicin sulphate was encapsulated within the vesicles, resulting in complete killing/inhibition of bacteria even if small amount of the antimicrobial was released to the external environment. The encapsulation concentration was then reduced for the JIS study.

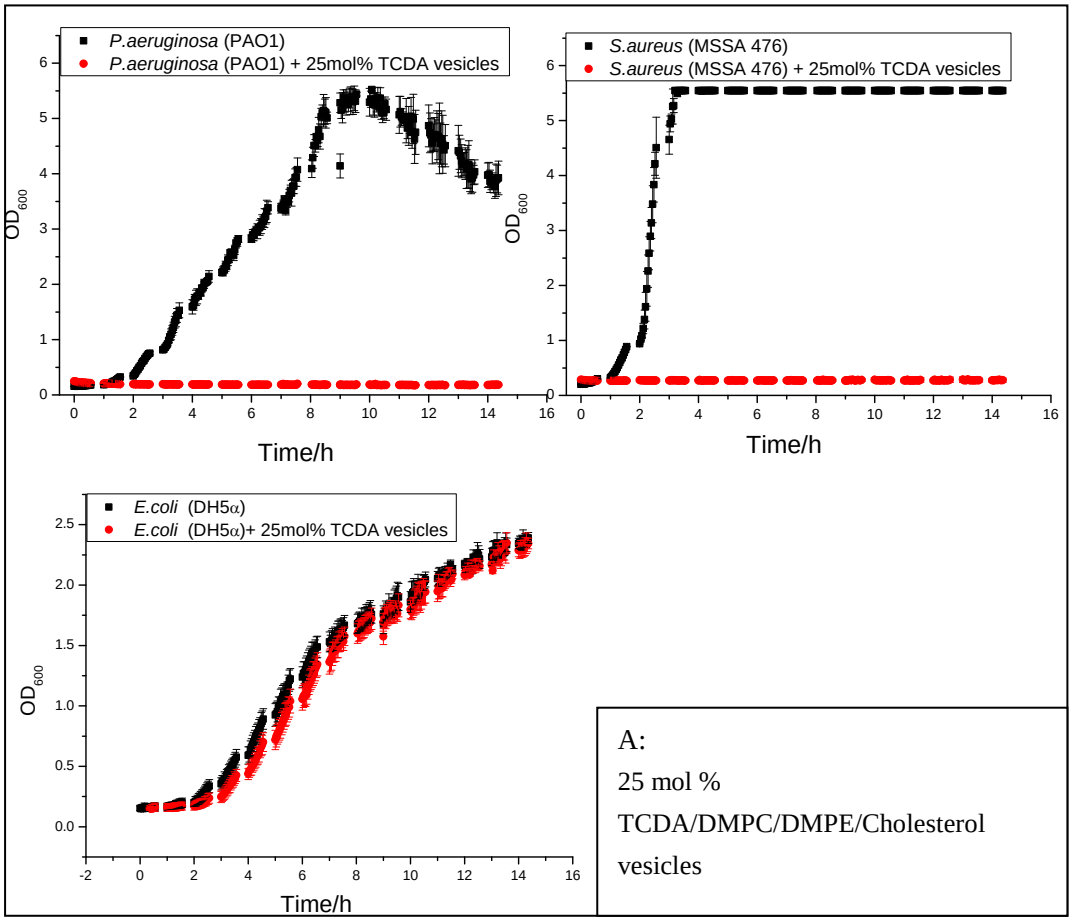

A:
25 mol %
TCDA/DMPC/DMPE/Cholesterol
vesicles

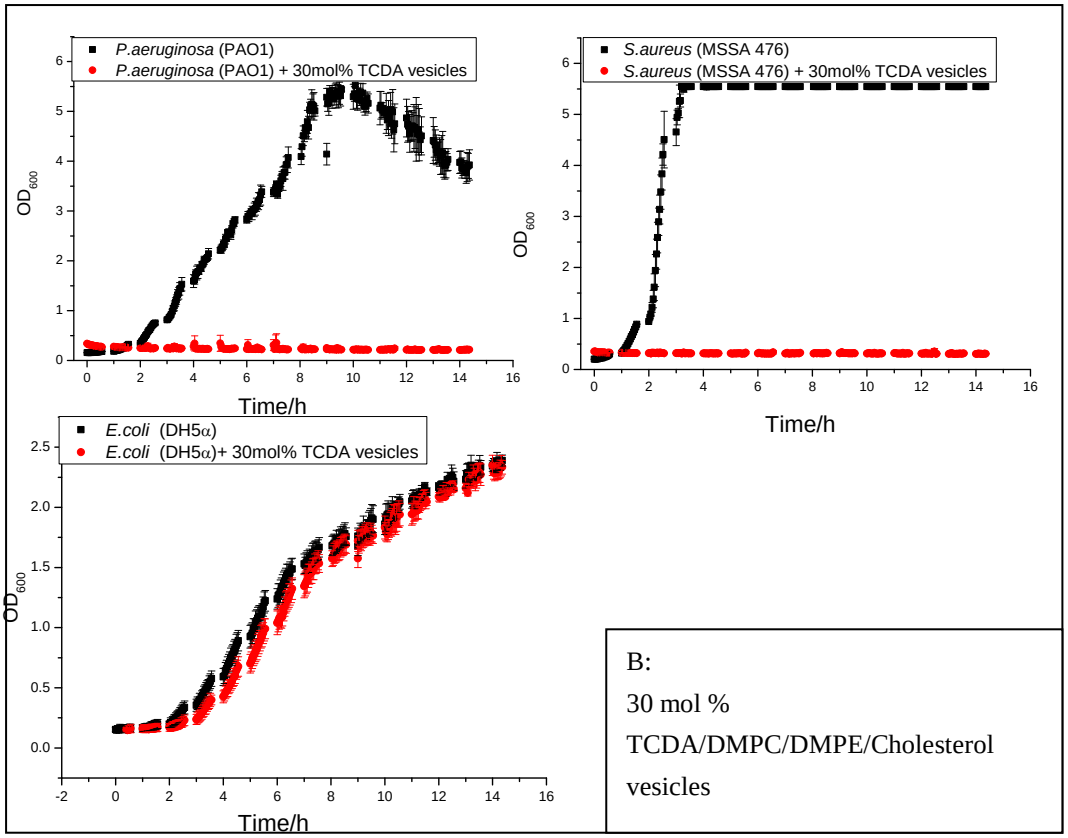

B:
30 mol %
TCDA/DMPC/DMPE/Cholesterol
vesicles

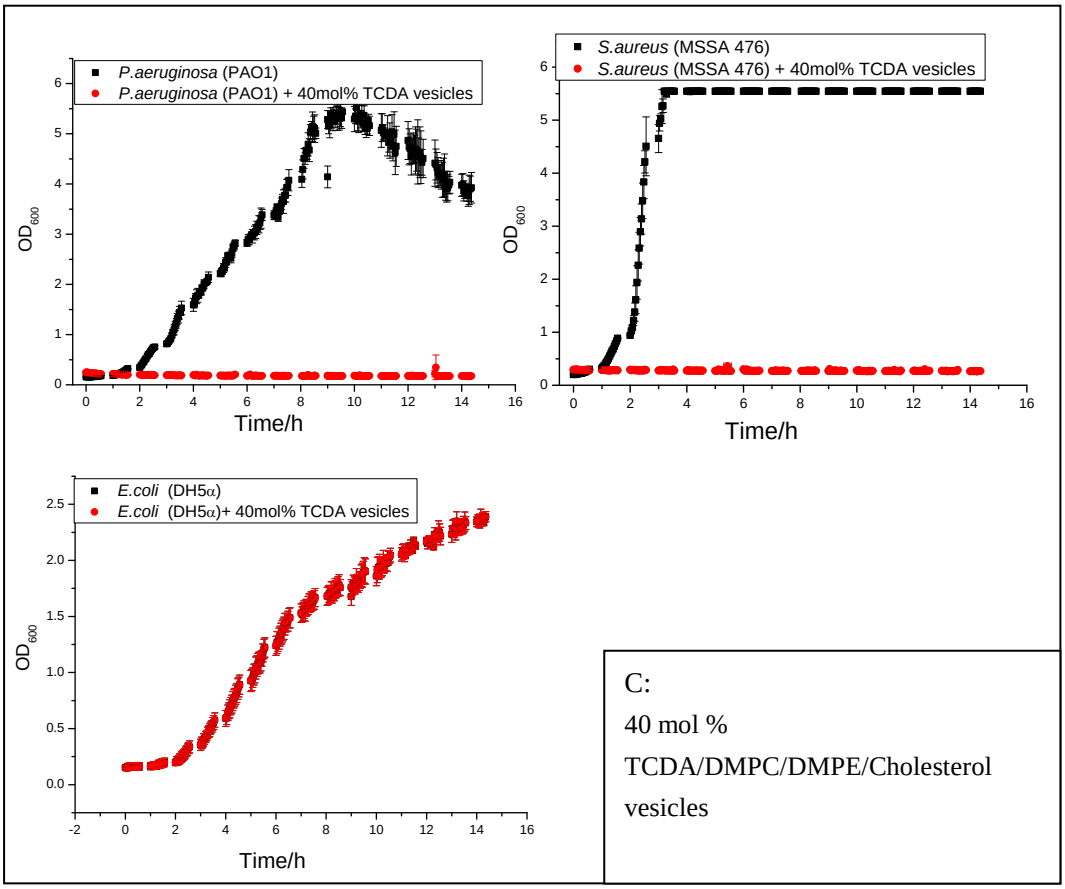

Figure 7.4: Time course of viable numbers of pathogenic and non-pathogenic bacteria incubated with phospholipid/PDA vesicles containing gentamicin sulphate.

A: Three strains of bacteria incubated with 25mol%TCDA vesicles. Black squares show normal growth curve of three strains of bacteria. *P. aeruginosa* PAO1 and *S. aureus* MSSA 476 were completely inhibited/killed by gentamicin sulphate released from vesicles. B: Three strains of bacteria incubated with 30mol%TCDA vesicles. Black squares show normal growth curve of three strains of bacteria. *P. aeruginosa* PAO1 and *S. aureus* MSSA 476 were completely killed/inhibited by gentamicin sulphate released from vesicles; C: Three strains of bacteria incubated with 40mol%TCDA vesicles. Black squares show normal growth curve of three strains of bacteria. Both *P. aeruginosa* PAO1 and *S. aureus* MSSA 476 were completely killed/inhibited by gentamicin sulphate after overnight. Error bars represent standard deviations based on three measurements of each sample.

7.2.4 Antimicrobial Activity on Vesicle Modified Fabrics ---JIS

JIS was used to detect the antimicrobial property of vesicle modified non-woven polypropylene. A primary gentamicin sulphate concentration of 5 mg mL $^{-1}$ was encapsulated inside 25, 30, 40 mol% TCDA vesicles for detecting antimicrobial activities in suspension. The concentration of gentamicin sulphate was later reduced to a value of 1 mg mL $^{-1}$ closer to MIC for JIS test in order to give a significant bacterial

response that proves fabric with antimicrobial encapsulated vesicles is capable of eliciting a correct bacterial response.

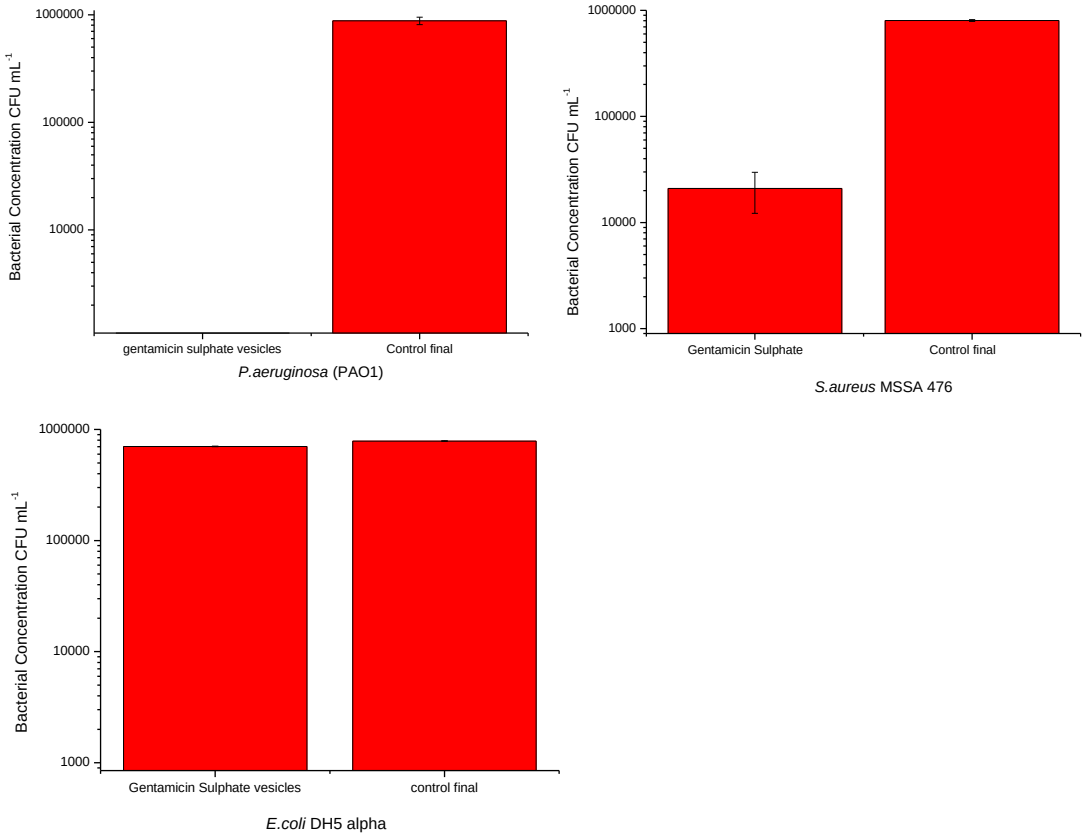

Figure 7.5: MIC results of TCDA vesicle (containing gentamicin sulphate) bound to pp-MA nonwoven polypropylene against three strains of bacteria.
Graphs show persistence and growth of two pathogenic (*S. aureus* MSSA 476 and *P. aeruginosa* PAO1) and one non-pathogenic strain *E. coli* DH5α on fabric modified with vesicles containing gentamicin sulphate in comparison to non-modified, UV sterilised nonwoven PP (control), over a 4 h period. The pathogenic bacteria secrete membrane damaging toxins which lyse the vesicles, releasing gentamicin sulphate at a concentration that inhibits bacterial growth, with 2.4 x 10^{4} CFU mL^{-1} of *P. aeruginosa* PAO1 and 25 CFU mL^{-1} of *S. aureus* MSSA 476 being measured after 4 h. Standard deviations represents standard deviations based on six measurements for each experiment.

Results in figure 7.5 show that the vesicle (30 mol% TCDA) modified nonwoven fabric inhibited the growth of both *P. aeruginosa* PAO1 and *S. aureus* MSSA 476, while the non-pathogenic *E .coli* DH5α (which did not secrete membrane damaging toxins) colonised the vesicle-modified fabric to almost the same extent as the non-modified control fabric. Growth of *P. aeruginosa* PAO1 was highly prevented as toxins produced lysed vesicles on the fabric, releasing gentamicin sulphate. *P. aeruginosa*

PAO1 was almost clearly inhibited/killed by gentamicin sulphate, with 25 CFU mL^{-1} of *P. aeruginosa* PAO1 being measured after 4 hour. *S. aureus* MSSA 476 test fabric samples also shows a high inhibition in the number of live bacteria present compared to control fabric samples (no vesicles). Bacterial growth was prevented, however to not as great an extent as *P. aeruginosa* PAO1. Furthermore, it can be concluded that the rate at which *P. aeruginosa* PAO1 was inhibited was greater than *S. aureus* MSSA 476 at low concentration of gentamicin sulphate from MIC_{50}, indicating that the difference in rate appears to superficially correlate with the JIS results of the two bacteria. However, other factors should be also taken into consideration such as expression levels of virulence factors from the two bacterial species, which are not clearly known.

Overall, vesicles encapsulated low concentration of gentamicin sulphate can retain good efficacy when bound to non-woven fabrics. However, antimicrobial tests with high concentration of gentamicin sulphate (15 mg mL^{-1}) encapsulated vesicles have been also measured both in suspension and on modified fabrics. All three strains were killed by gentamicin sulphate released from the vesicles. This is due to the fact that high encapsulated concentration of gentamicin sulphate and passive leakage from vesicles all cause complete killing/inhibition of bacterial growth.

7.3 Chlorhexidine

Chlorhexidine was used as an antimicrobial to be encapsulated within vesicles because it has a broad spectrum of activity and has high efficacy in both gram-positive and gram-negative bacteria.

7.3.1 Determination of Bacterial Susceptibility (MIC_{50})

A range finding test was firstly carried out to determine between which concentrations of chlorhexidine three strains of bacterial growth was inhibited. Chlorhexidine had a very low aqueous solubility and thus higher concentrations were not analysed. Table 7.4 shows the concentrations of chlorhexidine and between which concentrations bacterial

growth was inhibited.

Table 7.4: Range finding results for chlorhexidine agains three strains of bacteria (where '+' is positive growth and '-' indicated no growth)

[Chlorhexidine]mg mL $^{-1}$	*E.coli* DH5α	*P.aeruginosa* PAO1	*S. aureus* MSSA 476
0	+	+	+
0.00001	+	+	+
0.0001	+	+	+
0.001	-	-	-
0.01	-	-	-

The experiments of narrow range of concentrations of chlorhexidine against three bacterial strains were further performed on a BMG Labtech fluorimeter in absorbance mode at 600 nm. The concentrations of chlorhexidine to inhibit the three strains of bacteria are shown as follows:

- *E. coli* DH5α : 0.0001-0.001 mg mL $^{-1}$ chlorhexidine
- *P. aeruginosa* PAO1 : 0.0001-0.001 mg mL $^{-1}$ chlorhexidine
- *S .aureus* MSSA 476 : 0.0001-0.001 mg mL $^{-1}$ chlorhexidine

Based on the range of concentrations analysed above, optical density for varying concentrations were measured after overnight and plotted against log([chlorhexidine]), as presented in figure 7.6. The shapes of bacterial optical density-antimicrobials graphs give a clue that at which concentration of bacteria starts to respond to chlorhexidine and at which concentration of bacteria would be completely inhibited by the antimicrobial.

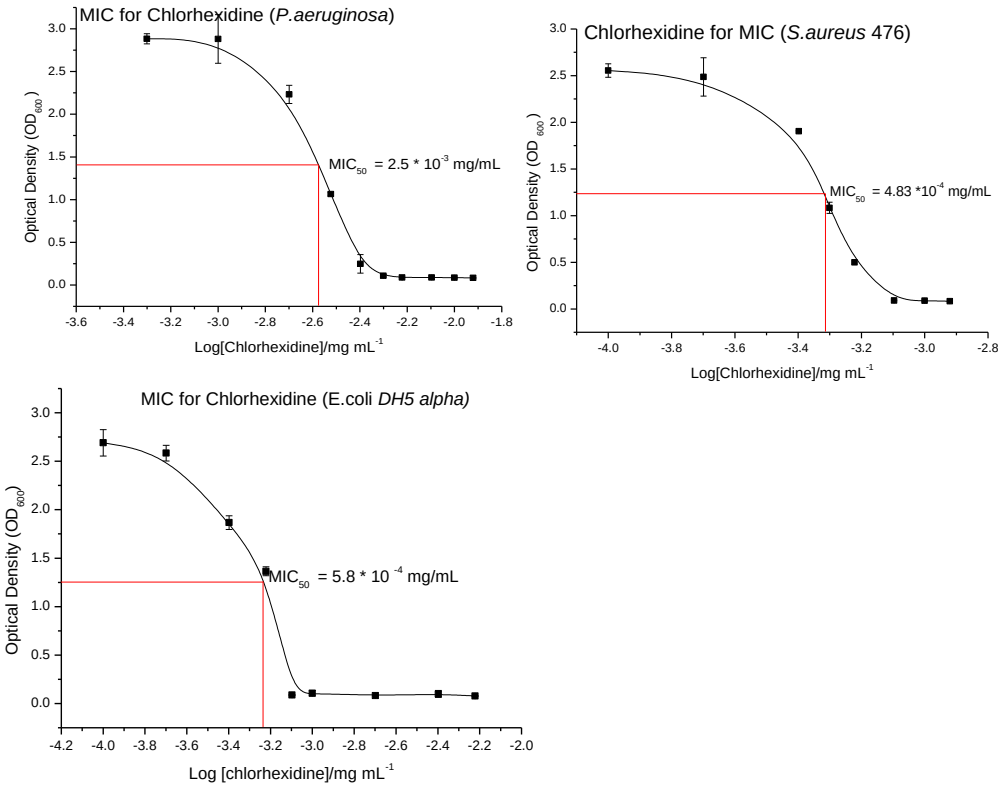

Figure 7.6:MIC_{50} of chlorhexidine versus the three strains of bacteria. Error bars represent standard deviations based on three measurements of each experiment.

The minimum inhibitory concentrations of chlorhexidine versus three bacterial strains were tested in solution and are summarised in table 7.5.

Table 7.5: Lists of MIC_{50} of three strains of bacteria

Antimicrobials	*P.aeruginosa* PAO1 MIC_{50}(mg mL^{-1})	*S. aureus* MSSA 476 MIC_{50}(mg mL^{-1})	*E.coli* (DH5α) MIC_{50}(mg mL^{-1})
Chlorhexidine	2.5 x 10^{-3}	4.83 x 10^{-4}	5.8 x 10^{-4}

It can be observed from the table that *S.aureus* are the most sensitive to chlorhexidine, which means that more *S.aureus* would be killed compared to *P.aeruginosa* PAO1 and *E. coli* DH5α using the same concentration of chlorhexidine, while *P.aeruginosa* showed the lest susceptible to chlorhexidine. Figure 7.6 shows that *P. aeruginosa* PAO1 started to respond (declines in concentration) to chlorhexidine at the concentrations of 0.6 µg mL^{-1} and was almost completely inhibited at concentration of 5µg mL^{-1}; *S .aureus*

MSSA 476 became sensitive to chlorhexidine at 0.25 μg mL^{-1} and need 0.9 μg mL^{-1} for complete inhibition; *E. coli* DH5α started to respond to chlorhexidin at concentration of 0.2 μg mL^{-1} and was completely inhibited at 1.12 μg mL^{-1}.

7.3.2 Minimum Encapsulation Concentration

The minimum concentration of chlorhexidine to be encapsulated within vesicles is calculated as follows:

Total encapsulated volume:

2.64×10^{-2} mL

The highest concentration of chlorhexidine to inhibit 50% of the three strains:

2.5×10^{-3} mg mL^{-1}

Therefore, the highest concentration of chlorhexidine which can completely kill/inhibit the three strains:

5×10^{-3} mg mL^{-1}

The minimum concentration of chlorhexidine to be encapsulated within vesicles:

$5 \times 10^{-3} / 2.64 \times 10^{-2} = 0.190$ mg mL^{-1}

Therefore, the calculated concentration of chlorhexidine is 0.190 mg mL^{-1}. A preliminary concentration of 2 mg mL^{-1} chlorhexidine was initially encapsulated within vesicles to ensure a high encapsulated concentration. MIC_{50} calculations give a chlorhexidine concentration when all vesicles obey ideal mechanisms; all are 100 nm in diameter, all are spherical, all are unilamellar and all encapsulate the same concentration of chlorhexidine. However, it is difficult to determine the exact dimensions of vesicles and so that the exact encapsulated concentration may not be the same as calculated.

7.3.3 Antimicrobial Activity of Vesicles Containing Chlorhexidine in Suspension

2 mg mL^{-1} chlorhexidine was encapsulated within vesicles to ensure high encapsulation concentration. Initially, antimicrobial activity of 30 mol% TCDA vesicles containing

chlorhexidine in the presence of three strains of bacteria (*E. coli* DH5α, *P. aeruginosa* PAO1, *S. aureus* MSSA 476) was measured in BMG Labtech fluorimeter in absorbance mode at 600nm. As usual, pure broth and pure bacterial solution were set up to detect contamination and bacterial standard growth curve. Figure 7.7 shows the result of bacteria incubated with vesicles with 30% TCDA overnight. *E. coli* DH5α was used as control system to provide important information on whether the fundamental hypothesis is correct: pathogenic bacteria lyse the vesicles and ensure their self-destruction, while non-pathogenic bacteria are largely unaffected.

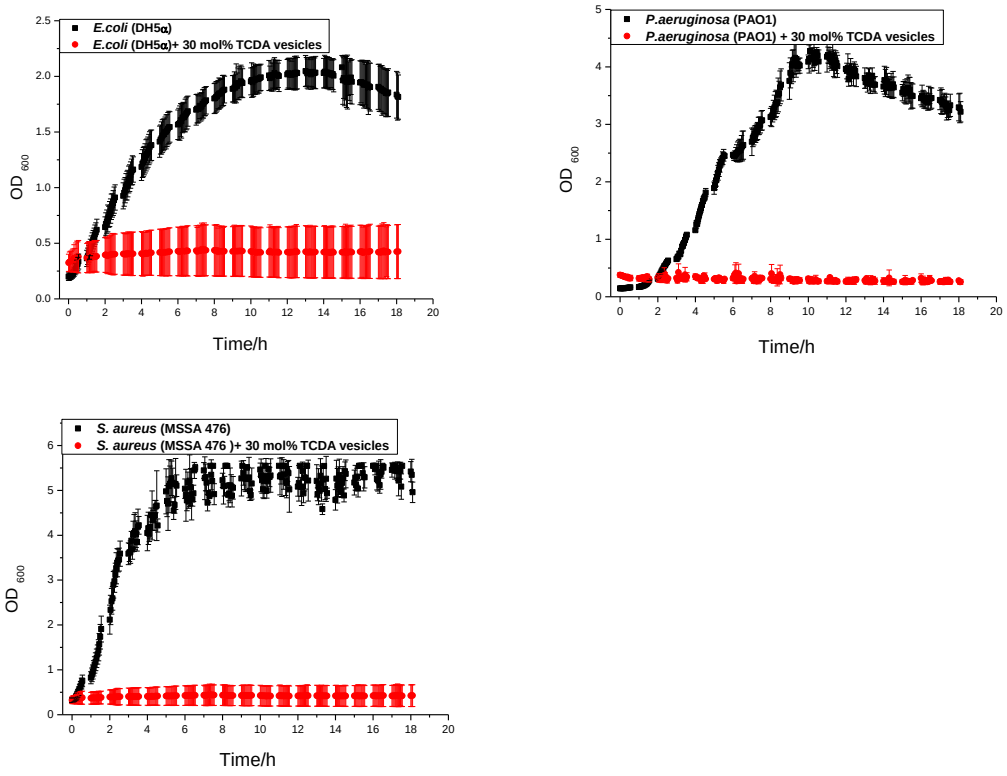

Figure 7.7: Overnight growth of pathogenic and non-pathogenic bacteria incubated with phospholipid/PDA vesicles containing chlorhexidine.
All three strains were all killed by chlohexidine released from the vesicles. Error bars represent standard deviations based on three measurements of each sample.

In figure 7.7, pure bacterial solution all showes a standard growth curve. Bacterial suspensions should have shown no effect on *E. coli* DH5α and a significant reduction in

the number of viable bacteria both in *P. aeruginosa* PAO1 and *S. aureus* MSSA 476. However, a large inhibition of growth was observed in all 3 strains, indicating that there must be free antimicrobials in solution. Efforts such as double filtration using NAP-25 columns and reducing encapsulation concentration of chlorhexidine (0.5 mg mL^{-1}) were attempted to obtain pure vesicles with chlorhexidine encapsulated inside. Subsequent antibacterial measurements in suspension were carried out to detect the efficacy of vesicles. However, the results showed vesicles still inhibited/killed all three strains. This indicates that most chlorhexidine was not encapsulated within the vesicles. It is thought to be relevant to poor solubility of chlorhexidine in aqueous solution and possible interaction between chlorhexidine and lipid bilayer of vesicles which makes chlorhexidine difficult to be encapsulated within vesicles. The mechanism of such interaction is not known. Therefore, chlorhexidine is not appropriate to be used in the further investigation on modified fabrics.

7.4 Conclusion

This chapter demonstrates that a simple vesicle bound to pp-MA non-woven fabrics can be used for controlling bacterial growth and infection. Three types of topical antimicrobials were separately encapsulated within vesicles and antimicrobial efficacy was evaluated.

Although TSB medium was later proved to be an optimal medium to grow *S. aureus* MSSA 476 as *S. aureus* MSSA 476 seems to produce more toxins in TSB medium. LB broth was used for growing three strains of bacteria in both MIC and antimicrobial assays in this work because TSB became available in the late period of this project and was only used for growing *S. aureus* MSSA 476 in section 5.5. It is possible that MIC result of *S. aureus* MSSA 476 grown in LB medium would be quite different from grown in TSB medium.

Chlorhexidine was assessed at an encapsulated concentration of 2 mg mL^{-1}.

Unfortunately, all three bacterial strains were all inhibited when incubated with vesicles containing chlorhexidine. The solution assay indicated that such antimicrobial was not suitable in the use of vesicle system and subsequent fabric test. Furthermore, chlorhexidine has poor aqueous solubility (0.08g/100 mL) which makes it a limited antimicrobial to be encapsulated within vesicles with relatively high concentration.

Silver nitrate was used as an alternative to be encapsulated within vesicles and antimicrobial measurement in solution showed all good responses in all three bacterial strains. The following fabric test (JIS) also showed good response in all three strains. Silver nitrate was selected as a suitable candidate to be encapsulated inside vesicles. However, silver nitrate has some issues regarding its inherent photosensitivity and solubility in aqueous solution. The compound stains a black colour and precipitates easily when it is exposed to light. Furthermore, it is reported that the use of silver can cause inherent cytotoxicity. Solutions of >1 % $AgNO_3$ are known to be cytotoxic which limits the development of more concentrated vesicles against bacteria. Therefore, low concentration of silver nitrate is suitable to be used for the antimicrobial development of vesicle system; while higher concentration of $AgNO_3$ will not be recommended to be used in the development of antimicrobial system in the long run.

Gentamicin sulphate, however, has good aqueous solubility compared to the other two compounds assessed and does not exist cytotoxicity issue. Antimicrobial measurements both in suspension and on fabrics showed all three strains had a good response to gentamicin sulphate released from vesicles. Gentamicin sulphate in addition has no cytotoxicity. Therefore, it can be used as an ideal compound to be encapsulated within vesicles for further use.

The main difficulty for the three compounds used in the work was the purification when they are encapsulated within vesicles. All three compounds in aqueous solution are colourless, meaning that purification is not accurate. This could be resolved by using double filtration by NAP-25 columns and removal of first 1 mL of eluate to ensure more

pure vesicle solution. It could also be resolved with the encapsulation of both dye such as carboxyfluorescein and antimicrobial within vesicles. This would maintain their antimicrobial efficacy whilst being more easily distinguishable during purification.

Chapter 8 Conclusions

This thesis has investigated an initial ‘smart’ wound dressing which releases antimicrobials and changes colour only in the presence of pathogenic bacteria. It has been shown that its contributions are of both theoretical and practical interest and serve as a good starting point for additional research. In this concluding chapter, all the key findings from different chapters are summarised and several future research directions are suggested.

8.1 Summary of Results

In chapter 4, preliminary work for designing a simple nanocapsule system for selectively recognising and killing/inhibiting pathogenic bacteria has been developed. The work has demonstrated that a simple vesicle system can be used for controlling bacterial growth and infection when antimicrobials are encapsulated within vesicles. Giant unilamellar vesicles with diameter of 1 μm were firstly applied to such system due to its high encapsulation volume and easy manipulation by using rotary evaporation methodology. Antimicrobials including sodium azide and gentamicin sulphate were encapsulated within GUVs to selectively inhibit/kill pathogenic bacteria. This is based on the concept that pathogenic bacteria can be used to be the agents of their own destruction by releasing toxins that rupture vesicles containing an antimicrobial agent. Antimicrobial measurements in suspension confirmed such a hypothesis: pathogenic bacteria can secrete membrane damaging toxins to lyse membranes of vesicles, while non-pathogenic bacteria do not secrete lytic toxins. Subsequent surface design was used in this work to attach GUVs via covalent bonding. Surface characterisation using FT-IR confirms that GUVs have been attached surface successfully. Subsequent JIS results prove that GUV bound pp-MA modified non-woven fabrics is capable of killing/inhibiting pathogenic bacteria. Such a system provides an idea to construct a wound dressing which can prevent bacterial infection as well as provide a simple colorimetric or fluorometric

response to give patients or clinicians early warning of wound infection. Later, a fluorescence response system has been developed and detailed in chapter 5 by utilising self-quenched carboxyfluorescein. The idea is based on the concept that at high concentration, carboxyfluorescein is non-fluorescent. Following breakdown of the lipid vesicle containers by bacterial toxins, the dye becomes diluted and "switches on".

However, there is some degree of passive leaching of encapsulated contents from the GUVs. This is apparent in antimicrobial detection using conventional agar plating. It is likely that some passive leakage of sodium azide limited the growth of *E. coli* DH5α to an extent. This leakage is most likely due to both tonic imbalance between the interior and exterior of vesicles and the thermal instability of the bilayer lipid vesicles. Furthermore, GUVs are not as stable as expected especially when it is exposed to partially dry conditions. Again, the physical properties of vesicles must be optimised to ensure stability over a long period of time. Hence, there was a motivation to introduce a novel vesicle system based on incorporation of diacetylene fatty acids as constituents in the lipid bilayer of a vesicle to yield robustness compared to phospholipid vesicles. The PAD/phospholipid vesicles can be irradiated with UV light and polymerised to form polymer cage. This rigid polymer part could provide the stability required to increase shelf life and thermal stability. Such polydiacetylene vesicle system fulfils both prerequisites and yields a satisfactory efficiency by varying the molar concentration of PDA part. TCDA as a diacetylene fatty acid was used to incorporate into lipid bilayer part. TCDA ensures a certain amount of stability; however the higher concentration of TCDA would enable the vesicle system less sensitive to external environment. Overall, the TCDA concentration for optimum stability was chosen as 30% which provides the relatively stability without compromising sensitivity to toxins produced by pathogenic bacteria.

Chapter 5 also explores physical properties of PDA/phospholipids. Such a vesicle system will undergo a colour transition after UV irradiation and may interfere with the result of the colorimetric response if a fluorophore is encapsulated within vesicles.

Stability and sensitivity measurements of vesicles provide that the ideal system is between 20 mol% - 30 mol% TCDA vesicles. In this range, the polydiacetylene part would not exhibit an intense colour. Hence, such colour transition will not significantly affect the colorimetric response if a fluorescent dye is encapsulated within vesicles.

Aside from exploration of optimal vesicle systems, bacterial detection with carboxyfluorescein shows very promising result in solution which provides proof of concept to fundamental theory here. Although the stability of phospholipid/PDA has been enhanced by incorporation of diacetylene fatty acids into the lipid bilayer, such a vesicle system still has leaching problems as can be seen from figure 5.11 with a relatively low concentration of TCDA and is not able to survive in completely dry conditions. Therefore, the attempts to immobilise the vesicles in hydrogels to maintain vesicles intact and stable as well as promote wound healing are detailed in chapter 7. Chapter 7 describes various methods used in this thesis to immobilise PDA/phospholipid vesicles. Pulse plasma deposited non-woven polypropylene with grafted collagen (gelatine) shows that such modified fabric can retain vesicles for at least one month at room temperature and maintain vesicles intact at 37 ^{o}C for 2 days. Subsequent bacterial test on the simple prototype suggests such system is capable of differentiating between pathogenic and non-pathogenic bacteria by releasing a fluorescent dye. The visual colour response can be observed under low power UV light. Other modified fabrics to stabilise vesicles and hydrogels to maintain the stability of vesicles are now being investigated in the group currently.

Apart from a simple colorimetric or fluorimetric response built into the system, the aim of this work is to attempt to engineer a ‘smart’ wound dressing system that only releases an encapsulated antimicrobial agent in the presence of pathogenic bacteria. The last chapter outlines three topical antimicrobials which can be encapsulated in the vesicles and subsequent antimicrobial measurements against three strains of bacteria were investigated. pp-MA treated non-woven polypropylene was chosen to attach vesicles and was used in the study of JIS. The antimicrobial measurements both in suspension and on

modified fabrics show silver nitrate and gentamicin sulphate had good performance on the antibacterial activity. Chlorhexidine would not be recommended in the use of the antimicrobial study due to its low solubility. Silver nitrate is not appropriate to be used with higher concentration as it also has low solubility in aqueous solution and will precipitate when exposed to light, without responding to harmless bacteria.

Rotary evaporation was the main methodology used in the synthesis of GUVs due to its relatively easy manipulation. However, the sizes of GUVs are not regular enough to obtain an accurate internal volume. Extrusion method was then applied to the synthesis of phospholipid/PDA vesicles by using Liposofast vesicle extruder. It is likely to be a better method for production with large capacity ready for scale up. The polycarbonate filters are stacked to give a very thorough processing of the bulk solution compared to rotary evaporation and to give a uniform size.

The purification of vesicles was used for all systems in both antimicrobials and fluorophore encapsulating vesicles. Empirically, it can be concluded that the purification of antimicrobials including sodium azide, gentamicin sulphate and silver nitrate was successful as they were able to selectively inhibit/kill the growth of pathogenic bacteria, while not responding to non-pathogenic bacteria. Double filtration is necessary for purifying vesicles with encapsulated antimicrobials to ensure pure vesicle solution. The fluorophore containing vesicles were proved to elute separately from the free fluorophore as shown in figure 4.5. NAP-25 columns are of larger volume than the NAP-10 columns and this allows better separation and resolution of the eluting times. Initial work of purification for GUVs relied on the use of NAP-10 columns as NAP-25 columns did not become available until starting the work of phospholipid/PDA vesicles. NAP-25 sephadex columns are proved to be more efficient to purify the vesicles from free antimicrobials/fluorescein.

8.2 Future Research Areas

There are several areas of this thesis that can be expanded at a future stage and some of these are outlined below:

8.2.1 Stability

In the short term, the physical properties of vesicles must be optimised to ensure stability over a long period of time. However, the incorporation of diacetylene moiety into lipid bilayer improves the stability of vesicles and enables such vesicle system to survive under partially dry condition. However, there is still some degree of passive leakage of encapsulated contents from the vesicles, as presented in figure 5.10 (a), (b). This is because the major constituent for constructing vesicles is phospholipid, which inevitably has some degree of leakage. On the other hand, the difference in length of hydrocarbon chains between TCDA fatty acids and DMPC can lead to the disruption of packing density of lipid bilayers, resulting in leakage of vesicle system. TCDA has 17 carbons after photopolymerisation, which is longer than alkyl groups in both DMPC and DMPE (14 carbons). The differentiation in the length of alkyl chains results in disrupting packing density of bilayer arrangement of PDA-phospholipid. This is shown in figure 8.1.

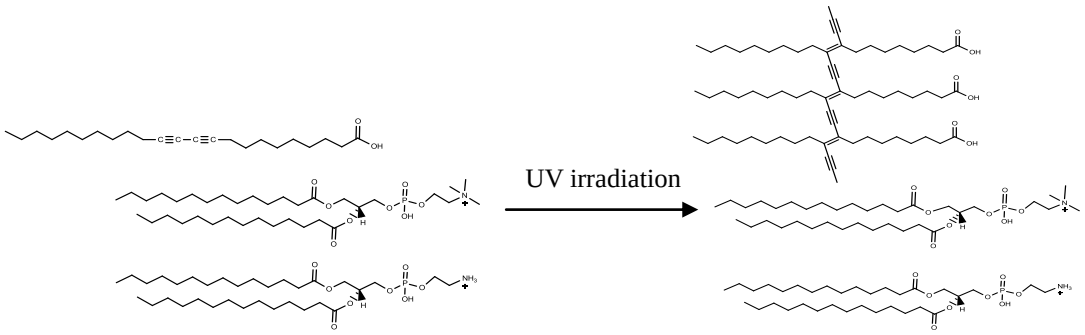

A

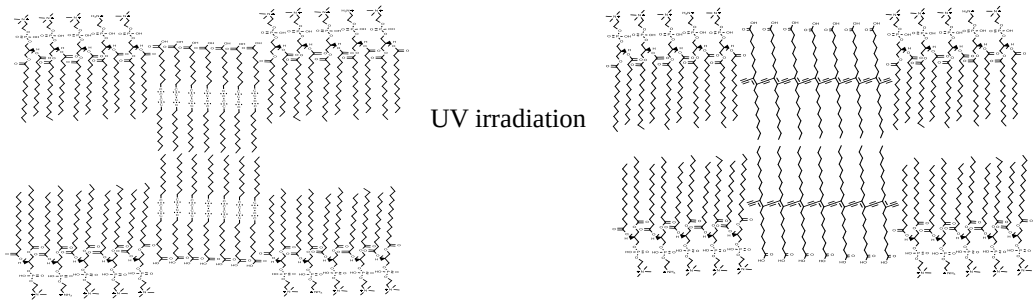

B

Figure 8.1: Bilayer arrangements before/after UV irradiation in phospholipid/TCDA vesicles.
Graphs show different length of alkyl groups in TCDA and phospholipid resulting in disrupting packing density of bilayer and subsequent resulting in possible leakage and instability of vesicles. (A): chemical structure of phospholipid and TCDA and their differences in the length of hydrophobic chains before and after photo-polymerisation; (B): different length of alkyl chains results in disruption of packing density of bilayer arrangement

Therefore, DMPC and DMPE replaced by other phospholipids with longer acyl chains are being studied in the group including DPPC (16:0) and DSPC (18:0). The current study of DPPC/DMPE/PDA suggests such system is quite stable if encapsulating carboxyfluorescein in solution for almost one month. Further study with pathogenic bacterial strains will be investigated. However, the closely packed bilayer between PDA and phospholipid would decrease the sensitivity and flexibility of the whole system as transition temperature would increase with longer alkyl chains of phospholipid. Cholesterol is also necessary to be used to insert the lipid bilayer to maintain the system both flexible and stable at room temperature. Hence, phospholipids including both PC and PE should be carefully selected to maintain vesicles both stability and sensitivity. Such study is also being investigated in the group.

8.2.2 Encapsulating Agents

Carboxyfluorescein is used as a main agent to be encapsulated within vesicles to give a fluorimetric colour response for early detection of pathogenic bacterial infection. It is known that carboxyfluorescein is pH dependent which means the carboxyfluorescein may be unstable or photo-bleached in either lower or higher pH environment. All work

in this thesis related to carboxyfluorescein was carried out in neutral environment. However, in reality the pH environment of chronic wounds has been recorded within the range of 7.15-8.9. As the wound progresses towards healing, the pH moves to neutral and then becomes acidic. Again, carboxyfluorescein is reported to be leaky if encapsulated in the vesicles and hence not suitable to be used as encapsulating agents for drug delivery. Therefore, more stable fluorescent dyes both in acidic and alkaline environment should be investigated and encapsulated in the vesicles for the further research.

Furthermore, more appropriate antimicrobials should be encapsulated and investigated in the same manner as sodium azide, gentamicin sulphate, $AgNO_3$ and chlorhexidine. More modern topical antimicrobials such cadexomer iodine,[1-2] fluoroquinolone[3] and laboratory synthesised antimicrobials can be chosen to be encapsulated within vesicles. A combination of antimicrobials (e.g. gentamicin and vancomycin combinations) is another possibility to be encapsulated in the vesicles. Zinc compounds such as zinc oxide and zinc pyrithione, a new area of antimicrobial research, could also be applied to the vesicles encapsulation.[4,5] Furthermore, organisms such as viruses and bacteriophages instead of antimicrobials are alternatives to be encapsulated in the vesicles which can detect bacterial strains very selectively. [6]

8.2.3 Bacteria Related to Wound Infection

Apart from *S. aureus* and *P. aeruginosa*, a large variety of organisms can be found in burn wound infections, such as *Enterococci*, *Acinetobacter*, *Klebsiella* and more virulent strains of *E.coil, S. epidermidis* and *S. pyogenes* are additional bacterial species commonly found in normal skin flora and are able to cause burn wound infection. Vesicle system should also be evaluated with a broader spectrum of bacterial strains and species. In addition, the rise of multi-drug resistant organism (MDROs) has resulted in inefficacy of used antimicrobials. The most commonly known MDRO is methicillin-resistant *Staphylococcus aureus* (MRSA), which is responsible for several

difficult-to-treat infections in humans. Therefore, vesicle system could be designed to deliver effective antimicrobials as well as reduce the rate of acquisition of bacterial resistance.

8.2.4 Prototype Construction

The ultimate of this project is to attempt to construct a ‘smart’ wound dressing system which can only release an encapsulated antimicrobial agent in the presence of pathogenic bacteria, without responding to commensal/harmless bacteria. Additionally, a simple colorimetric or fluorometric response could also be built into the device to give patients or clinicians early warning of wound infection. This proposed wound dressing is shown in figure 8.3. Various prototypes such as modified fabrics/hydrogels for maintaining both moist environment and vesicle integrity are now being developed in the group.

Wound Dressing Concept

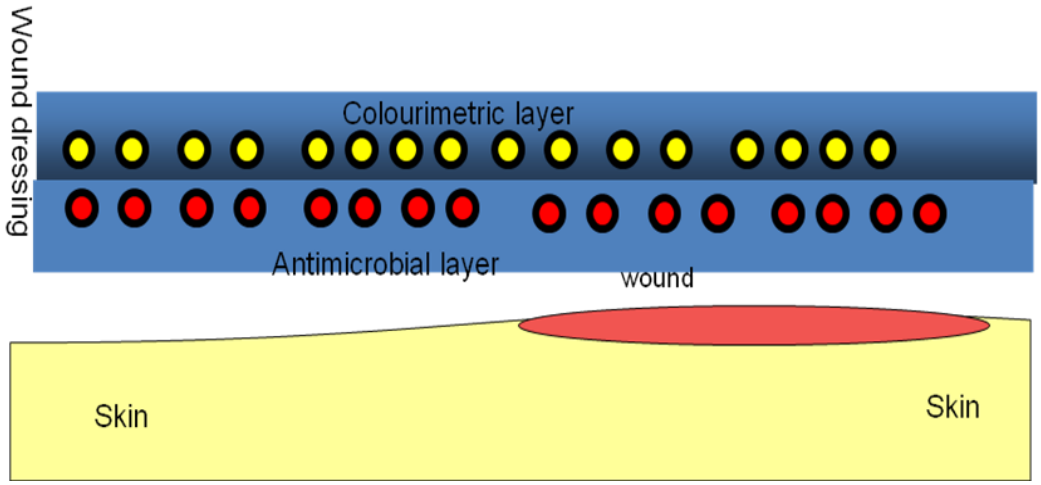

Mode of Action Following Infection

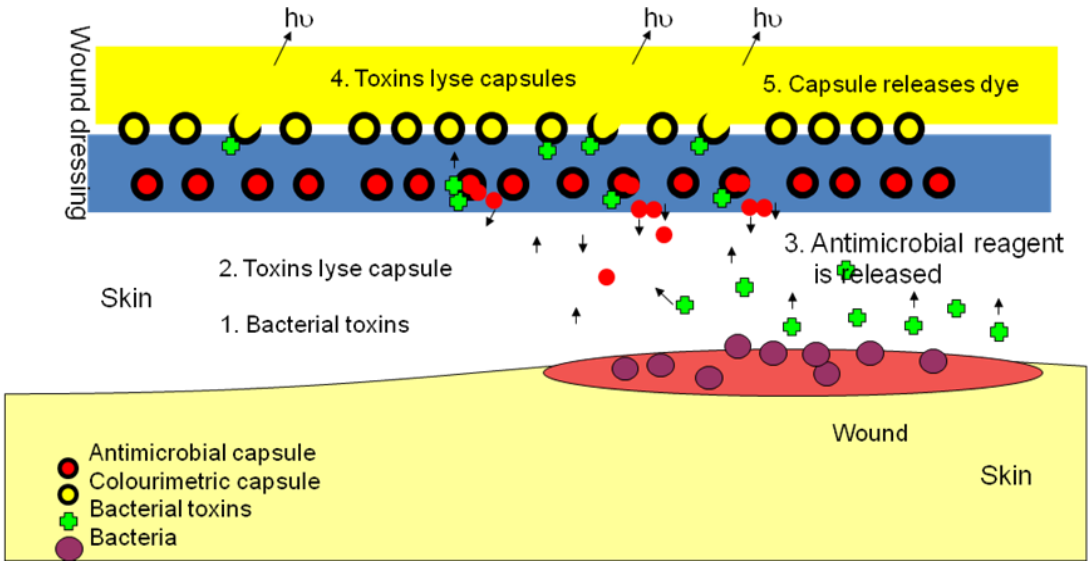

Figure 8.2: A proposed 'smart' wound dressing.
The graphs illustrate that it can respond to the presence of pathogenic bacteria: gives a fluorimetric/colorimetric response; releases an antimicrobial agent to inhibit/kill growth of pathogenic bacteria; promotes and supports tissue growth.

8.3 References

1 Lamme E.N., Gustafsson T.N., Middelkoop E., Cadexomer-iodine ointment shows stimulation of epidermal regeneration in experimental full-thickness wounds, *Arch. Dermatol. Res.*, 1998, *290*, 18-24.

2 Lipsky B.A., Hoey C., Topical antimicrobial therapy for treating chronic wounds, *Clin. Infect. Dis*., 2009, *49*, 1541-1549.

3 Kaye S., Tuft S., Neal T., Tole D., Leeming J., Figueiredo F., Armstrong M., McDonnell P., Tullo A., Parry C., Bacterial susceptibility to topical antimicrobials and clinical outcome in bacterial keratitis, *Immnol. Microbiol*. 2010, *51*, 362-368.

4 Rajendran R., Balakumar C., Mohammed Ahammed H.A., Jayakumar S, Vaideki S., Rajesh E.M., Use of zinc oxide nano particles for production of antimicrobial textiles, *Int. J. Eng. Sci. Tech.*, 2010, *2*, 202-208.

5 Lamore S.D., Cabello C. M., Wondrack G..T., The topical antimicrobial zinc pyrithione is a heat shock response inducer that causes DNA damage and PARP-dependent energy crisis in human skin cells, *Cell Stress Chaperon.*, 2010, *15*, 309-322.

6 Clark J.R., March J.B., Bacteriophages and biotechnology: vaccines, gene therapy and antibacterials, *Trends Biotechnol*., 2006, *24*, 212-218.

Appendix A Detailed Operations of Plasma Reactor

- Reactor cleaned manually: the reactor chamber and both flanges (reactor 1) were washed using acetone, water and ethanol, allowed to dry
- Reactor cleaned using oxygen plasma
- Monomer loaded to Young's flask. Freeze thawed several times (3+) by cooling flask with liquid nitrogen followed by gentle heating
- Substrate loaded to the main chamber at one end: Vacuum was removed, one electrode was detached using wing-nuts (reactor 1) or retaining strap (reactor 2), the substrate loaded, lines reattached and vacuum applied. System was allowed to reach base pressure (ca. 2 x 10^{-2} mbar)
- Monomer chamber was opened to vacuum, pressure was allowed to stabilise
- Monomer flow rate was measured by closing the vacuum tap for 30s, pressure readings were taken at start (P_s) and end (P_f) of this time period
- The RF generator was switched on, mode set to 'CW', plasma ignited (RF on) and desired input power set.
- Input impedance was manually matched using 'Tune' and 'Load' to minimise the reflected power. The reflected power was reduced to <0.5% of the input power at all times during deposition
- Deposition pressure was recorded along with the input and reflected power
- Deposition was stopped after desired time, then the monomer chamber was closed
- The substrate was removed after allowing the reactor to cool, then generally used immediately for analysis or biological assay

NB: The initial step of degassing or removal of impurities was applied only to non-melting monomers as those compounds which melt when heated or are liquid at room temperature instantly degas under vacuum.

Appendix B Original Publications

1 **Jin Zhou**, Adrew L.Loftus, Geraldine Mulley, A.Toby A. Jenkins, A thin film detection/response system for pathogenic bacteria, *J. Am. Chem. Soc*., 2010, *132*, 6566-6570.

2 **Jin Zhou**, Thet Naing Tun, Sung-ha Hong, June D.Mercer-Chalmers, Maisem Laabei, Amber E.R.Young, A.Tobias A. Jenkins, Development of a prototype wound dressing technology which can detect and report colonisation by pathogenic bacteria, *Biosensors and Bioelectronics*, 2011, published online.